Novel Nicotinic Acetylcholine Receptor Ligands based on Cytisine and Choline: Synthesis, *In vitro* Evaluation and Structure-Activity Relationships

Dissertation

zur

Erlangung des Doktorgrades (Dr.rer.nat.)

der Mathematisch-Naturwissenschaftlichen Fakultät

der

Rheinischen Friedrich-Wilhelms-Universität Bonn

vorgelegt von

Lenka Munoz

aus Nové Zámky

(Slowakei)

Bonn 2005

Angefertigt mit Genehmigung der Mathematisch-Naturwissenschaftlichen Fakultät der
Rheinischen Friedrich-Wilhelms-Universität Bonn

1. Referent: PD Dr. Daniela Gündisch

2. Referent: Prof. Dr. Christa E. Müller

Tag der Promotion: 2. November 2005

Die vorliegende Arbeit wurde im Zeitraum von Oktober 2001 bis September 2005 in der Abteilung Pharmazeutische Chemie des Pharmazeutischen Institutes der Rheinischen Friedrich-Wilhelm-Universität Bonn unter der Leitung von PD Dr. Daniela Gündisch angefertigt.

Ich danke herzlich Frau PD Dr. Daniela Gündisch für die wissenschaftliche Leitung dieser Arbeit sowie für ihre hervorragende Betreuung.

Mein Dank gilt ebenfalls Frau Prof. Dr. Christa E. Müller für die freundliche Übernahme des Koreferates.

For Alex…

Table of Contents

1 Introduction

1.1 Nicotinic Acetylcholine Receptors

1.1.1 The Structure of nAChRs

Nicotinic acetylcholine receptors (nAChRs) are members of the pentametric “cys-loop” superfamily of ligand-gated ion channels that also includes e.g. glycine, $GABA_A$ and $5\text{-}HT_3$ receptors.[1,2] The nAChR macromolecule is an ion-channel complex that is composed of five subunits assembled like the staves of a barrel around a central water-filled pore (Figure 1-1).[3] nAChRs can be divided into two groups: muscle receptors, located at the skeletal neuromuscular junction where they mediate neuromuscular transmission, and neuronal receptors, which are found throughout the peripheral and central nervous systems.[1]

Seventeen genes coding for five muscle and twelve neuronal nAChRs subunits have so far been cloned and they encode for peptides possessing sequence homology, sharing a general linear structure and having similar topologies.[4,5] Each receptor subunit is a three domain protein that divides the receptor channel into three parts (ligand-binding, membrane-

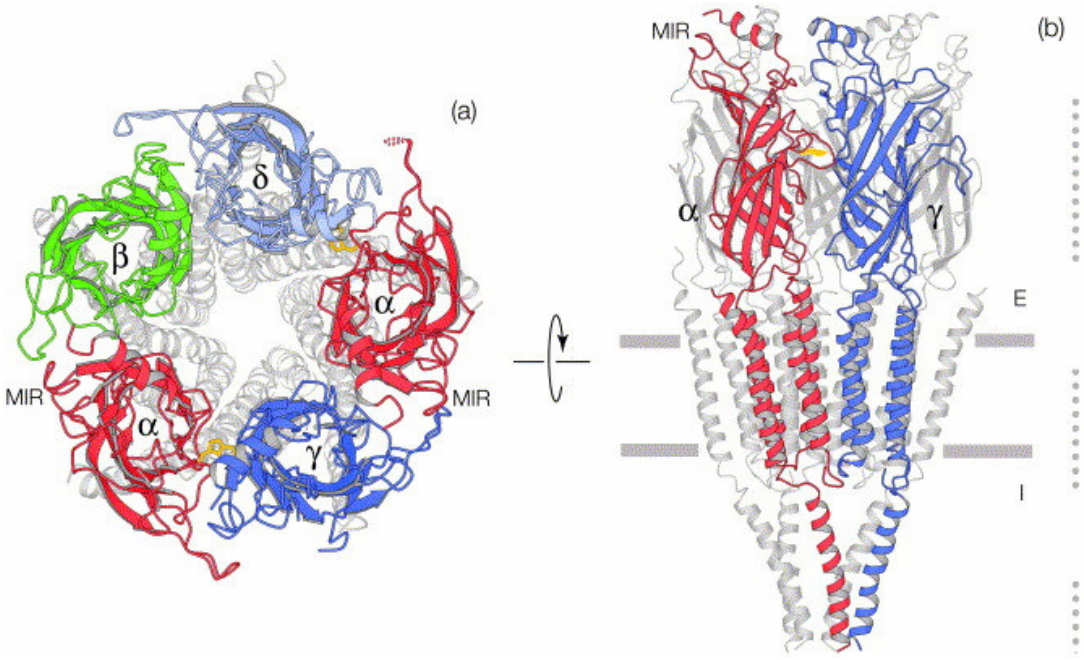

Figure 1-1 Ribbon diagrams of the whole receptor (muscle type), as viewed (a) from the synaptic cleft and (b) parallel with membrane plane. In the picture (a) only the ligand-binding domain is highlighted and in the picture (b) only the two front subunits are highlighted (α in red, β in green, γ in blue and δ in light blue). [Ref. 6]

spinning and intracellular part). Figure 1-2 illustrates the structure of a single subunit.[6] The amino and carboxy termini are located extracellularly. The N-terminal is built around a β-sandwich core consisting of ten β-strands (red and blue sheets) and one α-helix. The extracellular portion contains several loops that are critical for the receptor function (e.g. the Cys loop, the β1-β2 loop or the loops A, B and C). The membrane-spinning portion is composed of α-helical segments (M1 – M4) and their functionally important loops (M1-M2 and M2-M3). The intracellular portion is composed mainly of the extension of the sequence between M3 and M4 and a curved α-helix, termed MA.[6]

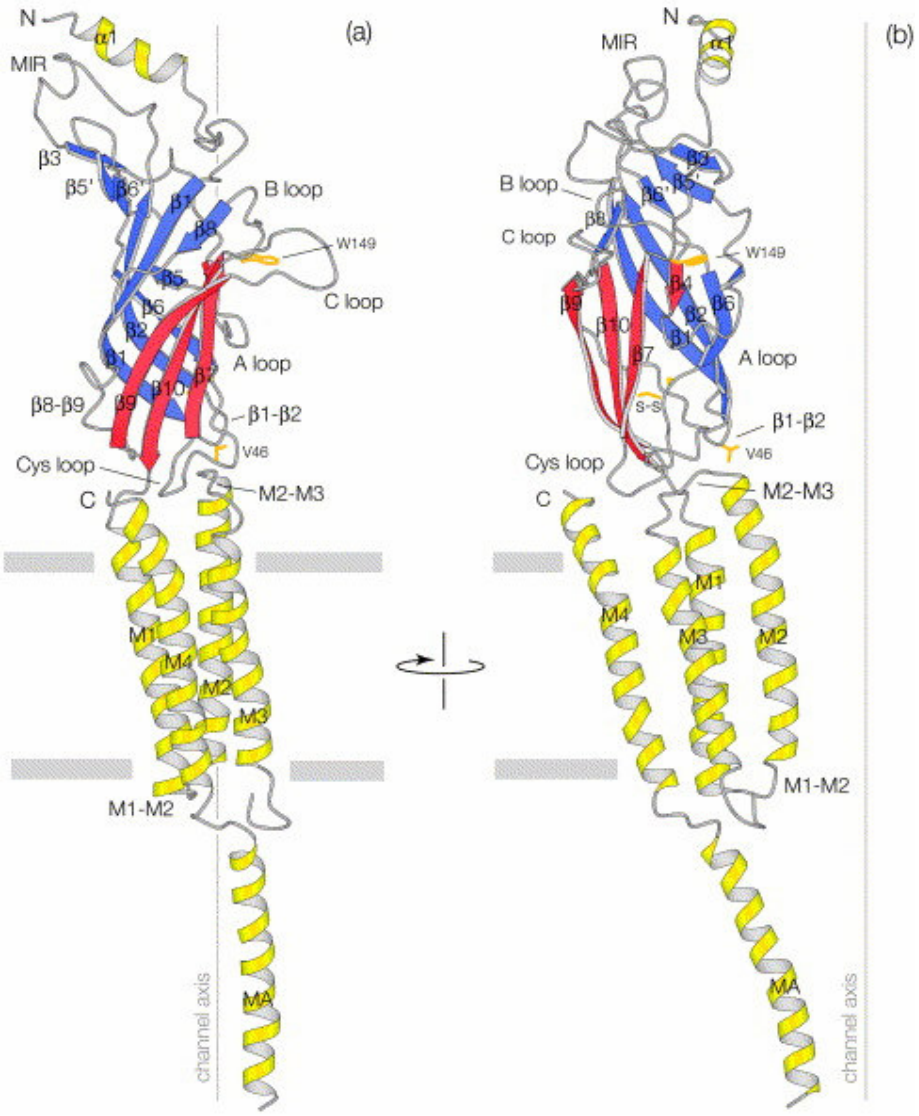

Figure 1-2 Ribbon diagrams of the α-subunit viewed parallel with the membrane plane, in orientations such that the channel axis (vertical line) is at the back (a) and to the side (b). The α-helices are in yellow, the β-strands composing the β sandwich are in blue (inner) and red (counter). [Ref. 6]

The most well characterised nAChRs are those found at the mammalian neuromuscular junction. The muscle nAChR shares many similarities with acetylcholine-binding sites found in the (muscle-derived) electric organ of *Torpedo californica* and this fish has provided for decades an extremely rich source of nAChRs for physiological and biochemical studies.[7] The muscle subtype is composed of two α1 subunits, one of each β1, δ and either γ or ε. During the development of the neuromuscular junctions, the γ subunit (embryonic form) is present, but after the synaptogenesis is complete, the ε subunit (adult form) replaces it.[8]

Neuronal nAChRs are much more diverse than the muscle type because many subunit combinations are possible. The assembly of the subunits in the neuronal nAChR is less tightly constrained than that of the muscle receptor. To date, nine neuronal subunits with the homology of muscle α1 (α2 – α10) and three non-α subunits (β2 – β4) have been identified.[9] In CNS these subunits form either heteromeric or homomeric complexes. The majority of the heteromeric receptor complexes identified are believed to contain a single type of α and a single type β subunit in $(\alpha)_2(\beta)_3$ stochiometry, e.g. $(\alpha4)_2(\beta2)_3$.[10] However, heteromeric receptors involving three types of subunits can be formed as well, e.g. the α3 and α5 subunits have been shown to form "triplet" receptors when co-expressed with other α or β subunits in the *Xenopus* expression system.[11] The properties of these triple receptors were distinct from those containing a single type of α and β subunit. The functional homomeric nAChR pentamers can be composed only of α7 – α10 subunits[12] (e.g. $(\alpha7)_5$, the homomeric subtype widely distributed in mammalian CNS).

A number of different approaches (e.g. photoaffinity labelling experiments[13], modelling of the putative three-dimensional structure of nAChRs[14], investigations with ligand probes and mutation of residues believed to be involved in ACh binding[15]) allowed elucidation of the structure of the ACh-binding site. It has been shown that the binding site in the heteromeric receptors is located on the interface between α and adjacent non-α (γ/ε or β) subunit, i.e. heteromeric receptors possess two binding sites. In the homomeric receptors, the binding site is placed on each interface between two α subunits. Therefore, five binding sites must be present in e.g. $(\alpha7)_5$ subtype. While α subunit contributes the principal component, the neighbouring subunit (γ, δ or ε for the muscle and β or α for the neuronal) builds the complementary component of the binding site.

Brejc et al[16] published the crystal structure of an acetylcholine-binding protein (AChBP), isolated from the fresh water snail, *Lymnaea stagnalis*. The soluble, homopentameric AChBP is 210 residues long and resembles the extracellular binding domain of nAChRs. X-ray diffraction analysis of this protein has provided valuable information about the nature of the binding pocket and confirmed its position on the interface between two subunits. The key

region of the nAChR binding domain is the convergence of three tyrosine and two tryptophan side chains, framing a 'box' of electron-rich aromatic rings. It is established that the cationic moiety of acetylcholine (or other nicotinic ligands) binds in this hydrophobic box with the α-subunit of the nAChR protein via strong π-cation interaction. Thus, the π-cation interactions, previously predicted in the binding of nicotinic agonists[17], are indeed decisive in high affinity binding. The other "bridge" in the binding mode is believed to be a hydrogen bond between a hydrogen bond donor (HBD) in the receptor and hydrogen bond acceptor (HBA) in the ligand.

1.1.2 nAChRs in Human Pathology

Nicotinic acetylcholine receptors have been implicated with a number of disorders affecting the nervous system (e.g. Tourette's syndrome, schizophrenia, epilepsy, depression, anxiety) as well as pathologies in non-neuronal tissues and cells (e.g. small-cell lung carcinoma or inflammatory bowel disease). However, the main focus in the field of these ligand-gated ion channels is on their involvement in neurodegenerative diseases such as Alzheimer's or Parkinson's and in antinociception.

Tourette's syndrome, characterised by uncontrolled obsessive behaviour as well as spontaneous motor and verbal tics, is usually treated with neuroleptics like haloperidol, however with little success. (-)-Nicotine in the form of chewing gum and patches improves the motor and verbal tics symptoms[18] and potentiates the behavioural effects of haloperidol in animals[19], suggesting that nAChR may play a role in the etiology of this neuropsychiatric disorder. The mechanism of the beneficial effect of nicotine remains unclear.

Schizophrenia, a chronically deteriorating psychosis (hallucination, disturbance of thought, self-awareness and perception) has been linked with nAChRs because of the high percentage of smokers among schizophrenics, 90% as compared to 33% in the general population.[20] This high nicotine intake in the schizophrenic population is accepted as a form of self-medication to compensate for a deficit in nicotinic neurotransmission.[21] It was observed that the density of α7 receptors has been reduced in the CA3 region of hippocampus in the brain of schizophrenics.[22] Using genome-wide analysis, a connection between schizophrenia and dinucleotide polymorphism at chromosome 15q13-14, a site of the α7-subunit gene CHRNA7 has been found.[20a]

Epilepsy, in particular Autosomal Dominant Nocturnal Frontal Lobe Epilepsy (ADNFLE, epileptic seizures occurring mainly during the sleep) is associated with mutation in the gene coding for either the α4 or β2 nAChR subunit.[23] These mutations have been reported to be

responsible only for some factors leading to the clinical manifestation of the disease, however not for all the symptoms of ADNFLE.[24] There are experimental indications that also α7 subunits are involved in seizure control.[25]

Depression/anxiety are also believed to be related to nAChR dysfunction. Direct evidence of altered nAChR function in individuals suffering from these disorders is missing, but genetic studies showed a positive correlation between tobacco dependence and major depression.[26] In addition, smoking is more prevalent in patients suffering from depression than in general population.[27]

Alzheimer's disease (AD) is a neurodegenerative disease characterised by a progressive loss of short-term memory and higher cognitive functions. The most marked changes in the neurotransmitter system of patients are the degeneration of the cholinergic innervation[28] and the reduction of the choline acetyl transferase activity[29] in the hippocampus and cerebral cortex. There is accumulating evidence that the function and density of neuronal nAChRs (especially α4β2 subtype) is reduced in the AD brains.[30] In addition, β-amyloid peptides which are part of the neuritic plaques found in AD brains, have been shown to bind to α7 nAChRs and are neurotoxic.[31] Thus, drugs targeted for treatment of AD through modulation of nAChRs should either target α4β2 subtype and cause receptor activation or activate α7 and improve cell survival.

Patients with **Parkinson's disease (PD)** suffer from motor dysfunction resulting in muscular rigidity, tremor and uncoordinated movement. PD is a neurodegenerative disease manifested by progressive degeneration of dopaminergic neurons in the substantia nigra pars compacta accompanied by parallel loss of high affinity nicotine binding in these regions.[32a] Nicotine improves the symptoms of PD patients and the beneficial effects of the tobacco alkaloid are consequences of increased dopamine levels in the substantia nigra[32b] and mesolimbic system[33], as well as of possible inhibition of monoamine oxidase B[34]. Once more, the risk of developing PD is inversely correlated with the number of cigarettes smoked.[35]

Pain and nAChRs are linked since the discovery of antinociceptive properties of the nicotinic agonist epibatidine, which possesses 200-fold higher analgesic effect than morphine in the hot-plate test.[36] The initial euphoria of this discovery disappeared because of the highly toxic effects of epibatidine mediated by peripheral nAChRs.[37] On the other hand, ABT-594, a selective nicotinic agonist for neuronal subtypes has been reported to be in clinical trials for the treatment of neuropathic pain[38], even if the side-effect profile of this compound is not improved compared to epibatidine[39].

Tobacco smoking, despite its positive effect in etiology of diseases such as Alzheimer's or Parkinson's, is the leading cause of preventable death worldwide.[40] Nicotine mediates its action through nAChRs in CNS, especially via dopamine release in the nucleus accumbens

or prefrontal cortex.[41] These brain regions are connected to the ventral tegmental area that is a part of the reward system in the human brain.[42] Nicotine administration in a form of gum, transdermal patch, nasal spray and inhaler or the non-nicotine based antidepressant bupropion is used for the treatment of nicotine addiction.[43] Administration of nicotine by any form is statistically more effective than placebos, but the long-term relapse rates are as high as 80%.[43] Thus, improving the long-term efficacy is a key component of novel pharmacotherapies for smoking cessation.

The existence of multiple nAChR subtypes and their connection to numerous human pathologies understandably requests development of suitably selective nAChRs ligands in order to target one receptor subtype mediating one certain therapeutically beneficial function, while eliminating undesired side effects. Subunit specific ligands would have wide-ranging effects in the laboratory as experimental tools and in the clinic as therapeutic agents. Thus, targeting nAChRs still remains an interesting opportunity to identify new potential drugs and this has led to a vast variety of compounds from different chemical classes.[44]

1.2 Nicotinic Acetylcholine Receptors Ligands

A great deal of synthetic effort has been applied towards the synthesis of potent, selective ligands for the nicotinic acetylcholine receptor[45] and the non-peptidic nAChRs ligands have been divided by Schmitt[46] into five classes. This classification is based on the structure, taking into account principal features of the endogenous ligand acetylcholine **1**, which are the cationic centre and HBA/π moiety (Figure 1-3). The binding affinity of the simplest nAChR agonist - tetramethylammonium ion (K_i = 480 nM, radioligand: [^{3}H]nicotine, tissue: rat brain; K_i = 2.3 μM, radioligand: [^{3}H]α-Bgt, tissue: rat brain)[47] reveals the importance of the ammonium head for recognition of nAChRs.

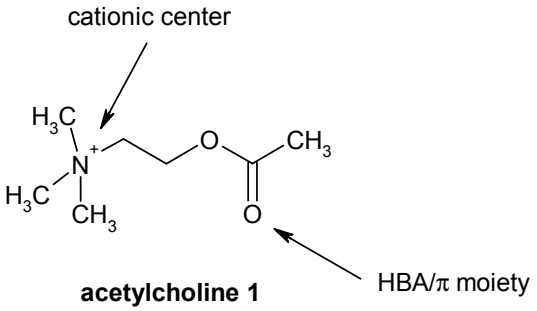

Figure 1-3 Structure of the nAChR endogenous ligand acetylcholine **1**. The pharmacophoric elements – cationic centre and HBA/π moiety – are pointed out.

1.2.1 Class A: Acyclic HBA/π and Acyclic Cation

Nicotinic ligands with acyclic HBA/π and cationic moieties belong to the *Class A* of Schmitt's classification.[46] These compounds are in general the most flexible nAChR ligands due to the missing ring constrain.

The prototype is acetylcholine **1**, which binds with high affinity to $\alpha4\beta2$ receptor subtype (K_i = 3-10 nM) but with lower affinity to [^{125}I]α-Bgt binding sites (K_i = 4,000 nM)[48]. However, ACh **1** lacks selectivity between nAChRs and mAChRs and the quaternised amino group of ACh **1** is associated with poor penetration through the blood-brain barrier. Carbacholine, an ACh analogue, in which the ester moiety of ACh is replaced by a carbamate group, is a mixed muscarinic-nicotinic acetylcholine receptor agonist (K_i = 750 nM for $\alpha4\beta2$ rat brain nicotinic binding site, K_i = 5 nM for [^{3}H]oxotremorine binding site)[49], but N-methylcarbamoylcholine **2** (MCC) displays nanomolar binding affinity to nAChRs (K_i = 23 nM)[49] with certain selectivity for neuronal receptors versus the muscarinic AChRs (K_i = 150 nM)[49] (Figure 1-4). MCC **2** was extensively studied at the beginning of the "nAChRs era" [50] and the tritium labelled MCC **2** was used as a radioligand for investigating the nicotinic recognition sites in brain tissue.[51] Introduction of another methyl group at the carbamate nitrogen of MCC **2** yields N,N-dimethyl-carbamoylcholine DMCC, which shows higher selectivity for nAChR (K_i = 20 nM, rat brain $\alpha4\beta2$ binding)[49] versus mAChR (K_i = 1,200 nM)[49] compared to MCC **2**.

Choline **3** (Figure 1-4), a precursor and a metabolite of acetylcholine **1**, is an effective agonist of $\alpha7$ nAChRs even if it presents very low affinity for this receptor subtype (K_i = 2,380 μM).[52] Choline **3** possesses higher affinity towards $\alpha4\beta2$ nACh receptor (K_i = 112 μM) and has been shown to protect neural cells from cytotoxicity induced by growth factor deprivation.[53]

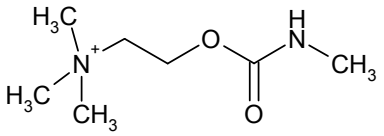

N-methylcarbamoylcholine **2** (MCC)
K_i = 23 nM ($\alpha4\beta2$, rat brain)
K_i = 44 nM ($\alpha7$, rat brain)

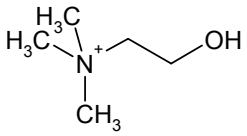

choline **3**
K_i = 112 µM ($\alpha4\beta2$, rat brain)
K_i = 2,380 µM ($\alpha7$, rat brain)

Figure 1-4 Chemical structure and affinities of MCC **2** and choline **3** [Ref. 49, 52]

1.2.2 Class B: Cyclic HBA/π and Acyclic Cation

Ligands in the *Class B* hold a cyclic HBA/π system and an open-chain cationic moiety.[46]

The first series of ligands in this group are choline derivatives. Radioligand binding studies of phenylether of choline **4,** a potent ganglion stimulant[54], revealed a high affinity of **4** for the central nAChRs, i.e. K_i = 22.3 nM for α4β2* and K_i = 196 nM for α7* binding (Figure 1-5).[55] Introduction of an amide moiety to the structure of phenylether of choline **4** yields a carbamate **5** that shows higher affinity for the α7* (K_i = 38.9 nM) than for the α4β2 nAChR subtype (K_i = 835 nM) (Figure1-5).[55]

Dukat *et al* studied a series of pyrrolidine ring-opened analogues of nicotine possessing a (3-pyridyl)-C-N^+ motif.[56] Although none of these analogues exhibited higher binding affinity than (-)-nicotine (K_i = 2.3 nM)[56], *3-(N-methyl-N-ethylaminomethyl)pyridine* **6** (Figure 1-5) binds with significant affinity (K_i = 28 nM). Substitution of the 6-position of **6** with methyl or halogen was well tolerated (K_i = 41 nM for 6-chloro; K_i = 93 nM for 6-fluoro and K_i = 66 nM for 6-methyl analogues), but methyl substitution in the position 2 or 4 caused a loss of the binding affinity (K_i = 4,614 and 1,745 nM, respectively).[56]

trans-Metanicotine **7** (also known as RJR-2403, *[E]-N-methyl-4-[3-pyridinyl]-3-butene-1-amine monofumarate*) is another ring-opened isomer of nicotine (Figure 1-5). RJR-2403 **7** binds with similar high affinity to both [^{3}H]nicotine binding nAChR subtypes expressed in rat brain and α4β2 expressed in transfected clonal cell line M10 (K_i = 26 nM). Despite its 6-fold lower affinity than the affinity of nicotine for the α4β2 nAChR, *trans*-metanicotine **7** is only slightly less potent and nearly as efficacious toward activation of the receptor.[57] Several modifications of *trans*-metanicotine **7** (e.g. methylation of the terminal amino group) resulted in lower binding affinity (K_i = 4,500 nM for N-methyl analogue of **7**) compared to the parent structure[58]. On the other hand, some structural modification led to an improved pharmacological profile and Targacept has recently identified a pyridine-substituted and α-branched analogue of *trans*-metanicotine TC-1734 **8** (*(S)-(E)-N-methyl-5-[3-(5-isopropoxypyridinyl)]-4-penten-2-amine*), an orally active novel neuronal nicotinic agonist with high selectivity for α4β2 nicotinic receptors (Figure 1-5).[59] TC-1734 binds with high affinity (K_i = 11 nM) to α4β2 nAChR labelled with [^{3}H]nicotine in membranes from rat cerebral cortex, but was not able to displace [^{125}I]α-Bgt binding (α7 nAChRs) in rat hippocampal membranes. Furthermore, phase I clinical trials demonstrated TC-1734's favourable pharmacokinetic and safety profile by acute oral administration.[59]

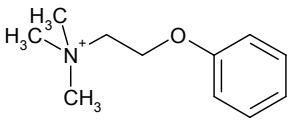

phenylether of choline **4**
K_i = 22.3 nM ($\alpha4\beta2$, rat brain)
K_i = 196 nM ($\alpha7$, rat brain)

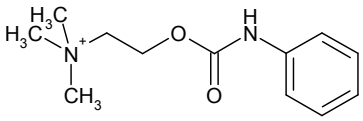

5
K_i = 835 nM ($\alpha4\beta2$, rat brain)
K_i = 38.9 nM ($\alpha7$, rat brain)

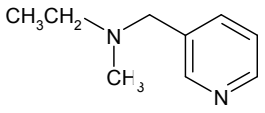

6
K_i = 28 nM ($\alpha4\beta2$, rat brain)

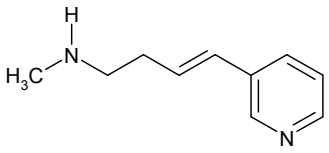

RJR-2403 **7**
K_i = 26 nM ($\alpha4\beta2$, rat brain & M10 cell line)

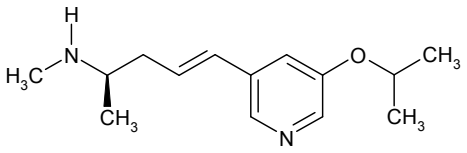

TC-1734 **8**
K_i = 11 nM ($\alpha4\beta2$, rat brain)
K_i > 50,000 nM ($\alpha7$, rat brain)

Figure 1-5 *Class B* ligands: structure and binding affinities for central nAChRs [Ref. 54 - 57, 59]

1.2.3 Class C: Cyclic HBA/π and Cyclic Cation

The *Class C* of nAChR ligands involves structures in which both the cationic centre and HBA/π moiety are cyclic.[46] *Class C* consists of ligands such as DMPP, nicotine, epibatidine and their analogues as well as highly potent group of 3-pyridylether derivatives.

The structure of N,N-dimethylphenylpiperazine **9** (DMPP, *N^1-dimethyl-N^4-phenylpiperazinium iodide*) (Figure 1-6) represents an unique pharmacophore for nAChRs binding due to its short internitrogen distance (see *1.3 nAChR Pharmacophore Models*). DMPP **9** binds with high affinity to the $\alpha4\beta2$ (K_i = 31 – 57 nM)[60] and $\alpha7$ (K_i = 7.6 μM)[61] receptors. On the contrary, the research group of Varani reported for DMPP **8** a K_i value of 250 nM (assays were completed with rat brain tissue labelled by [^{3}H]cytisine).[62] The same research group focused on the modification of the structure of DMPP **9** in order to improve its properties, since it is unlikely that quaternary compounds will cross the blood-brain barrier and distribute effectively into the CNS.[62] The variation of the lead **9** afforded several nonquaternary agents with improved affinity for central $\alpha4\beta2$ receptor subtype (e.g. for 1-methyl-4-pyridin-3-yl piperazine with K_i = 90 nM).

(-)-Nicotine **10** (*(S)-3-(1-methyl-2-pyrrolidinyl)-pyridine*) (Figure 1-6), the prototypical nAChR ligand, possesses a structure that appears to be well optimised for activity at the $\alpha4\beta2$ nAChR, since the simplest modifications lead to less potent analogues. The N-methyl pyrrolidine moiety and (S)-stereochemistry are critical features that contribute to the high $\alpha4\beta2$ affinity (K_i = 1 – 5 nM).[63]

The pyrrolidine ring expansion of nornicotine leads to anabasine **11** (Figure 1-6), an alkaloid also present in tobacco. In an assay published by Kem *et al*[64], anabasine **11** together with its dehydro analogue anabaseine **12** (an alkaloid isolated from a marine worm) (Figure 1-6) have substantially weaker affinity (K_i = 260 and 32 nM, respectively) than nicotine **10** (K_i = 4.1 nM) at $\alpha4\beta2$ receptors but actually exhibit somewhat improved potency at the $\alpha7$ subtype (K_i = 58 nM for anabasine **11** and anabaseine **12**) compared to nicotine **10** (K_i = 400 nM).[64] Anabaseine **12** has been used as a template for construction of $\alpha7$-selective compounds as it is substantially more efficacious than either (-)-nicotine **10** or acetylcholine **1** at rat $\alpha7$ receptors expressed in oocytes.[65] The 3-(2,4-dimethoxybenzylidine)-anabaseine derivative GTS-21 **13** has emerged as an important compound for characterisation of the $\alpha7$ function *in vivo*, even despite its weak potency (K_i = 650 nM) and low maximal efficacy (50% of ACh response).[66]

While substitution on the pyrrolidine ring causes loss of the binding affinity, the substitution on the pyridine ring of (-)-nicotine **10** is better tolerated, occasionally affording compounds with higher affinity. For example, the 5-ethynyl analogue of nicotine SIB-1508Y **14** (*(S)-(-)-5-ethynyl-3-(1-methyl-2-pyrrolidinyl)-pyridine*) (Figure 1-6), displaces [^{3}H]nicotine from rat cortical membranes with affinity equivalent to that of nicotine **10** (IC_{50} = 3 and 4 nM, respectively).[67] Since SIB-1508Y **14** is particularly efficacious in stimulating the release of dopamine, it was evaluated in an animal model of Parkinson's disease and selected for preclinical and clinical trials.[68]

With regard to the substitution of the position 6 in (-)-nicotine **10**, it was shown that the lipophilicity and bulkiness of the substituents influence the ligand's binding affinity for $\alpha4\beta2$ nAChR.[69] While 6-phenyl-nicotine exhibits very low binding affinity (K_i = 9,440 nM)[69], 6-(2-phenylethyl)-nicotine was found to bind at $\alpha4\beta2$ nicotinic receptor with high affinity (K_i = 15 nM) and antagonise the antinociceptive effects of (-)-nicotine **10** in mouse tail-flick assays in a dose-dependent fashion when administered via an intrathecal route.[70]

A series of nicotine analogues, in which the pyridine ring is replaced by isoxazole, isothiazole or pyrazole moieties, has been synthesized and claimed by Abbott Laboratories. Replacement of pyridine ring by 3-methyl-5-isoxazole moiety led to a structure known as ABT-418 **15** (Figure 1-6; K_i = 4.2 nM for [^{3}H]cytisine binding sites)[71], which has been shown to possess cognitive-enhancing and anxiolytic like activities in animal models with an improved safety profile compared to that of nicotine.[72] Unfortunately, ABT-418 **15** did not succeed in the clinical trials.[73]

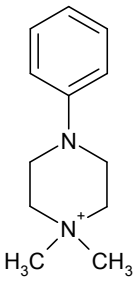

DMPP **9**
K_i = 57 nM (α4β2, rat brain)
K_i = 7,600 nM (α7, rat brain)

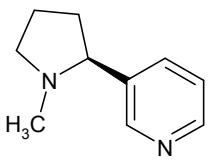

(*S*)-nicotine **10**
K_i = 1-5 nM (α4β2)
K_i = 400 nM (α7)

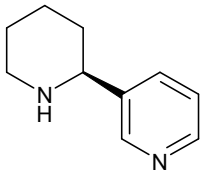

anabasine **11**
K_i = 260 nM (α4β2, rat brain)
K_i = 58 nM (α7, rat brain)

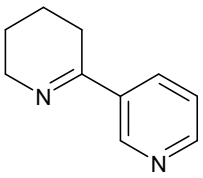

anabaseine **12**
K_i = 32 nM (α4β2, rat brain)
K_i = 58 nM (α7, rat brain)

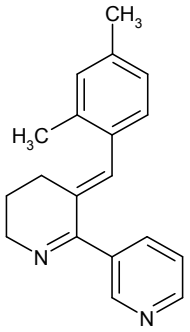

GTS-21 **13**
K_i = 19 nM (α4β2, rat brain)
K_i = 650 nM (α7, rat brain)

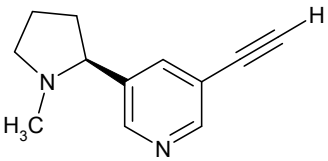

SIB-1508Y **14**
K_i = 3 nM (α4β2, rat brain)

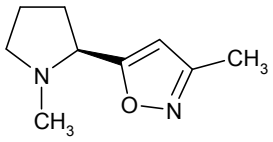

ABT-418 **15**
K_i = 4.2 nM (α4β2, rat brain)
K_i > 20,000 nM (α7, rat brain)

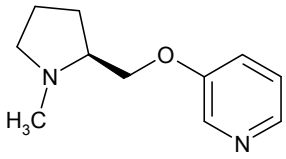

A-84543 **16**
K_i = 0.15 nM (α4β2, rat brain)
K_i = 1530 nM (α7, K28 cells)

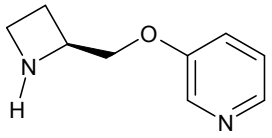

A-85380 **17**
K_i = 0.05 nM (α4β2, rat brain)
K_i = 100 nM (α7, rat brain)

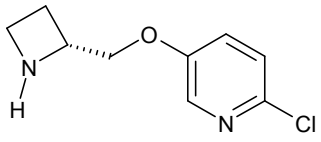

ABT-594 **18**
K_i = 0.037 nM (α4β2, rat brain)
0.177 nM (hα4β2, K177 cells)
K_i = 13,800 nM (α7, rat brain)
2,060 nM (hα7, K28 cells)

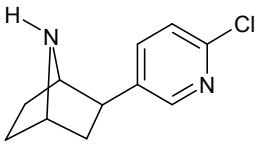

epibatidine **19**
(+)-epi K_i = 0.026 nM (α4β2, rat brain)
(-)-epi K_i = 0.018 nM (α4β2, rat brain)
K_i = 198 nM (α7, rat brain)

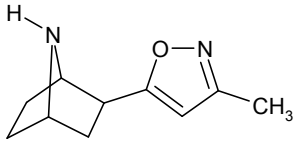

epiboxidine **20**
K_i = 0.6 nM (α4β2, rat brain)

Figure 1-6 nAChR ligands of the *Class C* (cyclic cation centre, cyclic HBA/π system) [Ref. 60, 61, 63, 64 - 67, 71, 74, 76, 78]

Incorporation of an ether link between the pyrrolidine and pyridine rings of nicotine results in a potent ligand A-84543 **16** (*3-((1-methyl-2-(S)-pyrrolidinyl)-methoxy)-pyridine*) (Figure 1-6), which binds to rodent $\alpha4\beta2$ nAChRs with 7-fold higher affinity than nicotine (K_i = 0.15 nM).[74] The exploration of the 3-pyridyl ether motif combined with pyrrolidine ring contraction to azetidine led to the discovery of A-85380 **17** (*3-(2-(S)-azetidinylmethoxy)-pyridine*) (Figure 1-6), an exceptionally potent and selective ligand for the human $\alpha4\beta2$ (K_i = 0.05 nM) over $\alpha7$ (K_i = 148 nM) and neuromuscular (K_i = 314 nM) nAChR subtypes.[75] In functional studies, A-85380 **17** was shown to be significantly more potent than (-)-nicotine **10** to activate ion flux through a number of nAChRs, to activate human $\alpha7$ nAChR channel currents and to facilitate the dopamine release.[75] The 6-halogen substitution improves *in vivo* activity and ABT-594 **18** (*5-(2-(R)-azetidinylmethoxy)-2-chloropyridine*) (Figure 1-6) possessing chlorine in the position 6 was identified as a potent nicotinic agonist with broad spectrum analgesic activity.[76] ABT-594 **18** is a potent inhibitor of [^{3}H]cytisine binding to $\alpha4\beta2$ nAChRs (K_i = 37 pM, rat brain; K_i = 55 pM, transfected human receptor) that displaces [^{125}I]α-bungarotoxin from the $(\alpha1)_2\beta1\delta\gamma$ neuromuscular nAChR with low affinity (K_i = 10,000 nM). Functionally, ABT-594 **18** is an agonist and pharmacologically, it has an *in vitro* profile distinct from that of the prototypic nicotinic analgesic epibatidine.[77] With the reduced side-effects (as a consequence of the very low binding to the muscle type nAChR), this compound represents a novel alternative for pain management.

Last, but by no means least, representative of *Class C* is epibatidine **19** (*exo-2-(6-chloro-3-pyridyl)-7-azabicyclo-[2.2.1]heptane*) (Figure 1-6), among the naturally occurring alkaloids the most potent nAChR ligand. Both enantiomers of epibatidine, (+)-**19** (the 1*S*,2*S*,4*R*-stereoisomer) and (-)-**19** (the 1*R*,2*R*,4*S*-stereoisomer) possess nearly equal affinity for the $\alpha4\beta2$ nAChR subtype (K_i = 26 and 18 pM, respectively).[78] Epibatidine **19** had proved to be 200-fold more potent than morphine as an analgetic[79], but also exhibited high potency and efficacy for activation of peripheral nAChRs which is the reason of its high toxicity. Numerous series of epibatidine derivatives have been synthesized so far, including changes in stereochemistry[80], alkylation of the NH group[81], changes in the 2'-chloropyridine ring[82], replacement of the 2'-chloropyridine ring with bioisosteric rings (e.g. by 3'-methylisoxazolyl ring resulting in compound named epiboxidine **20** (Figure 1-6)[83] or by substituted pyrimidine rings[84]), changes in the 7-azabicyclo[2.2.1]heptane ring system[85] or synthesis of conformationally-constrained analogues[86]. Many of the analogues retain the picomolar affinity, but the small therapeutic window has not been greatly improved.

1.2.4 Class D: Acyclic HBA/π and Cyclic Cation

Members of *Class D* contain an acyclic HBA/π moiety and a cationic site that is cyclic.[46]

(+)-Anatoxin-a **21** (the 1*R*,6*S*-stereoisomer) (Figure 1-7), an alkaloidal toxin produced by the freshwater cyanobacterium *Anabaena flos-aquae*, is a potent and stereoselective agonist at nAChRs in the periphery as well as in CNS.[87] The naturally occurring (+)-anatoxin-a **21** binds with high affinity to α4β2 (K_i = 3.5 nM) receptors and with 100-fold lower affinity to α7 (K_i = 380 nM) receptors.[88] Gündisch et al. reported even higher binding affinity of **21** for both α4β2 (K_i = 1.1 nM) and α7 (K_i = 90 nM) nicotinic receptor subtypes.[89] (+)-Anatoxin-a **21** is a potent agonist stimulating the $^{86}Rb^+$ influx into M10 cells, which express the nicotinic receptor subtype comprising α4 and β2 subunits, with EC_{50} value of 48 nM.[90] The semi-rigid structure of the azabicyclononene ring of (+)-anatoxin-a **21**, its stereoselectivity and functional group chemistry make the alkaloid an interesting template for SAR studies. However, no modification reported in the literature results in an increased affinity at either receptor subtype.[88,91]

Ferruginines are a group of 8-azabicyclo[3.2.1]oct-2-enes closely related to (+)-anatoxin-a **21**. In the natural (+)-ferruginine **22** (the 1R,5S-stereoisomer; potent neurotoxin from the arboreal species *Darlingia ferruginea* and *darlingiana*) as well as in the unnatural (-)-enantiomer **22** (Figure 1-7) the acetyl moiety is a pharmacophoric element. Although (-)-ferruginine **22** and its demethylated analogue (-)-norferuginine display lower affinity for α4β2 (K_i = 120 and 94 nM, respectively) and α7 protein (K_i = 330 and 110,000 nM, respectively) than (+)-anatoxin-a **21**, they served as templates for design of novel ferruginine-type nAChR ligands.[89,92] Replacement of the acetyl group in (-)-norferruginine **22** with 1,3-diazine (the structure then belongs to the *Class C* of Schmitt's classification[46]) resulted in 30-fold improvement in the affinity for the α4β2 subtype (K_i = 3.7 nM) combined with significant selectivity ratio between the α4β2 and α7 subtypes ($K_{i\,(\alpha4\beta2)}$ / $K_{i\,(\alpha7)}$ = 1,351).[89]

(-)-Lobeline **23** (the 2R,6S,10S-stereoisomer) (*2-[6-((S)-2-hydroxy-2-phenylethyl)-1-methyl-piperidin-2-yl]-1-phenylethanone*) (Figure 1-7), a major alkaloidal constituent of Indian tobacco (*Lobelia inflata*), is a unique nicotinic alkaloid bearing a 2,5-disustitued piperidine. (-)-Lobeline **23** binds to the α4β2 nAChR subtype with a similarly high affinity like (-)-nicotine **10** (K_i = 4 nM)[96b] and produces some, but not all pharmacological effects of (-)-nicotine **10** (e.g. nausea, tachycardia, anxiolytic activity).[93] Interestingly, the behavioural effects of (-)-lobeline **23** cannot be blocked by pre-treatment with nAChR antagonist mecamylamine, suggesting that the Indian tobacco alkaloid **23** might be binding to different,

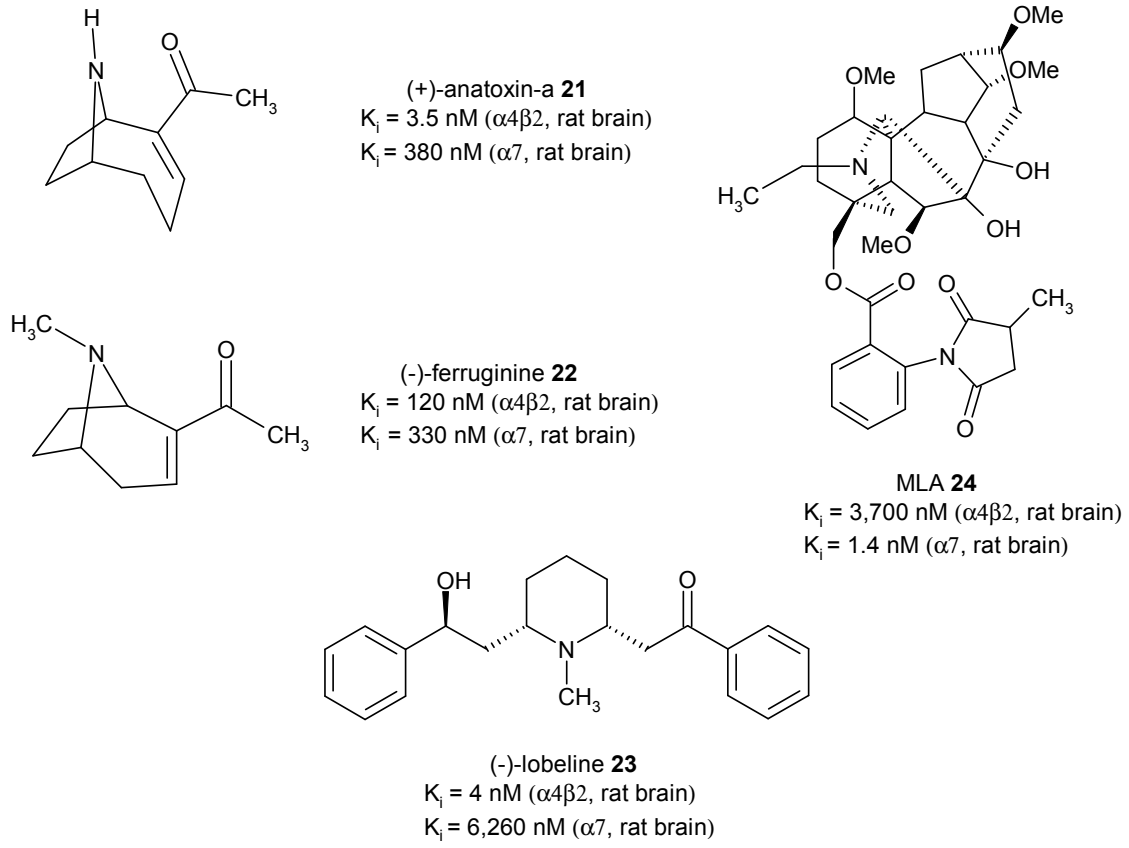

Figure 1-7 Naturally occurring alkaloids as members of the *Class D* [Ref. 88, 89, 96b, 99]

mecamylamine-insensitive subpopulations of nicotinic receptors than (-)-nicotine **10**.[94] Furthermore, lobeline-evoked overflow from [^{3}H]dopamine-preloaded striatal slices and synaptosomes is also mecamylamine-insensitive, indicating that this response is not mediated by nicotinic receptors.[95] The same authors declare, that (-)-lobeline **23** is a nAChR antagonist, as it inhibits the effects of (-)-nicotine **10** in several *in vitro* experiments. Structurally, (-)-lobeline **23** and (-)-nicotine **10** share very little similarities and (-)-lobeline **23** does not fit the classical nicotinic pharmacophore. However, SAR studies confirmed that the piperidine-ring nitrogen represents the onium feature and the carbonyl group rather than hydroxyl group represents the HBA/π feature.[96] All lobeline analogues that have been reported[96b,97] bind with lower affinity than the parent alkaloid. Only recently, (-)-lobeline **23** and especially lobelane (defunctionalised saturated lobeline analogue) were identified as weak vesicular monoamine transporter-2 (VMAT-2) ligands (K_i = 2.76 and 0.97 μM, respectively). A series of lobelane derivatives was evaluated for their affinity and selectivity for VMAT-2, through which psychostimulant drugs (e.g. amphetamine and metamphetamine) promote dopamine release responsible for the rewarding effects of the abused drugs. The most potent analogues display nanomolar affinities (K_i = 430 – 580 nM).[98]

Another plant-derived alkaloid of the *Class D* is methyllycaconitine **24** (MLA) (Figure 1-7), a competitive antagonist of nAChRs, with a significant preference for neuronal [^{125}I]-bungarotoxin binding sites (K_i = 1.4 nM).[99] This norditerpenoid alkaloid is present in *Delphinium brownii* seeds and possesses insecticidal properties.[100] Hydrolysis of the ester bond in MLA **24** to produce lycoctonine diminishes affinity for rat brain [^{125}I]Bgt binding sites 2500-fold, indicating that the ester linked 2-(methylsuccinimido)benzoyl group is necessary for the α7 subtype recognition, although the selectivity for α7-type nAChR resides in the norditerpenoid core.[101] High affinity, rapid binding kinetics and selectivity for α7 nAChR make [^{3}H]MLA **24** a suitable radioligand for pharmacological studies of α-Bgt sensitive nicotinic acetylcholine receptors.[102]

1.2.5 Class E: HBA/π and Cation in Fused Ring System

The nAChR ligands of the final *Class E* have both their HBA/π and cationic moieties fused in the same polycyclic or spiro system.[46]

Dihydro-β-erythroidine **25** (Figure 1-8) is a nAChR ligand that has HBA/π and cationic moieties locked in a nearly coplanar configuration. Dihydro-β-erythroidine **25**, an alkaloid present in the seeds of genus Erythrina, is a nicotinic receptor antagonist that binds to α4β2 protein with high affinity (K_i = 35 nM).[103]

Astra researchers synthesized and evaluated a quinuclidine-based nAChR ligand, designated as AR-R17779 **26** (*(-)-spiro[1-azabicyclo[2.2.2]octane-3,5'-oxazolidin-2'-one]*) (Figure 1-8).[104] This compound is a potent full agonist (efficacy = 96%) at the rat α7 nicotinic

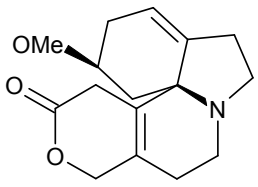

DHβE **25**
K_i = 35 nM (α4β2)

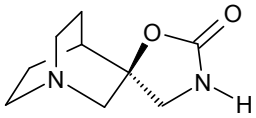

AR-R17779 **26**
K_i = 16,000 nM (α4β2, rat brain)
K_i = 92 nM (α7, rat brain)

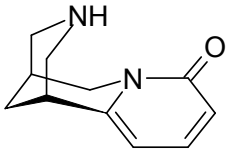

cytisine **27**
K_i = 0.122 nM (α4β2, rat brain)
K_i = 261 nM (α7, rat brain)

Figure 1-8 Nicotinic ligands of the *Class E* (HBA/π and cationic moieties fused in the same polycyclic or spiro system). [Ref. 103, 104, 118]

receptor subtype and exhibits remarkable selectivity for $\alpha7$ (K_i = 92 nM) receptor over $\alpha4\beta2$ (K_i = 16,000 nM). AR-R17779 **26** has been reported to enhance learning and memory function in rats[105], but it failed to improve the performance in rat's model of attention.[106] SAR of this restricted analogue of acetylcholine displayed that there is little space for change in its rigid molecule. The interaction of AR-R17779 **26** is stereosensitive and the (-)-enantiomer binds to the [^{125}I]α-Bgt nicotinic sites more tightly than the (+)-antipode (K_i = 9,400 nM). Changing the carbamate bond to a carbonate, ester or amide led to dramatic loss in $\alpha7$ receptor affinity.

(-)-Cytisine **27** also belongs to this class. This alkaloid is described in detail in Chapter 3.

1.3 nAChR Pharmacophore Models

Consideration of the structures of acetylcholine **1** and (-)-nicotine **10** reveals two fundamental nAChR pharmacophore elements – a quaternised or protonated/protonable nitrogen (N^+) and a hydrogen bond acceptor (HBA) (the carbonyl oxygen of ACh **1** and the pyridine's nitrogen in (-)-nicotine **10**). These basic elements were involved in the first useful pharmacophore model developed by Beers and Reich.[107] Sheridan et al. refined this model using a distance geometry approach and formulated a three-point pharmacophore.[108] They defined a third element, so-called dummy point (C), responsible for the spatial orientation of the HBA functionality. The distances of the triangle were proposed as follows: N^+---HBA 4.8 Å, HBA---dummy point (C) 1.2 Å and N^+---dummy point (C) 4.0 Å (Figure 1-9).

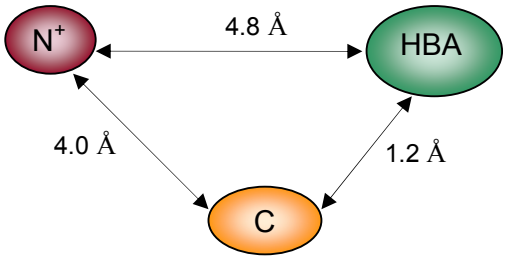

Figure 1-9 Pharmacophore model proposed by Sheridan et al. [Ref. 108]

Holladay et al.[109] developed a "four-point" model, in which numbers (1) and (2) mark the nitrogen functionalities (onium head and HBA) and numbers (3) and (4) represent locations on the nAChR protein with which they interact (Figure 1-10). The optimal internitrogen distance was proposed to be 4.85 Å.

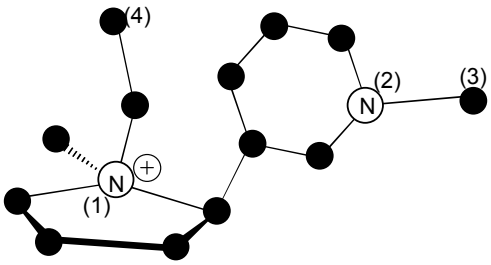

Figure 1-10 Pharmacophore model proposed by Holladay et al. [Ref. 109]

In the new vector model developed by Tønder et al.,[110] the authors suggested that the distance between the points *a* and *b* (i.e. points at the receptor where ligand's pharmacophores bind) define the binding better than the direct N---N distance. *Point a* is a site selected to be 2.9 Å in length from the onium group and *b* is a site selected to be 2.9 Å from a hydrogen bond acceptor. The *a---b* distance of approximately 7.3 – 8.0 Å was suggested to be optimal for high affinity. The same authors improved the vector model in an attempt to define three-point pharmacophore and included the dummy-point (C) (Figure 1-11).[111,112]

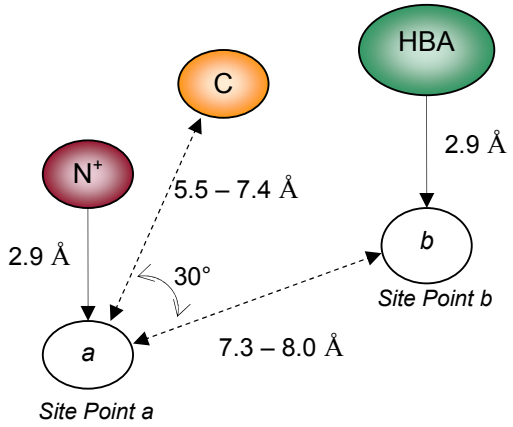

Figure 1-11 The improved vector model proposed by Tønder et al. [Ref. 111-112]

However, none of the proposed pharmacophore models seems to be "perfectly ideal" as they all fail to explain some of the available data. For example, the internitrogen distance of 4.8 Å proposed by Sheridan et al. as optimal for high binding affinity is not applicable to all nAChR ligands. In the Table 1-1 are listed several nAChR ligands that fit into the "distance model", but also several compounds in which the suggested internitrogen distance cannot be achieved. The N---N distance in epibatidine **19**, the most potent α4β2 ligand, was first reported to be 5.5 Å.[113] Later, with the discovery of azetidinylmethoxypyridine A-85380 **17**, it was shown that other low-energy conformers of epibatidine **19** were possible and these conformers possessed calculated internitrogen distance between 4.6 Å and 5.6 Å, but A-85380 **17** which is almost equipotent to epibatidine **19**, was reported to have an internitrogen distance of 6.1 Å (Table 1-1).[74a] Koren *et al* showed afterward that A-85380 **17** is a rather flexible molecule and has stable conformation with a internitrogen distance of 4.39 Å.[114] Thus, the Sheridan distance model[108] can be applied to the picomolar binding of epibatidine **19** and A-85380 **17**, however there are compounds which cannot achieve the short internitrogen distance and still display good affinity for nAChR, e.g. **30** and **31** (Table 1-1).[62b,115]

Table 1-1 Internitrogen distances and α4β2 binding affinities of representative nAChR ligands or ligands that do not fit into the Sheridan "distance model". The ligands are listed with regard to the increasing N---N distance.

Ligand	N --- N distance [Å]	K_i @ α4β2 [nM]	Reference
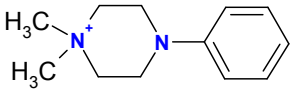 DMPP **9**	2.5 – 2.9	57	[62b]
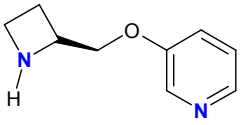 A – 85380 **17***	3.39	0.017	[114]
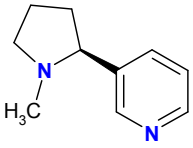 nicotine **10**	4.8	1-10	[108]
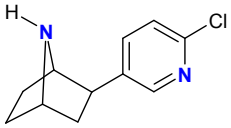 epibatidine **19**	4.6 – 5.6 5.5	0.043 0.050	[74a] [113]
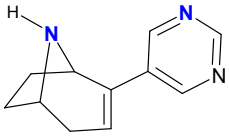 **28**	5.67 – 5.69	3.7	[89]
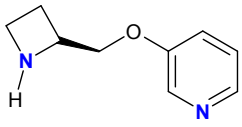 A – 85380 **17***	6.1	0.052	[74a]
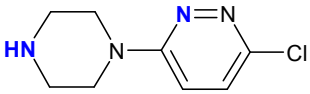 **29**	6.26	32	[116]
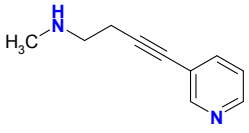 **30**	> 8	58	[115]
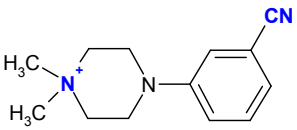 **31**	8.37	300	[62b]

*) A-85380 is positioned twice, as two different distance values are reported in literature

Compound **29** (Table 1-1) also gives support to the hypothesis that a longer internitrogen distance (~ 6.0 Å) than in the Sheridan model is still compatible with an affinity for the α4β2 receptor in the nanomolar range.[116] However, Gündisch *et al*[89] suggested that the internitrogen distance crucial for high affinity binding to nAChR should be closer to that found for the lowest-energy conformation of epibatidine (5.5 Å)[113], as they measured for high affinity compound **28** (K_i = 3.7 nM) an internitrogen distance of 5.67 – 5.69 Å (Table 1-1). In summary, the internitrogen distance *itself* cannot be used for prediction and/or rationalisation of binding affinity and activity of diverse sets of nicotinic agents.

The vector models fail e.g. to explain the very different affinity of aminoethoxypyridine (AXP) analogues, which were accounted by the vector model.[117] While N,N-dimethyl AXP **32** shows nanomolar α4β2 affinity (K_i = 21 nM), replacement of the ether oxygen by a methylene group affords compound **33** that lacks affinity (K_i > 10, 000 nM) (Figure 1-12).

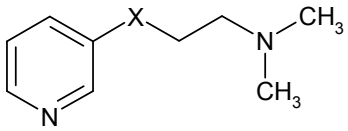

32 X = O K_i = 21 nM
33 X = CH_2 K_i > 10,000 nM

Figure 1-12 Examples of AXP-analogues which do not fit the vector pharmacophore model [Ref.117]

Recently, the "water-extension" concept has arisen among the nAChR community.[115] The idea is that a molecule of water might hydrogen bond to the 'short' ligands and converts them to 'long' ligands, meaning that the ligand's HBA or onium head hydrogen bonds to water, which in turn, hydrogen bonds with the receptor (Figure 1-13). Some unexpected results obtained in the laboratories have been rationalised with this concept, but it still requires further investigation.

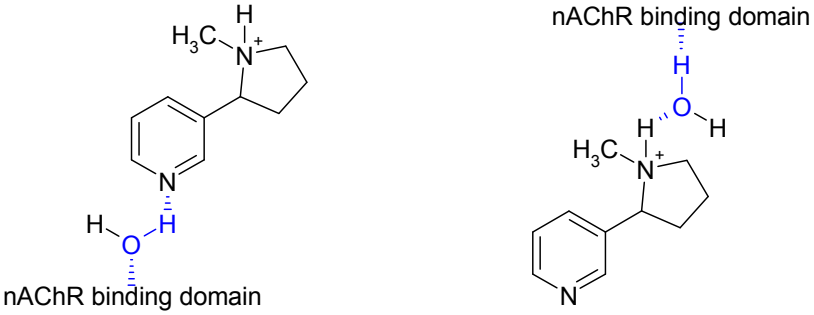

Figure 1-13 "Water-extension" concept applied to nicotine **10** [Ref. 115]

2 Objectives

The neuronal nAChRs have been associated with a great variety of pathological conditions, which results in a therapeutic potential of nAChR ligands. The nAChR pharmacopoeia is increasing and several agonists have entered clinical trials for the treatment of Alzheimer's (ABT-418, GTS-21, RJR-2403) or Parkinson's disease (SIB-1508Y). Unfortunately, the therapeutic use of compounds interacting with central nAChRs (i.e. $\alpha4\beta2$ and $\alpha7$ subtypes) is often associated with unwanted side effects. The side effects result from the interaction of the compound with the nAChRs in the peripheral nervous system (e.g. $\alpha3\beta4$ and $(\alpha1)_2\beta1\gamma\delta$ subtype). Thus, the medicinal chemistry research of nAChR ligands has to focus not only on development of ligands with high affinity, but also on development of agents that exhibit sufficient selectivity for central nAChRs over the muscle and ganglionic receptors.

The main goal of the presented thesis was to develop novel nAChR ligands based on (-)-cytisine **27** (Project I, main project) and choline **3** (Project II). Analogue design and biological evaluation of the novel compounds should help to understand which structure elements contribute to the compound's affinity and selectivity profile.

Project I

(-)-Cytisine **27**, a toxic alkaloid found in many plants of the Fabaceae family, displays picomolar affinity for $\alpha4\beta2$ nAChR (K_i = 0.122 nM)[118] and is a partial agonist with weak efficacy at this nAChR subtype.[119] The partial agonistic activity of (-)-cytisine **27** provides desired pharmacological effect for the treatment of smoking cessation. In this regard, the pure alkaloid (TABEX®)[120] is used in Bulgaria and varenicline (Pfizer), an azatricyclic compound imitating the structure of (-)-cytisine **27** is in Phase III clinical trials for the treatment of tobacco dependence.[121]

Structure-activity studies have concentrated on substitution of the secondary amine and halogenation of the pyridone ring.[118,122,123] While modification of the secondary amine decreased the affinity to a lesser or greater degree[123], the halogenation of the pyridone ring provided a series of analogues with generally high $\alpha4\beta2$ affinity[118]. Heterocyclic and (hetero)aryl cytisine derivatives have also been reported (Figure 2-1), but no binding affinity data has been published for these compounds, with one exception.[124] Roger et al. reported K_i values of 24 and 3,462 nM for 3-(2-fluoropyridinyl)-cytisine at $\alpha4\beta2$ and $\alpha7$ receptor subtypes.[125] In other words, very little is known about the impact of bulkier substituents at the pyridone fragment on the affinity and subtype selectivity for nAChRs.

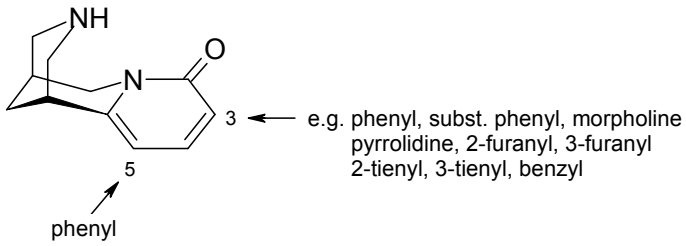

Figure 2-1 Structures of known (-)-cytisine analogues with unknown binding affinities

The target compounds should therefore feature bulkier substituents, i.e. substituted phenyl and heterocyclic moieties in the position 3 or 5 of the cytisine structure (Figure 2-2).

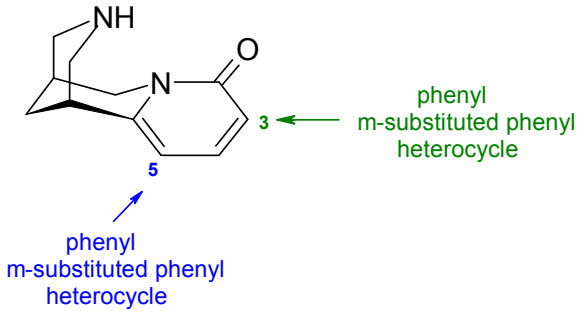

Figure 2-2 Structure of target compounds

The synthetic protocols reported for the incorporation of phenyl or aryl moieties into the cytisine backbone did not appear to be efficient for rapid synthesis of numerous derivatives required for SAR study, as they were complicated and lengthy, often using highly toxic stannane reagents. Thus, the work was focused on the development of rapid and more effective synthetic route to (hetero)aryl cytisine derivatives.

The assignment of the carbon and proton signals of cytisine **27** is poorly documented in the literature[126,127,128] and no publication deals with comprehensive NMR analysis of (-)-cytisine **27**. Moreover, no detailed study for distinguishing 3- and 5-substituted isomers has been reported. In order to correctly differentiate the isomeric 3- and 5-(hetero)aryl cytisine derivatives, a complete and correct set of ^{1}H and ^{13}C chemical shifts assignment for the unsubstituted alkaloid **27** was required. For that reason, another goal was to perform extensive NMR study of the parent alkaloid as well as of its several analogues. This study should provide information regarding the assignment of the ^{1}H and ^{13}C chemical shift to the cytisine skeleton and establish “diagnostical tools” for the differentiation of 3- and 5-isomers.

Although the cytisine analogues were aimed as potent α4β2 ligands, they were tested in radioligand binding studies not only for the affinity on the target receptor subtype, but also for their affinity towards different subtypes, i.e. α7*, α3β4* and $(\alpha1)_2\beta1\gamma\delta$ nAChRs. The determination of binding affinities will bring great impact on the current knowledge of structure-activity relationship, which is restricted due to the moderately big group of cytisine derivatives synthesized to date and very limited number of disclosed binding affinities. At the same time, the comparison of the binding profiles at different nAChRs subtype may help to understand the requests of each receptor for a selective ligand.

Project II

The nicotinic pharmacopoeia has expanded in the last decade with a number of novel synthetic ligands, however, the vast majority of these compounds is selective for α4β2 subtype and only a very limited number of potent α7-ligands is known to this point in time (e.g. α-bungarotoxin, MLA, anabaseine, GTS-21 or AR-R17779).

Choline **3**, a precursor and a metabolite of acetylcholine **1**, is an effective agonist of α7 nAChRs even if it presents very low affinity for the α7 nAChR (K_i = 2,380 μM).[52] Choline **3** has been shown to protect neural cells from cytotoxicity induced by growth factor deprivation[53] and it was suggested that the choline structure may serve as a template for the development of novel agents with both α7-nicotinic agonist activity and potential neuroprotective ability.[53] Nevertheless, the structure of choline **3** has attracted limited interest as a lead compound in the search for nAChR ligands and it was rationale to revisit this structure as a lead for development of novel nAChR ligands, with potential α7 selectivity.

The main goal of this project was to explore structural requirements of the nAChRs for a selective ligand based on choline. Our research group has shown, that phenylether of choline **4**, which shows nanomolar affinities for neuronal nAChRs and prevalence for α4β2* subtype is converted into an α7*-selective ligand **5** by an addition of amide moiety.[55] Thus, the question is: Does carbamate moiety between the pharmacophoric elements always result into α7-selective ligands?

In the target phenylcarbamate derivatives of **5**, the quaternary nitrogen will be incorporated into various azacyclic systems (N-methylpyrrolidine, N-methylpiperidine and quinuclidine), as compounds with tertiary amine groups have a higher probability to cross the blood-brain barrier. Additional substitution at the phenyl moiety should give deeper insight into the structure-activity relationships. Since the ortho and para position of the phenyl moiety in carbamates have been proved to strongly increase the affinity for muscarinic receptors as well as increase the anaesthetic effects, the meta position of the phenyl ring was selected for the introduction of various substituents (Br, CH_3, Ph and styryl).

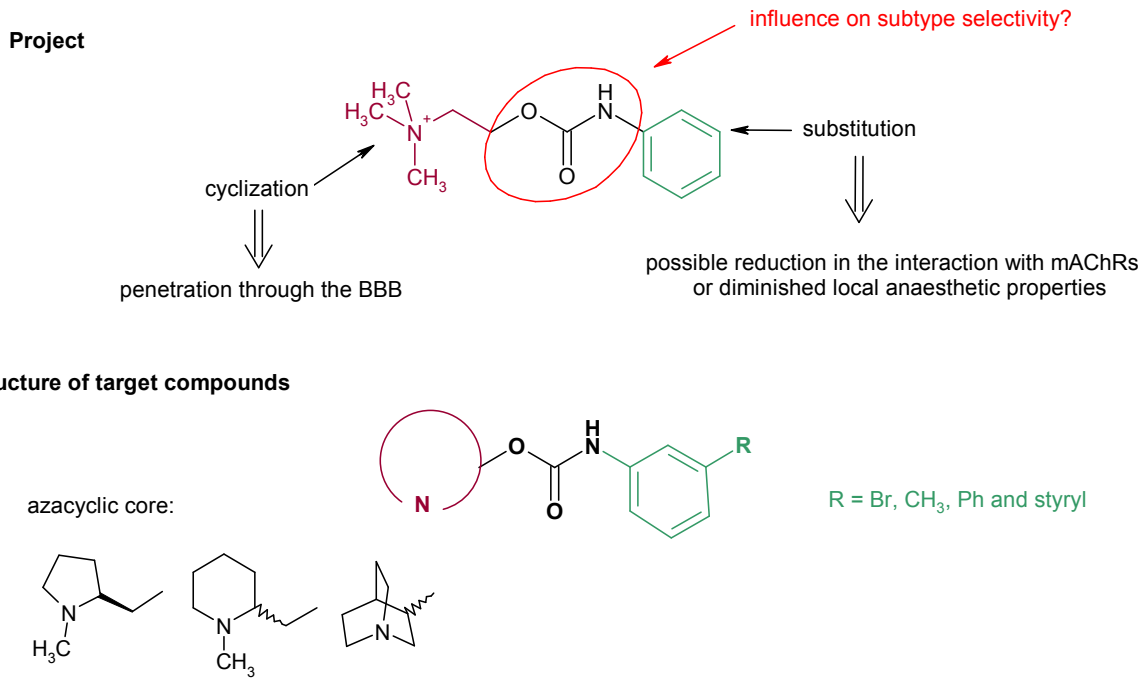

Figure 2-3 Development of nAChR ligands based on choline: project and structure of target compounds

The novel structures will be investigated in radioligand binding studies for their affinity towards nicotinic acetylcholine receptors, whereas the affinity for four subtypes, i.e. $\alpha4\beta2^*$, $\alpha7^*$, $\alpha3\beta4^*$ and $(\alpha1)_2\beta1\gamma\delta$ will be tested. This extensive pharmacological *in vitro* evaluation should provide valuable knowledge for the future development of nAChR ligands based on a phenylcarbamate template.

3 Project I: Development of Novel nAChR Ligands based on Cytisine

3.1 Cytisine as a Lead Compound

3.1.1 Introduction

(-)-Cytisine **27** was discovered in 1863 by Husemann and Marmé[129], as one of the poisonous alkaloids present in the seeds of *Laburnum anagyroides* (syn. *Cytisus laburnum*, Fabaceae). The physicochemical properties were for the 19th century extensively studied by Partheil[130] and he also established (-)-cytisine **27** to be identical with ulexin[131], discovered by Gerrard[132] in the seeds of *Ulex europeus*. More recently, Gorter proved its identity with baptitoxine, the alkaloid of the root of *Baptisia tinctoria.*[133] The structure of (-)-cytisine **27** was successfully established in the 1930s by H.R. Ing.[134]

(-)-Cytisine **27** *((7R,9S)-1,2,3,4,5,6-hexahydro-1,5-methano-pyrido[1,2-a][1,5]diazocin-8-one)* is a chiral quinolizidine alkaloid composed of an unsymmetrical, partially aromatic, bridged tricyclic skeleton (Figure 3-1). Quinolizidine alkaloids are derived from lysine and have two fused 6-membered rings that share nitrogen. At least 570 are known, but (-)-cytisine **27** and sparteine are the two most widely distributed quinolizidine alkaloids.[135] In the structure of (-)-cytisine **27** rings A and B form a bispidine framework that is fused to a 2-pyridone moiety (ring C) (Figure 3-1). The absolute configuration of the two chiral centres in the natural (-)-cytisine **27** was established to be 7*R* and 9*S*.[136] The absolute configuration of the unnatural (+)-enantiomer is 7*S*,9*R*. In the following work the signature "cytisine **27**" refers to the naturally occurring 7*R*,9*S*-cytisine, in cases of unnatural and racemic cytisine configurations, signs (+) and (±) will be used. The alternative numbering mostly used in the literature and in this thesis is not consistent with IUPAC numbering (Figure 3-1).

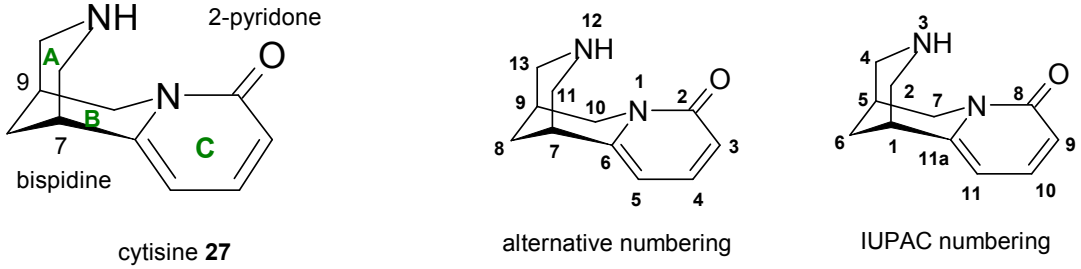

cytisine **27** alternative numbering IUPAC numbering

Figure 3-1 Structure of cytisine **27**. The rings A and B form a bispidine framework that is fused to a 2-pyridone moiety (C). The absolute configuration is 7*R*, 9*S*. Note: The alternative numbering mostly used in literature and in this thesis is not consistent with IUPAC numbering.

The lupin alkaloid cytisine **27** is present in many plants of the family Fabaceae. The isolation from e.g. Euchresta japonica[137], Maakkia tashiroi[138], Sophora exigua[139], Ormosia emarginata etc.[140], Echinosophora koreensis[141], Agryrolobium uniflorum[142] have been described in the literature.

In Europe, cytisine **27** can be easily isolated from seeds of *Laburnum,* a genus of two species, *L. anagyroides* and L. *alpinum*. Both species are bushy plants or small trees, cultivated throughout the Europe for their flowers, which appear early in the spring in rich, pendent, yellow clusters (Picture 3-1). However, most garden trees are the hybrid of the two species (termed *Laburnum x watereri)* which have the "benefit" of low seed production as *Laburnum* seed toxicity (i.e. cytisine toxicity) is a common cause of children's poisoning.[143] Symptoms of cytisine **27** poisoning are intense sleepiness, vomiting, convulsive movements and eventually death by respiratory failure. However, recovery from these symptoms occurs more or less speedily and only few cases were recorded in which death was the result.[144]

Picture 3-1 "Goldregen" tree (*Laburnum anagyroides*) in the spring and autumn

3.1.2 Pharmacological Characterisation of Cytisine

Compared to (-)-nicotine **10**, naturally occurring cytisine **27** is a more potent nAChR ligand with higher selectivity and subnanomolar affinity towards the $\alpha4\beta2$ subtype (Table 3-1). In the radioligand binding studies using rat brain membranes, Gündisch *et al* report for cytisine **27** K_i = 0.120 – 0.124 nM[118,145] while others report lower binding, i.e. K_i = 0.45 nM[146] and K_i = 3 nM.[123] To the $\alpha4\beta2$ receptor expressed in *Xenopus laevis* oocytes cytisine **27** binds with K_i values of 1.03 nM.[146] Similar binding of cytisine **27** to $\alpha4\beta2$ protein was found in assays performed with SH-EP1-h$\alpha4\beta2$ clonal cell lines that express human $\alpha4\beta2$ nACh receptors (K_i = 1.2 nM[147] and K_i = 1.07 nM[148]).

Table 3-1 K_i values of cytisine at various nAChR subtypes

	α4β2 [nM]	**Tissue**	**Reference**
K_i =	0.120	rat brain	[145b]
	0.122	rat brain	[118]
	0.124	rat brain	[145a]
	0.17	rat brain	[121]
	0.23	HEK 293 cell line	[185]
	0.45	rat brain	[146]
	1.03	*Xenopus laevis* oocytes	[146]
	1.2	SH-EP1-hα4β2 cell line	[147]
	1.5	rat brain	[122]
	3	rat brain	[123]
	α7 [nM]	**Tissue**	**Reference**
K_i =	8,000	SH-SY5Y-hα7 cell line	[147]
	4,200	IMR 32 cell line	[121, 185]
	261	rat brain	[118]
	α3β4 [nM]	**Tissue**	**Reference**
K_i =	18	pig adrenal	[183]
	54	rat adrenal	[183]
	56	*Xenopus laevis* oocytes	[146]
	81	rat ganglia	[122]
	220	KXα3β4R2 cell line	[150]
	840	IMR 32 cell line	[121, 185]
	$(\alpha 1)_2\beta 1\gamma\delta$ [nM]	**Tissue**	**Reference**
K_i =	250	cells electroplax	[121, 185]
	1,300	*Torpedo californica* electroplax	[183]

The K_i for cytisine **27** at other nACh receptor subtypes are listed in the Table 3-1. Cytisine **27** displaces [^{3}H]MLA from rat brain binding sites (i.e. α7 subtype) with K_i value of 261 nM[118] and α-[^{125}I]Bgt from SH-SY5Y-hα7 neuroblastoma clonal cell line with K_i value of 8.0 μM.[147] In the binding studies using *Xenopus laevis* oocytes K_i value of 8.36 μM was obtained.[148] Cytisine **27** has been shown to be a potent ligand also for α3β4 subtypes (K_i = 18 – 220 nM).[121,122,146,150,183,185] The K_i value of **27** for the $(\alpha 1)_2\beta 1\gamma\delta$ nAChR subtype at the neuromuscular junction is in the micromolar range (K_i = 1,300 nM).[183] Coe *et al* just recently reported a K_i value of 250 nM for cytisine affinity towards [^{125}I]-α-bungarotoxin binding sites expresed in cells electroplax.[121,185]

Functional data performed on known pairwise combinations of α and β subunits expressed in *Xenopus* oocytes showed that the effects of cytisine **27** on nAChRs are sensitive to receptor

subunit composition and the major factor in determining its efficacy is the nature of thee β subunit. Cytisine **27** was reported to be able to differentiate between receptors containing β4 and receptors containing β2 subunits. While nAChRs composed of α2, α3 or α4 in combination with β2 were insensitive to cytisine **27** compared to ACh **1**, and nAChRs composed of α2, α3 or α4 in combination with β4 were 3- to 17-fold more sensitive to cytisine **27** than to ACh **1**.[149]

Cytisine **27** acts as a true partial agonist for β2-containing nAChRs and can inhibit in the low concentration (20 nM) 50% of the α4β2 response to its endogenous neurotransmitter ACh **1** (1 μM) through a competitive mechanism. In the case of α4β2 receptors, cytisine **27** binds with high apparent affinity and low efficacy (the responses of α4β2-injected oocytes to the application of 1 mM cytisine **27** being only 14.7% of the response to 1 mM ACh **1**).[119]

Functional studies[103] with recombinant human nAChRs expressed in *Xenopus* oocytes exposed the same result, i.e. cytisine **27** displayed very low efficacy at β2-containing hnAChRs (hα2β2, hα3β2 and hα4β2) in contrast to its efficacy shown on β4-containing receptors (hα2β4, hα3β4 and hα4β4). In the same study, cytisine **27** was shown to possess a full agonist profile only on hα7 nAChRs.[103]

Partial agonist activity of cytisine **27** (59% efficacy compared to (±)-epibatidine **19**) was established also in K-177 cells expressing human α4β2 nAChR and in cultured cells expressing α3β4 receptors (62% efficacy compared to (±)-epibatidine **19**).[150]

The nicotine-like properties of cytisine **27** were first described by Dale and Laidlaw.[151] Although cytisine **27** is about 10-times more potent than (-)-nicotine **10** in binding experiments, it is less potent in producing the nicotine-like pharmacological effects.[152] Reavill *et al* confirmed that cytisine **27** has nicotine-like discriminative effect, but in much lesser extent than (-)-nicotine **10**.[153] The unimpressive behavioural effects of **27** were accounted at this point for its poor penetration to CNS due to the low lipophilicity (log k_w = 0.21 at pH 7.4, for comparison, (-)-nicotine **10** showed in the same experiment log k_w = 1.24).[153] Currently, the modern understanding of cytisine **27** being a partial agonist explains its pharmacological behaviour.

3.1.3 Radioligand [^{3}H]Cytisine

High affinity and selectivity of cytisine **27** for α4β2 nAChRs understandably led to the evaluation of tritium labelled [^{3}H]cytisine **27** in radioligand binding studies. In the pilot study, [^{3}H]cytisine **27** was found to bind with high affinity to α4β2 nAChRs (K_d = 0.96 nM, rat brain

tissues) and specific binding represented 60% – 90% of total binding at all concentrations examined (up to 15 nM).[154] Anderson and Arneric reported for [^{3}H]cytisine **27** binding in rat brain membrane fractions K_d value of 0.15 nM[155] and Khan et al. examined [^{3}H]cytisine **27** binding to membranes isolated from regions of the rat spinal cord. In their study, radioligand [^{3}H]cytisine **27** showed saturable, noncooperative binding to a single class of nAChRs with a K_d of 0.44 nM.[156] Gündisch *et al* reported for [^{3}H]cytisine **27** a K_d value of 0.120 nM.[145a] Currently, the tritium labelled cytisine **27** is being used in the radioligand binding experiments for the determination of affinities of various nAChR ligands.

Evaluation of the radioligand **27** in post mortem human brain revealed binding of [^{3}H]cytisine **27** to be of high affinity (K_d = 0.245 nM), saturable, reversible and labelling a single class of nAChRs. [157] The authors suggested that these characteristics make the radioligand useful for the quantisation of nicotinic cholinergic receptors in the human brain or in the tissues with low receptor density. *Ex vivo* labelling experiments using mouse brain and [^{3}H]cytisine **27** demonstrated that this radioligand is capable to label nAChRs.[158] However, a positron emission tomography (PET) attempt to visualise nicotinic cholinergic receptors in baboon brain with N-[^{11}C]methyl-cytisine failed.[159] The authors believed that the N-[^{11}C]methyl-cytisine crossed the blood-brain barrier very slowly and therefore the brain uptake of the radioligand was not different from blood radioactivity. However, the authors were mistaken with the affinity of caulophylline (N-methyl-cytisine) as they reported that caulophylline has a ten-fold higher potency than cytisine **27** in displacing [^{3}H]nicotine at brain nACh receptors. The real affinity of caulophylline (K_i = 5.7 nM)[118] is the reason why N-[^{11}C]methyl-cytisine is not a suitable tracer for PET studies of nAChR in primate brains, as PET methodology requires ligands with picomolar affinity, when monitoring neuroreceptors with low density.

3.1.4 Cytisine in Human Medicine

Nicotinic acetylcholine receptors are thoroughly investigated as potential drug targets in many therapeutic areas. nAChR ligands, including cytisine **27** and its derivatives, are claimed in the patent literature for the treatment of an endless list of pathologies, e.g. Alzheimer's disease, Parkinson's disease, Huntington's disease, Tourette's syndrome, mania, depression, anxiety, pain, jet-lag, glaucoma etc. The lists go up to thirty CNS- and non CNS-related disorders.[160] Cytisine **27** is mostly associated with the treatment of smoking and nicotine addiction.[124]

The first human smoking cessation study with cytisine **27** was performed in the 1960s. The study failed due to the poor effectivity resulting from poor bioavailability.[161] Several decades later, combination of nicotine replacement therapy with nAChR antagonist mecamylamine **34** (Figure 3-2) was found to be more effective than either treatment alone.[162] This discovery initiated a new therapeutical approach to smoking cessation using partial agonists. Sanofi-

Synthelabo developed a nAChR partial agonist SSR591813 **35** (Figure 3-2) that displays antiaddictive-like activity in animal models and reduces the dopamine-releasing and discriminating effects of nicotine.[163]

Cytisine **27** is currently on the market in Bulgaria as the main compound of Tabex® intended for treatment of tobacco dependence.[120] Even if Tabex® brought some positive results, the pure alkaloid has not found an application in the medicine outside of Bulgaria, most likely due to the small therapeutic window and the above mentioned poor bioavailability.

Pfizer recently described a novel series of compounds exhibiting a partial agonist profile and identified varenicline **36** (Figure 3-2), an azatricyclic compound imitating the structure of cytisine **27,** as the most suitable compound for the treatment of tobacco dependence.[121,164] The *in vivo* properties of varenicline **36** demonstrated its ability to attenuate the central dopaminergic response to smoking while simultaneously providing relief from withdrawal syndromes that accompany cessations attempts.[121]

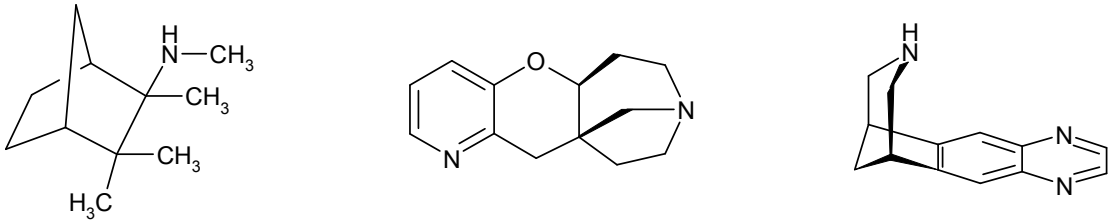

mecamylamine **34** SSR591813 **35** varenicline **36**

Figure 3-2 Chemical structures of nAChRs antagonist **34** and partial agonists **35** & **36** intended for the treatment of smoking cessation [Ref. 121, 162, 163]

3.1.5 Total Synthesis of Cytisine

The complex tricyclic structure of cytisine **27** has been an interesting chemical challenge for organic chemists over the decades. Several total syntheses of racemic cytisine **27** were described in the 1950s by van Tamelen[165], Bohlman[166] and Govindachari[167] and served to confirm its structure. However, these lengthy and low-yields resulting syntheses were not improved for nearly 50 years and only the identification of cytisine **27** as a potent nAChR ligand awoke new interest into the total synthesis of this alkaloid.

The first “new century” total syntheses of (±)-cytisine **27** were published by the Pfizer group in 2000. In the paper of O’Neill[168] the alkaloid (±)-**27** was prepared in five steps featuring an

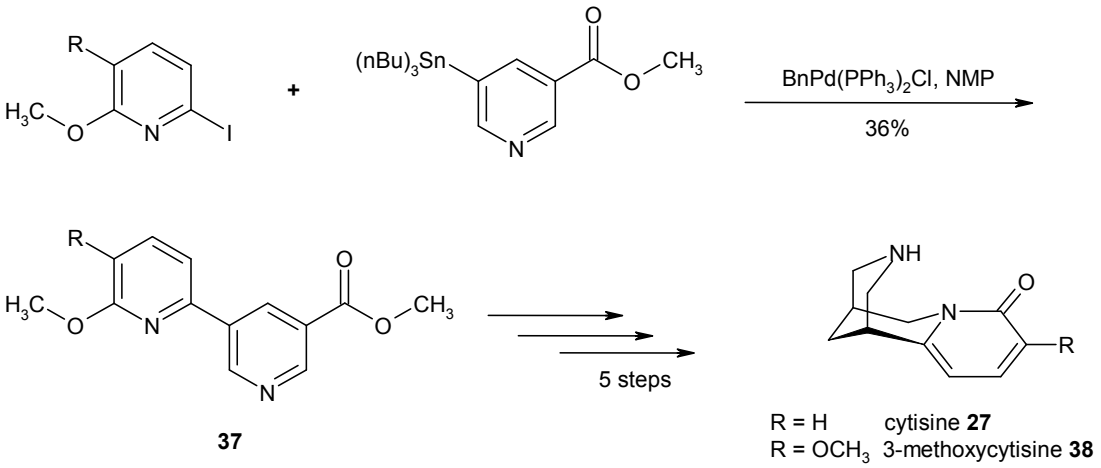

Scheme 3-1 First "new century" total synthesis of (±)-cytisine **27**, Stille cross-coupling reaction as a key step in the synthesis of the functionalised biaryl pyridine system **37** [Ref.168]

"in situ" Stille or Suzuki to provide the desired biaryl pyridine system **37** (Scheme 3-1). The utility of this procedure was established via synthesis of novel derivative 9-methoxycytisine **38** using similar sequence (Figure 3-1). At the same time, Coe described a concise 6-step synthesis of racemic (±)-cytisine **27** from cyclopent-3-enylmethanol.[169] This strategy featured the intramolecular Heck cyclization of glutarimide-derived ketene aminals to construct the tricyclic carbon skeleton of (±)-cytisine **27**, which was obtained in 16% overall yield. The crucial bipyridine **37** of the synthetic route published by O'Neill *et al*[168] was later synthesized by a French group via Negishi cross-coupling reaction.[170] Recently published novel strategy for the synthesis of racemic cytisine **27**, which was achieved in a total of 8 steps from commercially available starting materials, promises potential for more general application to the assembly of other lupine alkaloids.[171]

The first total enantioselective synthesis of (-)-cytisine **27** and its (+)-enantiomer was reported a few years later. The authors established 12-steps, 9%-overall yield synthesis of the enantiopure alkaloid **27** with ruthenium-catalysed ring closing metathesis representing the key step.[172] Enantiopure synthesis of (+)-cytisine **27** has been published together with synthetic routes of (+)-kuraramine and (+)-jussiaeiine, the oxidative metabolites of N-methylcytisine. These alkaloids were synthesized via samarium diiodide-promoted reductive deamination.[173]

3.1.6 Modification of the Cytisine Scaffold

Nevertheless, the above described routes still present a very complicated organic challenge and all novel analogues disclosed to date have been synthesized via modification of cytisine **27** obtained from natural sources and have been limited – with a few exceptions – to halogenation on the pyridone moiety and substitution of the secondary amine group. This chapter will discuss the chemistry of the cytisine derivatives, while the following Chapter 3.1.7 will focus on the biological data of these derivatives.

First halogenated derivative of cytisine **27** – 3,5-dibromo-cytisine **46** – was synthesized several decades ago. The alkaloid **27** was treated with excess of bromine in the aqueous acetic acid.[174] Imming *et al*[118] developed an effective one-step syntheses of halogenated derivatives of cytisine featuring a halogen substituent in the position 3 (**39**/**40**/**41**), in the position 5 (**42**/**43**/**44**) or both 3 and 5 (**45**/**46**/**47**) of the 2-pyridone fragment. The key step in syntheses was halogenation of N-12 protonated (-)-cytisinium acetate **48** (Scheme 3-2), prepared in situ by employing aqueous acetic acid as the solvent and utilising N-chloro, N-bromosuccinimide or iodine chloride as halogen transfer reagents (Scheme 3-2)[118].

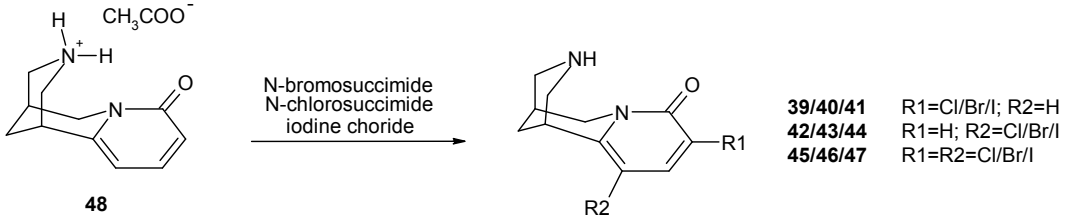

Scheme 3-2 Effective one-step syntheses of mono- and dihalogenated cytisine derivatives [Ref. 118]

Halogenated analogues of cytisine **39 – 47** were also disclosed in some Pfizer patents[124] and were prepared in a similar way, using halogenated succinimides as halogenation agents, but the bispidine nitrogen was *t*BOC-protected before the halogenation. The protecting group was subsequently removed with trifluoroacetic acid.

Several papers describe modification of the cytisine **27** structure by reactions at the secondary amino group. Substitution of the basic nitrogen with isocyanates and isothiocyanates afforded urea- and N-arylthiocarbamylderivatives of cytisine.[175,176] In the ex-Soviet Union, cytisine **27** deserved much attention in the 1970s due to its utilisation as a respiratory stimulant.[177] Recently, the remaining interest has produced many analogues, all of them presenting structural variation on the secondary amino group. N-alkyl- and sulfonamide derivatives of cytisine **27** were reported[178,179], as well as analogues of

cytisylmethylbarbituric acids[180]. Acylation of the alkaloid **27** with the benzocrown-ether carboxylic acid chlorides allowed incorporation of the benzocrown-ether fragment into the structure of cytisine **27**.[181]

A large group of N-substituted derivatives of cytisine **27** possessing an aliphatic, arylaliphatic or heteroaromatic substituent (Scheme 3-3, **49** representing a general structure) was synthesized together with compounds bearing a second cytisine unit, linked through an aliphatic or xylene chain (Scheme 3-3, **50** representing a general structure).[122,123]

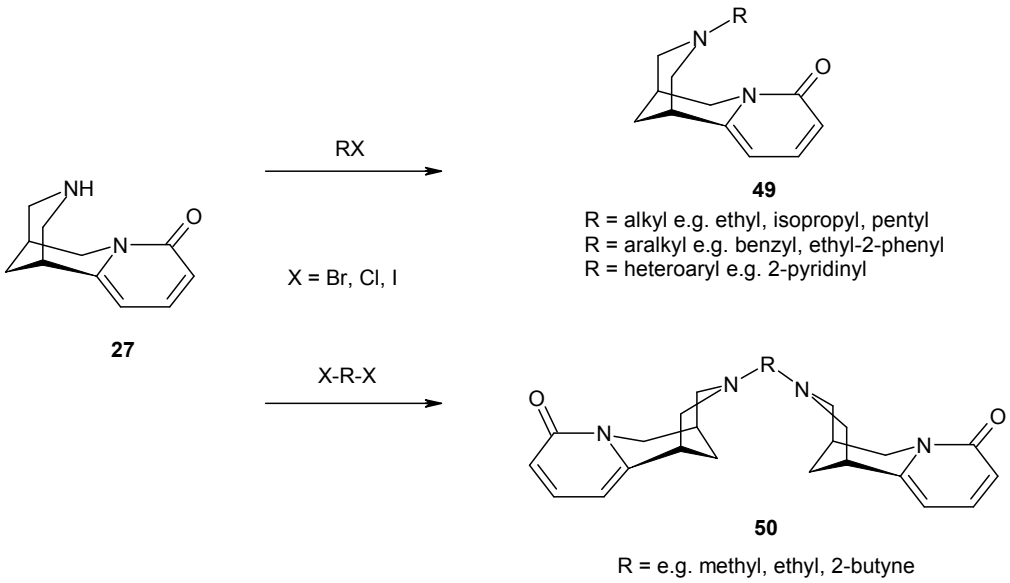

Scheme 3-3 Structural variation of the secondary amino group of cytisine **27** [Ref. 122, 123]

Oxygen-sulphur exchange with Lawesson's reagent under microwave irradiation allowed synthesis of bioisosteric thiocytisine **51** and via hydrogenation of double bonds tetrahydrocytisine **52** was synthesized (Figure 3-3).[118,182] N-methylation of cytisine **27** leads to an alkaloid known as caulophylline **53** (Figure 3-3). Several analogues featuring 2 or 3 modifications were also prepared, e.g. tetrahydrothiocytisine **54**, 3,5-dibromo-N-methylcytisine **55**, N-methyl-tetrahydrothiocytisine **56** (Figure 3-3).[118,182,183]

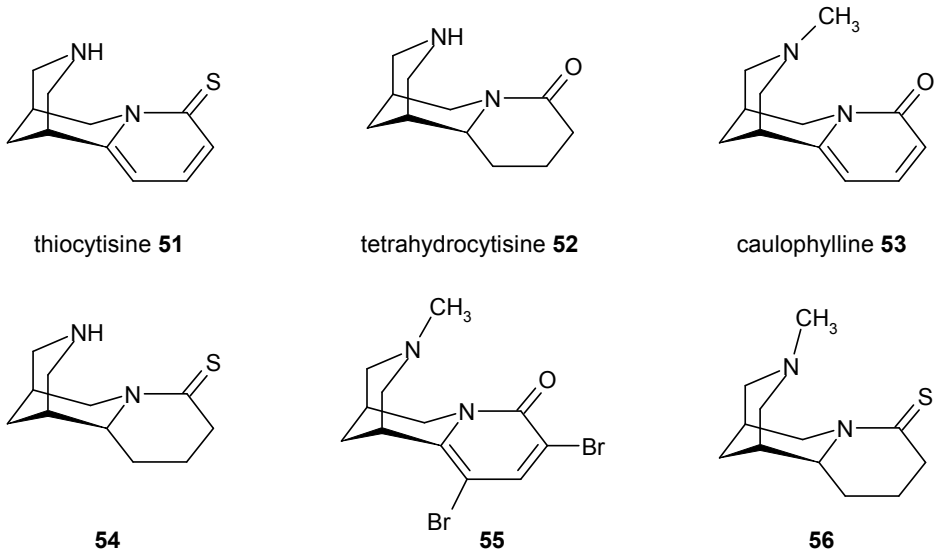

Figure 3-3 Structures of cytisine analogues. **51 – 53** possess one modification, while **54** – **56** feature two or three modifications compared to cytisine **27** [Ref. 118, 182, 183]

A series of cytisine derivatives with bulkier (hetero)cyclic substituents in the position 3 or 5 were disclosed in several Pfizer patents.[124] In order to develop PET ligands based on cytisine, 3-(4'-fluorophenyl)-cytisine[184] and (-)-3-(2-fluoropyridin-5-yl)-cytisine[125] were prepared via Stille cross-coupling reaction. These synthetic routes and structures are described in detail in Chapter 3.2.

Partial agonist properties of cytisine **27** and the involvement of $\alpha4\beta2$ nAChRs in mesolimbic dopaminergic system responsible for drug abuse as a pathway to treat smoking cessation led Pfizer to the development of racemic all-carbon-containing cytisine analogues **57** (Scheme 3-4), in which the pyridone ring was replaced by a substituted phenyl ring.[185] These analogues were generated via Heck cyclization protocol and followed the synthetic strategy for the total synthesis of racemic (±)-cytisine **27**[169] (Scheme 3-4).

57

e.g. R2 = OH, R3 = R4 = R5 = H
R2 = F, R3 = R4 = R5 = H
R3 = F, R2 = R4 = R5 = H
R3 = NO_2, R2 = R4 = R5 = H
R4 = NO_2, R2 = R3 = R5 = H

Scheme 3-4 Structure of all-carbon-containing cytisine analogues **57** [Ref.185]

3.1.7 Structure-Activity Relationship of Cytisine Derivatives

The knowledge of the structure-activity relationship for the lead compound **27** is very limited, since the binding affinity or the pharmacological activity data of the analogues disclosed in patent literature is not provided. Thus, the SAR for cytisine **27** as a lead compound is to date based on information obtained from research groups of Gündisch (University of Bonn, Germany), Cassels & Bermúdez (University of Chile & Oxford Brookes University, England), Sparatore (University of Genoa, Italy), Lasne (University of Caen-Basse-Normandie, France) and the most recent Pfizer publication[185].

SAR for α4β2 nAChR subtype

Cytisine **27** exhibits high affinity towards α4β2 nAChRs (K_i = 0.120 – 3 nM, Table 3-2).[121-123,145-147,185] The introduction of the substituent on the amine nitrogen always caused a dramatic loss in affinity dropping into the nanomolar range. This reduction of affinity was observed with a simple N-methylation of cytisine **27** to caulophylline **53** (K_i = 5.7 nM)[118], as well as with the introduction of a longer aliphatic, an arylaliphatic or a bulkier aryl moieties (K_i = 1.2 – 4,850 nM for compounds of general structure **49** in the Scheme 1-3)[123]. The compounds consisting of two cytisine units joined through an aliphatic or arylaliphatic moiety (**50**, Scheme 1-3) also showed a decrease in affinity. When the link between the bispidine's nitrogens involved 3-4 carbon atoms, the deterioration of affinity was smaller (K_i = 25 – 30 nM) than that observed with a chain of 2 or 6 carbon atoms (K_i = 96 and 313 nM).[123]

The introduction of halogen substituent into position 3 (**39** - **41**) resulted in an increase of the binding affinity to the rat brain α4β2 nAChRs (K_i = 0.010 – 0.022 nM).[118] 3-Bromocytisine **40** shows the highest affinity for α4β2 subtype (K_i = 10 pM), exceeding that of the parent alkaloid **27** by approximately one order of magnitude and comparable to the affinity of epibatidine **19** (K_i = 0.018 nM)[78]. The binding to α4β2 protein was reduced with halogenation of the position 5 (K_i = 0.23 – 2.5 nM for **42** - **44**) and dihalogenation of the positions 3 and 5 of the pyridone ring (K_i = 0.52 – 10.8 nM for **45** - **47**).[118]

Brominated cytisine analogues **40**, **43** and **47** have been also tested in the cell lines expressing hα4β2 receptor.[147,148] The rank of order of potency for blockade of [^{3}H]cytisine was 5-Br-cyt **43** (K_i = 1.54 μM) < 3,5-diBr-cyt **46** (K_i = 0.42 μM) < cytisine **27** (K_i = 1.07 nM) < 3-Br-cyt **40** (K_i = 0.082 nM). 3-Iodo-cytisine **41** was found to be less potent than **40**, but still showed a higher binding to the hα4β2 nAChR (K_i = 0.7 nM) than the parent alkaloid **27**.[148] 5-Iodo-cytisine **44** (K_i = 10 nM) was less potent than cytisine **27**, but possesses a higher affinity than the 5-bromo analogue **43**.[147]

The introduction of the nitro group into position 3 slightly decreases the binding affinity of the lead **27** (K_i = 0.42 nM for 3-nitrocytisine **58**). The 5-nitro counterpart **59** possesses approximately 150-fold lower affinity for $\alpha4\beta2$ nACh receptor (K_i = 65.6 nM).[183]

The divalent bioisosteric replacement of the lactam oxygen of cytisine **27** by sulphur yielded thiocytisine **51** and 7-fold affinity reduction (K_i = 0.832 nM) compared to cytisine **27** (K_i = 0.122 nM).[118] However, the thiolactam **51** showed the best affinity-selectivity profile for $\alpha4\beta2$ vs $\alpha7$ nAChR subtypes (K_i = 0.832/4000 nM, respectively).[118,182,183] The combination of two or three modifications of the cytisine **27** scaffold (e.g. bioisosteric replacement and halogenation) led to decrease of the $\alpha4\beta2$ binding affinities (Table 3-2).[183]

Table 3-2 Affinities of cytisine analogues with two or three modifications at $\alpha4\beta2$ nAChRs [Ref. 183]

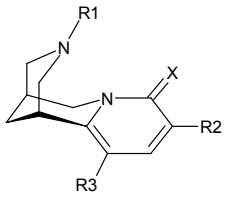

R1	R2	R3	X	K_i [nM]
H	H	H	O	0.122
CH_3	Br	H	O	1.37
CH_3	Br	Br	O	485
CH_3	I	H	O	1.0
CH_3	I	I	O	656
CH_3	H	H	S	6,000
H	Br	H	S	0.6
H	H	Br	S	8.1
H	Cl	H	S	1.48
H	H	Cl	S	55
-CO-CH_3	H	H	S	857

The impact of the bulky substitution in the position 3 or 5 cannot be evaluated, as biological data of the phenyl and aryl derivatives of cytisine **27** have not been disclosed[124], with one exception. Roger *et al* reported a K_i value of 24 nM for 3-(2-fluoropyridin-5-yl)-cytisine at $\alpha4\beta2$ receptor subtype.[125]

The structure-activity relationships for all-carbon derivatives of cytisine **57** exposed similar findings regarding the structure requirements for high affinity nAChRs ligands (Table 3-3)

Table 3-3 Structures and affinities of all-carbon analogues of cytisine **57** for hα4β2 nAChRs in HEK 293 cells [Ref.185]

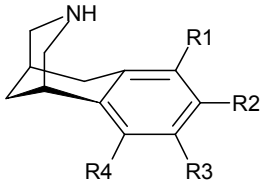

Compound	R1	R2	R3	R4	K_i [nM]
cytisine **27**	---	---	---	---	0.23
57a	H	H	H	H	34
57b	OH	H	H	H	2.9
57c	F	H	H	H	6.5
57d	H	F	H	H	2.0
57e	H	OMe	H	H	1.4
57f	H	NO_2	H	H	4.9
57g	H	H	NO_2	H	6.5
57h	H	H	H	NO_2	14
57i	F	F	H	H	0.44
57j	H	Ph	H	H	> 500

and controversial results regarding the α4β2 pharmacophore model.[185] High-affinity compounds (**57b** - **57i**) share a common substitution pattern of possessing electron-withdrawing group (OH, OMe, F, NO_2), preferably in the position that equals the position 3 in cytisine **27** (e.g. comparison of **57c** and **57d**). These groups are poor hydrogen bond acceptor (HBA) or are devoid of H-bond acceptor capability, which is believed to be crucial for receptor binding. The most potent compound **57i** combines two neighbouring fluorine atoms and shows affinity (K_i = 0.44 nM) comparable to the affinity of cytisine **27** (K_i = 0.23 nM).[185]

The SARs for cytisine **27** analogues is summarized in Figure 3-3.

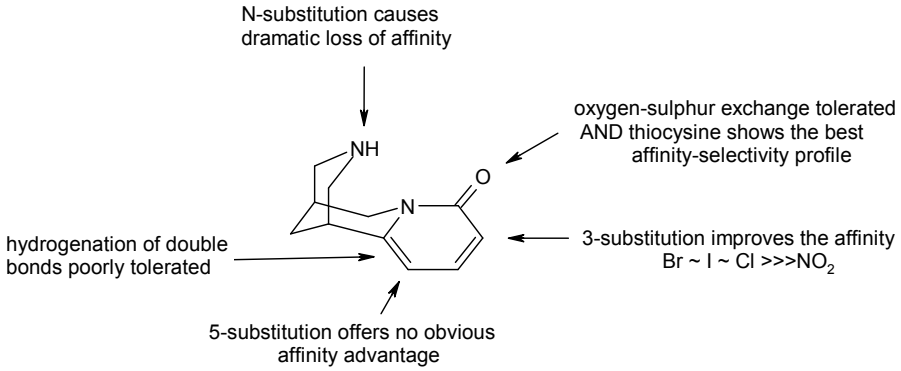

Figure 3-3 SARs for cytisine **27** analogues at α4β2 nAChR

SAR for α7 nAChR subtype

Cytisine **27** displays moderate binding to α7 nAChR (K_i = 261 nM)[118,183] and the structure-affinity relationship for this receptor subtype mostly follows the trend observed for SAR at α4β2 nicotinic acetylcholine binding sites.

The N-substitution greatly reduces affinity and the introduction of a methyl or dimethyl moiety at the secondary amine function yielded K_i values in micromolar range (K_i = 15,000 and 1,100 nM, respectively).[118]

The introduction of halogen atom into position 3 resulted in improved affinity (K_i = 1.5 – 2.5 nM), the rank of order for α7 affinity being 3-Cl **39** (K_i = 2.5 nM) < 3-Br **40** (K_i = 2.0 nM) < 3-I **41** (K_i = 1.5 nM).[118] While all 5-halogen derivatives of cytisine **42 – 44** showed reduced affinity for α4β2 receptor compared to the lead **27**; in the case of α7 nAChR, only 5-chlorocytisine **42** binds with lower affinity (K_i = 1,000 nM).[118] The introduction of bromine or iodine atoms into the position 5 of the pyridone moiety is favourable for the recognition of α7 receptor subtype and 5-bromo- and 5-iodo-cytisine **43** and **44** show approximately 10-fold higher affinity (K_i = 28 and 21 nM, respectively)[118] compared to the parent alkaloid **27**. Substitution of both positions with chlorine and bromine (**45** and **46**) afforded less potent ligands (K_i = 1,500 and 1,000 nM), but the same modification with iodine resulted in potent α7 ligand **47** (K_i = 41 nM).[118]

Houlihan *et al* tested brominated and iodinated analogues of cytisine in binding assays with SH-SY5Y-hα7 clonal cell lines, which overexpress the human α7 nAChR.[148] For the bromo analogues **40**, **43** and **46**, the following rank order of α7 affinities was obtained: 3,5-diBr-cyt **46** (K_i = 13.50 μM) < 5-Br-cyt **43** (K_i = 10.10 μM) < cyt **27** (K_i = 8.36 μM) < 3-Br-cyt **40** (K_i = 16 nM).[148] 3-Iodocytisine **41** (K_i = 7 nM) in the same test system showed a higher affinity than cytisine **27**, while 5-iodo analogue **44** exhibited the α7 affinity of cytisine **27** (K_i = 8 μM).[147]

Nitro analogues of cytisine showed different affinities for α7 receptor. While 3-nitrocytisine **58** inhibited the binding of [^{3}H]MLA with K_i of 40.7 nM, 5-nitrocytisine **59** showed affinity in micromolar range (K_i = 12,000 nM).[183]

Hydrogenation of double bonds and oxygen-sulphur exchange are detrimental for binding to α7 nAChR. However, the micromolar affinity of thiocytisine **51** for α7 (K_i = 4,000 nM) makes the bioisosteric lactam **51** the most α4β2/α7 selective ligand.[118] Halogenation of thiocytisine **51** in position 3 significantly improves the affinity for [^{3}H]MLA binding sites (K_i = 48 and 50 nM for 3-bromothiocytisine and 3-chlorothiocytisine, respectively) not only compared to thiocytisine **51** (K_i = 4,000 nM) but also to cytisine **27** (K_i = 261 nM).[183] The introduction of a

bulky 4-fluorophenyl moiety into the position 3 resulted in a ligand with low α7 binding affinity (K_i = 3,462 nM).[125]

In the series of all-carbon cytisine derivatives **57**, the compounds bearing fluorine **57c** (R1 = F), **57d** (R2 = F) as well as difluoro analogue **57i** (R1 = R2 = F) displaced [^{125}I]-αBgt with a significantly higher affinity (K_i = 350 – 830 nM) than cytisine **27** did in the same test system (K_i = 4,200 nM).[185] Other analogues (e.g. **57e**, R2 = OMe) tested for their α7 affinity also showed a higher binding to the α7 nAChR subtype (K_i = 2,400 nM) than the lead **27**.[185]

The SAR of cytisine **27** analogues for the α7 subtype is summarized in the Figure 3-4.

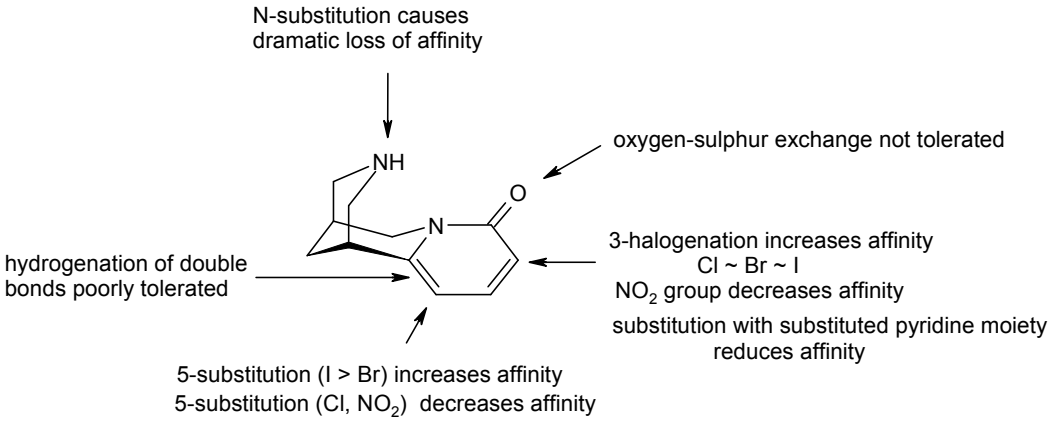

Figure 3-4 SARs for cytisine **27** analogues at α7 nAChR

SAR for α3β4 nAChR subtype

Cytisine **27** binds to [^{3}H]epibatidine labelled binding sites in pig adrenals with K_i = 19 nM.[183] The rate of the decreased α3β4 affinity via N-substitution depends on the bulkiness of the substitutent, e.g. K_i = 1,500 nM for caulophylline **53** *vs.* K_i = 5,500 nM for N-benzylcytisine.[183]

Halogenation of position 3 leads to an increase of binding affinity, the rank of order being cytisine **27** (K_i = 19 nM) < 3-Cl-cyt **39** (K_i = 1.1 nM) < 3-Br-cyt **40** (K_i = 0.61 nM) < 3-I-cyt **41** (K_i = 0.35 nM).[183] Identical rank was obtained for 5-halogenated analogues **42 – 44** {cyt **27** (K_i = 19 nM) < 5-Cl-cyt **42** (K_i = 14.3 nM) < 5-Br-cyt **43** (K_i = 5.0 nM) < 5-I-cyt **44** (K_i = 3.25 nM)}.[183]

Introduction of the nitro group into position 3 yields ligand **58** with affinity (K_i = 12 nM) nearly identical to the affinity of the parent alkaloid **27**. Nitro group in the position 5 significantly reduces binding to the α3β4 protein (K_i = 1,000 nM for **59**) compared to the affinity of cytisine **27** (K_i = 19 nM).[183]

Hydrogenation of the double bond in the pyridone moiety (compound **52**) as well as bioisosteric replacement of oxygen by sulphur (compound **51**) leads to compounds with lower $\alpha3\beta4$ affinity (K_i = 385 nM and 632 nM, respectively) than that of the parent alkaloid **27**.[183]

Selected all-carbon cytisine derivatives **57** (for structure see Table 3-3) have been tested for their affinity to the $\alpha3\beta4$ nACh receptor expressed in IMR32 cells.[185] In this assay, cytisine **27** displaced [^{3}H]epibatidine with K_i value of 840 nM and only two compounds showed lower binding affinity (K_i = 340 and 710 nM for **57f** (R2 = NO_2) and **57d** (R2 = F), respectively). Derivatives **57e** (R2 = OMe) and **57i** (R1 = R2 = F) bind to $\alpha3\beta4$ nAChR with the same affinity as cytisine **27** (K_i = 810 nM).[185]

The structure-activity relationship of cytisine **27** analogues for the $\alpha4\beta3$ nAChR subtype is summarized in Figure 3-5.

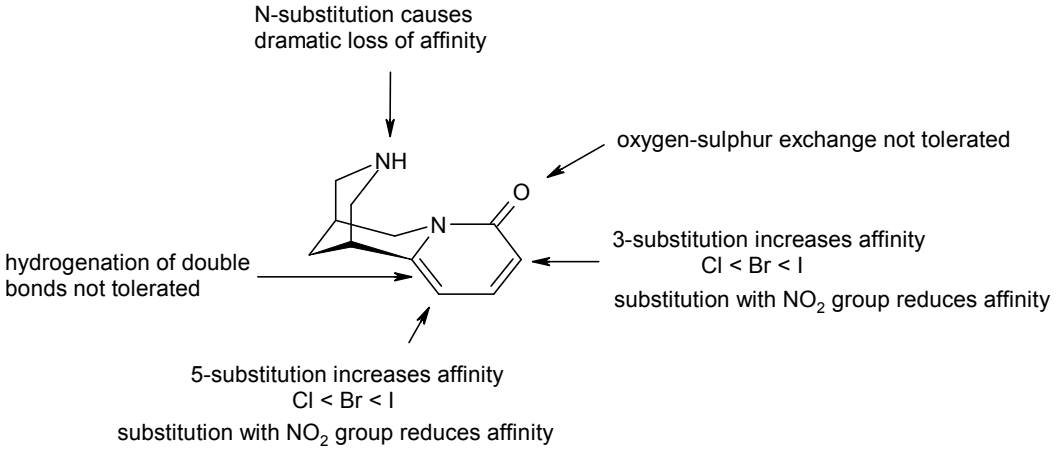

Figure 3-5 SARs for cytisine **27** analogues at $\alpha3\beta4$ nAChR

SAR for $(\alpha1)_2\beta1\gamma\delta$ nAChRs

Cytisine **27** possesses micromolar affinity to the nAChRs at the neuromuscular junction (K_i = 1,300 nM).[183] All modifications introduced into the structure of **27** led to ligands with reduced affinity (K_i > 1,300 nM), except for halogenation of position 3. While 3-chlorocytisine **39** shows affinity (K_i = 1,332 nM) identical with the affinity of cytisine **27**, 3-bromo- and 3-iodo-analogue **40** - **41** with K_i = 627 and 413 nM, respectively, are more potent ligands for muscle nACh receptors than the parent alkaloid **27**.[183]

3.2 Syntheses of Novel nAChRs based on Cytisine

The method of choice for the synthesis of novel nAChRs ligands was the Suzuki cross-coupling reaction carried out under microwave accelerated conditions. This choice can be rationalised firstly with the fact that the Suzuki reaction (palladium-catalysed cross-coupling of arylhalides and organoboron compounds in the presence of a base) is one of the most versatile cross-coupling reactions used in modern organic synthesis for creating C-C bonds. Secondly, heating and driving chemical reactions by microwave energy has recently been reported to dramatically reduce the reaction time (from days and hours to minutes and seconds) of various chemical reactions, including the Suzuki cross-coupling reaction.

3.2.1 Suzuki Cross-Coupling Reaction

Suzuki reaction[186] together with Grignard[187], Stille[188], Hiyama[189] or Sonogashira[190] reactions (named after the pioneers in the field) build a group of reactions termed as “cross-couplings” (Scheme 3-5). These reactions are based on transmetallation of organometallic nucleophiles and share many mechanistic aspects, although some differences exist in the activation of the organometallic nucleophile. The Suzuki (or Suzuki-Miyaura) coupling of organoboron compounds has been recognised after more than three decades of intensive research (first papers describing these reactions appeared at the end of the 1970s and at the beginning of the 1980s) as the most general and selective palladium-catalysed cross-coupling reaction.[191] Heck reaction[192] or “coupling process” differs from the family of “coupling reactions” as the transmetallation step is absent in the Heck reaction. In the arylation/alkenylation of olefins, the C-C bond is formed by an addition-elimination mechanism, i.e. the addition of ArPdX (X = halogen or triflate) is followed by the elimination of HPdX to form the substituted alkene product.[193]

In 1979, Suzuki reported that cross-coupling reactions between alkenylboranes and 1-alkenyl halides are effectively catalysed by tetrakis(triphenylphosphine)-palladium [$Pd(PPh_3)_4$] in the presence of a base and water.[186a,b] This publication started the historical period of “Suzuki reaction” which attracts as much attention today as it did at the beginning. Nowadays, the Suzuki cross-coupling reaction is not limited only to the formation of $C(sp^2)$-$C(sp^2)$ bonds but also $C(sp^3)$-$C(sp^3)$, $C(sp^2)$-$C(sp^3)$ or $C(sp)$-$C(sp^2)$ bonds can be formed using the Suzuki protocol under carefully selected reaction conditions. The need of a base due to the activation of the low nucleophilicity possessing organoborane is the most noteworthy difference between Suzuki cross-coupling and all other cross-coupling reactions.[191c]

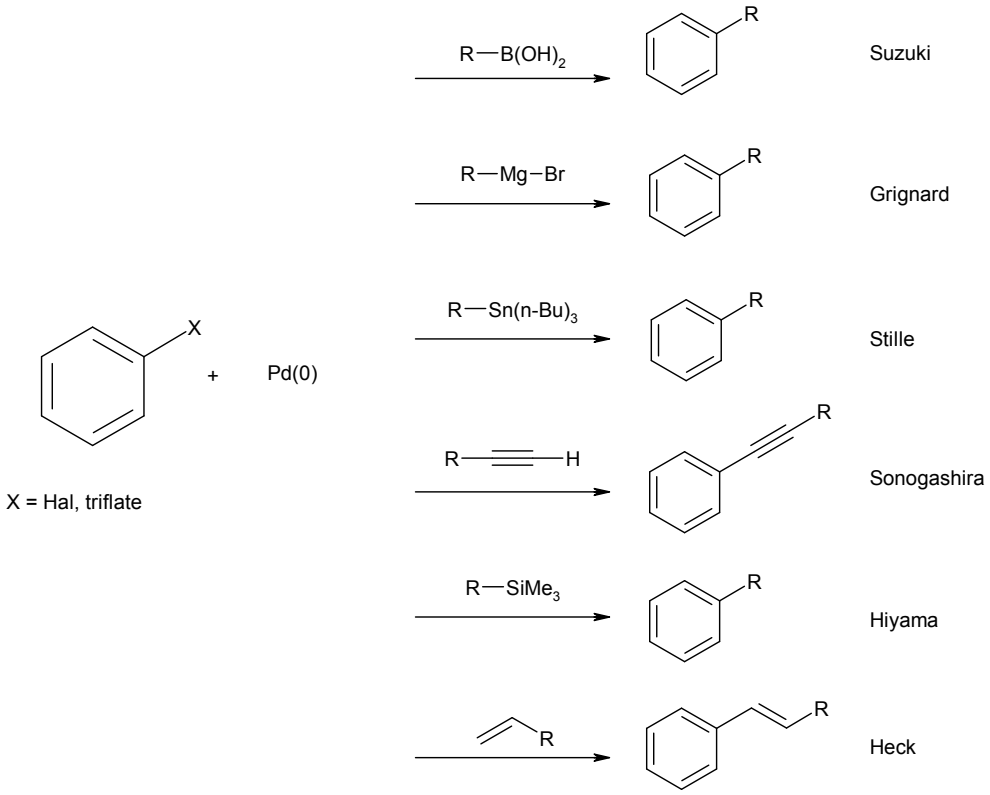

Scheme 3-5 Cross-coupling reactions [Ref. 186 – 192]

3.2.1.1 Mechanism

A catalytic cycle for the cross-coupling reaction of organoboron compounds with organic halides (iodides, bromides and electron deficient chlorides) and organic triflates follows a general catalytic cycle of organometallics, involving: (A) oxidative addition of organic halides or other electrophiles to a palladium(0) complex yielding R_1-Pd(II)-X **60**; (B) transmetallation between R_1-Pd-X and R_2-$B(OH)_2$ with the aid of bases affording R_1-Pd(II)-R_2 **61**; and (C) reductive elimination of R_1-R_2 **62** to regenerate the palladium(0) complex (Scheme 3-6).[191]

The oxidative addition of organic electrophiles R_1X to Pd(0) complex affords a stable *trans*-palladium(II) complex **60**. The first step of the cross-coupling reaction takes place usually by aromatic nucleophilic substitution (S_{N2} reaction). Oxidative addition is reported to be the rate-determining step in the catalytic cycle and the order of reactivity of electrophilic partners has been established as I >> OTf ~ Br >> Cl. Electron-withdrawing substituents on aryl and 1-alkenyl halides lead to rate acceleration.[191]

The transmetallation involves nucleophilic displacement of R_1-Pd(II)-X **60** with the borate complex $[R_2B(OH)_3]M$ **63**, yielding R_1-Pd(II)-R_2 **61**, $B(OH)_3$ and MX.[191c]

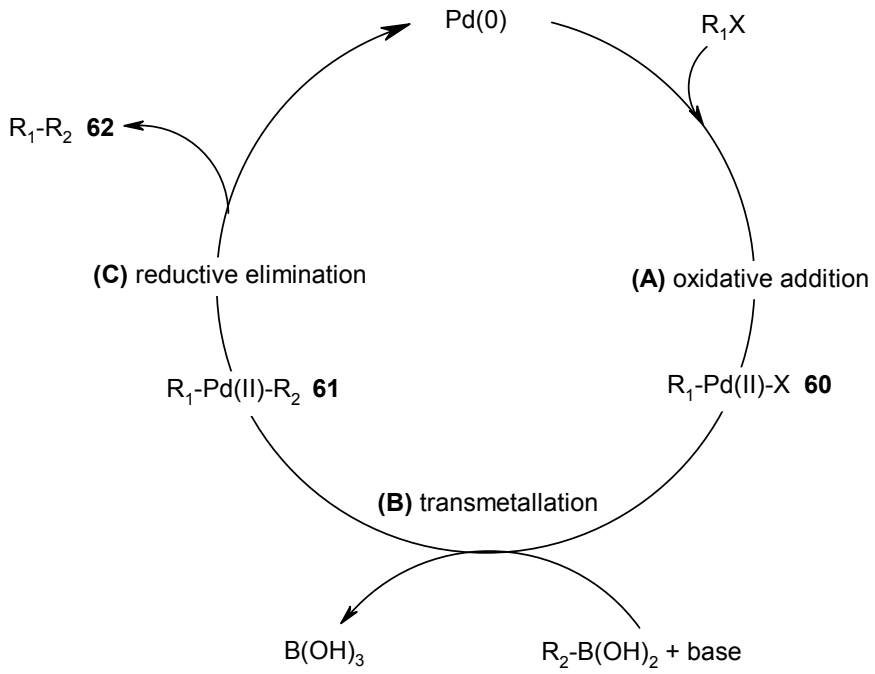

Scheme 3-6 Catalytic cycle of Suzuki cross-coupling reaction [Ref. 191]

Due to the low nucleophilicity of the borane reagents (compared with organostannanes, for example) the Suzuki reaction requires the use of a base in order to take place. The essential role of the base is to generate a more reactive borate complex by coordination of the hydroxide ion to the boron. The quarterization of the boron atom with a negatively charged base enhances the nucleophilicity of the organic group on the boron atom, and the corresponding "ate" complex easily undergoes the coupling reaction with R_1-Pd(II)-X **60**.[191c]

Reductive elimination of organic partners from R_1-Pd(II)-R_2 **61** yields the desired product R_1-R_2 **62** and reproduces the palladium(0) complex.[194] The reaction takes place directly from *cis*-isomer, the *trans*-isomers react after their *trans*-*cis* isomerization to the corresponding *cis*-complex.[191a]

3.2.1.2 Reaction Conditions

The nature of the organoborane, the aryl, vinyl or alkyl halide, the palladium catalyst and the base significantly influence the yields of products and formation of byproducts.

3.2.1.2.1 Palladium Catalyst

The most commonly used catalyst is $[Pd(PPh_3)]_4$. Freshly synthesized, this catalyst is a bright-yellow crystalline powder, which darkens over time and with exposure to air and temperatures above 0°C, leading to a decreased activity of the catalyst.[195] $[Pd(PPh_3)]_4$ is commercially available and some chemical suppliers provide this catalyst in good quality. Another catalyst employed in Suzuki cross-coupling reaction is $PdCl_2(PPh_3)_2$, which is reduced *in situ* to the reactive palladium(0) species.[196] Although this catalyst is air and temperature stable and less expensive than $[Pd(PPh_3)]_4$, it has been used in smaller extents. The addition of a phosphine ligand to $[Pd_2(dba)_3]$, $[Pd(dba)_2]$ or $Pd(OAc)_2$ is an alternative method for preparing analogous palladium(0)/phosphine catalyst.[191c]

3.2.1.2.2 Base

A carefully selected base is essential for a successful Suzuki cross-coupling. The "standard" Na_2CO_3 is effective for a variety of coupling reactions, but it is not suitable for alkyl and alkynyl coupling or for reactants that are sterically hindered. For example, the reaction of mesitylboronic acid with iodobenzene shows the following rate of reactivity: TlOH > $Ba(OH)_2$, Tl_2CO_3 > NaOH > Cs_2CO_3, K_3PO_4 > Na_2CO_3 > $NaHCO_3$.[197] Thallium salts have been successfully used also in the alkyl-aryl or alkyl-vinyl coupling reactions.[198] It is acknowledged that Cs_2CO_3 in the presence of water accelerates the coupling reaction carried out at room temperature.[199] Stronger bases such as NaOH, TlOH and NaOMe were shown to perform well in THF/H_2O solvent systems, whereas weaker bases such K_2CO_3 and K_3PO_4 were more successful in DMF.[200,209]

The different effect of a base can be explained with different stability constant of counter cations for halide and hydroxide anions. The base has been proposed to be involved in several steps of the catalytic cycle, but most notably in the transmetallation process, whereas the most essential role of the base is the conversion of the boronic acid into the more reactive borate species **63** (Scheme 3-7).[210a]

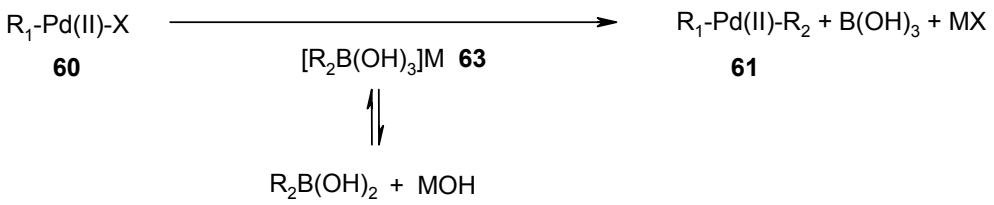

Scheme 3-7 The role of a base in the transmetallation process [Ref. 201]

The concentration of the hydroxyborate complex $[R_2B(OH)_3]M$ **63** exists in an alkaline solution in equilibrium with a free boronic acid and increases by increasing the basic strength ($OH^- > MPO_4^- > MCO_3^- > HCO_3^-$).[201] Furthermore, the stability constant of cations for OH^- becomes smaller when moving down the periodic table ($Cs^+ < K^+ < Na^+ < Li^+$).[201] Thus, cesium bases yield a higher concentration of $[R_2B(OH)_3]Cs$ than do the smaller alkali. Additionally, the transmetallation step is faster when bases with counter cations of a high stability constant for halide anions ($Ag^+ > Tl^+ >> Ba^{2+} > Cs^+ > K^+$) are employed. [202]

As the presence of water greatly accelerates the reaction[203], aqueous solutions of bases (e.g. 2 M Na_2CO_3) or hydrated bases (e.g. $K_3PO_4*3H_2O$) are employed in the Suzuki cross-coupling reaction.

3.2.1.2.3 Organoboron Coupling Partner

The advantages of organoboron reagents are their high selectivity in cross-coupling reactions and the tolerance of functional groups on either coupling partners (hydroxy, amino, nitro, phenyl, ester, ketone, cyanide, aldehyde groups).[191,210a] In addition, they are in general thermally stable and inert to water and oxygen, thus allowing handling without special precautions.[191] The great variability of commercially available organoboron reagents makes the Suzuki reaction very attractive for the lead modification.

It has been confirmed that all kinds of carbon-boron bonds, i.e. (sp^3)C-B, (sp^2)C-B and (sp)C-B, can be employed as cross-coupling partners in coupling reactions. However, (sp^2)C-B derivatives remain the most used boron coupling partners.

Preparation and Coupling of Aryl- and Alkenylboron Derivatives

The classical synthesis of aryl- and 1-alkenylboronic acids or esters is the transmetallation of Grignard or lithium reagents to alkoxyborates. Subsequent treatment of the alkoxyborates with aqueous acid provides arylboronic acids (Scheme 3-8/A).[204] Arylboronic esters can be

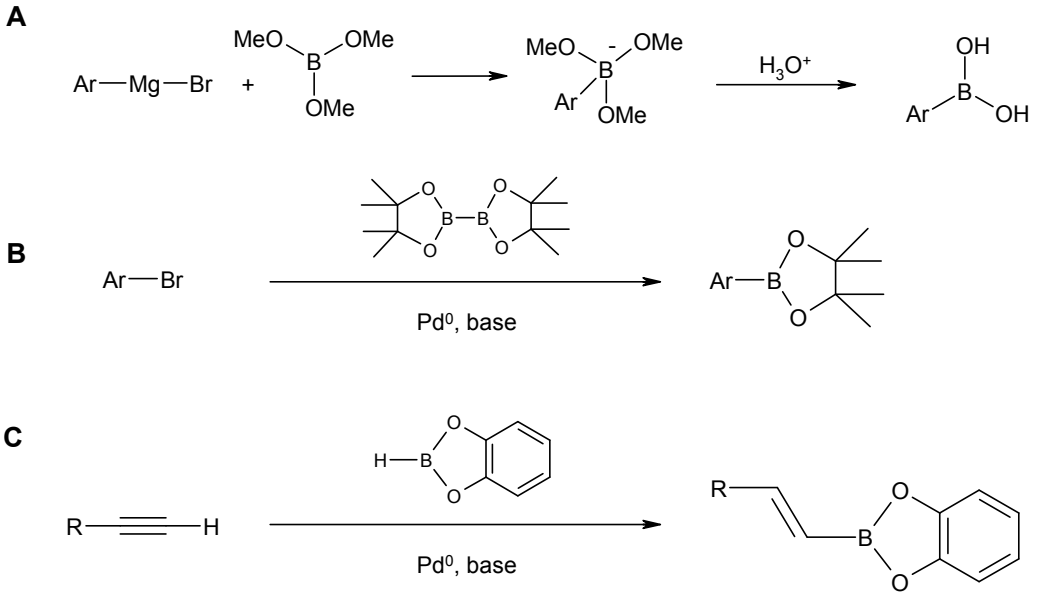

Scheme 3-8 Synthesis of (sp^2)C-B organoboron reagents [Ref. 204 – 206]

directly synthesized via cross-coupling of aryl halides/triflates with (alkoxy)diboron compounds (Scheme 3-8/B).[205] Hydroboration of a terminal alkyne with catecholborane produces 1-alkenylboronic ester (Scheme 3-8/C).[206]

Preparation and Coupling of Alkynylborane Derivatives

Sonderquist et al. reported that alkynyl(methoxy)borates **64** prepared *in situ* from an alkynyllithium and the B-methoxy-9-borabicyclo[3.3.1]nonane **65** (B-methoxy-9-BBN) are stable complexes that couple with 1-alkenyl (R2-X) and aryl halides (ArX) (Scheme 3-9/A).[207] An analogous reaction of an allylboronate complex **66** with arylhalides (ArX) affords allylarenes in high yields (Scheme 3-9/B).[208]

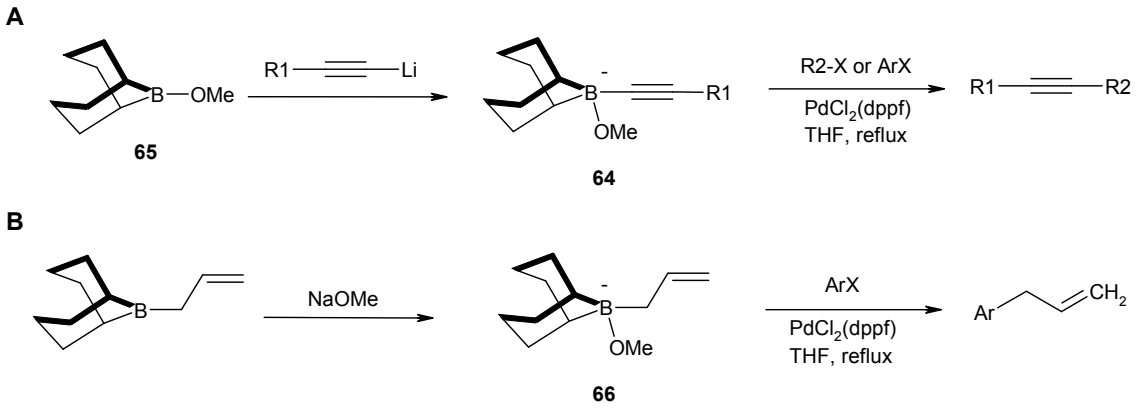

Scheme 3-9 Preparation and cross-coupling reaction of alkynyl **64** and allyl boron reagent **66** [Ref. 207, 208]

Preparation and Coupling of Alkylboron Derivatives

Hydroboration of terminal alkenes with 9-borabicyclo[3.3.1]nonane **67** (9-BBN) is the most convenient method to furnish the desired alkylboron reagents **68**[209], which are highly sensitive to air, but they can be used directly for subsequent coupling reaction without isolation (Scheme 3-10).

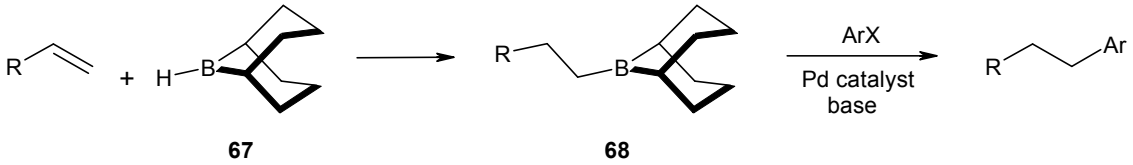

Scheme 3-10 Preparation and coupling of C(sp^3) organoboron reagent **68** [Ref. 209]

The tendency of the alkyl-palladium complex to undergo β-hydride elimination instead of reductive elimination can be prevented with the right choice of the catalyst, base and solvent. The most used ligand for alkyl-alkenyl, alkyl-aryl and alkyl-alkyl coupling is [$PdCl_2$(dppf)] or [$PdCl_2$(dppf)]/$AsPh_3$ and the use of aqueous base or hydrated inorganic bases (e.g. K_3PO_4*nH_2O) is recommended.[199] Solvents such as THF, DMF, dioxane or toluene are usually employed.

The connection of two fragments via the hydroboronation-cross-coupling sequence has found a wide range of applications in the synthesis of natural products.[210a] Danishefsky et al. have reported a total synthesis of the promising anticancer agent (-)-epothilone B using B-alkyl Suzuki-Miyaura coupling method as shown in Scheme 3-11 and a sister compound epothilone A was synthesized by a similar procedure.[210b-e] The key step is the hydroboronation of terminal alkene **69** which is directly followed by cross-coupling with iodoalkene **70** to furnish the desired *cis*-alkene **71**.

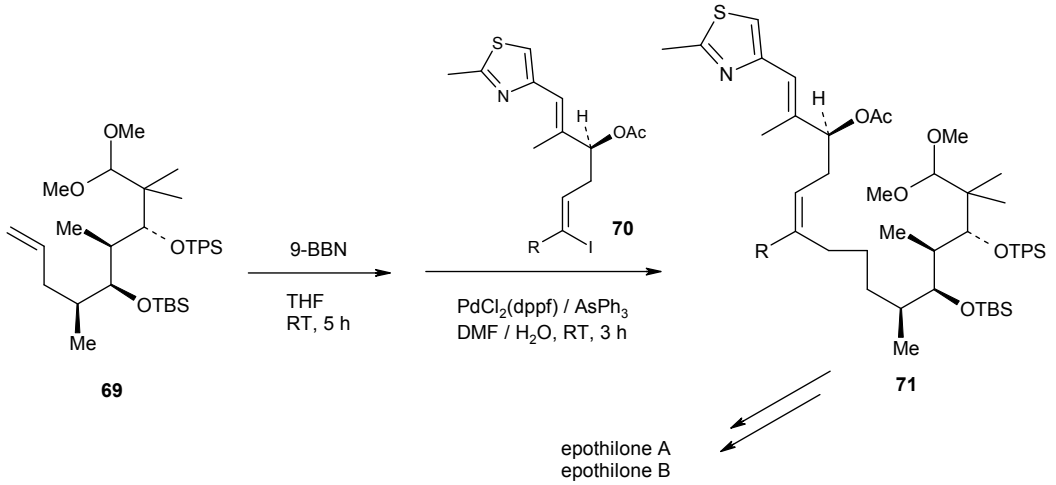

Scheme 3-11 Hydroboronation-cross-coupling sequence in the synthesis of the cytotoxic agents epothilone A and epothilone B [Ref. 210a-e]

3.2.1.2.4 Organic Halides / Pseudohalides as Coupling Partners

Aryl and alkenyl halides or triflates are mostly employed in the Suzuki coupling. Alkyl halides are not common substrates for the Suzuki reaction due to their slow rate of oxidative addition and their fast β-hydride elimination from the derived palladium intermediate. However, under the right conditions, alkyl halides will also react with organoboron coupling partners (see below).

Coupling of Aryl Halides

Aryl halides often used in the Suzuki reaction are bromides and iodides. Arylchlorides do not participate in the coupling reaction, except when used in conjugation with electron-deficient groups.[191a]

The first observed method to prepare biaryls is shown in Scheme 3-12.[186c] Various modifications (base, catalyst, solvent) of Suzuki protocol have been reported, but it can be concluded that the "standard" Suzuki conditions ($Pd(PPh_3)_4$/aq.Na_2CO_3/DME) work satisfactorily in most cases. The reaction is successful for aryl triflates, iodo- and bromoarenes and some of π-deficient heteroaryl chlorides.[191a]

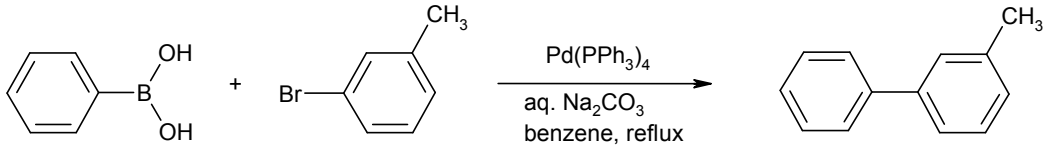

Scheme 3-12 First biaryl Suzuki cross-coupling reaction [Ref. 186a]

Noteworthy improvements of biaryl coupling during the years of investigation are e.g. Suzuki coupling of extremely sterically bulky boronic acid with halopyridines in non-aqueous solvent with potassium *t*-butoxide giving the best result among the bases examined[211], ambient temperature Suzuki-type biaryl coupling[212], "ligandless" $Pd(OAc)_2$-catalysed biaryl formation in water in the presence of tetrabutylammoniumbromide (TBAB)[213] or synthesis of axially chiral biaryls.[214]

Coupling of Alkenyl Halides

Cross-coupling reactions of 1-alkenylboron compounds with 1-alkenyl halides afford stereodefined dienes, trienes and further conjugated polyenes. 1-alkenylboronic acids couple with iodoalkenes when relatively strong base (TlOH > NaOH > K_3PO_4 > Na_2CO_3 > NaOAc)[215] and a phosphine-based Pd-catalyst ($Pd(PPh_3)_4$ or $PdCl_2(PPh_3)_2$) are employed.[216] Thallium

hydroxide is an excellent base that enables completion of the alkenyl-alkenyl coupling within few hours even at room temperature.[217] The protocol has been successfully used for a number of syntheses of natural products, including (-)-bafilomycin A.[218]

Coupling of Alkyl Halides

Iodoalkanes were reported to react with alkyl boranes in the presence of K_3PO_4 and catalytic amounts of tetrakis(triphenylphosphine)palladium. The reaction was performed in dioxane and generated corresponding coupling products in moderate to good yields (45% – 71%). $PdCl_2$(dppf) did not act as an efficient catalyst in this protocol.[210a]

Coupling of Triflates

Triflates (trifluoromethanesulphonates) have been discovered to undergo cross-coupling with organoboron compounds in the same way as coupling with organostannanes, aluminium or zinc compounds.[219] The triflates are easily accessed from phenols or carbonyl enolates.[220] Catalysts such as $PdCl_2$(dppf) or $Pd(PPh_3)_4$ and powdered K_3PO_4 suspended in THF or dioxane result in successful coupling of triflates with arylboronic acids.[191]

3.2.2 Suzuki vs. Stille Cross-Coupling Reaction

Palladium-catalysed cross-coupling of organotin reagents with organic electrophiles, alias Stille reaction[221], is shown in the Scheme 3-13. This reaction is very similar to the Suzuki cross-coupling, but alkyltin reagents are used instead of boronic acids.

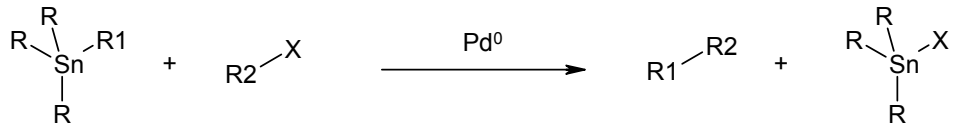

R = Me, n-Bu
R1 = alkyl, aryl R2 = aryl, vinyl product unwanted byproduct

Scheme 3-13 Stille cross-coupling reaction [Ref. 221]

Catalytic cycle of Stille coupling follows the one of the Suzuki coupling, i.e. the first step is oxidative addition of R2-X to the active palladium species (PdL_2) to give R2-PdL_2-X, followed by transmetallation to give R1-PdL_2-R2 and finally reductive elimination to give R1-R2.[222] This catalytic cycle performs well in THF, HMPA[223], NMP[222] or in ionic liquids[224]. $Pd(PPh_3)_4$ is referred to as “traditional favourite”, while $PdCl_2(PPh_3)_2$ is the “traditional” catalyst.[222] Addition of CuCl or LiCl to $Pd(PPh_3)_4$ or $ZnCl_2$ to $PdCl_2(PPh_3)_4$ was reported to increase yields of the coupling reactions.[225]

Stille cross-coupling is a very flexible and versatile chemical reaction as organotin coupling partners can be synthesized from any bromine involving organic compound. Recently, this reaction has attracted many chemists working on the total synthesis of natural products.[226] For example, a stannylpyridine **72** was used in the key step of the synthesis of (±)-epibatidine **19** (Scheme 3-14).[227]

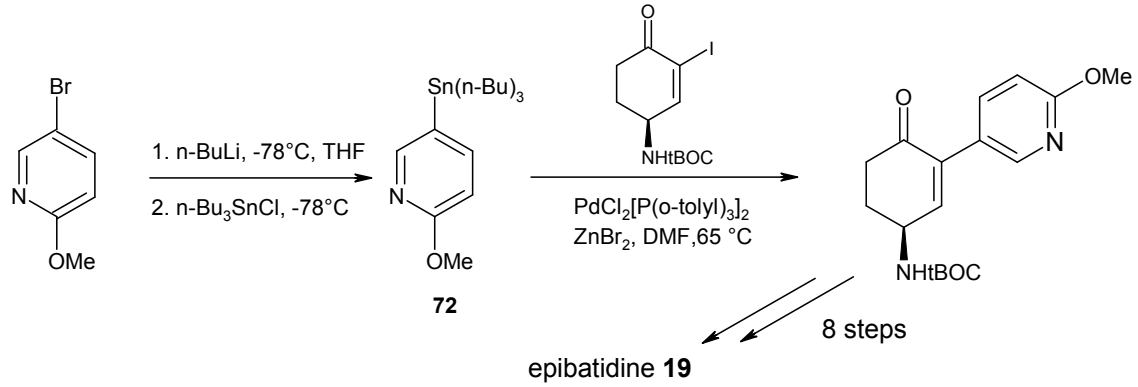

Scheme 3-14 Stille cross-coupling in the total synthesis of (±)-epibatidine **19** [Ref. 227]

However, it is important to point out, that the organotin compounds are highly toxic and the presence of the organotin residue ("unwanted byproduct") hampers the purification of the desired product, since the separation of tin compounds present in the reaction mixture is rather difficult. An ideal reaction system would be one in which the product can be obtained free from byproducts, but such a system has not been reported so far.

On the other hand, organoboron reagents employed in the Suzuki reaction are non-toxic, commercially available and coupling products can be obtained in very high purity, given that the right purification methods are applied (e.g. high performance liquid chromatography).

3.2.3 Suzuki Reaction in Microwave Assisted Organic Synthesis

Traditionally, organic synthesis is carried out by conductive heating with an external heat source (oil bath). This is a comparatively slow and inefficient method for transferring energy into the system since it depends on the thermal conductivity of various materials that must be penetrated. In 1986, two independent groups reported accelerating effects of microwaves in the organic synthesis[228], but the research in this field had not boomed until the late 1990s. The use of domestic microwave appliances was lacking the control of temperature and pressure, meaning that the risk of flammability of organic solvents was high. Besides, results obtained in "kitchen" microwave ovens had very low reproducibility. The introduction of microwave reactors designed for organic synthesis with efficient temperature and pressure

control system did not only increase the safety of microwave synthesis in the laboratories, but also led to reproducible synthetic conditions. As expected, this resulted in a real "microwave boom" and microwave assisted organic synthesis (MAOS) has attracted a great amount of attention in last 5 years, which is documented in several reviews[229] and books[230]. Several research groups, e.g. of Hallberg and Larhed (Uppsala University), Leadbeater (Kings College, London) or Kappe (Karl-Franzens University, Graz) have demonstrated over the past decade that the microwave heating greatly accelerates transition-metal-catalysed carbon-carbon bond forming, including the Suzuki cross-coupling reaction.

3.2.3.1 Microwave

A microwave is a form of electromagnetic energy in the frequency range of 0.3 to 300 GHz. All domestic "kitchen" microwaves and all microwave reactors used for industrial, scientific or medical applications operate at a frequency of 2.45 GHz (which corresponds to a wavelength of 12.24 cm) to avoid interference with telecommunication and cellular phone frequencies. Microwaves move at the speed of light (300,000 km/sec) and the energy of microwave photon in this frequency region is 0.037 kcal/mole.[229,230] This energy is very low compared to the typical energy required to break chemical bonds (80-120 kcal/mole), thus it is clear that microwaves cannot affect the structure of an organic molecule and induce a chemical reaction.[231,232]

3.2.3.2 Microwaves as a Heating Source in Organic Synthesis

Although some chemical reactions proceed under ambient conditions, in most cases the organic synthesis is carried out at high temperature and the definition from the chemistry dictionary[233] of N. Macquer edited in 1775 "*All the chemistry operations could be reduced to decomposition and combination; hence, the fire appears as an universal agent in chemistry as in nature*" is still valid.

The conventional heating source - the oil bath - produces slow conductive heating, i.e. the heat is driven into the substance passing through the walls of the vessel in order to reach the solvents and reactants and it is dependent on the thermal conductivity of materials that have to be penetrated. Until the thermal equilibrium is achieved, the temperature of the vessels is higher than the temperature of the reaction mixture and overall, the control of the chemical reaction is rather difficult.[230a]

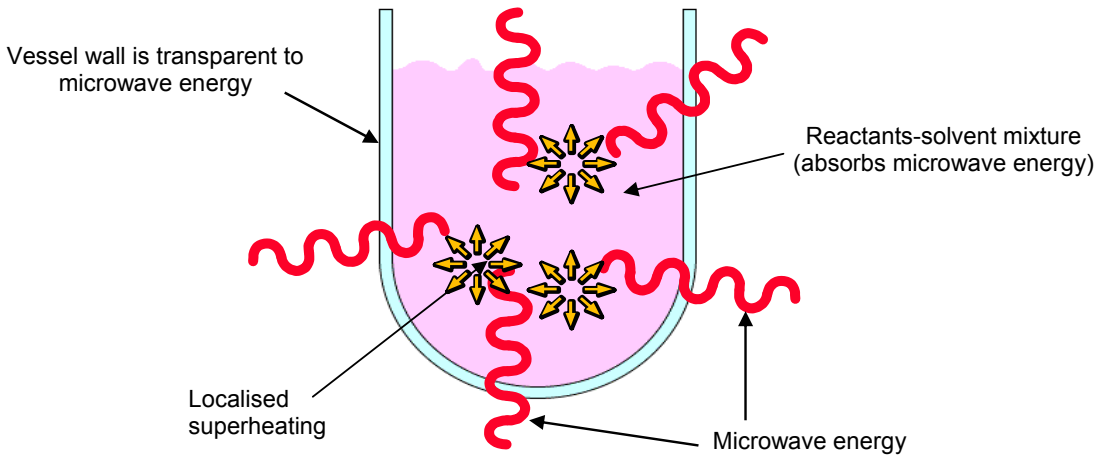

Figure 3-6 Schematic presentation of heating the reaction mixture with microwaves [Ref. 230a]

In contrast, microwave irradiation generates efficient internal heating by direct coupling of microwave energy with the molecules (solvents, reagents, catalysts) that are present in reaction mixture. Because this process does not depend on the thermal conductivity of the vessel materials, the result is an instantaneous localised superheating of any molecule that couples with microwaves (Figure 3-6). [234]

The electric component of the electromagnetic field of the microwave causes heating by two main mechanisms – dipole rotation (dipolar molecules rotate to align themselves with the fluctuating electric field of the microwave) and ionic conduction (migration of dissolved ions with the oscillating electric field).[229,230]

The ability of a particular substance to heat under microwave irradiation conditions is dependent upon two factors. The first one is the efficiency with which the substance absorbs the microwave energy, described by dielectric constant ε', also known as the relative permittivity, a value dependent on both temperature and frequency. The second factor is the efficiency with which the absorbed energy can be converted to heat, described by the loss factor ε''. The ability of a specific substance to convert electromagnetic energy into heat at a given frequency and temperature is determined by loss tangent or tangent delta (**tan δ**). It is expressed as the tangent of the ratio of the loss factor and the dielectric properties (Eq. 1).[235]

$$\tan \delta = \varepsilon'' / \varepsilon' \qquad \text{(Eq. 1)}$$

Solvents with a high **tan δ** value efficiently absorb the microwave energy and will, therefore, provide rapid heating. The loss factors for some common organic solvents are summarised

Table 3-4 Loss tangent (tan δ) of different solvents, measured at 2.45 GHz and 20°C*

Solvent	tan δ	Solvent	tan δ
high absorbing	> 0.5	DMF	0.161
ethylene glycol	1.350	1,2-dichloroethane	0.127
ethanol	0.941	water	0.123
DMSO	0.825	chlorobenzene	0.101
2-propanol	0.799	low absorbing	< 0.1
formic acid	0.722	chloroform	0.091
methanol	0.659	acetonitrile	0.062
nitrobenzene	0.589	ethyl acetate	0.059
1-butanol	0.571	acetone	0.054
medium absorbing	0.5 – 0.1	tetrahydrofuran	0.047
2-butanol	0.447	dichloromethane	0.042
1,2-dichlorobenzene	0.280	toluene	0.040
NMP	0.275	hexane	0.020
acetic acid	0.174		

*) Data from Ref. 230a

in Table 3-4. In general, solvents can be divided into three groups: high (**tan δ** > 0.5), medium (**tan δ** 0.1 – 0.5) and low microwave absorbing (**tan δ** < 0.1). Less polar or non-polar solvents, such as carbon tetrachloride, benzene and dioxane, are more or less microwave transparent. However, the addition of polar substances/mediums (e.g. fluid salts or ionic liquids) significantly increases the absorbance level of the reaction environment.[230a]

Some microwave-enhanced reactions have produced different products than the conventionally heated counterpart synthesis carried out at the same temperature. These findings have led to speculation on existence of “specific” or “non-thermal” microwave effects.[236] Although this topic has been intensely discussed[237], there is a general agreement that rate enhancement observed in MAOS is merely due to the superheating effect of microwave irradiation. The unique microwave dielectric heating mechanism can rapidly superheat solvents at atmospheric pressure above their boiling points (up to 26°C above the conventional boiling point) and this cannot be achieved with any conventional heating.[229c]

3.2.3.3 Microwaves in Suzuki Cross-coupling Reaction

High-speed Suzuki coupling carried out under controlled microwave conditions has been known for several years. In 1996, Larhed and coworkers[238] coupled 4-methylphenyl bromide **73** and phenyl boronic acid **74** in less than 4 min, showing that microwave irradiation indeed shortens reaction times from hours to minutes (Scheme 3-15). More interestingly, the reaction worked smoothly on solid support affording high yields of products.[239]

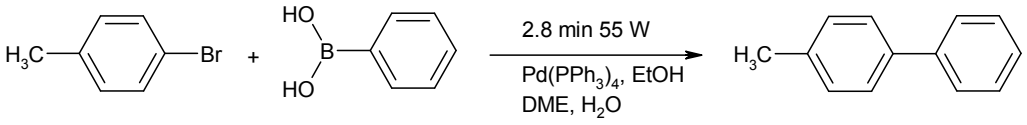

73 **74**

Scheme 3-15 First microwave promoted Suzuki reaction [Ref. 238]

A significant advance in Suzuki chemistry has been the observation that the coupling reaction can be carried out using water as the solvent in conjunction with microwave heating. Water is cheap, readily available nontoxic solvent with a high loss tangent (tan δ) making it an excellent solvent for microwave-mediated synthesis. Water as a solvent has been used in the synthesis of poly(ethyleneglycol)-esterified biaryls via Suzuki cross-coupling under the "ligandless" (i.e. no ligands such as PPh_3 present in the reaction mixture) palladium acetate-catalysed condition.[240] Also Leadbeater and Marco described very rapid, ligand-free palladium-catalysed aqueous Suzuki couplings of aryl halides (including chlorides) with aryl boronic acids.[241] The common drawback of using water as a solvent (limited solubility of substrates and stability of metal catalyst in aqueous medium) has been overcome by the use of 1.0 equivalent of tetrabutylammonium bromide (TBAB) as a phase-transfer catalyst. The addition of TBAB facilitates the solubility of organic substrates and activates the boronic acid by formation of $[R_4N]^+[ArB(OH)_3]^-$. Under these optimised reaction condition various aryl halides were coupled with aryl boronic acids within 5 min (Scheme 3-16).[241]

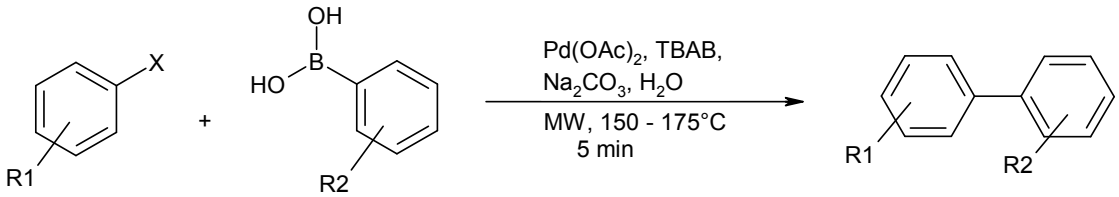

Scheme 3-16 Ligand-free Suzuki reaction with TBAB as an additive [Ref. 241]

Deactivated, non-activated and activated aryl chlorides (normally not efficient coupling partners) were shown in another study to undergo coupling with boronic acids, when microwave energy is used for heating. The reactions were performed in 1,4-dioxane in the presence of 2 equivalents of K_3PO_4.[242] However, microwaves brought the most unexpected development in the Suzuki chemistry via a breakthrough discovery by Leadbeater and Marco indicating that the "Suzuki reaction takes a naked hot bath".[244] They reported a successful coupling of aryl bromides (e.g. **75**) and iodides with electron-poor or electron-neutral boronic acids (e.g. **74**) in the water without a palladium catalyst (Scheme 3-17). The transition-metal-free aqueous Suzuki-type coupling again utilised 1.0 equivalent of TBAB as an additive, 3.8 equivalents of Na_2CO_3 as a base and 1.3 equivalent of corresponding boronic acid.[243] This astonishing finding denies the long understanding of the mechanism of aryl-aryl couplings of aryl halides in which a transition metal is required to break the strong C(sp^2)-X bond. The exact mechanism of this novel transformation remains unknown, but there are various speculations. One possibility is that the reaction occurred through a radical mechanism.[244]

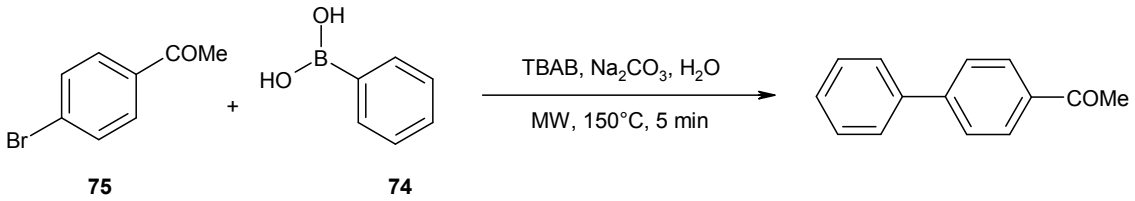

75 **74**

Scheme 3-17 Transition-metal-free Suzuki-type coupling [Ref. 243]

In summary, the beneficial impact of microwave irradiation on Suzuki coupling (shorter reaction time, higher yield and cleaner reaction environment) has been well established and the use of microwaves in the organic synthesis is limited only to the high equipment costs.

3.2.4 Isolation of Cytisine

3.2.4.1 Introduction

In Europe cytisine **27** may be easily isolated from seeds of *Laburnum anagyroides medicus* (*Fabaceae)*[182,184,245] known as "Goldregen" in Germany. This bushy plant or small tree contains the highly toxic alkaloid **27** with the greatest amount found in black seeds.

Protocols describing the extraction of cytisine **27** from the seeds of *L. anagyroides* follow the general method of alkaloids isolation and vary basically only in the type of solvent or acid/base used (Table 3-5). The yields of the isolation alter (0.1% to 1.8% reported in the literature)[182,184,245] and cannot be taken as a consequence of the chosen method of isolation. The content of cytisine **27** is believed to be influenced by the age of the plant and climatic conditions. Additionally, *L. anagyroides* has been often replaced by hybrid *Laburnum* x *watereri*, with a significantly lower amount of the main alkaloid **27**, in order to prevent intoxication by cytisine **27**.[143]

Table 3-5 Selected procedures used for cytisine **27** extraction from *Laburnum anagyroides* as reported in the literature [Ref. 182, 184, 245]

	Bojadshiewa et al.[245]	**Marriére et al.**[184]	**Klaperski**[182]
seeds dissolved in	perchlorethylene	CH_2Cl_2 /MeOH	$CHCl_3$
alkalization	10% NH_4OH	25% NH_4OH	10% KOH
acidification	5% H_2SO_4	0.5 N HCl	1% HCl
alkalization	25% NH_4OH	25% NH_4OH	10% KOH
extraction	$CHCl_3$	CH_2Cl_2	CH_2Cl_2
flash chromatography	---	CH_2Cl_2/MeOH/NH_4OH 85 : 15 : 1	$CHCl_3$/MeOH 5 : 1
recrystallization	perchlorethylene	---	---

3.2.4.2 Method / Results

The enantiopure cytisine **27** needed for further synthesis was isolated from the seeds of *Laburnum anagyroides* and *watereri*, collected in the Köln/Bonn area during September and October. Air-dried plant materials were extracted with a mixture of dichloromethane, methanol and 25% ammonia through Ultra-turrax homogenization. The extracts were concentrated under reduced pressure and extracted with 1M hydrochloric acid. The aqueous acid solution was made alkaline with ammonium hydroxide and extracted at least 10 times with dichloromethane. The organic solvent was evaporated *in vacuo* and the brown thick

residue was chromatographed on a silica gel column using mixture of chloroform and methanol as a mobile phase. Recrystallization from perchlorethylene afforded cytisine **27** as light yellow crystals (0.11% – 0.48%), which was used for spectroscopic analysis and further synthesis.

3.2.4.3 Discussion

This isolation protocol was based on the procedure published by Marriére *et al*[184], however it was modified at few steps. The time of ultra-turrax homogenization and subsequent maceration was extended from 1 hour to 8 hours and 1 M hydrochloric acid was used for acidification. For the flash chromatography a mixture of $CHCl_3$/MeOH was used. However, in this way obtained cytisine **27** did not possess satisfying purity and more purification steps were required. Recrystallization from perchloroethylene afforded cytisine **27** as light yellow crystals in 0.11% – 0.18% yields. Much higher yields were achieved when seeds were separated from their pouches before the actual extraction (0.27% – 0.48%). Seeing that perchlorethylene is a highly toxic solvent, circumvention of its usage was necessary. Therefore, the recrystallization was replaced by high performance liquid chromatography (HPLC) purification of the N-protected cytisine, i.e. cytisine **27** obtained after flash chromatography was directly used in the next step (the protection of the bispidine nitrogen) and purified with HPLC (see Chapter 3.2.5).

3.2.5 Protection of the Secondary Amino Group of Cytisine

3.2.5.1 Introduction

The lone electrons pair on the amino group may be easily protonated and is generally reactive towards electrophiles. In order to decrease the reactivity of this functional group, it is usually converted to an amide or a carbamate, since the carbonyl group effectively withdraws electron density from the nitrogen and renders it unreactive.[246]

Many amine protecting groups of the carbamate (-NCOOR) or of the amide (-NCOR) type have been developed. *tert*-Butoxycarbonyl (*t*BOC) protective group is an example of protecting groups of carbamate type and is widely used for protection of secondary amines. *tert*-Butoxycarbonyl group is introduced with reagents such as di-tert-butoxycarbonate[247] or *t*-BOC-azide[248]. *t*BOC protective group is not hydrolysed under basic conditions and is inert to many nucleophilic reagents.[249] These characteristics make *t*-butyl carbamate a perfect protective group of the secondary amine in cytisine **27**, which is later employed in the Suzuki reaction, carried out in the presence of a base and with nucleophilic organoboron coupling partners.

The synthesis of N-*t*BOC-cytisine **76** had been reported and provided useful information for fast and efficient synthesis of the N-protected alkaloid **76**.[124,125] The protection was performed with di-*tert*-butoxycarbonate in a presence of aqueous sodium carbonate solution, THF or dichloromethane were used as solvents. The reaction times differ extremely – the protection was quantitative after 48 hrs, when THF was employed[125] and after 90 min, when dichloromethane was used[124]. Other protecting groups (-NO, -COOMe) for the secondary amine of cytisine **27** were reported as well.[184]

3.2.5.2 Method / Results

N-*t*BOC-protected alkaloid **76** from crystalline cytisine **27** was easily prepared by employing 1.2 eq of di-*tert*-butylcarbonate and sodium carbonate (Scheme 3-18). The product was recrystallised from petroleum ether and obtained in high yields (77% – 90%).

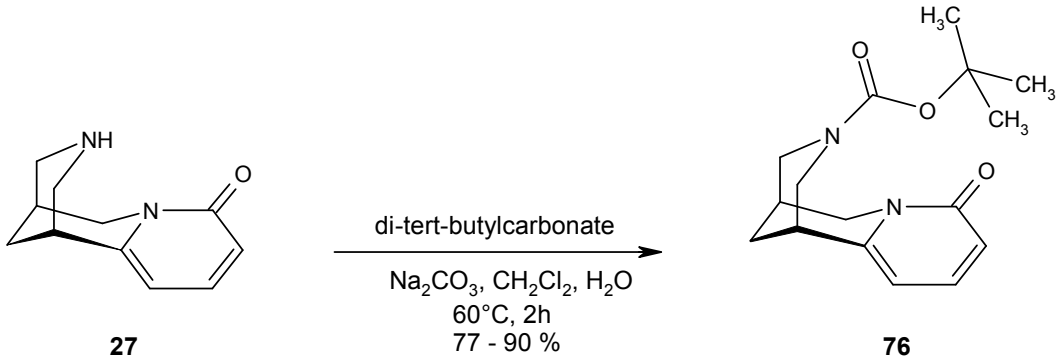

Scheme 3-18 Synthesis of *t*BOC-protecting cytisine **76**

In the second method, the introduction of the protecting group was part of the isolation/purification process. Herein, cytisine **27** obtained after flash chromatography was dissolved in dichloromethane and treated with an excess of aqueous sodium carbonate and di-*tert*-butyldicarbonate at reflux temperature. The reaction was monitored by TLC in order to achieve quantitative substitution. The N-protected alkaloid **76** was purified with HPLC using isocratic methanol/water mixture (60:40 v/v) on a reverse phase C18 (RP-C18) column (t_r = 6.9 min). The combined aqueous fractions of product were concentrated under reduced pressure and the remaining solvent (i.e. water) was removed by lyophilization for at least 24 hours. The amount of isolated alkaloid **27** was calculated from the quantity of N-*t*BOC-cytisine **76**. Yields represent ratio of cytisine **27** amount to the quantity of plant material (1,000 g) and are listed in the Table 3-6.

Table 3-6 Amount of cytisine **27** calculated from the amount of N-*t*BOC-cytisine **76**. Yields calculated as the ratio of cytisine **27** quantity to the amount of plant material (1,000 g)

Experiment	N-*t*BOC-cytisine **76**	Cytisine **27**	Yields
1	1.80 g	~ 1.18 g	0.12%
2	1.76 g	~ 1.15 g	0.11%
3	2.70 g	~ 1.77 g	0.17%
4	2.30 g	~ 1.51 g	0.15%
5	2.06 g	~ 1.35 g	0.13%

3.2.5.3 Discussion

Using crystalline cytisine **27**, the reaction was performed in dichloromethane with 1.2 eq of di-tert-butoxycarbonate and sodium carbonate as a base. The product **76** was recrystallised from petroleum ether and obtained in high yields (77% – 90%).

In order to avoid the use of perchloroethylene (in the isolation step), the brownish cytisine **27** obtained after flash chromatography was dissolved in dichloromethane and treated with an excess of aqueous sodium carbonate and di-*tert*-butoxycarbonate. The reaction was stopped when the quantitative substitution was achieved (monitored by TLC). The N-protected alkaloid **76** was purified with HPLC and obtained as white crystalline powder. The yields of this isolation/purification process were ranging from 0.11% to 0.17% and were identical to the yields of extraction, when perchlorethylene was used for recrystallization (0.11% – 0.18%). The results demonstrate that protection of the N-12 as a part of the isolation process improved the known conventional methods of cytisine **27** purification. The alkaloid **27** (in the N-*t*BOC- protected form **76**) was obtained in the same yields, but in higher purity and without using highly toxic solvent.

3.2.6 2-Pyridone Scaffold

Since all of the following chemistry includes modification of the 2-pyridone moiety of the cytisine **27**, a short review of this structure is given here. Many naturally occurring and synthetic compounds contain a 2-pyridone ring and its chemistry is well documented.[250-267]

Among the naturally occurring substances which incorporate the 2-pyridone nucleus are e.g. ricinine[250], fredericamycin A[251] and tenellin.[252] Camptothecin **77** (Figure 3-7), isolated from the tree *Camptotheca acuminata* Decne *(Nyssaceae)* possesses antileukemic activity[253] and its decarboxylated E-ring analogue, mappicine ketone (MPK) was shown to possess potent activity against the herpesviruses HSV-1, HSV-2 and human cytomegalovirus.[254] The 2-pyridone ring can be also found in the structure of paraensidimerins **78** (Figure 3-7) and

vepridimerins, a large group of dimeric quinoline alkaloids.[255] Additional members of this group are quinolizidine alkaloids cytisine **27** and anagyrine.

2-Pyridone scaffold is further present in a specific non-nucleoside reverse transcriptase inhibitor of human immunodeficiency virus-1 L-697,661 (Figure 3-7)[256] or in the structure of cardiotonic agents Milrinone **79** and Amrinone **80** displaying selective PDE-3 inhibitor activity (Figure 3-7).[257] Some 2-pyridones are also reported to be human rhinovirus (HRV) 3C protease (3CP) inhibitors.[258] 3-Aryl-2-pyridone derivatives were designed and tested as selective kappa opioid receptor agonists.[259]

However, the vast majority of papers discuss synthetic approaches to 2-pyridones[253-255,258,260] and only very few papers involve the Suzuki coupling performed on the pyridone moiety.[259,262,263,266,267] The latter reactions are discussed together with the coupling reactions on the cytisine backbone and are divided into Chapters 3.2.8 and 3.2.9, concerning the position of the substitution.

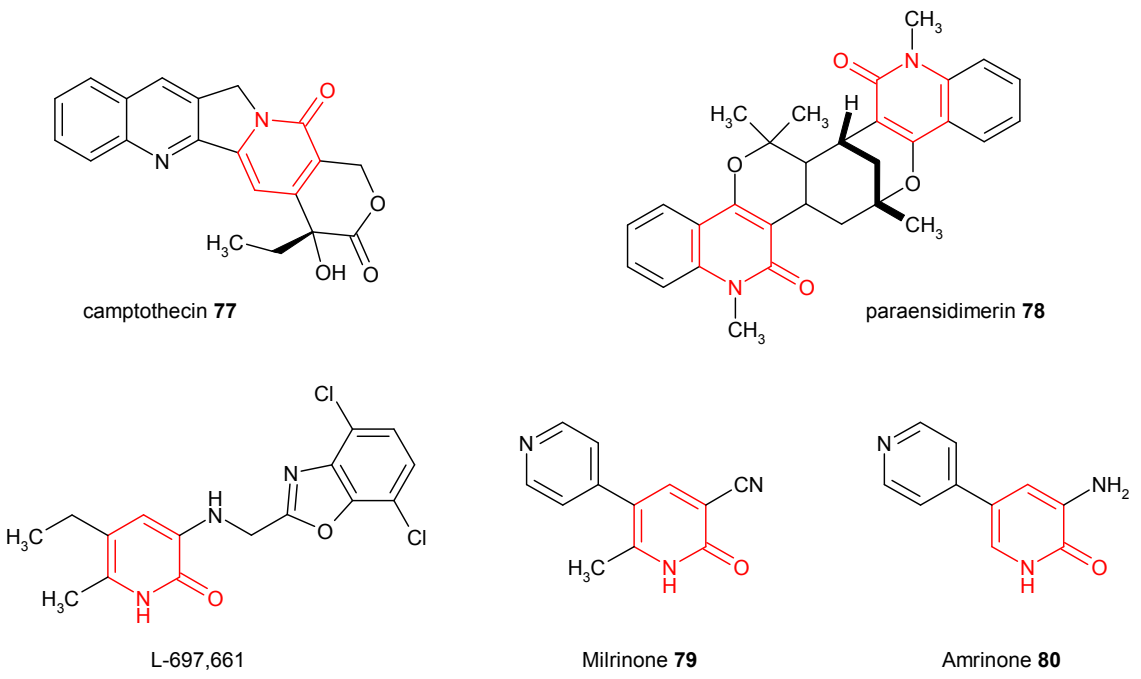

Figure 3-7 Structure of pharmacologically interesting compounds possessing 2-pyridone scaffold (in red) [Ref. 253, 255 - 257]

3.2.7 Bromination of Cytisine

3.2.7.1 Introduction

The target molecules - (hetero)aryl analogues of cytisine – were planned to be synthesized via a palladium-catalysed Suzuki reaction. In a cross-coupling reaction one coupling partner possesses a halide or a pseudohalide while the other coupling partner is an organoboron reagent. As the arylboronic acids are commercially available in great variety, only the type of halide/pseudohalide that should be introduced into the molecule of N-*t*BOC-cytisine **76** was considered. The synthesis of a triflate derivative requires hydroxyl or carbonyl group[193] and the introduction of any of them into the structure of cytisine **27** could be a multistep chemical challenge.

Halogenation, e.g. bromination of cytisine **27** offers a simpler, faster route for the preparation of a cytisine-derived coupling partner. Bromination can be done with elementary bromine, which has an advantage of an easy control of the dosage and the high selectivity.[261] However, elementary bromine is too expensive for technical purposes and has been replaced by other bromination agents, such as bromotrichloromethane, *t*-butylhypobromit or N-bromosuccinimide (NBS). NBS is widely used in free radical, allylic or benzylic brominations and also for the electrophilic substitution of aromatic rings.[261]

Semple *et al*[259a] prepared 3-bromopyridone by treatment of 2-pyridone with bromine in KBr solution, however in low yields (22%). For the halogenation of the position 5 of 2-pyridone scaffold N-bromosuccinimide was employed and the desired product was obtained in 55% yields. 3-Bromo and 5-bromopyridone were successfully coupled with a wide range of boronic acids under Suzuki conditions.[259a]

Bromination of cytisine **27** has been previously reported.[118,124,174,182,184] Excess of bromine in acetic acid afforded 3,5-dibromocytisine **46**.[174] Similarly, avoiding the introduction of protecting groups, monobrominated cytisine derivatives **40** and **43** were prepared by treatment of cytisine **27** in aqueous acetic acid with one equivalent of NBS.[118,182] Using a manifold excess of bromine transfer reagent, 3,5-dibromocytisine **46** predominated.[118,182] Other studies[124,184] performed bromination after protecting the secondary amine group of cytisine **27**. N-protected alkaloid **76** was treated with NBS in different solvents (CH_2Cl_2, DMF, MeCN, H_2O/H^+) and the influence of the solvent on the 3-bromo/5-bromocytisine ratio was studied. The substitution time was 30 – 90 minutes.

3.2.7.2 Method / Results

Bromination of the pyridone ring was carried out with N-bromosuccinimide in dichloromethane. Adding one equivalent of NBS, a mixture of two monosubstituted isomers, namely 3-bromo-N-*t*BOC-cytisine **81** and 5-bromo-N-*t*BOC-cytisine **82** was obtained (Scheme 3-19).

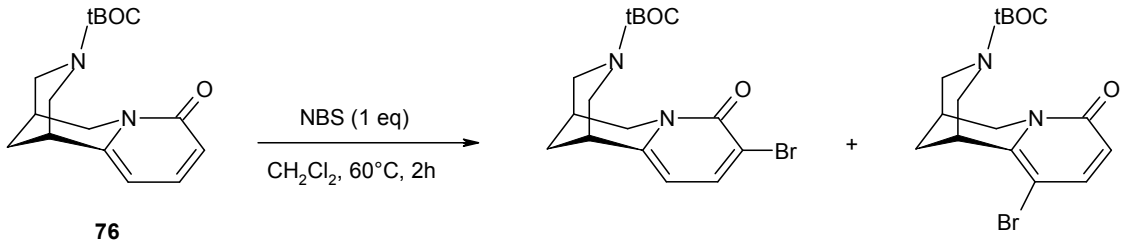

76 **81** 38.0 - 51.4 % **82** 28.1 - 42.2 %

Scheme 3-19 Synthesis of monobrominated analogues of cytisine **81** and **82**

The separation of the two regioisomers **81** and **82** was successfully performed with HPLC using isocratic MeOH/H_2O mixture as a mobile phase. The compounds **81** (38.0% – 51.4%) and **82** (28.1% – 42.2%) were obtained as white crystalline powders that were further used for the coupling reaction.

Bromine transfer reagent in a twofold excess afforded a third product, 3,5-dibromo-N-tBOC-cytisine **83**, next to the small quantity of monobrominated isomers **81** and **82**. The reaction products were easily separated on a RP-C18 column with methanol/water mixture as a mobile phase and dried via evaporation and lyophilization of the solvents. The yields of this reaction are listed in Table 3-7.

Table 3-7 Yields of monobrominated and dibrominated cytisine derivatives **81** – **83** when 2 eq of NBS were applied

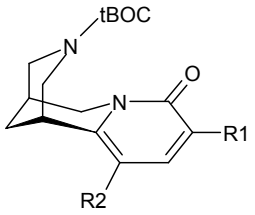

Cpd.	R1	R2	Yields
81	Br	H	19.8%
82	H	Br	13.2%
83	Br	Br	42%

3.2.7.3 Discussion

When one molar equivalent of NBS was used, the reaction afforded two monosubstituted regioisomers, 3-bromo-N-*t*BOC-cytisine **81** (43%) and 5-bromo-N-*t*BOC-cytisine **82** (32%). The resulting mixture was successfully separated with preparative high performance liquid chromatography (HPLC). This method showed a clear advantage over the purification and separation of the products on silica gel (CH_2Cl_2/MeOH 99:1), which had been performed before the HPLC method was established. The similar lipophilicity of isomers **81** and **82** resulted in close R_F values (R_F = 0.21 and 0.33 for **81** and **82**, respectively, CH_2Cl_2/MeOH 99:1), thus complicating the separation of the isomers. The 3-bromo isomer **81** contained 5-bromo isomer **82** and vice versa. On the other hand, RP-C18 phase and automatization yielded each isomer in a high purity.

3-Bromo analogue **81** has been obtained in higher yields than the corresponding 5-substituted derivative **82**, which is in agreement with literature.[124,184] The ratio of 3- and 5-regioisomers seems to be dependent not only on the solvent used for the reaction,[184] but also on the nature of the protecting group (Table 3-8). Bromination of the N-12 protonated cytisinium acetate gave the isomers in the same yields (27%, Table 3-8)[118], while protection of the nitrogen with -*t*BOC or –COOMe yielded 3-bromo isomer in higher yields compared to its 5-halogenated counterpart (Table 3-8).[184] However, using *t*BOC as a protecting group and CH_2Cl_2 as a solvent showed the advantage of obtaining smaller 3-/5-isomer ratio (1.34) compared to the 2.10 ratio, when the bromination was performed in dichloromethane on the –COOMe-protected cytisine (Table 3-8).[184] Thus, the conditions described herein offer so far the best protocol for the synthesis of 5-bromo-N-*t*BOC-protected cytisine derivative **82**.

Table 3-8 Yields of monobrominated regioisomers in different solvents and with different N-protecting groups, using 1 eq of NBS

Solvent	Protecting group	3-bromo isomer [%]	5-bromo isomer [%]	3,5-dibromo analogue [%]	3- / 5-ratio
CH_2Cl_2	-*t*BOC	43[a]	32[a]	0	1.34
60% CH_3COOH[b]	none	27	27	5	1.00
CH_2Cl_2[c]	-COOMe	65	31	4	2.10
MeCN[c]	-COOMe	72	19	9	3.79
DMF[c]	-COOMe	73	23	2	3.17
H_3O^+[c]	-COOMe	75	18	5	4.16
THF[c]	-COOMe	85	15	0	5.66

a) average of 8 experiments, SEM = ± 5.2 for the 3-isomer; SEM = ± 5.9 for the 5-isomer
b) taken from Ref. 118
c) taken from Ref. 184

Adding two molar equivalents of the halogenating agent, the product **83** predominates, but the monobrominated isomers were obtained as well (**81**/**82**/**83** 20%/13%/42%). Imming et al. reported nearly quantitative substitution of both positions (3 and 5) when manifold excess of the NBS was employed.[118] The yield of 3,5-dibromo-N-*t*BOC-cytisine **83** did not increase with an extended reaction time (up to 5 hrs) or an addition of N-bromosuccinimide (up to 4 mmol).

3.2.8 3-Phenyl Analogues of Cytisine

3.2.8.1 Introduction

Pfizer claimed synthesis of 3-phenyl-cytisine and a series of 3-aryl analogues of cytisine via Suzuki cross-coupling reaction.[124] In this route, firstly N-*t*BOC-cytisine-3-boronic acid **84** was prepared from bromine counterpart **81** via n-BuLi promoted transmetallation with triisopropylborate **85** (Scheme 3-20). The boronic acid of the alkaloid was subsequently coupled with (hetero)arylbromides (e.g. **86**) using the standard Suzuki conditions $Pd(PPh_3)_4/Na_2CO_3$ in ethanol/water solution. The protecting group was removed by treatment with trifluoroacetic acid in methylene chloride and the final products were obtained as hydrochlorides.[124] A synthesis of 3-(2,6-difluorophenyl)cytisine hydrochloride **87** shown in the Scheme 3-20 is an example of this method. Although the patent literature disclose a large number of cytisine derivatives, only limited NMR analysis data are available and the information about yields is missing. The structures of the analogues were confirmed merely with high-resolution mass spectrometry (HRMS). Therefore, it is difficult to evaluate the success of this protocol.

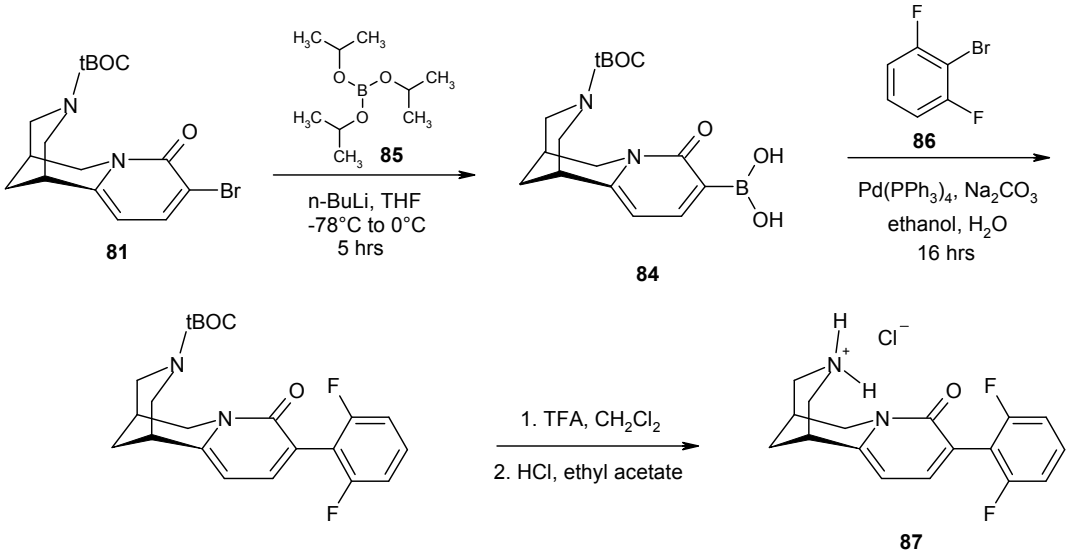

Scheme 3-20 Synthesis of **87** as an example of synthetic protocol developed for the synthesis of 3-phenylsubstituted cytisine analogues [Ref. 124]

Marriére et al.[184] synthesized 3-(4'-fluorophenyl)-cytisine by coupling stannylcytisine with 4-fluorobromobenzene (Stille reaction) using two types of catalyst systems ($Pd_2(dba)_3/AsPh_3$ and $PdCl_2(PPh_3)_2/LiCl$) and different protecting groups. The yields of these two transformations are satisfying (37% – 72%), but the long reaction times (12 to 60 hours) and the need of synthesizing the stannane coupling partners hamper the use of this protocol for the rapid synthesis of numerous derivatives required for a SAR study.

Suzuki coupling on 2-pyridone moiety was successfully applied in the total synthesis of indoloquinoline alkaloid cryptotackieine **88** (syn. neocryptolepine).[262] Coupling of **89** with N-pivaloylamino phenylboronic acid in the presence of a palladium catalyst afforded the biaryl **90**, which is considered to be the key intermediate for preparation of the alkaloid **88** (Scheme 3-21).

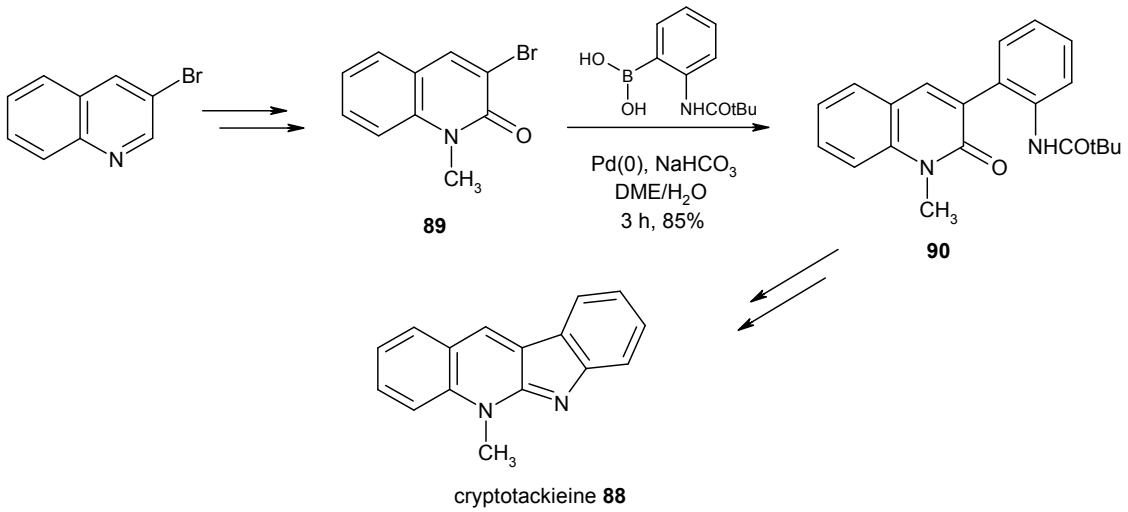

Scheme 3-21 Suzuki coupling in the position 3 of the pyridone moiety in the total synthesis of cryptotackieine [Ref. 262]

Similar approach to 3-arylsubstituted 2-pyridones has been published by Semple et al. as a part of synthesis of kappa opioid receptor agonists.[259] Herein, N-substituted 3-bromo-2-pyridone was coupled with various boronic acid under the catalysis of $Pd(OAc)_2$. Dioxane was employed as a solvent, $NaHCO_3$ as a base and the reaction time was 4 hours. Yields of 40% – 90% were reported.

Collins and Castro prepared 3-trifluoromethanesulfonyloxy-2-pyridone **91** (Scheme 3-22) by Vilsmeier formylation and cyclisation of acyl enamine.[263] The triflate **91** was then found to undergo a range of palladium-catalysed cross-coupling reactions (one of them being Suzuki coupling) giving a synthetic sequence of general use for the preparation of substituted 2-pyridones **92** (Scheme 3-22). Unfortunately, these results do not provide any helpful

information for the scope of this investigation, as the addition of a triflate moiety to the structure of cytisine **27** would be more lengthy and complicated than bromination.

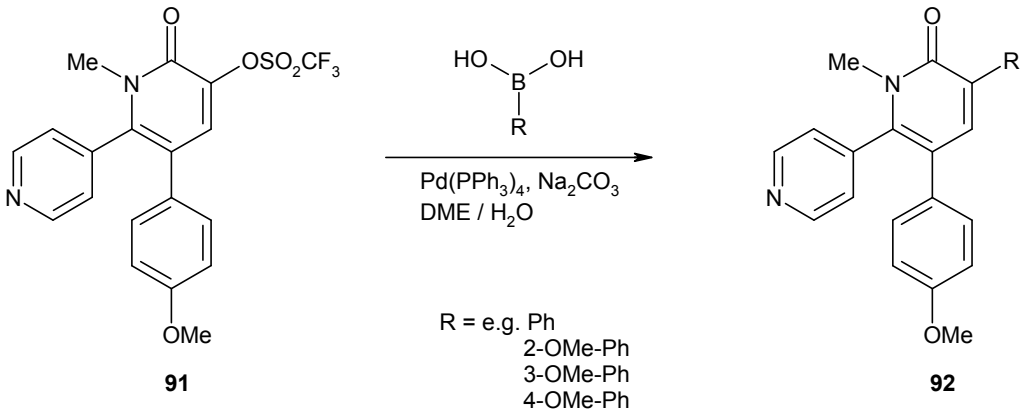

Scheme 3-22 Palladium-catalysed coupling of 2-pyridone **91** and various boronic acids [Ref. 263]

3.2.8.2 Method / Results

A series of known* and novel cytisine analogues was synthesized via Suzuki cross-coupling reaction. All coupling reactions were performed in a single mode microwave cavity using power of no more than 30 W. $Pd(PPh_3)_4$ catalysed coupling reaction of **81** with phenylboronic acid **74** or differently m-substituted phenylboronic acids provided in the presence of sodium carbonate *t*BOC-protected phenyl analogues of cytisine **93 – 100** in less than 30 minutes (Scheme 3-23). Dimethoxyethane (DME) and water were employed as solvents. After solid phase extraction of lipophilic catalyst residues the coupling products were isolated with preparative HPLC system, using methanol/water mixture as a mobile phase and RP C-18 column. The composition of the mobile phase was chosen with regard to the lipophilicity of

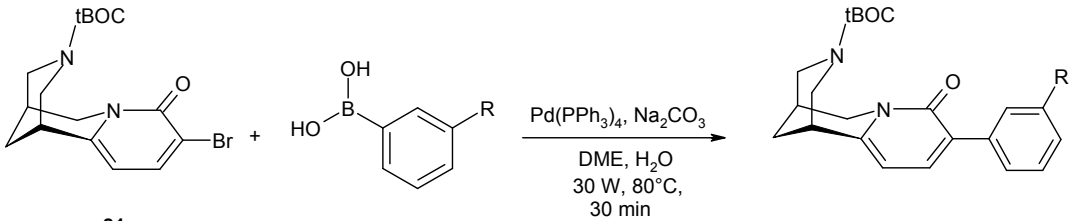

Scheme 3-23 Suzuki cross-coupling between 3-bromo-N-*t*BOC-cytisine **81** and different boronic acids

* 3-phenyl-N-*t*BOC-cyt **93** and 3-(3'-fluorophenyl)-N-*t*BOC-cyt **99** have been synthesized previously[124]

the substituent in order to achieve retention time of the product between 10-20 min. The concentrated aqueous solution of the coupling product was directly used for the removal of the protecting groups.

3.2.8.3 Discussion

The key step in the addition of phenyl group as well as differently m-substituted phenyl moieties into the structure of cytisine **27** is the Suzuki cross-coupling reaction under microwave accelerated conditions. All coupling reactions of 3-bromo-N-*t*BOC-cytisine **81** and various boronic acids were performed in a single mode microwave cavity using power of no more than 30 W to avoid the decomposition of the catalytic system. In addition, hydrolysis of the carbamate bond was observed within the first experiments, when a higher energy (50 – 100 W) was used. This is very beneficial for the deprotection chemistry, as it offers a new, convenient and fast removal of the *t*BOC protecting group. However, in order to avoid the decomposition of the catalyst and the use of buffered aqueous solutions for preparative HPLC purification of the coupling product as a free base, the microwave energy was kept under 30 W.

Application of the standard Suzuki protocol ($Pd(PPh_3)_4$, Na_2CO_3, DME/H_2O) and microwave irradiation as a heating source afforded known and novel cytisine analogues **93 – 100** in less than 30 minutes in moderate to excellent yields (36% – 83%). Compared to conventional heating, microwave dielectric heating shortened the reaction time from the 4 hours reported for coupling of 3-bromo-2-pyridones[259] and 16 hours reported for the coupling of cytisine-3-boronic acid **84**[124] to 30 min.

All syntheses were performed on a milligram scale. From the medicinal chemistry point of view, it is more efficient at the lead modification/optimization stage to use chromatography for purification than to search for more efficient, higher-yielding, alternative synthetic routes and crystallization techniques.[264] Chromatography on silica gel was found not to separate the coupling product from bromine reactant, which was mostly present in a small quantity in the reaction mixture. However, high performance liquid chromatography on a reverse phase C-18 column allowed excellent separation and purification of the wanted coupling product. Isocratic mixture of methanol/water in composition with regard to the lipophilic nature of the substituent yielded the coupling product in high purity.

Microwave-assisted Suzuki coupling was “discovered” nearly a decade ago[238] and since then, numerous papers report the advantage of microwave on the coupling process.[229,230] Yet, the vast majority of the published microwave-enhanced Suzuki reaction employed

simple coupling partners, which were very similar to those used in the first microwave promoted Suzuki reaction, i.e. 1-bromo-4-methyl-benzene **73** and phenylboronic acid **74**.[238] Thus, the efficient coupling of 3-bromo-N-*t*BOC-cytisine **81** with various boronic acids enlarges the limited number of papers reporting the use of Suzuki cross-coupling reaction for the high-speed modification of various heterocyclic scaffolds of pharmacological or biological interest. [265]

3.2.9 5-Phenyl Analogues of Cytisine

3.2.9.1 Introduction

In the patent literature orientated on the diversification of the cytisine scaffold[124], three 5-substituted analogues of cytisine were claimed. 5-Methyl-, 5-vinyl- and 5-phenyl-cytisines were synthesized via Stille cross-coupling reaction (Scheme 3-24). Of particular interest is up to date the only one analogue of cytisine with aryl substituent in position 5. 5-Phenyl-N-*t*BOC-cytisine was synthesized via coupling of 5-bromo-N-*t*BOC-cytisine **82** and tributylphenyltin under $PdBnCl(PPh_3)_2$ catalysis. The reaction time of this substitution was 48 hours (Scheme 3-24).[124]

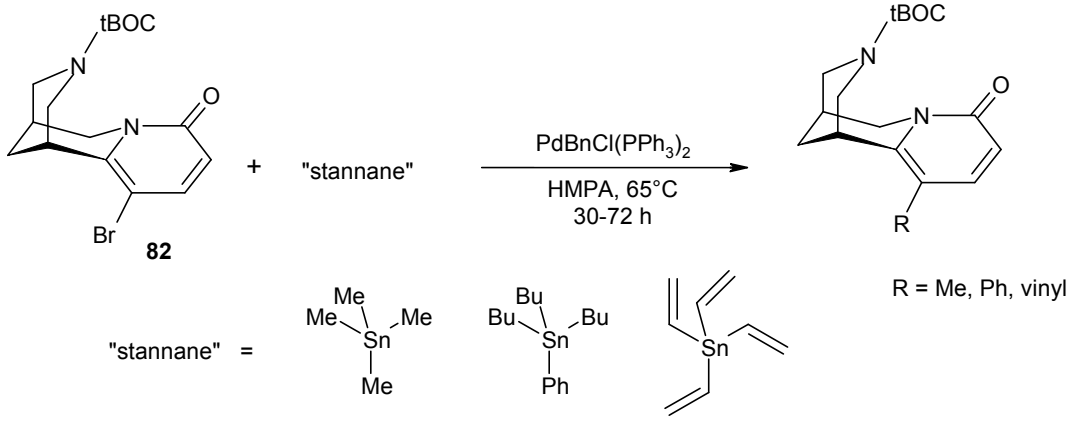

Scheme 3-24 Stille cross-coupling reactions of 5-bromo-N-*t*BOC-cytisine **82** [Ref. 124]

Arylation of the position 5 of the pyridone moiety is documented also by a single report. Nadin[266] coupled tricyclic 5-triflate-pyridone **101** with o-, m- and p-methoxyphenyl-boronic acid under common Suzuki condition ($Pd(PPh_3)_4$, Na_2CO_3, DME/H_2O). The coupling products **102** were isolated in high yields (76% – 93%) (Scheme 3-25).

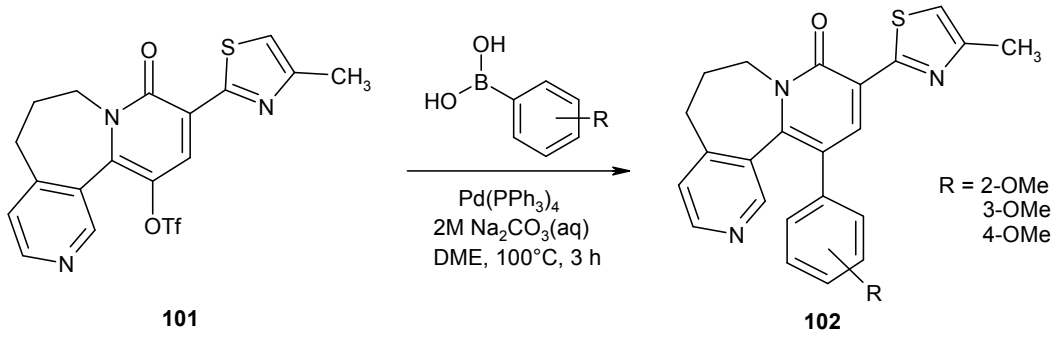

Scheme 3-25 Introduction of aryl moiety into the position 5 of a pyridone ring in **101** via Suzuki cross-coupling reaction [Ref. 266]

3.2.9.2 Method / Results

Microwave irradiation (30 W) allowed incorporation of unsubstituted or substituted phenyl moieties into position 5 of the pyridone ring in less than 30 minutes. 5-phenyl analogues of cytisine **103** – **100** (except for **108**) were synthesized under standard Suzuki conditions - $Pd(PPh_3)_4$, Na_2CO_3, DME/H_2O in 27% – 81% yields (Scheme 3-26). Solid phase extraction (RP-C18) followed by HPLC purification afforded separation of the products from the reagents and side products. The concentrated aqueous solutions of coupling products were directly used in the deprotection step. The reaction products were always identified via NMR and HRMS analysis of the final deprotected ligands. For the synthesis of 5-(3'-chlorophenyl)-N-*t*BOC-cytisine **108,** potassium phosphate was used as a base and the reaction time was extended to 60 min. The desired product, however, was obtained in low yield (23%).

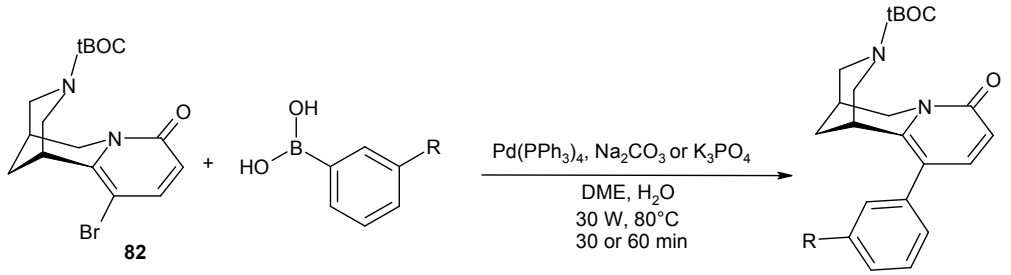

R = H **103** NO_2 **104** CH_3 **105** CF_3 **106**
OCF_3 **107** Cl **108** F **109** Ph **110**

Scheme 3-26 Suzuki cross-coupling of 5-bromo-N-*t*BOC-cytisine **82** and 3-substituted phenylboronic acids

3.2.9.3 Discussion

Triflates have been shown to be efficient leaving groups for Suzuki couplings on the pyridones in the position 3[263], 4[267] and 5[266]. However, the introduction of a triflate moiety into any position of the cytisine's pyridone ring would require several steps. The better documented bromination of pyridone moiety in the cytisine structure[118,124,174,182,184] yielded efficient N-protected 3-bromocytisine coupling partner **81** and it was somehow expected that bromine in the position 5 will also be an efficient leaving group for Suzuki cross-coupling.

Indeed, microwave irradiation (30 W) and standard Suzuki conditions [$Pd(PPh_3)_4$, Na_2CO_3, DME/H_2O] allowed phenyl substitution in the position 5 of the pyridone ring within 30 min (Scheme 3-26), compared to 48 hours when the Stille protocol was applied.[124] Moreover, the method described herein afforded a successful cross-coupling of 5-bromo-N-*t*BOC-cytisine **82** with various m-substituted phenyl boronic acid (Table 3-9). The method was changed for the synthesis of 5-(-3'-chlorophenyl)-N-*t*BOC-cytisine **108**. Sodium carbonate as a base did not provide the coupling product in yields higher than 5%, even if the reaction time was extended from 30 min to 60 min. Replacing sodium carbonate by a stronger base - potassium phosphate - gave at the reaction time of 60 min the desired product (23%).

Table 3-9 Retention times and yields of coupling products synthesized via Suzuki reaction

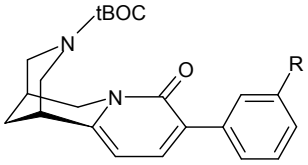

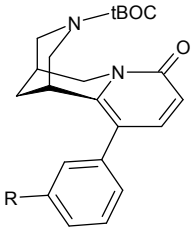

Compound	t_r* [min]	Yields** [%]	R	Compound	t_r* [min]	Yields** [%]
93	16.73[A]	58	H	**103**	17.32[A]	39
94	17.18[A]	83	NO_2	**104**	16.70[A]	62
95	16.27[B]	65	CH_3	**105**	16.17[B]	58
96	19.28[B]	52	CF_3	**106**	17.05[B]	64
97	21.28[B]	64	OCF_3	**107**	21.12[B]	27
98	20.39[B]	47	Cl	**108**	20.52[B]	23
99	13.70[B]	46	F	**109**	12.32[B]	81
100	27.29	36	Ph	**110**	27.65[C]	62

*) A, B, C stand for methods used by the HPLC purification
A) MeOH/H_2O 60:40 v/v
B) MeOH/H_2O 65:35 v/v
C) MeOH/H_2O 65:35 v/v for 15 min, the gradient to MeOH/H_2O 80:20 v/v in 15 min

**) yields calculated over two steps – coupling reaction and deprotection, however, as the deprotection was quantitative, the final yields can be considered as the yields of the coupling reaction

5-Phenyl analogues were like their 3-phenyl counterparts purified with isocratic methanol/water mixture on a RP-C18 phase, using preparative HPLC. The retention times of the corresponding 3- and 5-derivatives differentiate slightly, indicating very similar lipophilic properties of the counterparts (Table 3-9). For example, the retention times of 3- and 5-(m-tolyl)-N-*t*BOC-cytisine **95** and **105** are 16.27 min and 16.17 min, respectively (Table 3-6). It should be noted that the preparative HPLC does not focus on the peak profile monitoring for quantitative estimation and elution time measurement. The aim of the preparative HPLC is an actual collection of an eluted component, i.e. the separation and purification of synthetic products. In addition, mass overload leads to changed retention times and as a consequence, the retention times obtained from the preparative HPLC cannot be taken as identification parameters.[268] Indeed, it was observed that the retention time depended on the quantity on the coupling product. While in the analytical HPLC exact concentration of a substance is loaded on the column (e.g. 1 µg/1 mL), in the preparative HPLC, reaction mixture with unknown concentration of the reaction product is used. The concentration of the sample mixture can be only estimated from the masses of applied reactants.

The expectation of position 5 being less reactive than the position 3 was confirmed in most syntheses (Table 3-9). An exception to the rule is the yield of 5-(3'-fluorophenyl)-derivative **109** (81%), which highly exceeds the yield of 3-(3'-fluorophenyl)-N-*t*BOC-cytisine **99** (46%).

Suzuki coupling can be accompanied with several side reactions. A phenyl-coupling product derived from triphenylphosphine is an important side-product in the cross-coupling reaction of electron-rich haloarenes having no steric hindrance of an ortho substituent.[269] However, the pyridone moiety of cytisine **27** is rather electron-deficient and both positions (3 and 5) have ortho-substituents (2-oxo and bulky bispidine moiety, respectively). Another side reaction is oxygen-induced homocoupling of arylboronic acids, which occurs when the reaction mixture is exposed to air. The homocoupling is very slow under neutral conditions, but is very rapid in the presence of an aqueous base.[270] Therefore, the coupling reactions were performed under argon atmosphere and with an excess of boronic acid (1.5 eq). Nevertheless, the complete absence of oxygen cannot be achieved and the use of an aqueous Na_2CO_3 solution could lead to an undesired homocoupling of employed arylboronic acids. As the side products of the coupling reaction were not identified, also the participation of phophine-bound phenyl in the coupling cycle of cytisine **27** cannot be excluded. These, and maybe some other unknown side reactions together with the lower reactivity of the position 5 can rationalise the varying yields of the coupling reactions.

3.2.10 Heterocyclic Derivatives of Cytisine

3.2.10.1 Introduction

Up to date, all heterocyclic analogues of cytisine possess heterocycle only in the position 3. In the Pfizer patent[124] they have been synthesized either via the Suzuki coupling of N-*t*BOC-cytisine-3-boronic acid **84** and corresponding heteroaryl bromides (analogous synthesis to Scheme 3-20) or via Pd-catalysed Buchwald-Hartwig reaction. Coupling of 3-bromo-N-*t*BOC-cytisine **81** and morpholine, using bis[1,2-bis(diphenylphosphino)ethane]-palladium(0) as a catalyst and sodium *tert*-butoxide as a base yielded N-protected 3-morpholino-cytisine **111** (Scheme 3-27). Also 3-pyrrolidino-cytisine was prepared through this procedure.[124]

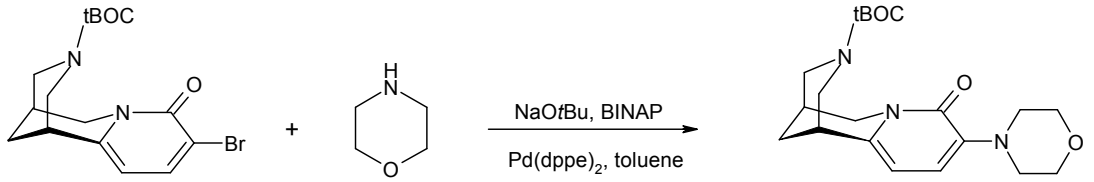

81 **111**

Scheme 3-27 Buchwald-Hartwig coupling as key step for synthesis of heterocyclic analogue of cytisine **111** [Ref. 124]

In the development of 3-(2-[^{18}F]fluoropyridinyl)-cytisine[125], intended as a suitable radiotracer for use in PET, the synthesis of the N-protected "cold" counterpart **112** has been described. The key step was Stille cross-coupling reaction of N-protected 3-iodocytisine **113** or N-protected 3-trimethylstannylcytisine **114** derivative with corresponding coupling partners **115** and **116** (Scheme 3-28).[125]

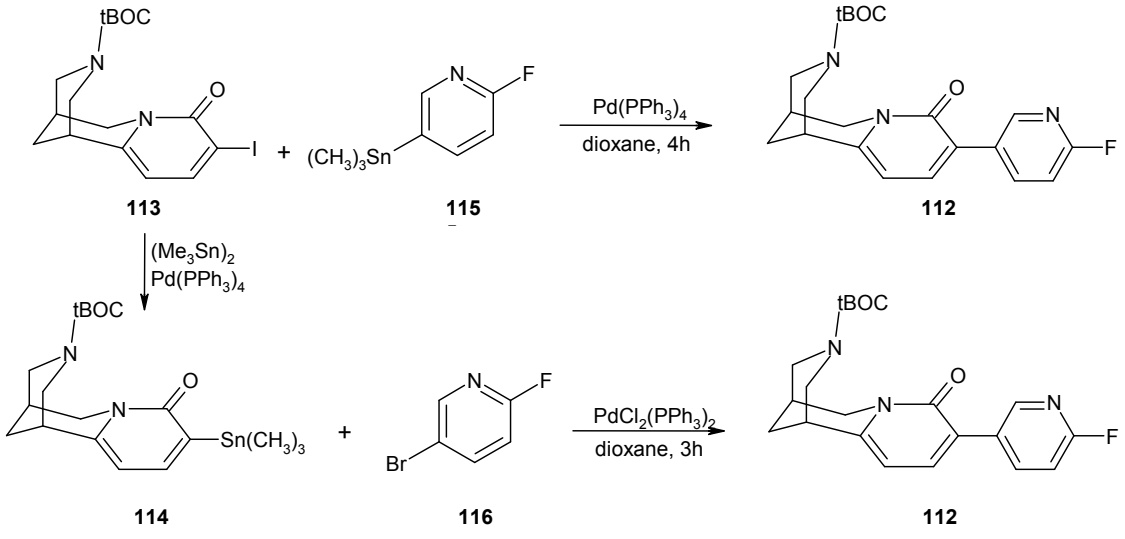

113 **115** **112**

114 **116** **112**

Scheme 3-28 Stille coupling as a key step in the synthesis of 3-(2-fluoropyridine)-N-*t*BOC-cytisine **112** [Ref. 125]

Suzuki cross-coupling reaction with heteroaryl boronic acids has been performed on the pyridone scaffold.[263] 3-Triflate-2-pyridone undergoes coupling with 3-thienyl and 4-pyridinyl boronic acid under standard Suzuki conditions ($Pd(PPh_3)_4/Na_2CO_3$/DME-H_2O).[263] The coupling reaction of 4-triflate-2-pyridone and 2-thienyl boronic acid proceeds greatly at room temperature in the presence of $Pd(PPh_3)_4/K_2CO_3$/THF-DMA 1:1 (96% yields).[267]

3.2.10.2 Method / Results

The introduction of heterocyclic scaffolds of biological interest into the position 3 or 5 of the cytisine structure is shown in Schemes 3-29 and 3-30. While coupling of 5-indolylboronic acid with both **81** or **82** performed well under "standard" condition (entry **117** and **123**), the same condition afforded incorporation of 3,4-methylenedioxyphenyl group only into the more reactive position 3 of the pyridone moiety (entry **118**). For the same coupling with 5-bromo-N-*t*BOC-cytisine **82** sodium carbonate had to be replaced by $Ba(OH)_2$ and the reaction time extended to 60 min (entry **124**). The application of K_3PO_4 as a base afforded synthesis of 3-(3'-pyridyl)-N-*t*BOC-cytisine **119** within 60 min, but the stronger base $Ba(OH)_2$ had to be employed for the synthesis of the corresponding 5-substituted counterpart (entry **125**). The same observation was made for incorporation of 1-methyl-1*H*-pyrazol-4-yl moiety. Whereas the coupling reaction in the presence of K_3PO_4 as a base gave the desired coupling product **122** in 30 min, the corresponding 5-substituted analogue (entry **126**) was synthesized only when $Ba(OH)_2$ was employed and the reaction time extended to 60 min. Potassium phosphate also allowed incorporation of 4-pyridyl and quinolin-8-yl into the position 3 of the pyridone moiety (entry **120** and **121**), however, the introduction of these substituents into position 5 was not successful. All attempts to synthesize 5-(4'-pyridyl)- and 5-(quinolin-8'-yl) analogue failed. The syntheses were carried out under a variety of conditions with regard to the base (Na_2CO_3, K_2CO_3,, Cs_2CO_3 or $Ba(OH)_2$), solvent (DME or DMF) and reaction time. The microwave heating was stopped after 60 or 90 minutes. However, no combination allowed incorporation of quinolin-8-yl and 4-pyridyl moieties into position 5. For every Suzuki cross-coupling of **81** or **82** with heterocyclic boronic acids, $Pd(PPh_3)_4$ was employed as a catalyst and DME/H_2O as solvents. Since the unsuccessful syntheses were performed with the same catalyst ($Pd(PPh_3)_4$), employing different catalyst systems (e.g. $PdBnCl(PPh_3)_2$ or $Pd(OAc)_2/PPh_3$) could allow incorporation of 4-pyridyl and quinolin-8-yl moieties into position 5.

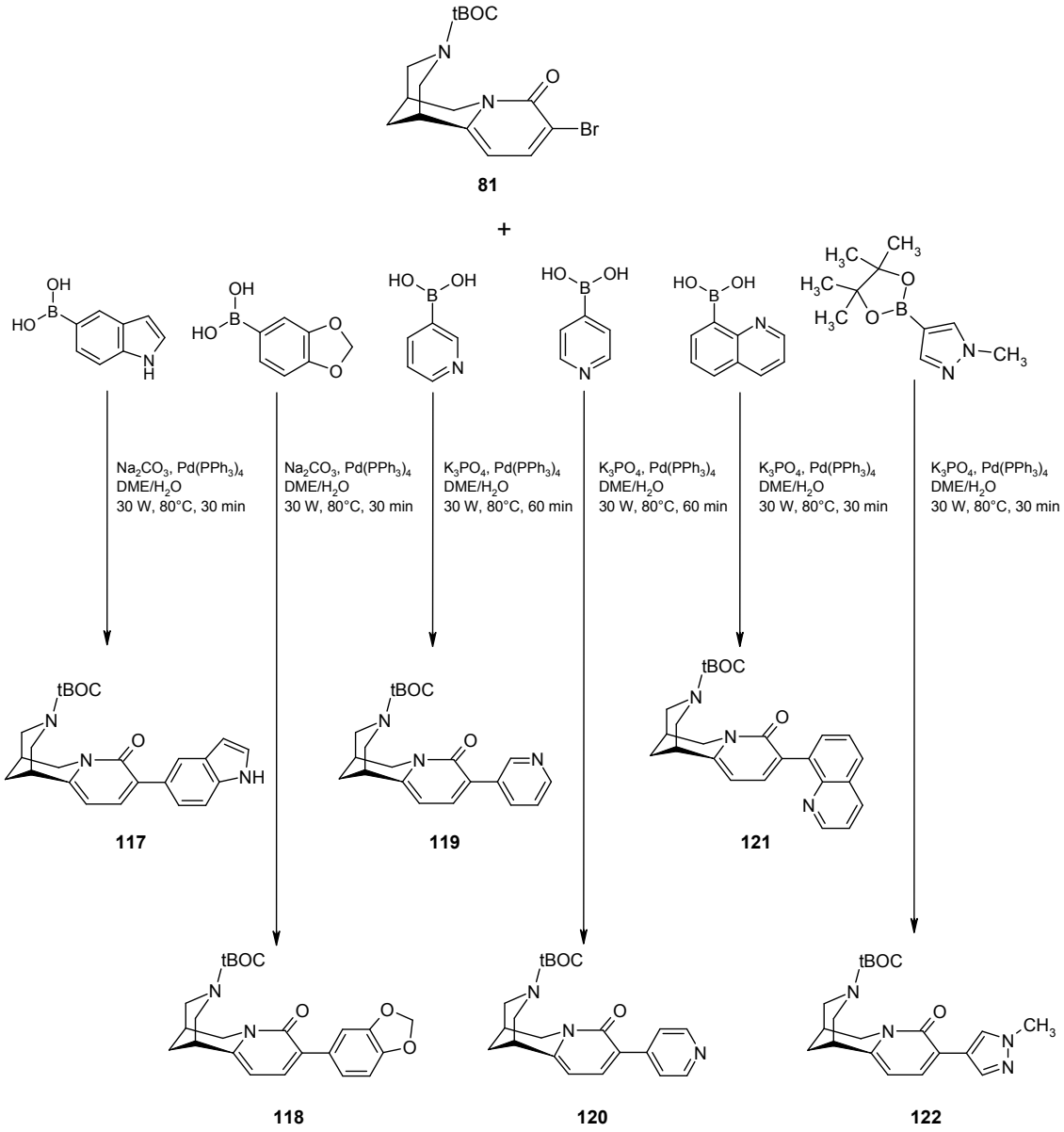

Scheme 3-29 Introduction of heterocyclic or heteroaryl moieties into the position 3 of cytisine

The purification of all N-protected reaction products **117** – **126** consisted of a solid phase extraction of the highly lipophilic catalyst and a separation of the reaction products from reactants and side products, which was performed with HPLC using isocratic methanol/water mixture.

The coupling reactions with heterocyclic boronic acids confirmed the higher reactivity of position 3. 5-Substituted coupling products were always achieved in lower yields (Table 3-10) and all attempts to introduce quinol-8-yl and 4-pyridyl moieties into the position 5 failed. Similarly, coupling reactions of 3- or 5-bromo-N-*t*BOC-cytisine **81** – **82** with 2-chloro-5-

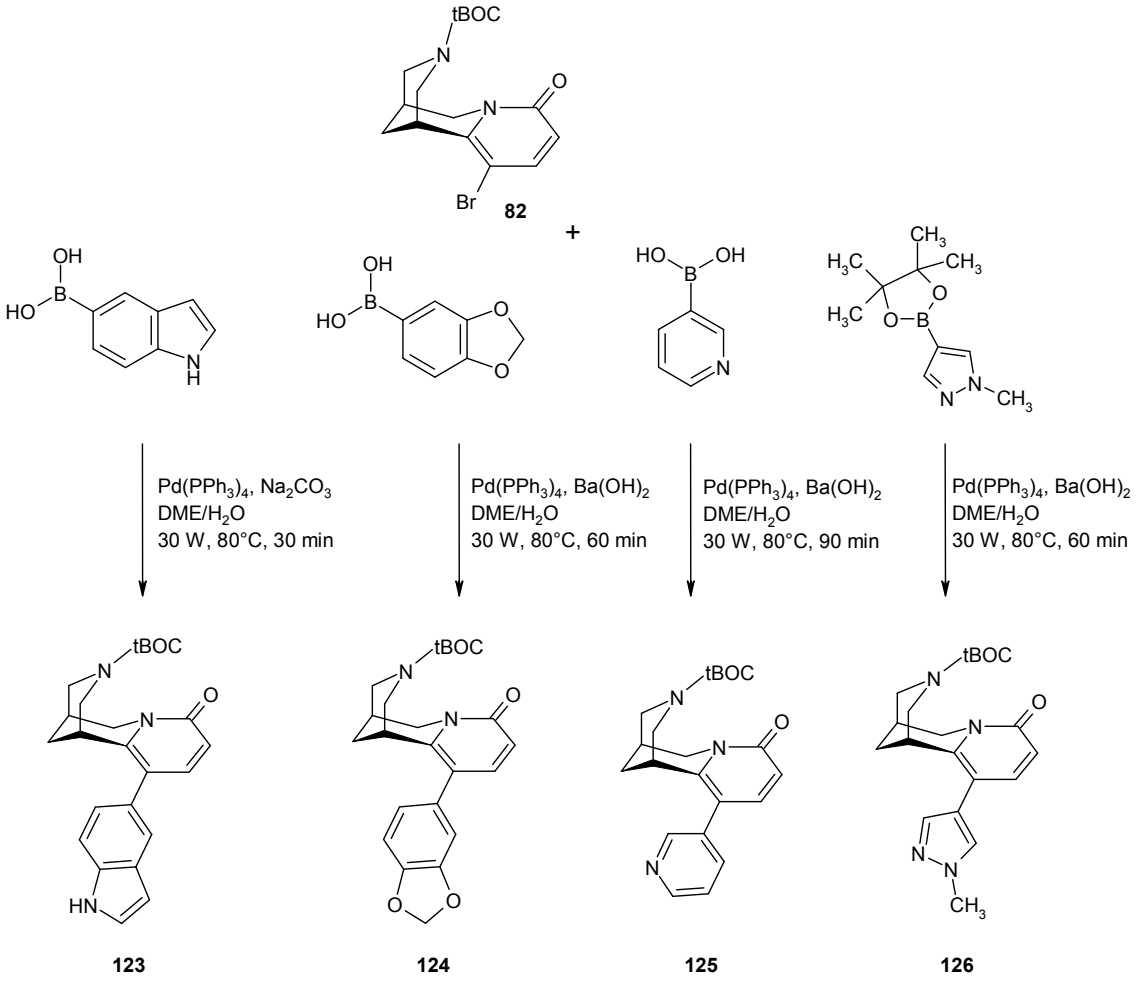

Scheme 3-30 Modification of position 5 via the introduction of heterocyclic moieties

pyridylboronic acid yielded the desired coupling product in trace. This could be explained with the fact that boronic acids containing heteroatoms easily undergo in aqueous milieu hydrolytic B-C bond cleavage.[271] This side reaction is accelerated in electron-deficient boronic acids[272] and 2-pyridylboronic acid was reported not to give coupling products because of its very rapid deprotonation.[168,191c] Electron-withdrawing effect of the chlorine in the 2-chloro-5-pyridyl boronic acid is probably responsible for the hydrolytic cleavage of the B-C bond.

Table 3-10 Retention times and yields of heterocyclic cytisine derivatives **117** – **126** prepared via Suzuki reaction

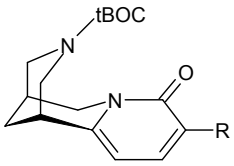

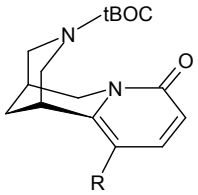

Compound	t_r* [min]	Yields** [%]	R	Compound	t_r* [min]	Yields** [%]
117	16.12[A]	37	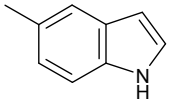	**123**	15.55[A]	26
118	18.99[A]	36	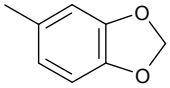	**124**	18.69[A]	25
119	16.05[B]	66	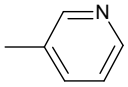	**125**	14.52[B]	32
120	17.80[B]	62	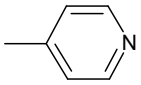	not purified		< 5
121	18.43[A]	44	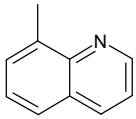	not purified		< 5
122	15.32[B]	70	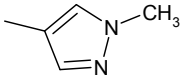	**126**	12.65[B]	19

*) A and B stand for methods used for the HPLC purification
A) MeOH/H_2O 60:40 v/v
B) MeOH/H_2O 50:50 v/v

**) yields calculated over two steps – coupling reaction and deprotection, however, as the deprotection was quantitative, the yields can be considered as the yields of the coupling reaction

3.2.10.3 Discussion

The results of Suzuki cross-coupling with heteroaryl boronic acids extend the original observation from the synthesis of aryl analogues. Microwave activation as an unconventional energy source demonstrated beneficial impact also with the introduction of a heterocyclic unit of pharmacological interest into the structure of cytisine **27**. A new strategy for the straightforward and fast synthesis of heterocyclic cytisine analogues yielded ten novel derivatives **117 – 126** featuring bulky heterocycle in the position 3 or 5.

However, the reaction condition described for phenyl derivatives (Chapters 3.2.8 and 3.2.9) had to be modified in some protocols, as using the "standard microwave conditions" [$Pd(PPh_3)_4$, Na_2CO_3, DME/H_2O, 30 W, 30 min], gave only very fair yields. The syntheses of **117** – **126** were carried out under a variety of conditions regarding the base (Na_2CO_3, K_2CO_3,

K_3PO_4, Cs_2CO_3 or $Ba(OH)_2$), solvent (DME or DMF) and reaction time. Replacement of DME by DMF did not increase yields while the addition of K_3PO_4 or $Ba(OH)_2$ exerted a remarkable affect on the acceleration of the coupling rate.

The rate and yield enhancing effect of a base is a result of the increasing basic strength of counter anions (HCO_3^- < MCO_3^- < MPO_4^- < OH^-). Furthermore, counter cations possess different stability constant for halides (Na^+ < K^+ < Cs^+ < Ba^{2+} << Tl^+ < Ag^+) and for hydroxide anions (Cs^+ < K^+ < Na^+ < Li^+).[191c, 201] Thus, in the example of the synthesis of 3-(4'-pyridyl)-N-*t*BOC-cytisine **120** (Scheme 3-27), a stronger base $K_2PO_4^-$ yields in the transmetallation step a higher concentration of 4-pyridylboronate complex **127** than $NaCO_3^-$ does (Scheme 3-31).

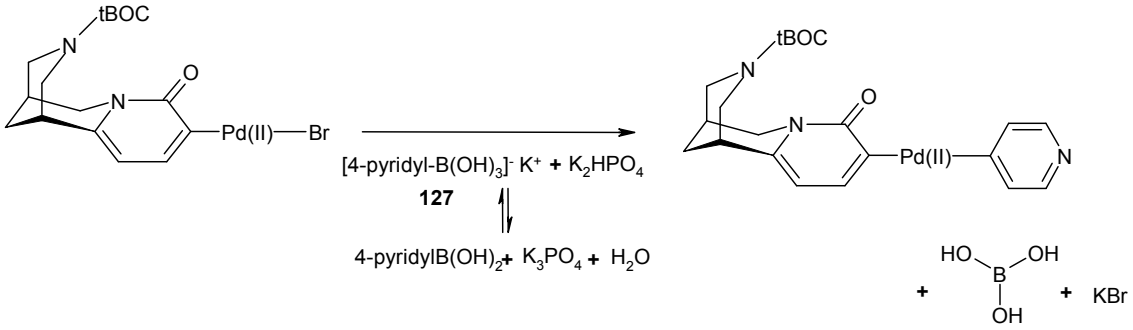

Scheme 3-31 Hypothetical transmetallation process in the synthesis of 3-(4'-pyridyl) derivative **120**

Moreover, K^+ supports a higher concentration of the boronate **127** because it possesses a lower stability constant for hydroxide anion than Na^+. On the other hand, potassium cation has a higher stability constant for bromide than Na^+, meaning that the transmetallation is faster with potassium salts (e.g. K_2CO_3, K_3PO_4) than with sodium salts (e.g. Na_2CO_3).

3.2.11 3,5-Disubstituted Analogues of Cytisine

3.2.11.1 Introduction

The published 3,5-dihalogenated cytisine analogues possess either the same or different halogen atoms in positions 3 and 5, e.g. 3,5-dichlorocytisine **45** and 3-bromo-5-chlorocytisine.[118,182] The mixed dihalogenated cytisine analogues were synthesized via "step by step" halogenation with common halogen transfer reagents such as N-bromo- or N-chlorosuccinimide.[182] A twofold excess of halogen transfer reagent (e.g. N-chlorosuccinimide) yielded derivatives with the same halogen in positions 3 and 5, e.g. 3,5-dichlorocytisine **45**.[118]

The introduction of methyl-, ethyl-, vinyl- and phenyl moieties into positions 3 and 5 has been claimed, but synthetic protocol only for the synthesis of 3,5-dimethylcytisine was disclosed.[124] The target derivative was synthesized once more via the Stille cross-coupling reaction of 3,5-dibromo-N-*t*BOC-cytisine **83** and a 10-fold excess of tetramethyltin under the catalysis of *trans*-benzylchloro-bis(triphenylphosphine)palladium in HMPA. The reaction was completed after 12 hours.[124]

3.2.11.2 Method / Results

The synthetic routes to disubstituted cytisine analogues **128** and **129** started with 3,5-dibromo-N-*t*BOC-cytisine **83** (Scheme 3-32). The Suzuki-cross coupling reaction with phenylboronic acid **74** was selectively performed with the bromine in position 3. When Na_2CO_3 was used as a base, only the bromine in the position 3 of the pyridone moiety coupled with phenylboronic acid. Using 3-pyridylboronic acid and potassium phosphate led to an addition of the 3-pyridyl substituent again only to position 3. For both reactions $Pd(PPh_3)_4$ was applied as a catalyst and DME/H_2O as solvents. The microwave irradiation of the maximum 30 W was stopped after 30 or 60 min. The purification procedure of the coupling products followed the protocol described for phenyl and heterocyclic derivatives (SPE and HPLC separation).

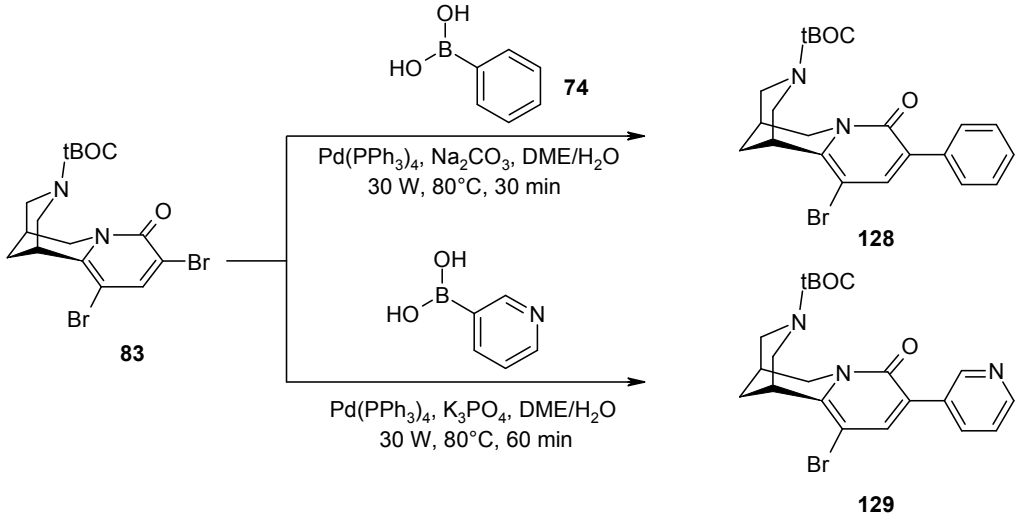

Scheme 3-32 Selective cross-coupling in the position 3 of 3,5-dibromo-N-*t*BOC-cytisine **83**

3.2.11.3 Discussion

The conditions used in the selective Suzuki cross-coupling reaction were chosen due to previous experience revealing that the more reactive position 3 of the pyridone moiety undergoes coupling with the boronic acid easier and faster. Thus, employing bases such as

Na_2CO_3 or K_3PO_4 afforded coupling reaction only in position 3, while the bromine in position 5 was not attacked. In this way obtained 3-phenyl-5-bromo- and 3-(3'-pyridyl)-5-bromo analogues **128** and **129** are novel disubstituted cytisine derivatives.

Selective coupling has been previously reported, but selective only by the means of different reactivity of iodine and bromine towards the Suzuki reaction (Scheme 3-33). The coupling of 4-boronic acid of anisole and bromo-iodo-phenanthroline **130** affords coupling product **131**. The results of this study demonstrate that positions with leaving groups of different reactivity can selectively undergo the coupling reaction under carefully chosen conditions.[191b]

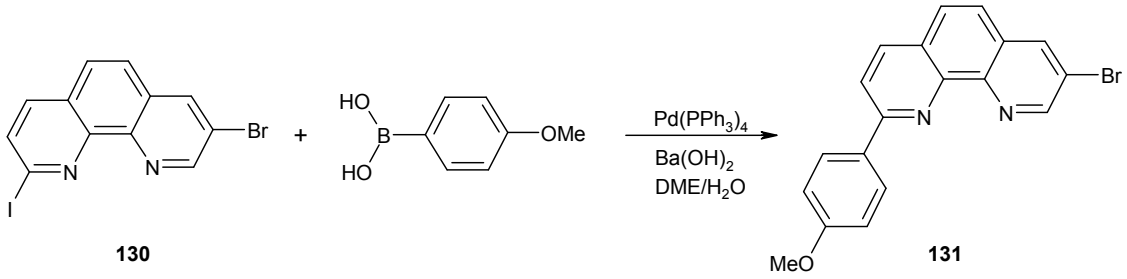

130 **131**

Scheme 3-33 Selective Suzuki cross-coupling reaction [Ref. 191b]

3.2.12 Removal of the *t*BOC Protecting Group

3.2.12.1 Introduction

Traditionally, the *t*BOC group is cleaved by acidic hydrolysis using hydrochloric acid in ethylacetate[273] or trifluoroacetic acid (TFA) in dichloromethane[124]. 10% Sulphuric acid in dioxane has been used as well.[274] The *t*BOC group can be also removed thermally, either neat[275,276] or in diphenyl ether[277].

Microwave irradiation has been shown to be effective in the deprotection methods, especially in protocols requiring harsh conventional conditions. Extensive research on microwave-accelerated deprotection[278] yielded new protocols for alternative cleavage reactions. For example, the use of irritating and corrosive TFA can be eliminated with microwave irradiation. A solvent-free deprotection of N-*t*BOC group occurs upon exposure to microwaves in the presence of neutral alumina with aluminium chloride.[279] Cleavage of *t*BOC can be achieved by coupling microwave irradiation and silica gel.[280] Recently, an absolute deprotection of *t*BOC protected amino acid and peptide esters employing *p*-TsOH in toluene under microwave irradiation was found to be completed in 30 second. The method worked well also in methanol and acetonitrile.[281]

3.2.12.2 Method/Results

Hydrochloric acid quantitatively (reaction time > 24 hours) removed the *t*BOC group and after extraction of a free base into chloroform, final products **93e** – **100e** and **103e** – **110e** were obtained as off-white crystalline powders (Scheme 3-34, Method A).

However, it was observed that heating the Suzuki reaction with microwave irradiation quantitatively removed the *t*BOC protecting group. Therefore, after the HPLC purification, the aqueous fraction containing the N-protected product was concentrated to approximately 80 mL and the removal of the carbamate was achieved by thermal fission (150°C) of CO_2 and isobutene using microwave irradiation of 150 W for 30 minutes (Scheme 3-34, Method B). As the reaction was quantitative, no purification was required and lyophilization of water for at least 24 h afforded ligands **117e** – **126e** as white or yellowish crystalline powders.

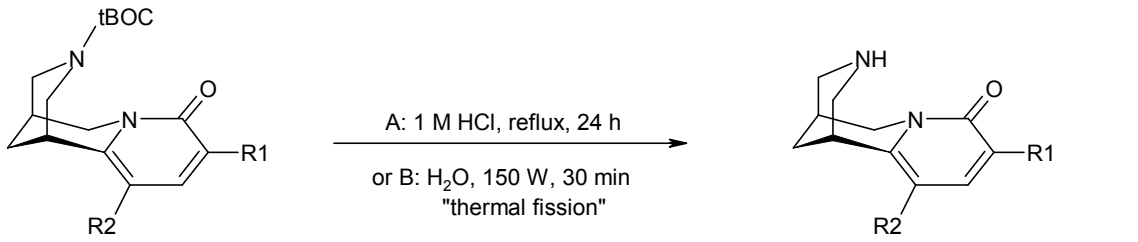

93e - **100e** R1 = aryl, R2 = H
103e - **110e** R1 = H, R2 = aryl
117e - **122e** R1 = heterocycle, R2 = H
123e - **126e** R1 = H, R2 = heterocycle
128e R1 = phenyl, R2 = Br
129e R1 = 3-pyridyl, R2 = Br

Scheme 3-34 Removal of the *t*BOC-protecting group by acidic hydrolysis (A) or thermal fission promoted with microwave irradiation (B)

3.2.12.3 Discussion

The removal of the *t*BOC-protecting group was performed directly in the concentrated aqueous solution of the coupling product, obtained from HPLC purification.

Trifluoroacetic acid caused too many side products that had to be removed by flash chromatography, which resulted in a significant loss of the little quantity of the coupling product. Therefore, hydrochloric acid was used for the hydrolysis of the carbamate bond. The reaction was monitored by TLC in order to achieve quantitative yields. Free base was extracted into chloroform and after evaporation of the solvent under reduced pressure the ligands **93e** – **100e** and **103e** – **110e** were obtained as off-white crystalline powders.

A great improvement was the discovery that the *t*BOC protecting group can be quantitatively removed with the microwave heating. Quantitative thermal fission of carbon dioxide and isobutene was achieved with microwave-enhanced fast heating within 30 min. The final products **117e** – **126e** (free bases) were obtained after lyophilization of solvent (i.e. water) as white or yellowish crystalline powders.

This protocol offers a high-speed, efficient and quantitative cleavage of the *t*BOC-protecting group. Microwave irradiation of the aqueous solution of the N-*t*BOC protected amine improves previously reported similar approaches.[279-281] While the thermal fission of *t*BOC group with conventional heating required two hours[276], alternative dielectric heating completed the same reaction within 30 minutes. Microwaves were shown to enhance deprotection of secondary amines, however in the presence of organic solvents (e.g. toluene) or reactants (e.g. silica gel). The method presented herein requires water as a solvent and no reagents.

3.3 ^{1}H and ^{13}C NMR Chemical Shifts Assignment for the Novel nAChRs Ligands

3.3.1 Overview of used NMR Spectroscopy Methods

The aim of the standard **^{1}H NMR** experiment is to record a routine proton NMR spectrum in order to obtain structure-related information for the protons of the sample, i.e. chemical shifts, spin-spin couplings and intensities.[282] The aim of the standard **^{13}C NMR** experiment is to record a ^{13}C spectrum with proton broad-band decoupling and data accumulation so as to acquire chemical shift information for the compound's carbon skeleton.[283]

Well separated resonances in the ^{1}H NMR spectrum can be selectively irradiated by relevant decoupler frequencies, this method is called **Single-Frequency Decoupling** (SFD). In the ^{13}C NMR spectrum, the signal of the carbon atom adjacent to the irradiated proton will be detected as a singlet, the other carbon resonances are off-resonance decoupled, with splitting dependent on the frequency distance from the decoupler frequency applied. Although time consuming, this procedure affords plentiful information about the C,H coupling behaviour of the spin system in question.[283]

Distortionless Enhancement by Polarization Transfer (DEPT) produces subspectra for distinguishing the CH, CH_2 and CH_3 carbons. In the DEPT-135 spectrum, CH and CH_3 carbon are presented by positive signals and CH_2 by negative signals, whereas signals of quaternary carbons are missing.[285]

While conventional NMR spectra (**1D NMR**) are plots of intensity vs. frequency, in two-dimensional spectroscopy (**2D NMR**) intensity is plotted as a mutual correlation of two resonance frequencies. 2D NMR spectrum means a spectrum in which both axes show chemical shifts, with the intensity of the correlation peaks constituting a third dimension. From a practical point of view, the most useful 2D spectra are those that show either homonuclear ^{1}H-^{1}H or heteronuclear ^{1}H-^{13}C correlations.[284]

The 2D hydrogen **Correlated Spectroscopy** (COSY) is a valuable source of information regarding the coupling partners. The one-dimensional ^{1}H NMR spectrum can be found along the top and left sides of the 2D COSY spectrum. Cross peaks exist in the 2D COSY spectrum where there is a spin-spin coupling between hydrogens.[285]

2D-Incredible Natural Abundance Double Quantum Transfer Experiment (INADEQUATE) detects the ^{13}C nuclei connected to another ^{13}C nucleus and reveals connectivities of neighbouring carbons. This experiment is relatively insensitive, thus time-consuming and a large sample of the analysed structure is necessary.[285]

One particularly useful experiment is to record a two-dimensional spectrum in which the co-ordinate of a peak in one dimension is the chemical shift of one type nucleus (e.g. proton) and the co-ordinate in the other dimension is the chemical shift of another nucleus (e.g. carbon) which is bound to the first nucleus (**heteronuclear correlation experiments**).[286] **Heteronuclear Single Quantum Coherence** (HSQC) shows correlations between directly bonded atoms, e.g. ^{13}C-^{1}H. The 2D data set reveals cross peaks corresponding to the carbon atoms and protons attached to them. Such spectra are very useful as aids to signal assignment, e.g. if the proton spectrum has already been assigned, the HSQC spectrum will give the assignment of all carbons linked to the protons.[287]

Another 2D NMR onset is called **Heteronuclear Multiple Bond Correlation** (HMBC) which provides 2- and 3-bond coupling correlation information ($^{2/3}J_{C,H}$ coupling). The purpose of HMBC is to suppress correlations via $^{1}J_{C,H}$. Since this suppression is not perfect, $^{1}J_{C,H}$ are still observable, but those arising from $^{2/3}J_{C,H}$ are predominant.

3.3.2 Project

The assignment of the carbon and proton signals of cytisine **27** is poorly documented in the literature. The absolute configuration and stereochemistry of some quinolizidine alkaloids (e.g. sparteine or anagyrine) have been extensively studied with NMR experiments[288], but no publication deals with comprehensive structural analysis of cytisine **27**.

The structure of the alkaloid **27** was established in the 1930s by Ing.[134] In the 1950s three independent groups described the total syntheses of racemic cytisine **27**, which served to confirm its structure.[165-167] A first assignment of ^{13}C chemical shifts of cytisine **27** was performed by Bohlmann[126] (Table 3-11), however the author did not provide any argumentation of the assignment. The assignments of ^{13}C chemical shifts of cytisine **27** reported afterwards are in agreement with the first assignment[127,128,142] (Table 3-11), but one has to take into consideration that the assignment published by Bohlman[126] always served as a primary work for the identification of cytisine **27**. Publications[168-173] describing the total synthesis of enantiopure or racemic cytisine **27** provide ^{1}H and ^{13}C chemical shift data, however no assignment of the chemical shifts is reported.

Furthermore, no detailed study for distinguishing 3- and 5-substituted isomers has been reported. In the Pfizer patent[124] the 3- and 5-bromo isomers **81** and **82** were differentiated by NMR techniques with regard to the ^{1}H chemical shifts of H3 (δ 6.38 ppm) and H5 (δ 5.99 ppm). Similarly, the thesis focusing on structural modification of the cytisine scaffold[182] does not offer any additional experiments required for a correct assignment of ^{1}H and ^{13}C chemical

Table 3-11 ^{13}C chemical shifts of cytisine **25** [Ref. 126-128,142]

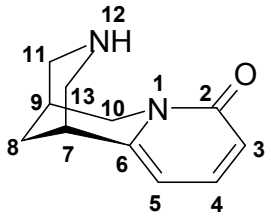

	^{13}C chemical shifts [ppm] as reported by			
	Bohlmann[126] ($CDCl_3$)	Takamatsu[127] (CD_3OD)	Asres[128] ($CDCl_3$)	El-Shazly[142] ($CDCl_3$)
C2	163.6	166.6	163.6	163.6
C3	116.5	117.8	116.5	116.7
C4	138.7	142.1	138.5	138.7
C5	104.9	108.9	104.6	104.9
C6	151.2	153.4	151.4	151.0
C7	35.5	36.9	35.3	35.6
C8	26.2	27.3	25.3	26.3
C9	27.7	29.5	27.8	27.8
C10	49.7	51.8	49.9	49.7
C11	52.9	53.6	62.1	52.9
C13	53.9	54.6	46.1	53.9

shifts for positions 3 and 5, although numerous 3- and 5-haloderivatives of cytisine have been reported in this thesis.

In order to differentiate the isomeric 3- and 5-(hetero)aryl cytisine derivatives, a correct and complete set of ^{1}H and ^{13}C chemical shift assignment for the unsubstituted alkaloid **27** was required. The details regarding assignment of the ^{1}H chemical shifts for cytisine **27** were not found in the literature. Similarly, the publication of Bohlmann[126] did not provide any rationalisation for the assignment of ^{13}C chemical shifts. Therefore not only the standard ^{1}H and ^{13}C spectra, but also the 2D correlation maps (COSY, HSQC, HMBC, INADEQUATE) of cytisine **27** were measured in two different solvents - deuterated chloroform ($CDCl_3$) and methanol (CD_3OD).

Detailed 2D NMR COSY, HSQC and HMBC spectra were performed also for the phenyl substituted analogues **93e** and **103e** in order to establish “diagnostical tools” for their differentiation. For the heteroaryl cytisine derivatives **117e**, **119e**, **121e**, **124e** 2D COSY as well as HSQC spectra were measured, as those would facilitate an assignment of ^{1}H and ^{13}C chemical shifts of the heteroaryl moieties.

3.3.3 Spectral Assignments of ^{1}H and ^{13}C Chemical Shifts

3.3.3.1 Cytisine 27

The ^{1}H NMR, ^{13}C NMR and DEPT-135 spectra of cytisine **27** in $CDCl_3$ are pictured in Figure 3-8. Cytisine **27** possesses sp^2 and sp^3 carbons. Three sp^3 carbons (C11, C13 and C10) are connected to the nitrogen atom. The sp^2 carbons are part of a pseudoaromatic pyridone moiety. In the ^{1}H spectra the protons H3, H4 and H5 arise in the aromatic downfield region (δ 5.5 – 7.5 ppm), while the aliphatic protons of the bispidine ring appear in the upfield part (δ 1.5 – 4.0 ppm).

Starting with the aliphatic region of the ^{1}H NMR spectrum (Figure 3-8/A), the most upfield shifted peak (δ 1.70 ppm) which integrates for 2 protons was identified as H8. This signal provided the starting point for assignments of the remaining bispidine protons. In the 2D COSY spectrum of cytisine **27** (Figure 3-9), H8 displayed cross peaks with singlets at δ 2.08 and δ 2.69 ppm and with a multiplet at δ 2.73 – 2.83 ppm. The two singlets at δ 2.08 ppm and δ 2.69 ppm may be assigned only to H7 and H9, concerning the information obtained in the COSY map. The δ 2.08 ppm peak was correlated firstly to a doublet at δ 3.85 ppm and secondly to a doublet of doublet ("dd") at δ 3.63 ppm, both being signals of protons $H10_{\beta}$ and $H10_{\alpha}$, respectively (shifted downfield as they are linked to a carbon with a nitrogen attachment). Therefore, the δ 2.08 ppm singlet was assigned to H9 and the singlet at δ 2.69 ppm to H7. To conclude, the multiplet δ 2.73 – 2.83 was assigned to protons H11 and H13.

The geminal coupling of the protons $H10_{\alpha}$ and $H10_{\beta}$ was recognised as ^{2}J = 15.6 Hz and the vicinal coupling of one of them (dd at δ 3.63 ppm) to H9 as ^{3}J = 6.6 Hz.

The dd at δ 7.05 ppm correlated with two doublet signals at δ 6.17 ppm and δ 5.77 ppm, respectively. Coupling constants of ^{3}J = 6.9 Hz and ^{3}J = 9.1 Hz were observed and the signal at δ 7.05 was attributed to H4. Another two doublets at δ 5.77 ppm (^{3}J = 6.9 Hz) and at δ 6.17 ppm (^{3}J = 9.1 Hz), representing the olefinic protons H3 and H5, could not be unambiguously assigned at this point.

After completing the assignments of the cytisine's ^{1}H chemical shifts (except for H3 and H5), ^{13}C spectra were recorded and analysed along with the HSQC and HMBC ^{1}H – ^{13}C 2D shift correlation experiments. In the DEPT-135 spectrum (Figure 3-8/C) four methine carbons were found (δ 25.6; 49.1; 52.3 and 53.3 ppm). HSQC correlations (Figure 3-10) allowed straightforward assignment of signals at δ 25.6 ppm and δ 49.1 ppm to C8 and C10. In order to assign the signals at δ 52.3 and 53.3 ppm to either carbon C11 or C13, it was necessary

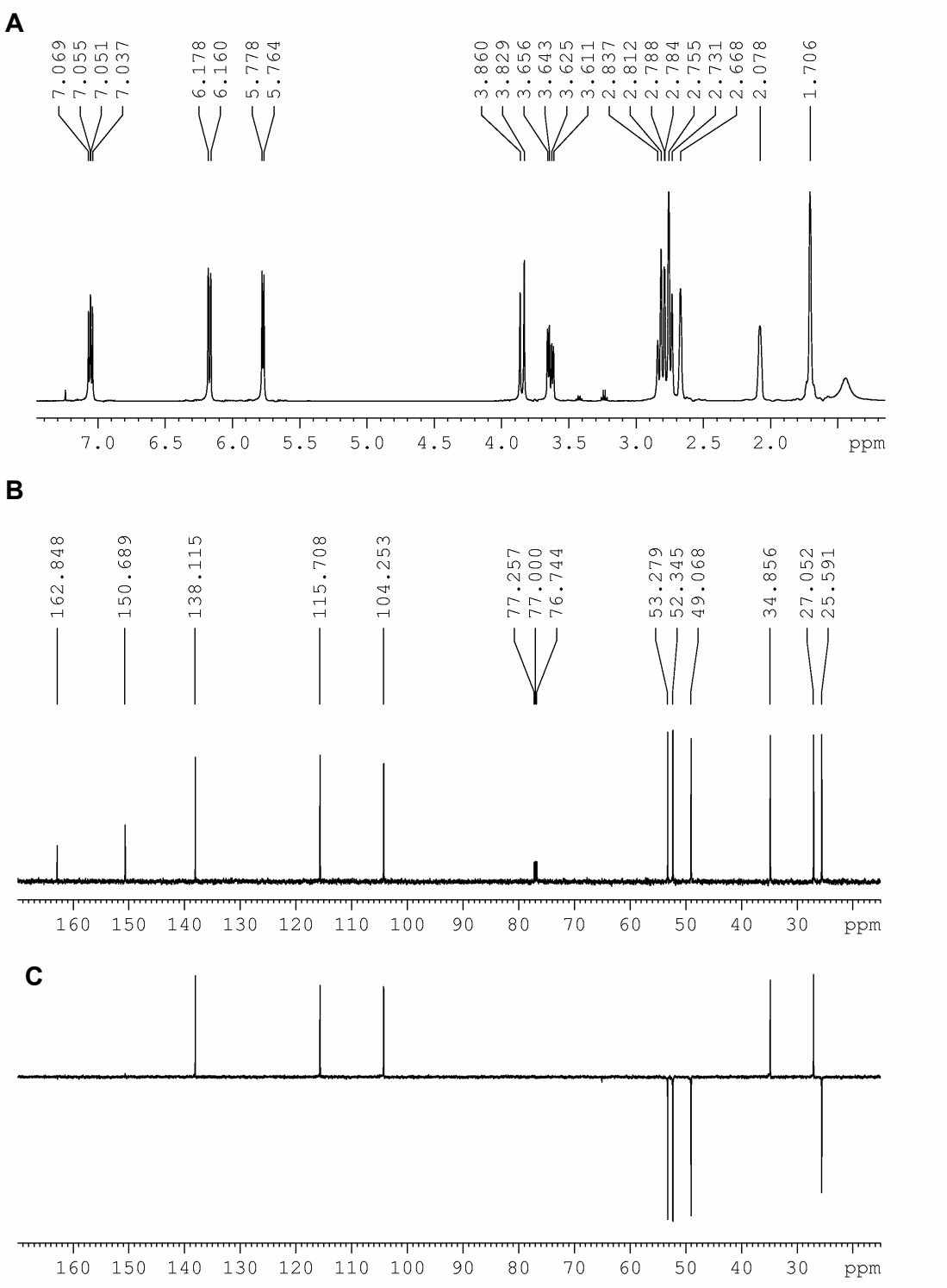

Figure 3-8 ^{1}H NMR (A), ^{13}C NMR (B) and DEPT-135 (C) spectra of cytisine **27** [$CDCl_3$, 125 MHz (^{13}C NMR) and 500 MHz (^{1}H NMR)]

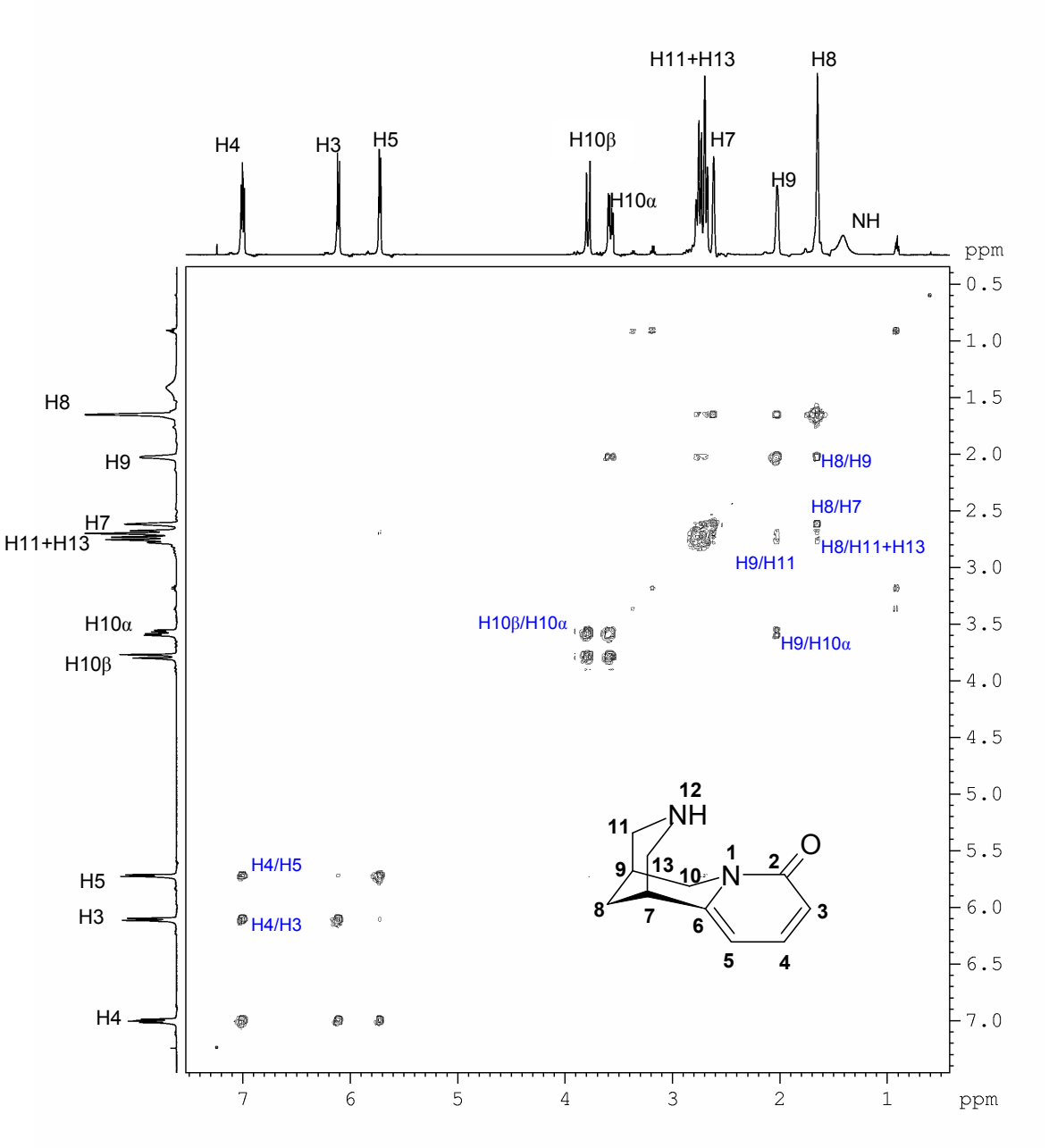

Figure 3-9 2D COSY contour plot of cytisine **27** ($CDCl_3$, 500 MHz)

to examine their two- and three bond ^{1}H and ^{13}C correlations in the HMBC spectrum (Figure 3-11). Of particular interest was the long-range coupling of both H10 protons to the signal at δ 52.3 ppm, whereas a correlation to the signal at δ 53.3 ppm is missing (Figure 3-11). This cross peak must arise from a coupling of C11 to H10 over three bonds. Therefore, the δ 52.3 ppm chemical shift was assigned to carbon C11 and the signal at δ 53.3 ppm corresponds to C13. Two positive signals of the DEPT-135 spectrum at δ 27.0 ppm and δ 34.9 ppm were identified as aliphatic CH groups and the HSQC correlation map (Figure 4-3) was used to

assign the respective protons (H9 and H7). Thus, the chemical shift of C9 was located at δ 25.6 ppm and the carbon C7 possesses a chemical shift of δ 34.9 ppm.

In the aromatic part of the ^{13}C NMR spectrum, the most downfield shifted signal (δ 162.8 ppm) was attributed to the carbonyl group (C2). The one-bond ^{1}H-^{13}C correlation detected in the HSQC spectrum identified the signal at δ 138.1 ppm as C4 (Figure 3-10). The same spectrum allowed the attribution of the proton at δ 5.77 ppm to the carbon at δ 104.2 ppm and the proton at δ 6.17 ppm to the carbon at δ 115.7 ppm. Thus, the remaining signal at δ 150.7 ppm belongs to C6 (Figure 3-10).

However, the major problem in analysing the cytisine's NMR spectra was the identification of C3/H3 and C5/H5 (δ 6.17/115.7 ppm vs. δ 5.77/104.2 ppm). In the HMBC experiment, two and three bond correlations emerged from the carbon C2 to the doublet at δ 6.17 ppm and, furthermore, from the carbon C7 towards the doublet at δ 5.77 ppm (Figure 3-11). Since the detection of ^{5}J correlation in the HMBC spectrum is unlikely and may be excluded (i.e. C7 to H3), the doublet at δ 5.77 ppm was assigned to H5. Thus, with these findings in mind, signals at δ 6.17/115.7 ppm were attributed to H3/C3 and the set of signals at δ 5.77/104.2 ppm to H5/C5, respectively.

An INADEQUATE experiment was performed in order to obtain the connectivity pattern of the skeleton atoms. Unfortunately, the connectivity between C6 and C5 was not detected and the carbonyl C2 was found to couple with the signal at δ 104.2 ppm (Figure 3-12). Both one-bond couplings $^{1}J(C,C)$ and long-range couplings $^{n}J(C,C)$ (n = 2 or 3) have been described by INADEQUATE measurements.[285] Since the cross-signal of C2 - C(δ 104.2 ppm) had a lower intensity when compared to other correlations and more cross-signals of that intensity were found in the INADEQUATE map (Figure 3-12, red circles), this cross-signal was attributed to the long-range coupling over three bonds, i.e. carbonyl C2 to C5. The INADEQUATE conclusions about the carbon-carbon connectivity of the bispidine moiety confirmed the ^{13}C assignment which had been obtained through HSQC and HMBC experiments.

In order to verify the ^{1}H and ^{13}C signals assignment to positions 3 and 5, a natural proton-coupled ^{13}C NMR spectrum was measured (Figure 3-13/B). The signal at δ 104.2 ppm was obtained as a doublet of doublet of doublet (DDD; $^{1}J_{C5/H5}$ = 166.3 Hz; $^{3}J_{C5/H3}$ = 7.5 Hz; $^{3}J_{C5/H7}$ = 3.3 Hz) and the signal at δ 115.71 ppm appeared as a doublet of doublet (DD, $^{1}J_{C3/H3}$ = 167.1 Hz; $^{3}J_{C3/H5}$ = 7.3 Hz). Single-frequency decoupling (SFD) via selective irradiation at δ 2.69 ppm (H7) (Figure 3-13/C) revealed the signal at δ 104.2 ppm as a doublet of doublet (DD; $^{1}J_{C5/H5}$ = 162.2 Hz; $^{3}J_{C5/H3}$ = 8.2 Hz), whereas the ^{3}J coupling of C5 to H7 was missing.

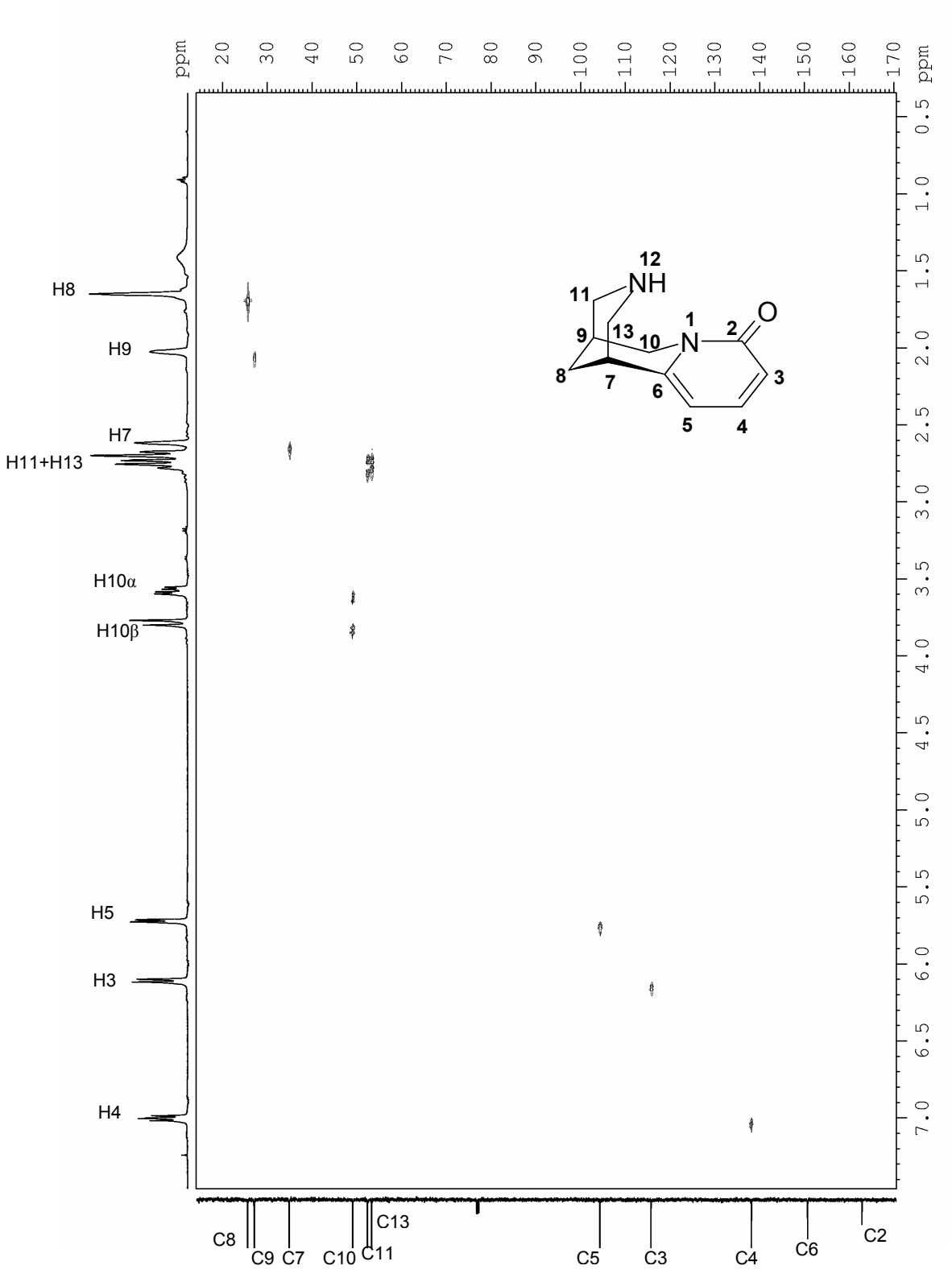

Figure 3-10 2D HSQC contour plot of cytisine **27** [$CDCl_3$, 125 MHz (^{13}C NMR) and 500 MHz (^{1}H NMR)]

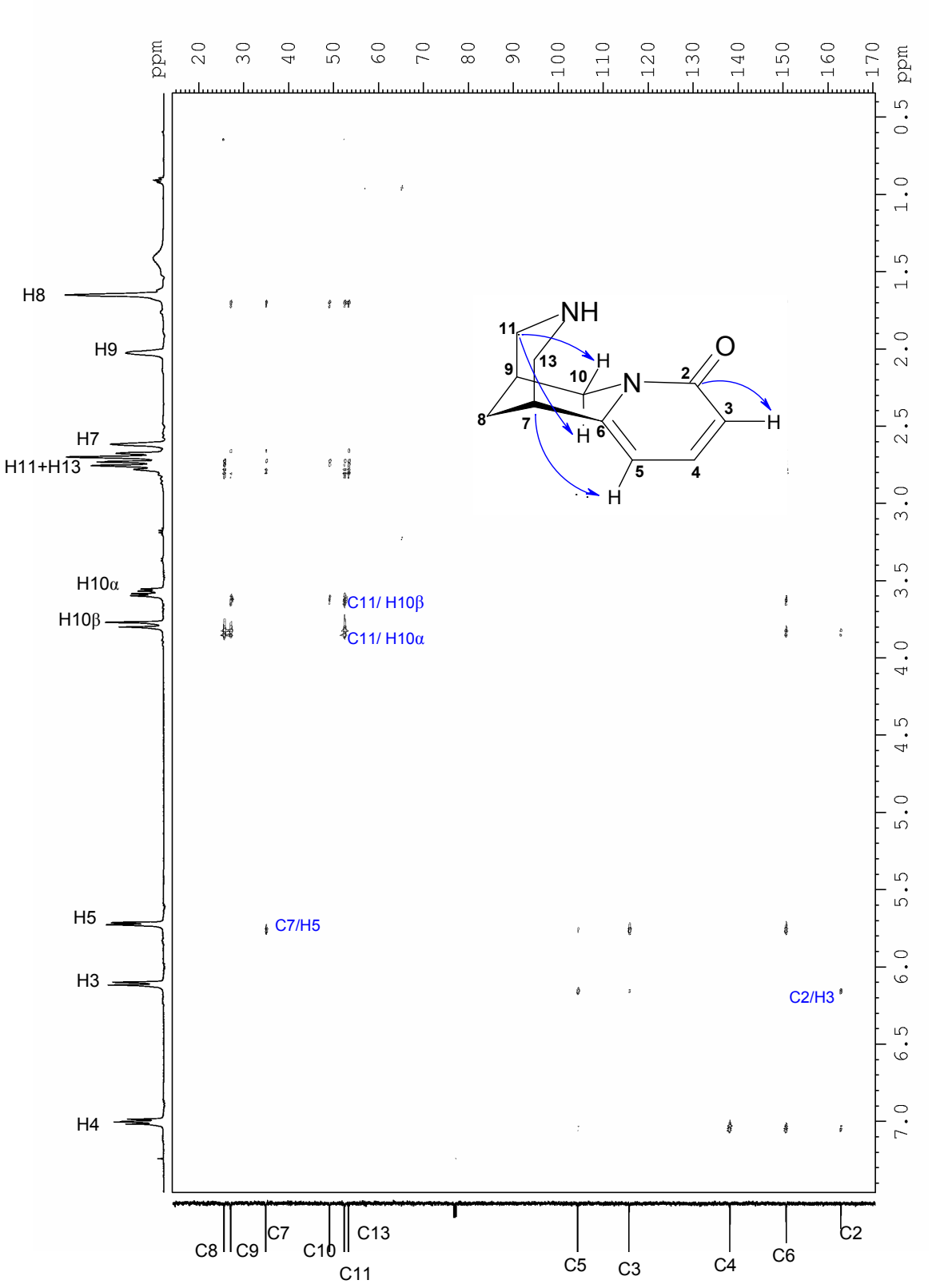

Figure 3-11 2D HMBC contour plot of cytisine **27**. Cross-peaks of particular interest are highlighted in blue. [$CDCl_3$, 125 MHz (^{13}C NMR) and 500 MHz (^{1}H NMR)]

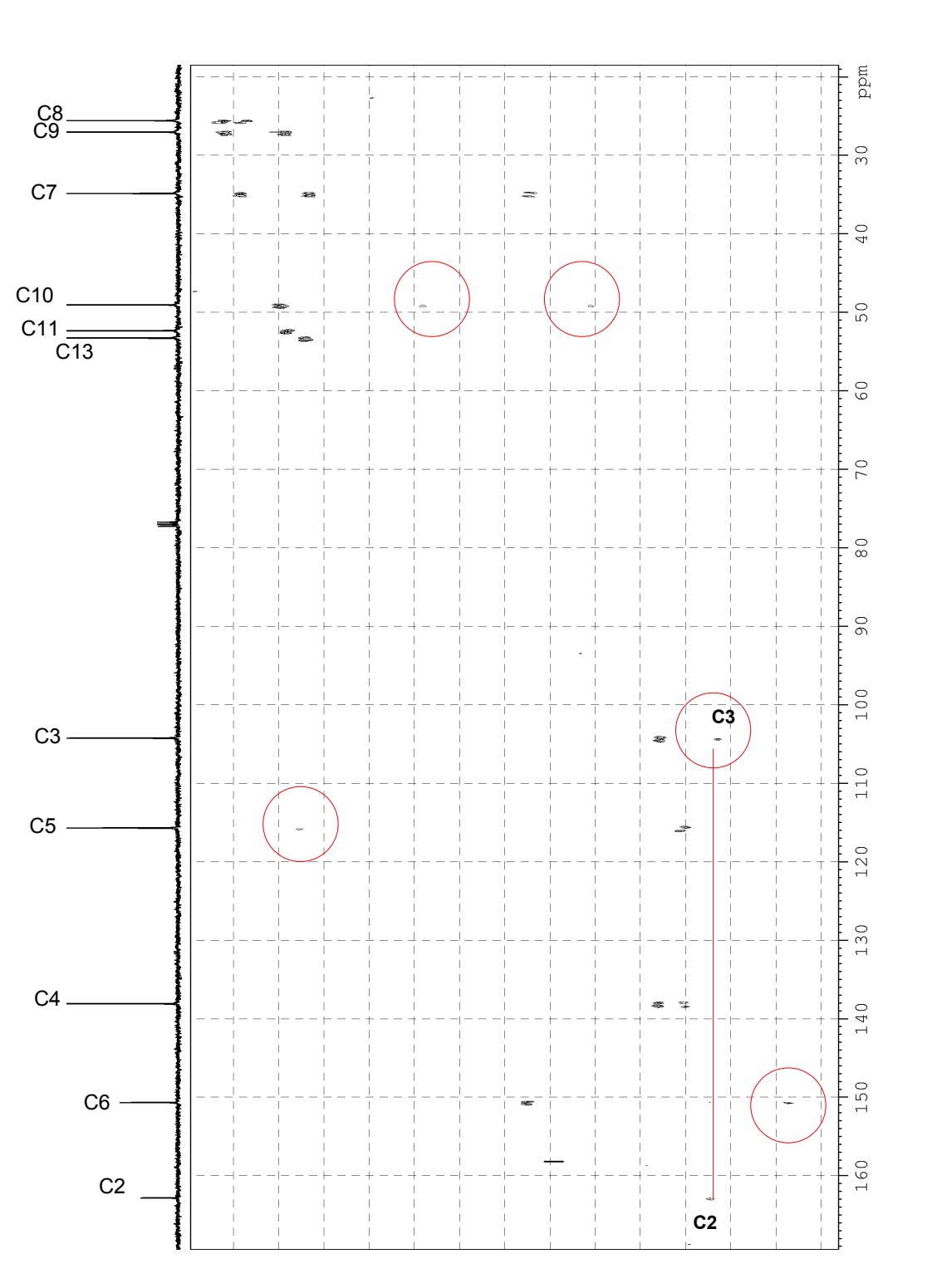

Figure 3-12 2D INADEQUATE spectrum of cytisine **27** ($CDCl_3$, 125 MHz). Red circles pointing out correlations over two or three bonds.

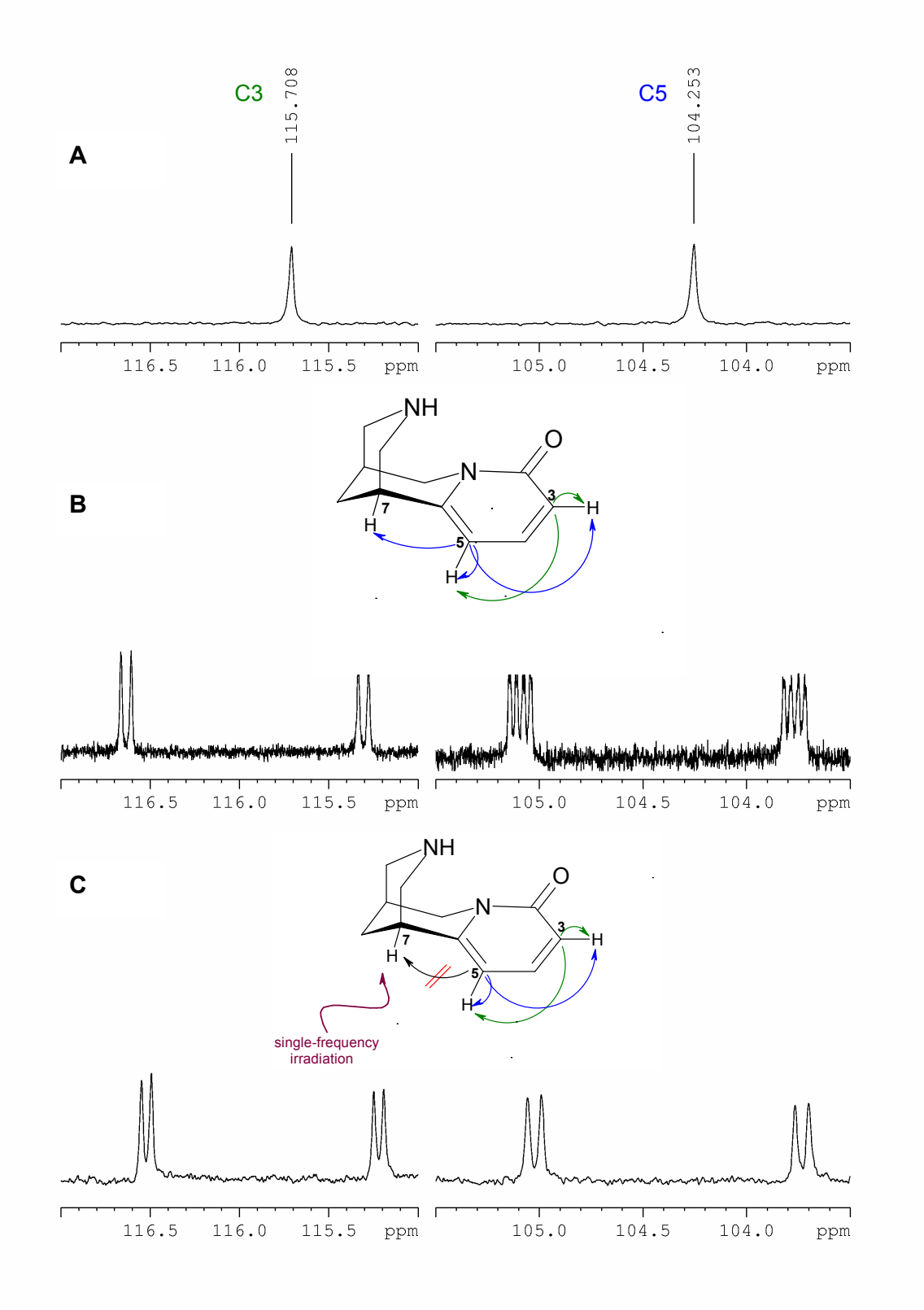

Figure 3-13 Part of decoupled ^{13}C spectrum (**A**), coupled ^{13}C spectrum (**B**) and single frequency decoupled (δ 2.69 ppm) ^{13}C spectrum (**C**) of cytisine **27** ($CDCl_3$, 125 MHz)

The signal at δ 115.7 ppm remained unchanged (DD, $^{1}J_{C3/H3}$ = 163.5 Hz $^{1}J_{C3/H5}$ = 7.0 Hz) (Figure 3-13/C). Therefore, this signal was unequivocally assigned to C3 and the signal at δ 104.2 ppm was assigned to C5. Consequently, H3 appeared at δ 6.17 ppm and proton H5 was located to δ 5.77 ppm.

Except for SFD, all experiments were repeated in deuterated methanol (CD_3OD). There are some subtle differences in the ^{1}H and ^{13}C NMR spectra measured in deuterated chloroform and methanol (Table 3-12). In CD_3OD (compared to $CDCl_3$), the proton H5 is shifted downfield (Δ δ 0.53 ppm) more than the proton H3 (Δ δ 0.27 ppm). Therefore, these two questionable protons (H3 and H5) appear much closer to each other in CD_3OD (δ 6.44 and 6.30 ppm) than they appear in $CDCl_3$ (δ 6.17 and 5.77 ppm). The signals of both H3 and H5 are doublets of doublets with ortho couplings to H4 ($^{3}J_{H4,H5}$ = 6.9 Hz; $^{3}J_{H3,H4}$ = 9.1 Hz) and a mutual meta coupling ($^{4}J_{H3,H5}$ = 1.4 Hz). All aliphatic protons are shifted downfield in CD_3OD by 0.3 ppm, as compared to the chemical shifts in $CDCl_3$.

The ^{13}C chemical shifts of cytisine **27** in CD_3OD were slightly shifted downfield (app. Δ δ 1-4 ppm) when compared to results from experiments performed in $CDCl_3$ (Table 4-2). The most pronounced downfield shift was observed for C5 and the smallest shift for C3. As in the ^{1}H NMR spectrum, also in the ^{13}C NMR chemical shift map, the signals of C3 and C5 approximated each other. Results from the 2D NMR experiments (HSQC, HMBC, INADEQUATE) performed in CD_3OD allowed unambiguous assignments of all ^{1}H and ^{13}C signals in the cytisine **27** skeleton and confirmed the assignments of the signals obtained from $CDCl_3$ – experiments (Table 3-12).

Table 3-12 ^{1}H and ^{13}C chemical shifts of cytisine **27**

	^{1}H NMR (500 MHz)			^{13}C NMR (125 MHz)	
	$CDCl_3$ δ [ppm]	CD_3OD δ [ppm]		$CDCl_3$ δ [ppm]	CD_3OD δ [ppm]
H3	6.17	6.44	**C2**	162.8	165.8
H4	7.05	7.49	**C3**	115.7	117.0
H5	5.77	6.30	**C4**	138.1	141.3
H7	2.69	2.99 – 3.11	**C5**	104.2	108.0
$H8_A$	1.70	2.04	**C6**	150.7	153.3
$H8_B$	1.70	1.98	**C7**	34.9	36.6
H9	2.08	2.39	**C8**	25.6	26.9
H10α	3.63	3.92	**C9**	27.0	29.0
H10β	3.85	4.09	**C10**	49.1	51.3
H11	2.73 – 2.83	2.99 – 3.11	**C11**	52.3	53.4
H13	2.73 – 2.83	2.99 – 3.11	**C13**	53.3	54.4

Thus, the extensive NMR study of the cytisine **27** approved the ^{13}C chemical shift's assignment of Bohlmann *et al*[126] and provided a detailed assignment of the ^{1}H chemical shifts for the first time. The final ^{1}H and ^{13}C signal assignment ($CDCl_3$) is shown in Figure 3-14.

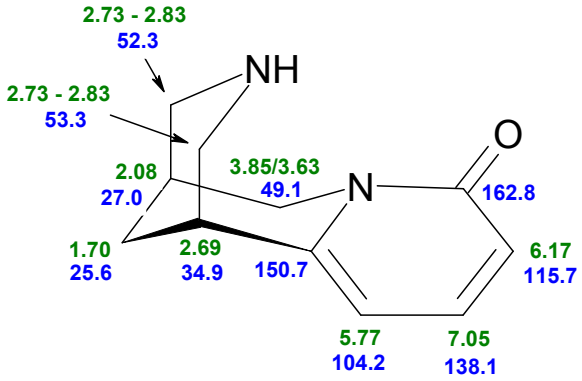

Figure 3-14 Complete assignment of ^{1}H (in green, $CDCl_3$, 500 MHz) and ^{13}C (in blue, $CDCl_3$, 125 MHz) chemical shifts (δ, ppm) for cytisine **27**

3.3.3.2 3-Phenyl- and 5-Phenyl-cytisine 93e & 103e

^{1}H and ^{13}C NMR chemical shifts of 3-phenyl-cytisine **93e** and 5-phenyl-cytisine **103e** are listed in Table 3-13. An introduction of a phenyl moiety into position 3 or 5 leads to downfield shifts of all ^{1}H signals ($\Delta\ \delta$ 0.27 – 0.46 ppm) when compared to cytisine **27**.

Significant differences between the isomers **93e** and **103e** might be seen in the ^{1}H NMR spectrum of the bispidine ring moiety. Bispidine as such is a symmetrical molecule (Figure 3-15/A) and the protons herein designated as H8 are chemically and magnetically equivalent, thus they appear in the ^{1}H spectrum as a singlet (δ 1.42 ppm)[289]. The annelation of a pyridone moiety to the bispidine ring system resulting into the structure of cytisine **27** disturbs the symmetry of the bispidine moiety and the H8 protons become magnetically different. In the ^{1}H NMR spectra the protons $H8_A$ and $H8_B$ are expected to arise as separated peaks. However, the used experimental conditions were not able to detect these two protons separately and the H8 protons gave a sharp singlet in the ^{1}H NMR spectrum of cytisine **27**

Table 3-13 ^{1}H and ^{13}C chemical shifts of cytisine **27**, 3-phenyl-cytisine **93e** and 5-phenyl-cytisine **103e** ($CDCl_3$, 500 MHz)

	cytisine **27** δ [ppm]	3-Ph-cyt **93e** δ [ppm]	5-Ph-cyt **103e** δ [ppm]		cytisine **27** δ [ppm]	3-Ph-cyt **93e** δ [ppm]	5-Ph-cyt **103e** δ [ppm]
H3	6.10	---	6.49	**C2**	162.8	162.1	163.1
H4	7.00	7.46	7.21	**C3**	115.7	127.4	116.1
H5	5.72	6.09	---	**C4**	138.1	137.4	141.4
H7	2.62	2.91	3.04	**C5**	104.2	105.0	119.3
$H8_A$	1.65	1.96	1.84	**C6**	150.7	150.3	147.5
$H8_B$			1.92	**C7**	34.9	35.7	31.6
H9	2.03	2.34	2.30	**C8**	25.6	26.3	26.4
H10α	3.57	3.96	4.19	**C9**	27.0	27.9	27.4
H10β	3.77	4.19	3.95	**C10**	49.1	50.2	50.4
$H11_A$	2.70 – 2.75	3.02 – 3.07	3.12	**C11**	52.3	53.0	52.2
$H11_B$			2.92	**C13**	53.3	54.0	53.0
$H13_A$	2.70 – 2.75	3.02 – 3.07	2.81	**C1'**	---	137.0	138.5
$H13_B$			2.69	**C2'**	---	128.6	129.8
H2'	---	7.69	7.19	**C3'**	---	128.0	128.6
H3'	---	7.38	7.37	**C4'**	---	127.2	127.4
H4'	---	7.29	7.31	**C5'**	---	128.0	128.6
H5'	---	7.38	7.37	**C6'**	---	128.6	129.8
H6'	---	7.69	7.19				

(Figure 3-15/B). The H8 signal simplicity remained the same in 3-phenyl-cytisine **93e** (Figure 3-15/C). Only in the spectrum of 5-phenyl-cytisine **103e** the protons attached to the C8 appear as expected separated doublets at δ 1.84 ppm and δ 1.92 ppm with a geminal coupling of ^2J = 13 Hz (Figure 3-15/D).

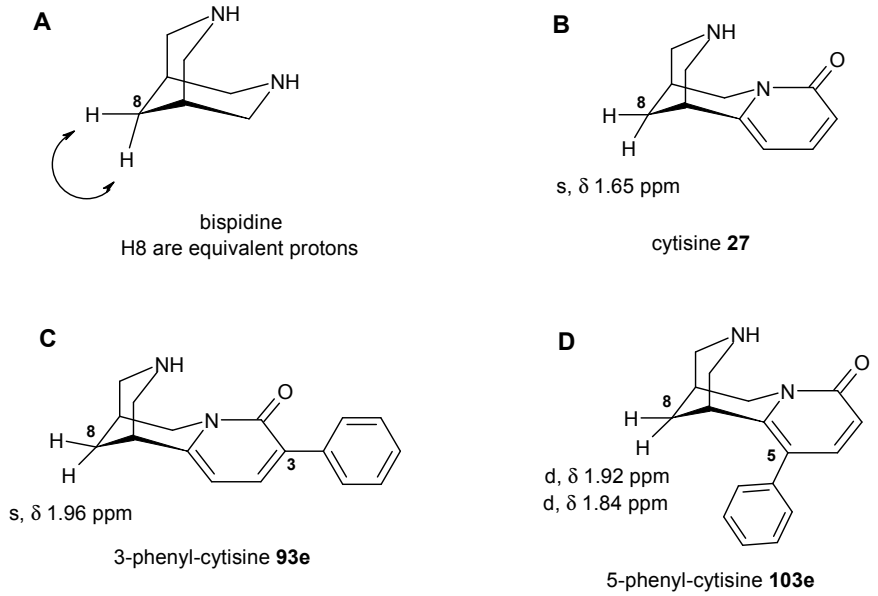

Figure 3-15 Bispidine moiety as a symmetrical molecule (**A**). H8 protons appear as singlets in cytisine **27** (**B**) and 3-phenyl-cytisine **93e** (**C**). In the spectrum of 5-phenyl-cytisine **103e** the H8 protons give two separated doublets (**D**).

Furthermore, in the spectrum of **103e** each proton of the methylene groups in the position 11 and 13 showed separated doublet instead of overlapping doublets as seen in cytisine **27** (δ 2.73 – 2.83 ppm, Figure 3-8/A) and 3-phenyl-cytisine **93e** (δ 3.02 – 3.07 ppm, Figure 3-16). The COSY spectrum of **103e** (Figure 3-17) revealed cross peaks between the doublet at δ 2.81 ppm and the doublet of doublet at δ 2.69 ppm. These cross peaks emerged from the geminal coupling (^2J = 12 Hz) of the H13 protons, which showed a "roof effect". Additionally, both H13 protons gave cross signals to H7, but only one of them was detected as a doublet of doublet (^3J = 2.5 Hz, ^2J = 12 Hz). The doublets at δ 3.12 ppm and δ 2.92 ppm showed a lone mutual cross peak (^2J = 12 Hz) and were assigned to the methylene group in the position 11.

Differences between the ^{1}H NMR spectrum of 3-phenyl- and 5-phenyl-cytisine **93e** and **103e** were also observed in the chemical shifts of the phenyl substituent. In the ^{1}H NMR spectrum of **93e**, the "ortho" protons (H2' and H6') are shifted downfield (δ 7.69 ppm) as compared to the chemical shift of the same protons in the spectrum of **103e** (δ 7.19 ppm) (Table 3-13).

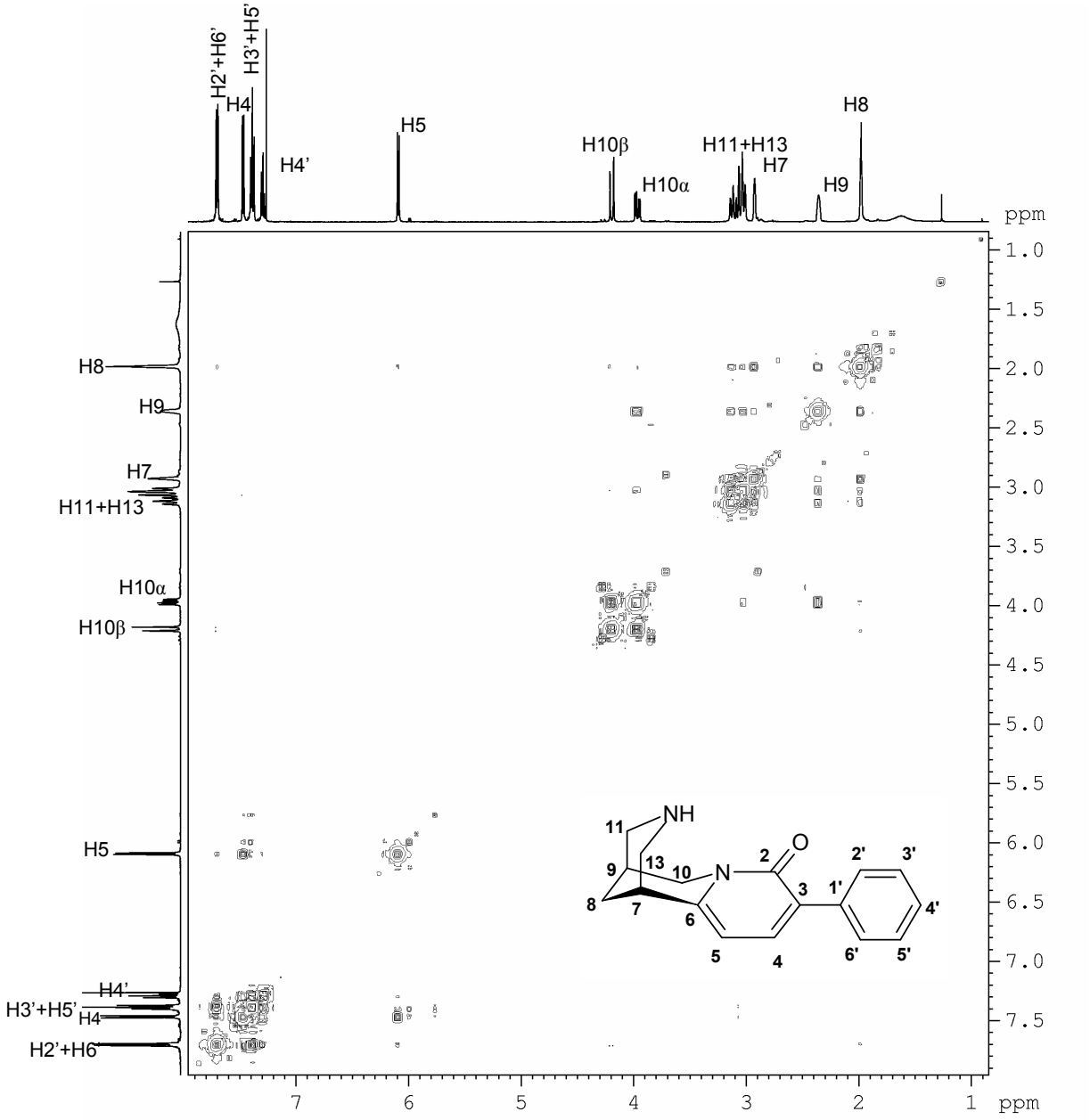

Figure 3-16 2D COSY contour plot of 3-phenyl-cytisine **93e** ($CDCl_3$, 500 MHz)

This relative downfield shift of “ortho” protons in **93e** may be explained by an inductive effect of the 2-carbonyl group or through an anisotropic effect mediated thereby.

In the 3-phenyl- and 5-phenyl-cytisine **93e** and **103e** the pyridone protons H4/H5 and H3/H4 each represent an AB system. Similarly to the data obtained from the analysis of cytisine’s ^1H chemical shifts, the coupling constant of H3/H4 was bigger ($^3J_{H3,H4}$ = 9.5 Hz) than that of H4/H5 ($^3J_{H4,H5}$ = 7.2 Hz).

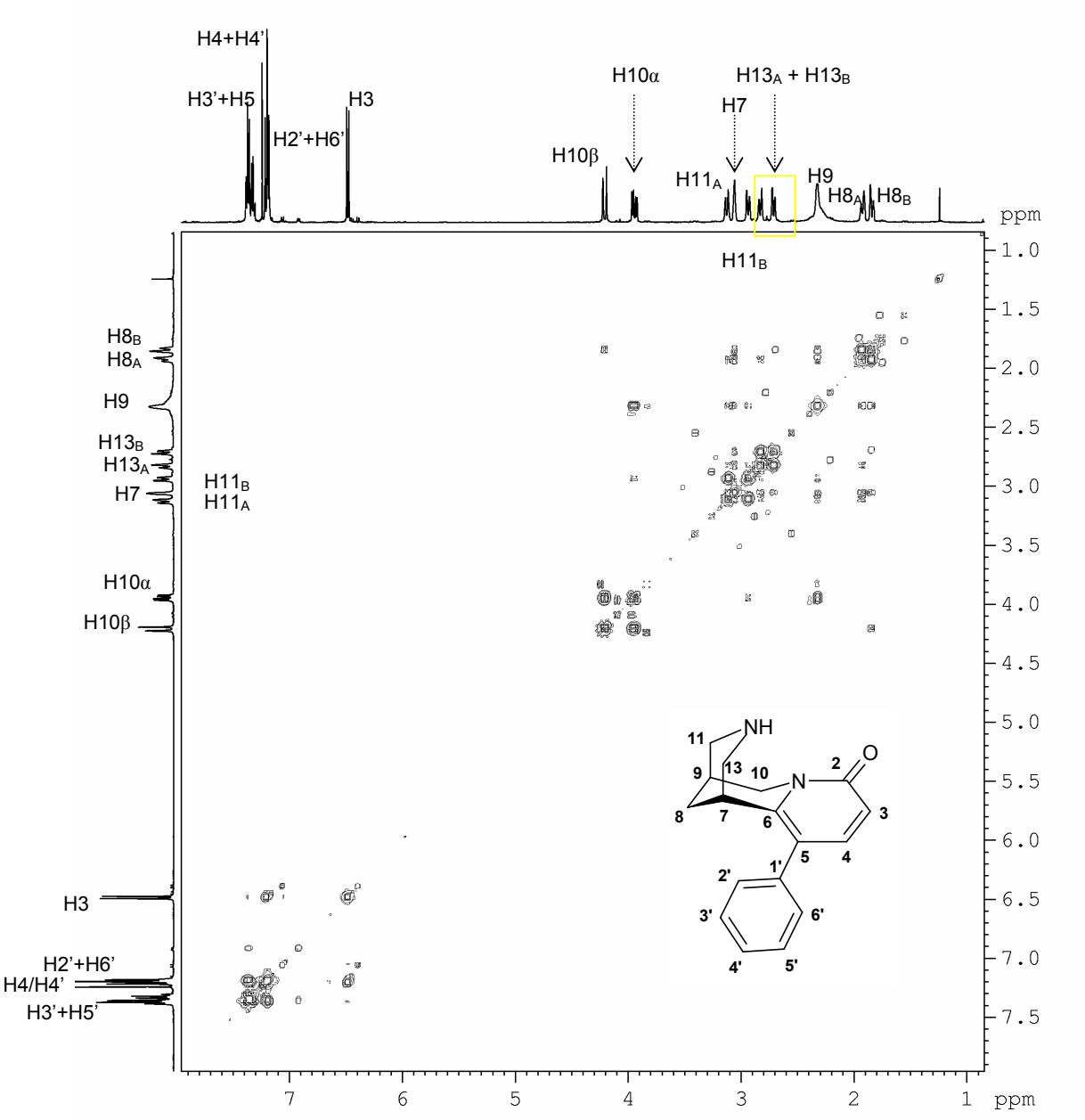

Figure 3-17 2D COSY contour plot of 5-phenyl-cytisine **103e** ($CDCl_3$, 500 MHz)

The substitutions in position 3 or 5 led to a downfield shift of ^{13}C signals, $\Delta\,\delta$ 11.7 ppm for the substituted C3 and $\Delta\,\delta$ 15.1 ppm for the substituted C5, when compared with the chemical shifts found in cytisine **27** (Table 3-13). Simultaneously, a phenyl substitution in position 5 caused an upfield shift of C6 ($\Delta\,\delta$ 3.2 ppm) and C7 ($\Delta\,\delta$ 3.3 ppm). In 3-phenyl-cytisine **93e**, the carbons C6 and C7 retained the ^{13}C chemical shift values measured in cytisine **27**. HSQC correlation maps assigned ^{13}C signals to all secondary and tertiary carbons of 3-phenyl and 5-phenyl-cytisine **93e** and **103e** (Figure 3-18 and 3-19).

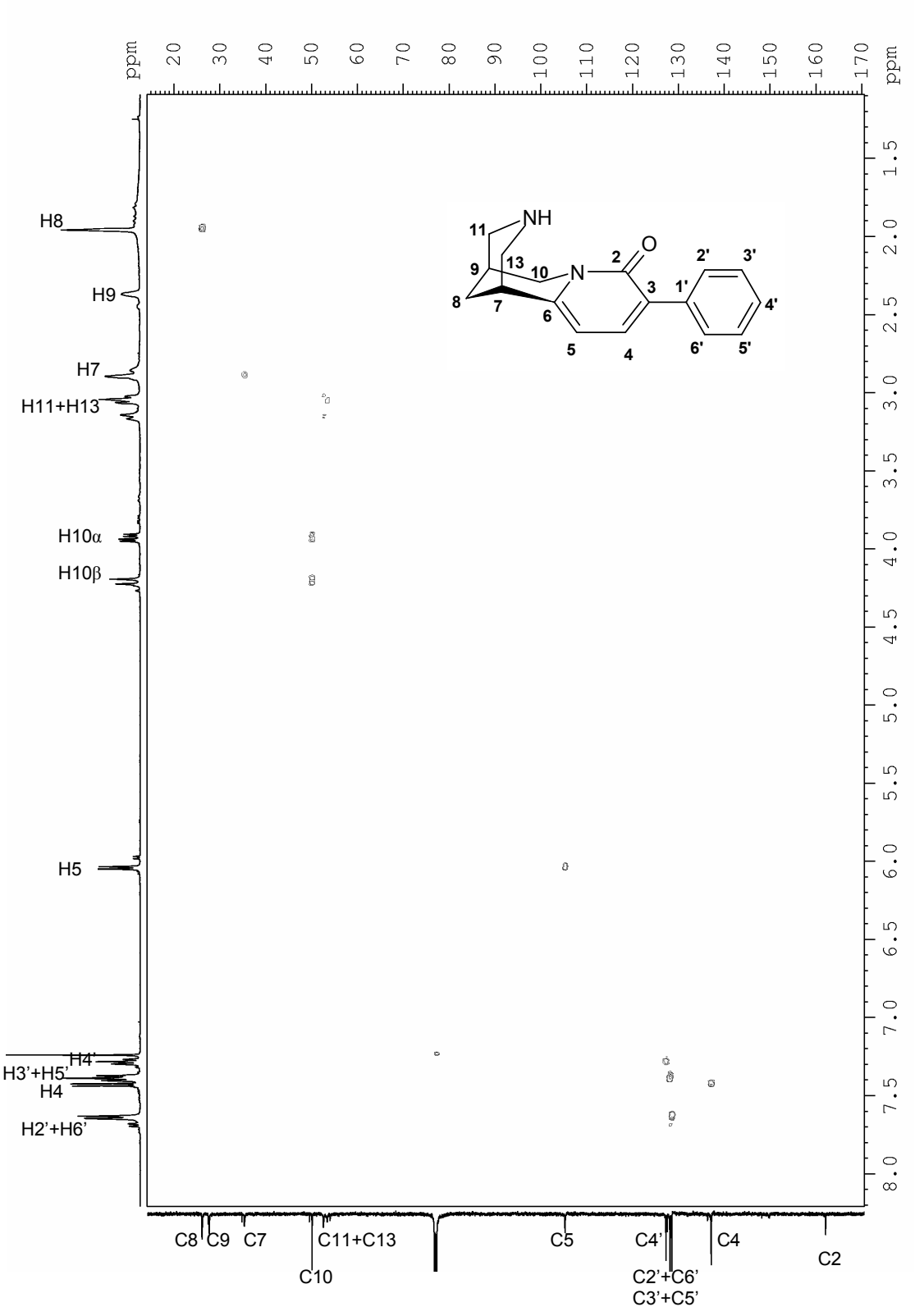

Figure 3-18 2D HSQC contour plot of 3-phenyl-cytisine **93e** [$CDCl_3$, 125 MHz (^{13}C NMR) and 500 MHz (^{1}H NMR)]

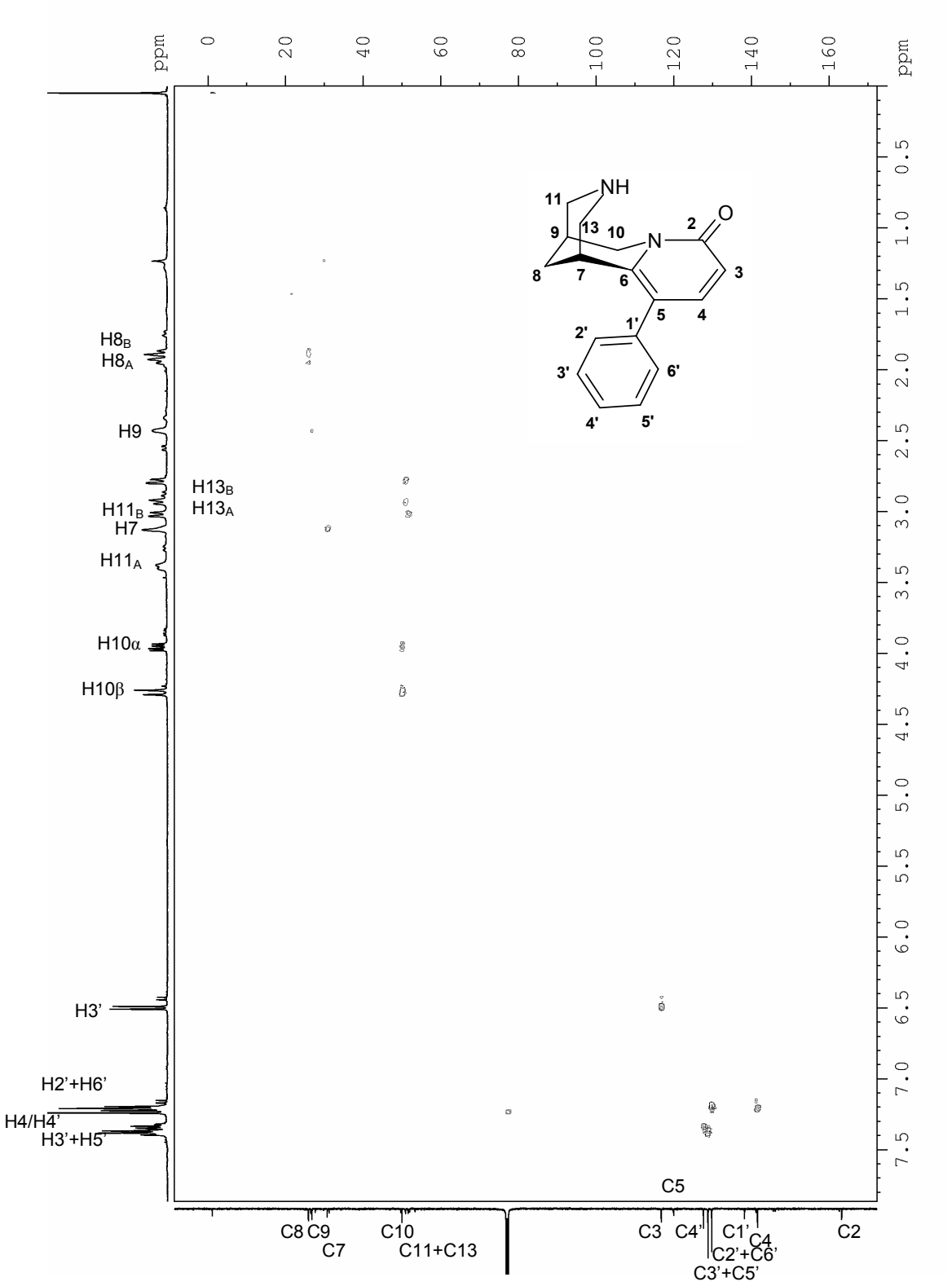

Figure 3-19 2D HSQC contour plot of 5-phenyl-cytisine **103e** [$CDCl_3$, 125 MHz (^{13}C NMR) and 500 MHz (^{1}H NMR)]

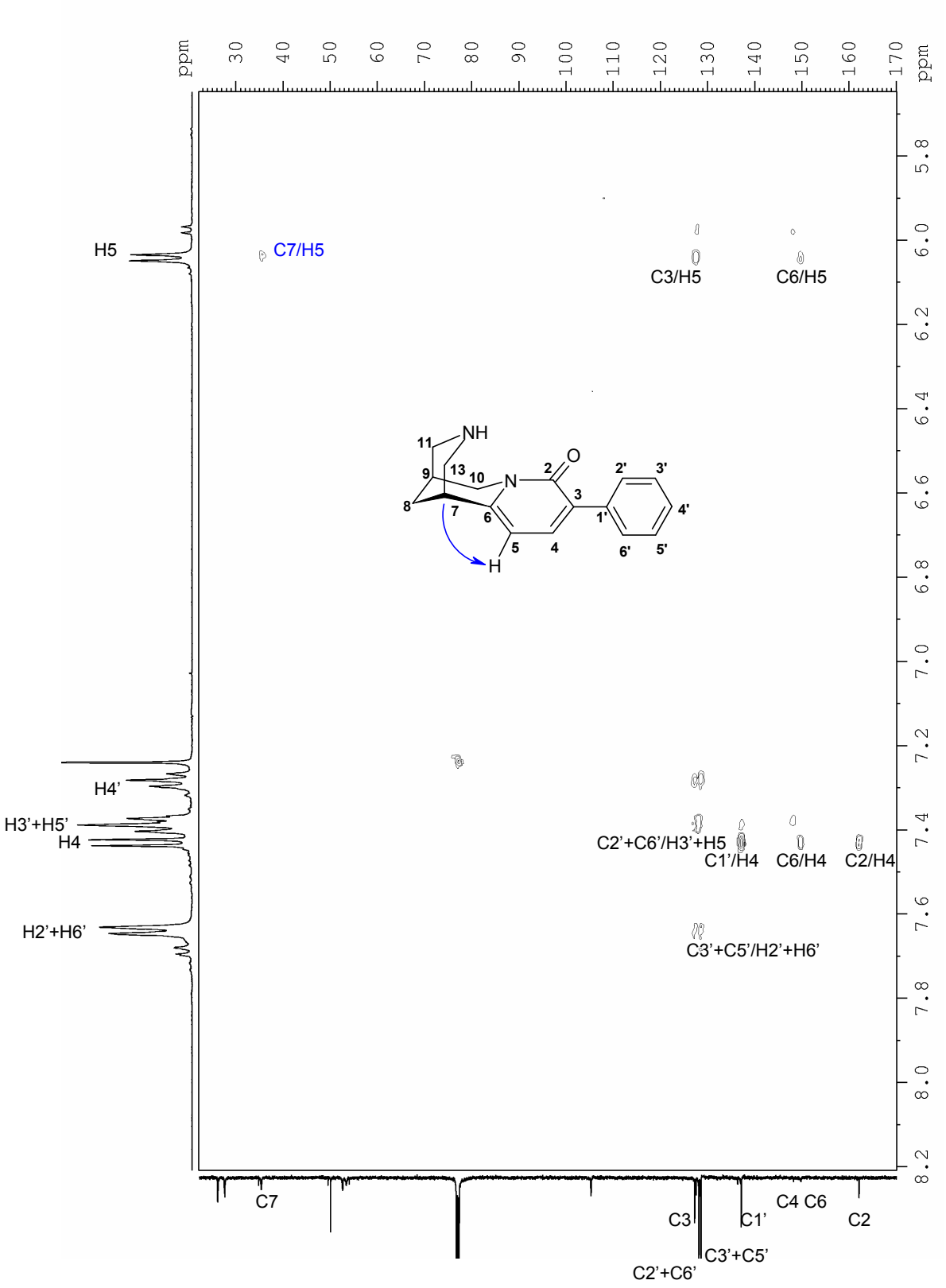

Figure 3-20 2D HMBC contour plot of 3-phenylcytisine **93e**. Decisive correlation C7/H5 highlighted in blue. [$CDCl_3$, 125 MHz (^{13}C NMR) and 500 MHz (^{1}H NMR)]

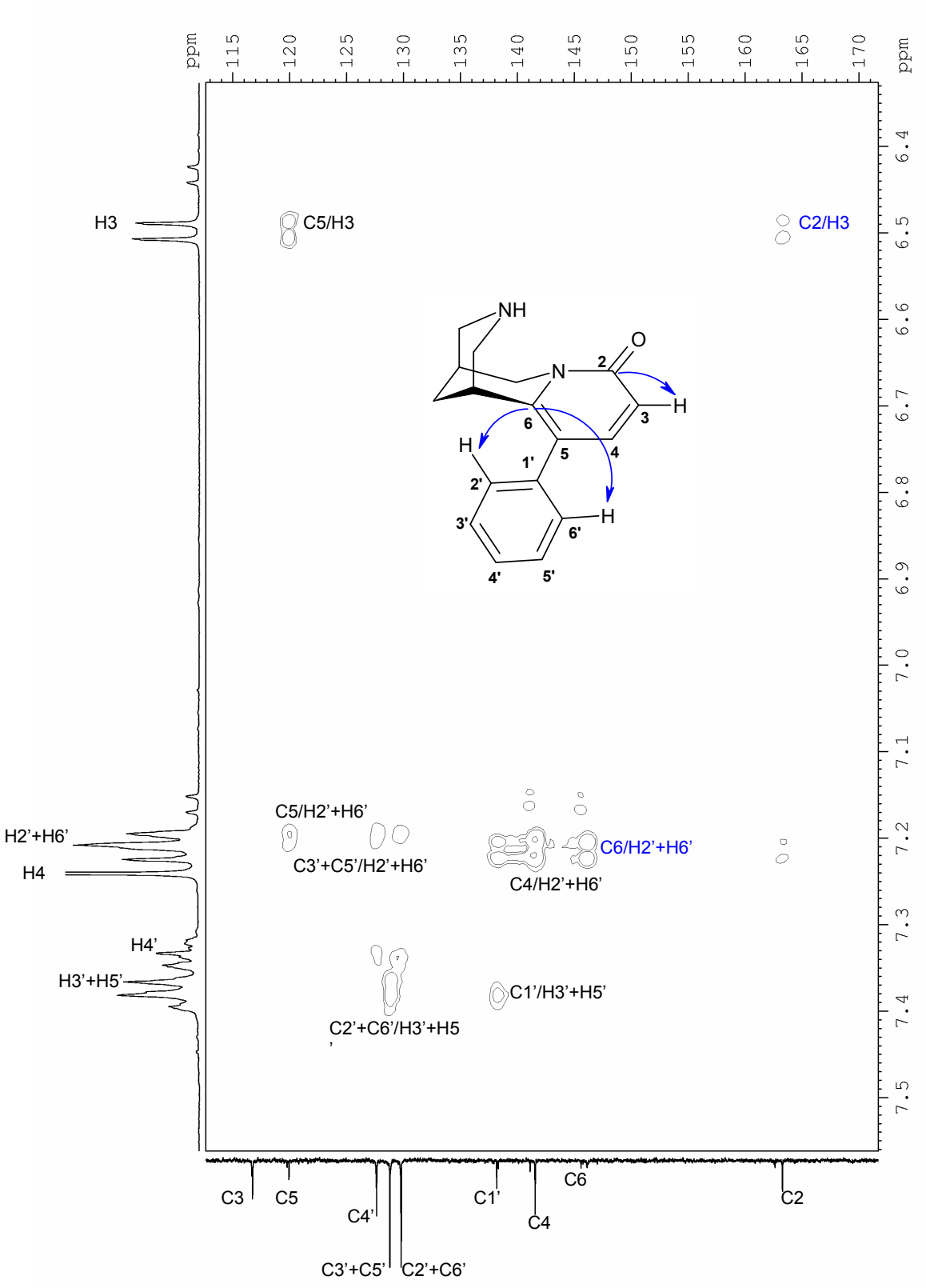

Figure 3-21 2D HMBC contour plot of 5-phenyl-cytisine **103e**. Decisive correlations highlighted in blue. [$CDCl_3$, 125 MHz (^{13}C NMR) and 500 MHz (^{1}H NMR)]

Examinations of the long-range ^{1}H-^{13}C correlations in the HMBC spectra of 3-phenyl-cytisine **93e** (Figure 3-20) and 5-phenyl-cytisine **103e** (Figure 3-21) confirmed the structure of these two isomers. While in the HMBC spectrum of **103e** the carbon C6 is long range coupled over four bonds to the "ortho" protons H2' and H6' (Figure 3-21), in the HMBC of its 3-phenyl counterpart **93e** a cross peak between C6 and H2'/H6' is not observed (Figure 3-20). On the other hand, in the HMBC chemical shift map of **93e**, a correlation peak between C7 and H5 is present (Figure 3-20).

In summary, the most important differences between the two phenyl isomers **93e** and **103e** are:

1. H8 protons appear in 5-phenyl-cytisine **103e** as the two most upfield shifted doublets. These protons give in 3-phenyl-cytisine **93e**, like in cytisine **27,** a singlet peak.
2. Protons H2' and H6' ("ortho" protons of the phenyl substituent) experience a stronger deshielding (δ 7.69 ppm) in the 3-phenyl-cytisine **93e** than in 5-phenylcytisine **103e** (δ 7.19 ppm).
3. The ^{13}C shifts of C6 in 3-phenyl-cytisine **93e** remain similar to the corresponding cytisine **27** carbon (δ 150.3/150.7 ppm, respectively). Likewise, the ^{13}C chemical shifts of C7 do not significantly differ (δ 35.7/34.9 ppm, respectively). In the ^{13}C NMR spectrum of 5-phenyl-cytisine **103e**, the chemical shifts of C6 and C7 are shifted upfield by approximately Δ δ 3 ppm (δ 147.5 and 31.6 ppm, respectively).
4. The coupling constant ^{3}J between H3 and H4 is bigger ($^{3}J_{H3,H4}$ = 9.5 Hz) than that of the coupling between H4 and H5 ($^{3}J_{H4,H5}$ = 7.2 Hz).

These differences are shown in the Figure 3-22 and may be used as "diagnostical" tools to distinguish a 3- and a 5-aryl substitution in the cytisine skeleton.

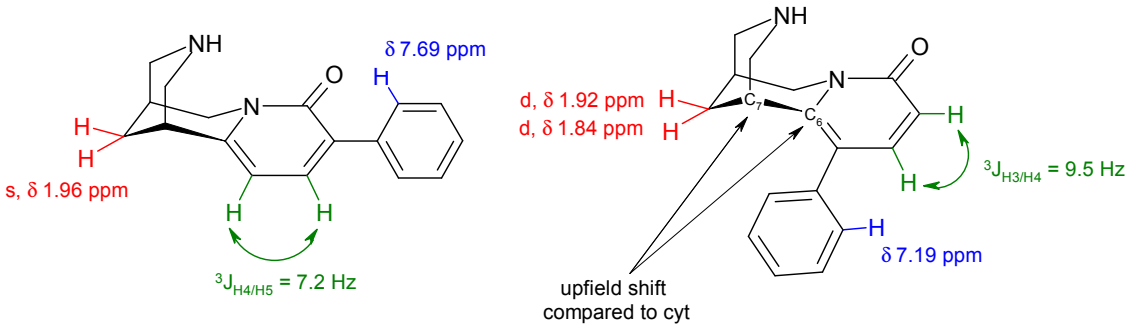

3-phenyl-cytisine **93e** 5-phenyl-cytisine **103e**

Figure 3-22 ^{1}H and ^{13}C NMR spectrum differences between 3-phenyl- and 5-phenylcytisine **93e** and **103e** [$CDCl_3$, 125 MHz (^{13}C NMR) and 500 MHz (^{1}H NMR)]

3.3.3.3 3-Aryl Analogues of Cytisine

All ^{1}H chemical shifts of the 3-aryl substituted cytisine analogues **94e** – **100e** were easily assigned with the help of the complete assignment of ^{1}H NMR signals for 3-phenyl-cytisine **93e** (Table 3-14).

Methyl-substitution of the phenyl ring in the structures **94e** – **100e** did not display any significant effect on the ^{1}H chemical shifts of the bispidine and pyridone moieties. The alteration of ^{1}H chemical shifts of the "cytisine part" in the aryl substituted analogues **94e** – **100e** remain within $\Delta\ \delta \pm 0.03$ ppm, compared to the ^{1}H chemical shift of 3-phenyl-cytisine **93e** (Table 3-14). In the phenyl moiety of **94e** – **100e**, the H3' chemical shifts are missing and the resulting protons H2', H4', H5' and H6' show expected multiplicities and chemical shifts, depending on the nature of the meta substitution (Table 3-14).

All data obtained from ^{1}H NMR spectra are in agreement with the "diagnostical" tools suggested in the previous chapter (3.3.3.2 3-Phenyl and 5-Phenyl-cytisine **93e** and **103e**). The coupling constant of the AB system (H4 and H5) in **94e** – **100e** is δ 7.00 – 7.30 Hz, the protons H8 always appear as broad singlets around δ 1.96 ppm and the magnitude of the downfield shift of H2' is always bigger than that observed in 5-aryl analogues.

^{13}C chemical shifts of 3-aryl derivatives of cytisine **94e** – **100e** are listed in the Table 3-15. The ^{13}C chemical shifts of the cytisine moiety in the structures **94e** – **100e** were largely unaffected by the introduction of the meta substituent (Table 3-15). Except for the carbon C3, which reflected the differences in various aromatic ring substituents, the cytisine part of the molecules retained the chemical shifts observed in 3-phenyl-cytisine **93e**. The ^{13}C chemical shifts of C3 in the structures **94e** – **100e** were shifted slightly (δ 124.7 – 129.1 ppm) when compared to the chemical shift of C3 in 3-phenyl-cytisine **93e** (δ 127.4 ppm) (Table 3-15).

The analysis and assignment of the ^{13}C NMR signals for the aryl moieties in **94e** – **100e** had been performed mainly on the basis of the additivity rule, known as substituent–induced chemical shift "SCS".[283,286] All phenyl ring substituents caused downfield shifts of the α-carbon (C3', δ 128.0 ppm), their magnitudes being correlated with their electronegativity. Increasing electronegativity of the substituent increased the downfield shift of the α-carbon (Table 3-15). Therefore, a strong inductive effect of fluorine in **99e** led to the most pronounced deshielding of the α-carbon ($\Delta\ \delta$ 35.6 ppm); nitro (entry **94e**) and trifluoromethoxy (entry **97e**) substituents caused lower, yet significant, downfield shifts ($\Delta\ \delta$ 20.2 and 21.0 ppm, respectively). The lower electronegativity of chlorine resulted only in a moderate downfield shift ($\Delta\ \delta$ 5.9 ppm, entry **98e**). Methyl substitution of C3' (entry **95e**) or a

Table 3-14 ^{1}H chemical shifts of 3-aryl derivatives of cytisine **93e** – **100e** ($CDCl_3$, 500 MHz)

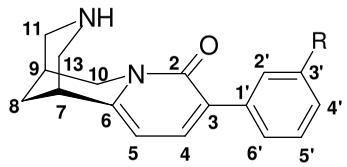

	^{1}H chemical shifts [ppm]							
R =	H **93e**	NO_2 **94e**	CH_3 **95e**	CF_3 **96e**	OCF_3 **97e**	Cl **98e**	F **99e**	Ph **100e**
H4	7.46 (d)	7.54 (d)	7.43 (d)	7.49 (d)	7.45 (d)	7.44 (d)	7.45 (d)	7.51 (d)
H5	6.09 (d)	6.13 (d)	6.06 (d)	6.11 (d)	6.07 (d)	6.08 (d)	6.08 (d)	6.09 (d)
H7	2.91 (br s)	2.95 (br s)	2.91 (br s)	2.94 (br s)	2.91 (br s)	2.92 (br s)	2.92 (br s)	2.93 (br s)
H8	1.96 (br s)	1.97 (br s)	1.97 (br s)	1.96 (br s)	1.95 (br s)	1.96 (br s)	1.96 (br s)	1.97 (br s)
H9	2.34 (br s)	2.38 (br s)	2.34 (br s)	2.35 (br s)	2.35 (br s)	2.35 (br s)	2.36 (br s)	2.35 (br s)
H10α	3.96 (dd)	3.95 (dd)	3.94 (dd)	3.95 (dd)	3.93 (dd)	3.94 (dd)	3.93 (dd)	3.97 (dd)
H10β	4.19 (d)	4.17 (d)	4.18 (d)	4.16 (d)	4.17 (d)	4.16 (d)	4.17 (d)	4.19 (d)
$H11_A$	3.03 (d)	2.98 – 3.14	3.00 – 3.11	2.99 – 3.13	2.95 – 3.12	3.11 (d)	3.12 (d)	3.00 – 3.13
$H11_B$	3.02 (d)	(m)	(m)	(m)	(m)	3.00 (d)	3.01(d)	(m)
$H13_A$	3.07 (dd)	2.98 – 3.14	3.00 – 3.11	2.99 – 3.13	2.95 – 3.12	3.06 (dd)	3.06 (dd)	3.00 – 3.13
$H13_B$	3.02 (d)	(m)	(m)	(m)	(m)	3.00 (d)	2.98 (d)	(m)
H2´	7.69 (dt)	8.53 (t)	7.52 (br s)	7.95 (s)	7.58 (br s)	7.69 (t)	7.43 (br d)	7.91 (t)
H3´	7.38	---	---	---	---	---	---	---
H4´	7.29 (tt)	8.11 (m ovl)	7.09 (d)	7.52 (d)	7.11 (dqui)	7.58 (dt)	6.96 (tdd)	7.51 (dd)
H5´	7.38 (t)	7.52 (t)	7.26 (t)	7.47 (t)	7.38 (t)	7.28 (d)	7.32 (dt)	7.44 (t)
H6'	7.69 (dt)	8.11 (m ovl)	7.43 (d)	7.91 (d)	7.63 (ddd)	7.23 (dd)	7.43 (br d)	7.69 (ddd)

Table 3-15 ^{13}C chemical shifts of 3-aryl derivatives of cytisine **93e** – **100e** ($CDCl_3$,125 MHz)

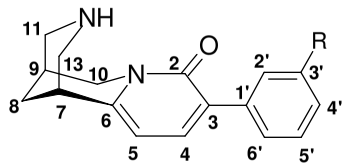

	^{13}C chemical shifts [ppm]							
R =	H **93e**	NO_2 **94e**	CH_3 **95**e	CF_3 **96e**	OCF_3 **97e**	Cl **98e**	F **99e**	Ph **100e**
C2	162.1	161.7	162.2	161.9	161.8	161.8	161.9	162.1
C3	127.4	124.7	127.6	125.8	125.6	125.9	126.0	129.1
C4	137.4	137.6	137.0	137.4	137.3	137.3	137.3	137.6
C5	105.0	105.0	105.0	104.9	105.0	104.9	105.0	105.3
C6	150.3	152.0	150.0	151.4	151.1	151.0	150.7	150.4
C7	35.7	35.7	35.6	35.7	35.6	35.7	35.5	35.3
C8	26.3	26.1	26.3	26.2	26.1	26.2	26.1	26.3
C9	27.9	27.7	27.8	27.8	27.7	27.8	27.7	27.5
C10	50.2	50.3	50.1	50.3	50.2	50.2	50.1	50.2
C11	54.0	52.9	52.8	53.0	52.8	53.0	52.7	53.0
C13	53.0	53.8	53.9	54.0	53.7	53.9	53.6	53.9
C1'	137.0	139.0	137.5	138.1	139.3	139.1	139.4	137.8
C2'	128.6	123.3	129.3	123.8	119.5	128.6	114.0	---*
C3'	128.0	148.2	137.3	130.4	149.0	133.9	163.6	141.4
C4'	127.2	121.9	128.1	125.3	121.1	127.2	115.6	---*
C5'	128.0	128.9	128.0	128.4	129.2	129.2	129.4	---*
C6'	128.6	134.7	125.7	131.9	126.9	126.7	124.1	---*

*) the signals of the biphenyl moiety could not be unambiguously assigned

phenyl attachment (entry **100e**) both caused downfield shifts (Δ δ 9.3 and 13.4 ppm, respectively), owing to the rule $\delta(C_{tert}) < \delta(C_{quart})$.

The large deshielding effect observed on the ^{13}C shift of a carbon atom directly attached to a halogen atom (e.g. fluorine) or to a substituent with negative inductive effect (e.g. nitro or trifluoromethoxy group) does not apply to the chemical shifts of the β- and γ-carbons. In the cases of the electronegative substitution, the ^{13}C chemical shifts of the corresponding γ-carbons are reported to move upfield.[286] Indeed, the ^{13}C chemical shift of C5' in 3-(3'-fluorophenyl)-cytisine **99e** showed an upfield shift of Δ δ 1.4 ppm. The SCSs (i.e. the additivity increments) of various groups for the ^{13}C chemical shifts of the phenyl carbons in the series of 3-aryl-cytisine **93e** – **99e** are given in Table 3-16. The data found are in agreement with the literature SCSs data.[286] The additivity increments for OCF_3 substitution (**97e**) are not listed, since the literature data for SCSs of a trifluoromethoxy group are still not available.

Table 3-16 Additivity increments [ppm] of various groups for the ^{13}C chemical shifts of the phenyl carbons in the series of 3-aryl cytisine derivatives (**94e** – **96e** and **98e** – **99e**), literature SCSs values shown in parentheses[286]

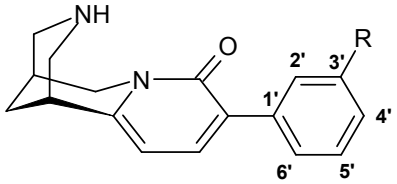

		Additivity Increments [ppm]				
	R = H **93e** [δ,ppm]	NO_2 **94e**	CH_3 **95e**	CF_3 **96e**	Cl **98e**	F **99e**
C1'	137.00	**2.0** (0.8)	**0.5** (0.0)	**1.1** (-0.3)	**2.1** (1.0)	**2.4** (0.9)
C2'	128.6	**-5.3** (-5.3)	**0.7** (0.6)	**-4.8** (-2.6)	**0.0** (0.2)	**-14.6**(-14.3)
C3'	128.0	**20.2** (19.6)	**9.3** (9.3)	**2.4** (2.6)	**5.9** (6.4)	**35.6** (35.1)
C4'	127.2	**-5.3** (-5.3)	**0.9** (0.6)	**-1.9** (-2.6)	**0.0** (0.2)	**-11.6** (-14.3)
C5'	128.0	**0.9** (0.6)	**0.0** (0.0)	**0.4** (-0.3)	**1.2** (1.0)	**1.4** (0.9)
C6'	128.6	**6.1** (6.0)	**-2.9** (-3.1)	**3.3** (-3.2)	**-1.9** (-2.0)	**-4.5** (-4.4)

The ^{13}C chemical shift assignment of the biphenyl substituent in **100e** remains incomplete, as nine tertiary carbons of the biphenyl moiety possess nearly identical chemical shifts in the range δ 125.5 ppm to δ 127.6 ppm. Only the assignments of the quaternary carbons C1' (δ 137.8 ppm), C3' (δ 141.4 ppm) and C1'' (δ 141.0 ppm) could be estimated, however, they might be reversed. Due to the small amount of the substance, detailed 2D NMR correlation experiments (e.g. HSQC or HMBC) required for a complete and final assignment were not measured.

In the ^{13}C NMR spectrum of 3-(3'-fluorophenyl)-cytisine **99e** a doublet was observed at δ 163.6 ppm, corresponding to an aromatic C-F coupling, with a $^{1}J_{C,F}$ = 244.1 Hz. Generally, the long range coupling of fluorine with their neighbouring aromatic carbons greatly facilitate the assignment of the remaining ^{13}C chemical shifts. The fluorine-carbon couplings observed here ranged over two bonds to C2' ($^{2}J_{C,F}$ = 21.2 Hz) and C4' ($^{2}J_{C,F}$ = 22.4 Hz), over three bonds to C1' ($^{3}J_{C,F}$ = 8.2 Hz) and to C5' ($^{3}J_{C,F}$ = 8.5 Hz) as well as over four bonds to C6' ($^{4}J_{C,F}$ = 2.7 Hz) and C3 ($^{4}J_{C,F}$ = 2.3 Hz) and all of them agreed with literature citation[286] (Table 3-17).

Table 3-17 ^{13}C ^{-19}F Coupling constants in 3-(3'-fluorophenyl)-cytisine **99e**, the respective coupling carbon atom given in parentheses

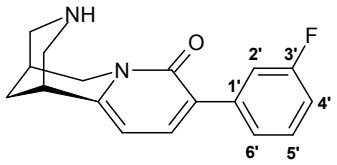

99e

	^{13}C ^{-19}F Coupling constant [Hz]		
	literature[286]	**found**	
$^{1}J_{C,F}$	245	244.1	(C3')
$^{2}J_{C,F}$	21	21.2	(C2')
		22.4	(C4')
$^{3}J_{C,F}$	8	8.2	(C1')
		8.5	(C5')
$^{4}J_{C,F}$	3	2.3	(C3)
		2.7	(C6')

Also in the ^{13}C NMR spectra of 3-(3'-trifluoromethyl-phenyl)-cytisine **96e** and 3-(3'-trifluomethoxy-phenyl)-cytisine **97e,** the ^{13}C-^{19}F couplings were apparent and raised several quartets. The characteristic coupling constants ($^{1}J_{C,F}$ = 272.5 Hz; $^{2}J_{C,F}$ = 31.7 Hz; $^{3}J_{C,F}$ = 3.7 Hz) found in the spectrum of **96e** originate from the direct and the long range couplings between fluorine and its adjacent carbons. The constants are nearly identical with the literature values reported (Table 3-18). The quartet at δ 121.2 ppm in the ^{13}C chemical shifts spectrum of 3-(3'-trifluoromethoxyphenyl)-cytisine **97e** with coupling constant of $^{1}J_{C,F}$ = 257 Hz was assigned to the carbon of the trifluoromethoxy group. Additionally, in the spectrum of **97e** a long range $^{13}C3'$-^{19}F coupling was observed (^{3}J = 1.5 Hz).

Table 3-18 ^{13}C ^{-19}F Coupling constants in 3-(3'-trifluoromethyl-phenyl)-cytisine **96e**

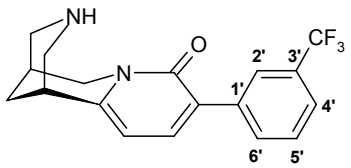

96e

	^{13}C ^{-19}F Coupling constant [Hz]		
	literature[286]	**found**	
$^{1}J_{C,F}$	272	272.5	(CF_3)
$^{2}J_{C,F}$	32	31.7	(C3')
$^{3}J_{C,F}$	4	3.7	(C2')
		3.7	(C4')

3.3.3.4 5-Aryl Analogues of Cytisine

The ^{1}H and ^{13}C chemical shifts of the 5-aryl derivatives of cytisine **103e** – **110e** are listed in Tables 3-20 and 3-21. Assignment of ^{1}H and ^{13}C signals was carried out by comparison with the assignments for 5-phenyl-cytisine **103e** as well as through the increment additivity rules.

The ^{1}H chemical shifts of the cytisine moiety of the 5-aryl derivatives **104e** – **110e** compare greatly to those of the cytisine part in the 5-phenyl analogue **103e** (Table 3-20). Protons H8 (assigned to a sharp methylene singlet in the ^{1}H spectra of the 3-aryl derivatives **93e** – **100e)** appeared in the spectra of the 5-aryl derivatives as two separated broad singlets (**104e**, **107e** and **108e**) or as two broad doublets with geminal couplings $^{2}J_{H8\alpha/H8\beta}$ between 12.6 and 13 Hz (**105e**, **106e** and **109e**). The A and B doublets of the 11 and 13 methylene AB systems are all well separated and may be correlated to their geminal partners with the aid of their "roof" effect.

The protons H3 and H4 of the 5-substituted pyridone moiety in the series of 5-aryl derivatives **103e** – **110e**, always representing an AB system, display cis coupling constants $^{3}J_{H3,H4}$ = 9.1 – 9.3 Hz. The respective vicinal coupling constants $^{3}J_{H3,H4}$ = 9.1 and 9.5 Hz were established in the ^{1}H spectrum of cytisine **27** and 5-phenyl-cytisine **103e**. These results suggest that the meta-substitution on the phenyl ring does not particularly influence the vicinal coupling of the H3 and H4 protons.

However, the meta-substituent changed the ^{1}H chemical shifts of phenyl moiety in **104e** – **110e** when compared to the chemical shifts of 5-phenyl-cytisine **103e** (Table 3-20). The assignment of the four protons H2', H4', H5' and H6' was feasible through their multiplicities and substituent chemical shifts. Significant differences between the chemical shifts of H2' in 5-aryl and 3-aryl analogues were observed. The H2' protons of 3-aryl substituted cytisines **94e** – **100e** were deshielded by the neighbouring carbonyl group while in the 5-aryl derivatives **103e** – **110e** this neighbour effect was lacking (Table 3-19).

Table 3-19 ^{1}H chemical shifts of H2' protons in 3- and 5-aryl derivatives of cytisine (signed as 3-H2' and 5-H2') ($CDCl_3$, 500 MHz)

	^{1}H chemical shifts of H2' [ppm]						
	R = H	**CH_3**	**Cl**	**NO_2**	**CF_3**	**F**	**OCF_3**
3-H2'	7.69	7.52	7.69	8.53	7.95	7.43	7.58
5-H2'	7.21	7.00	7.32	8.10	7.46	6.90	7.08
$\Delta\delta$	0.48	0.52	0.37	0.43	0.49	0.53	0.50
	$\Delta\delta$ = 0.47 ± 0.06 ppm						

Table 3-20 ^{1}H chemical shifts of 5-phenyl derivatives of cytisine **103e** – **110e** ($CDCl_3$, 500 MHz)

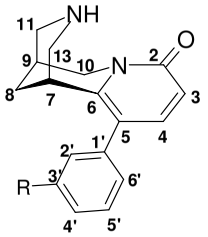

	^{1}H chemical shifts [ppm]							
R =	H **103e**	NO_2 **104e**	CH_3 **105e**	CF_3 **106e**	OCF_3 **107e**	Cl **108e**	F **109e**	Ph **110e**
H3	6.49 (d)	6.52 (d)	6.47 (d)	6.49 (d)	6.50 (d)	6.49 (d)	6.47 (d)	6.51 (d)
H4	7.21 (d)	7.18 (d)	7.19 (d)	7.17 (d)	7.19 (d)	7.17 (d)	7.16 (d)	7.26 (d)
H7	3.04 (br s)	2.93 (ovl)	3.07 (br s)	2.93 (br s)	3.11 (br s)	3.04 (br s)	3.07 (br s)	3.09 (br s)
$H8_A$	1.92 (d)	1.94 (br s)	1.92 (br d)	1.93 (br d)	1.91 (br s)	1.93 (br s)	1.91 (br s)	1.94 (br d)
$H8_B$	1.84 (d)	1.87 (br s)	1.83 (br d)	1.82 (br d)	1.84 (br s)	1.81 (br s)	1.84 (d br)	1.84 (br d)
H9	2.30 (br s)	2.35 (s)	2.29 (br s)	2.31 (br s)	2.46 (br s)	2.34 (br s)	2.31 (br s)	2.30 (br s)
H10α	3.95 (dd)	3.96 (dd)	3.93 (dd)	3.94 (dd)	3.95 (dd)	3.95 (dd)	3.92 (dd)	3.96 (dd)
H10β	4.19 (d)	4.19 (d)	4.19 (d)	4.18 (d)	4.26 (d)	4.21 (d)	4.17 (d)	4.22 (d)
$H11_A$	3.12 (d)	3.10 (d)	3.04 (d)	3.06 (d)	3.39 (d)	2.73 (d)	3.03 (d)	3.07 (d)
$H11_B$	2.92 (d)	2.93 (ovl)	2.91 (d)	2.90 (d)	3.07 (d)	2.73 (d)	2.93 (br s)	2.91 (d)
$H13_A$	2.81 (d)	2.74 (ovl)	2.81 (d)	2.75 (d)	2.92 (dd)	2.95 (d)	2.79 (br d)	2.85 (d)
$H13_B$	2.69 (dd)	2.74 (ovl)	2.68 (dd)	2.69 (dd)	2.82 (d)	2.81 (dd)	2.71 (br d)	2.72 (d)
H2'	7.21 (d)	8.09 – 8.11	7.00 (s ovl)	7.46 (s)	7.08 (d)	7.32 (m ovl)	6.90 (dt)	7.55 – 7.58 (m)
H3'	7.37 (tt)	---	---	---	---	---	---	---
H4'	7.31 (tt)	8.16 – 8.21	7.12 (br d)	7.39 (d)	7.20 (ddd)	7.32 (m)	7.01 (tdd)	7.17 (dt)
H5'	7.37 (tt)	7.55 – 7.50	7.25 (t)	7.50 (t)	7.41 (t)	7.21 (t)	7.32 (td)	7.41 – 7.46 (m)
H6'	7.18 (tt)	7.55 – 7.50	6.98 (br d)	7.58 (d)	7.15 (dt)	7.09 (dd)	6.96 (dt)	7.41 – 7.46 (m)

Table 3-21 ^{13}C chemical shifts of 5-phenyl derivatives of cytisine **103e** – **108e** and **109e** – **110e** ($CDCl_3$, 125 MHz)

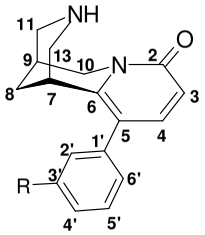

	^{13}C chemical shifts [ppm]						
R =	H **103e**	NO_2 **104e**	CH_3 **105e**	CF_3 **106e**	OCF_3 **107e**	F **109e**	Ph **110e**
C2	163.1	163.0	163.1	163.0	163.2	163.0	163.1
C3	116.1	116.3	116.0	116.4	117.0	116.2	116.1
C4	141.4	141.0	141.4	140.8	141.1	140.9	141.3
C5	119.3	117.2	119.5	117.6	116.4	118.0	119.1
C6	147.5	148.1	147.4	148.0	148.3	147.6	147.7
C7	31.6	32.1	31.6	31.7	30.5	31.6	31.4
C8	26.4	26.3	26.4	26.3	25.5	26.2	26.4
C9	27.4	27.7	27.4	27.3	26.4	27.3	27.4
C10	50.4	50.5	50.4	50.5	49.8	50.4	50.5
C11	52.2	52.0	52.2	52.1	50.4	52.1	52.3
C13	53.0	52.9	53.0	53.0	51.2	52.8	53.0
C1'	138.5	140.0	138.4	139.3	140.0	140.6	139.0
C2'	129.8	124.2	130.4	126.5	120.0	116.8	---
C3'	128.6	148.4	138.3	130.9	149.3	163.6	140.6
C4'	127.4	121.9	128.1	124.3	122.3	114.4	---
C5'	128.6	129.2	128.4	129.2	130.2	130.1	---
C6'	129.8	135.5	126.8	133.2	128.2	125.6	---

^{13}C chemical shifts of the phenyl moieties in **103e** – **110e** are in agreement with ^{13}C chemical shifts of the corresponding carbons in their 3-aryl counterparts **93e** – **100e** as well as with the predicted values (i.e. ^{13}C chemical shifts of the phenyl ring in **103e** ± SCS of the substitutent with regard to the position[286]). Thus, the additivity increments calculated from the experimental data are in good accordance with literature SCSs data[286] (Table 3-22).

Table 3-22 Additivity increments [ppm] of various groups for the ^{13}C chemical shifts of the phenyl carbons in the series of 5-aryl cytisine derivatives (**104e** – **106e** and **109e**), literature SCSs values shown in parentheses[286]

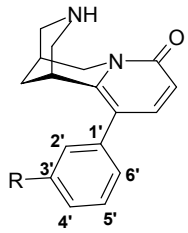

		Substituent chemical shifts [ppm]			
	R = H **103e** [δ, ppm]	NO_2 **104e**	CH_3 **105e**	CF_3 **106e**	F **109e**
C1'	138.5	**1.5** (0.8)	**-0.1** (0.0)	**0.8** (-0.3)	**2.1** (0.9)
C2'	129.8	**-5.6** (-5.3)	**0.6** (0.6)	**-3.3** (-2.6)	**-13.0** (-14.3)
C3'	128.6	**19.8** (19.6)	**9.7** (9.3)	**2.3** (2.6)	**35.0** (35.1)
C4'	127.4	**-5.5** (-5.3)	**0.7** (0.6)	**-3.1** (-2.6)	**-13.0** (-14.3)
C5'	128.6	**0.6** (0.6)	**-0.2** (0.0)	**0.6** (-0.3)	**1.5** (0.9)
C6'	129.8	**5.7** (6.0)	**-3.0** (-3.1)	**3.4** (-3.2)	**-4.2** (-4.4)

One of the "diagnostical tools" to distinguish the 3- and 5-substituted counterparts is the chemical shift difference of approximately δ 3 ppm between the carbons C6 and C7 in the 3-substituted **93e** – **100e** and 5-substituted analogues **103e** – **110e**. While in the ^{13}C NMR spectra of cytisine **27** and the 3-phenyl derivatives **93e** – **100e** the carbons C6 and C7 display signals around δ 150 ppm and δ 35 ppm, respectively (Table 3-15), the same carbons are shifted upfield in the ^{13}C spectra of the 5-substituted analogues **103e** – **110e** (Table 3-21). Hence, their carbons C6 are located between δ 147.4 – 148.1 ppm and their C7 between δ 30.5 – 32.1 ppm. Similar shift mutation, however in the opposite direction, was observed for C4 of the 5-substituted derivatives. While 3-substitution did not alter the ^{13}C chemical shift of C4 compared with cytisine **27** (δ 137.0 – 137.6 ppm) (Table 3-15), a 5-substitution resulted in a medium downfield shift of Δ δ 2.27 ± 0.23 ppm (n=6) and thereby, the C4 signals were found between δ 140.8 and 141.4 ppm (Table 3-21). The ^{13}C chemical shifts of the remaining carbons in the bispidine and pyridone ring maintained the values

found in the spectra of the unsubstituted alkaloid **27** and the 3-substituted analogues **93e** – **100e**.

In the ^{13}C spectra of the compounds **106e**, **107e** and **109e** containing fluorine, characteristic ^{13}C-^{19}F couplings were observed (Table 3-23). C-F doublets in the 5-(3'-fluoro)-phenyl analogue **109e** and C-F_3 quartets in the spectrum of **106e** supported the carbon assignment when literature data[286] were considered. The C-F doublet in **109e** was found at δ 163.6 ppm (literature: δ 163.6 ppm)[286] and the chemical shift of the CF_3 – quartet in **106e** (δ 124.9 ppm) also definitely agreed with the value published (δ 124.5 ppm)[286]**.** The presence of a CF_3-group gave hints towards the C3', C2' and C4' signals (δ 130.9; 126.5 and 124.3 ppm, respectively) which were split into quartets, their shifts matching the literature ppm values (δ 130.8 ppm for C3' and δ 125.4 ppm for ortho C2' and C4').[286]

Table 3-23 $^{13}C^{-19}F$ Coupling constants in 5-(3'-trifluoromethylphenyl)-cytisine **106e** (A) and 5-(3'-fluorophenyl)-cytisine **109e** (B), coupling carbon given in parentheses

A

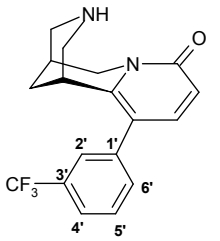

106e

	^{13}C ^{-19}F Coupling constant [Hz]		
	literature[286]	**found**	
$^{1}J_{C,F}$	272	272.5	(<u>C</u>F_3)
$^{2}J_{C,F}$	32	32.3	(C3')
$^{3}J_{C,F}$	4	3.8	(C2')
		3.8	(C4')

B

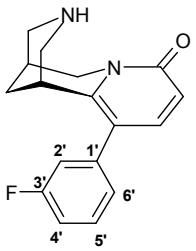

109e

	^{13}C ^{-19}F Coupling constant [Hz]		
	literature[286]	**found**	
$^{1}J_{C,F}$	245	247.6	(C3')
$^{2}J_{C,F}$	21	21.0	(C2')
		21.0	(C4')
$^{3}J_{C,F}$	8	7.7	(C1')
		8.5	(C5')
$^{4}J_{C,F}$	3	2.7	(C6')
		1.7	(C5)

3.3.3.5 Heterocyclic Analogues of Cytisine

^{1}H and ^{13}C chemical shifts of the cytisine derivatives **117e** – **126e**, substituted in 3- and 5-position with heterocycle are listed in the Tables 3-24, 3-25 and 3-26.

In general it may be concluded that a 3-substitution with a heterocyclic moiety moved all the ^{1}H chemical shifts of the cytisine moiety downfield when compared to the unsubstituted alkaloid **27** (Table 3-24). The examination of the ^{13}C data obtained from cytisine **27** and its 3-heterocyclic derivatives **117e** – **122e** revealed only a difference in the chemical shift of C3, whereas the chemical shifts of other cytisine carbons (C2-C13) were largely unaffected (Table 3-25).

The substitution of the position 5 with a heterocycle (**123e** – **126e**) also caused a downfield shift of all ^{1}H signals for cytisine moiety (Table 3-26). The ^{13}C chemical shifts of the bispidine and pyridone moieties in the structures of the 5-substituted analogues **123e** – **126e** were consistent with the trends reported for 5-aryl derivatives **103e** – **110e** (i.e. upfield shift of C6 and C7 signals) (Table 3-26).

Structures and assignment of NMR signals of the heterocyclic analogues **117e** – **126e** is discussed separately for each set of corresponding 3- and 5-isomer.

3.3.3.5.1 3- and 5-(5'-Indolyl)-cytisine **117e** & **123e**

The ^{1}H chemical shifts of 3-(5'-indolyl)-cytisine **117e** are listed in Table 3-24. The doublet at δ 6.06 ppm (^{3}J = 7.0 Hz) was assigned to H5. This signal provided the starting point for assignments of the remaining aromatic protons located in the region δ 8.3 – 6.0 ppm. In the COSY 2D spectrum of **117e** (Figure 3-24), H5 displayed a cross peak to a doublet at δ 7.47 ppm (^{3}J = 7.0 Hz), which therefore was assigned to H4. A broad singlet at δ 8.28 ppm appeared as the most downfield shifted signal, it was assigned to the indolic NH group. Another singlet at δ 7.92 ppm was recognised as H2' and it showed only one correlation towards the doublet at δ 7.52 ppm. This doublet had an additional cross peak with the doublet at δ 7.38 ppm, therefore these two signals were identified as H7' (coupling with H2' and H6') and H6' (coupling with H7'). A pseudotriplet at δ 7.16 ppm produced a cross peak with the NH group at δ 8.28 ppm, thus it was assigned to the proton H4'. Finally, the cross signal between δ 7.16 ppm and δ 6.54 ppm could only arise from a coupling between H4' (δ 7.16 ppm) and H3' (δ 6.54 ppm).

Table 3-24 ^{1}H chemical shifts of 3-heterocyclic derivatives of cytisine **117e** – **122e** ($CDCl_3$, 500 MHz)

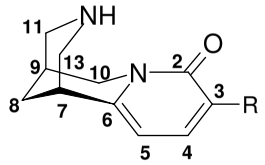

R	H cytisine **27**	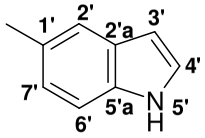 **117e**	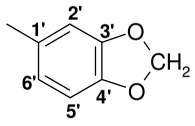 **118e**	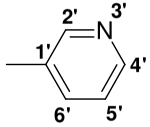 **119e**	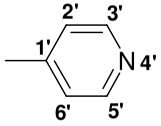 **120e**	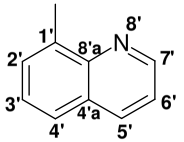 **121e**	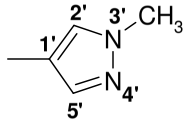 **122e**
H3	6.10	---	---	---	---	---	---
H4	7.00	7.47	7.38	7.49	7.57	7.58	7.56
H5	5.72	6.06	6.05	6.11	6.13	6.16	6.05
H7	2.62	2.89	2.90	2.95	2.94	2.95	2.90
H8	1.65	1.96	1.95	1.96	1.96	1.96	1.94
H9	2.03	2.34	2.34	2.36	2.36	2.33	2.33
H10α	3.57	3.96	3.93	3.94	3.95	3.96	3.94
H10β	3.77	4.22	4.16	4.16	4.16	4.21	4.18
$H11_A$	2.70 – 2.75	3.12	3.11	3.11	3.11	3.08	3.09
$H11_B$		3.00 – 3.06	3.00	2.99 – 3.03	3.00		2.96
$H13_A$	2.70 – 2.75	3.00 – 3.06	3.06	3.06	3.07	3.02	3.03
$H13_B$			3.00	2.99 – 3.03	3.04	3.13	2.99
H2'	---	7.92	7.26	8.78	7.67	7.85	7.80
H3'	---	6.54	---	---	8.57	7.56	---
H4'	---	7.16	---	8.49	---	7.78	---
H5'	---	8.28 (NH)	6.81	7.29	8.57	8.15	8.29
H6'	---	7.38	7.12	8.16	7.67	7.35	---
H7'	---	7.52	---	---	---	8.86	---
			5.94 ($C\underline{H}_2$)				3.90 ($C\underline{H}_3$)

Table 3-25 ^{13}C chemical shifts of 3-heterocyclic derivatives of cytisine **117e** – **122e** ($CDCl_3$, 125 MHz)

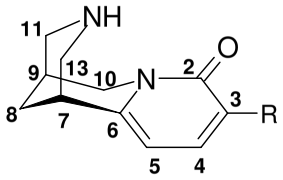

R	H cytisine **27**	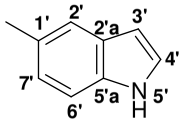 **117e**	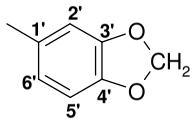 **118e**	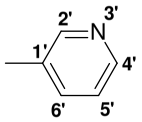 **119e**	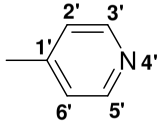 **120e**	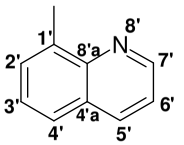 **121e**	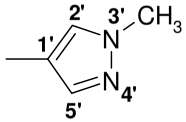 **122e**
C2	163.7	162.6	162.1	161.9	161.5	162.5	161.2
C3	116.8	128.9	127.1	123.9	122.8	136.5	119.8
C4	138.8	136.7	136.4	137.2	137.8	139.8	132.4
C5	105.1	105.1	104.9	105.0	104.9	104.8	105.1
C6	150.9	148.9	149.9	151.5	152.6	150.4	148.0
C7	35.5	35.6	35.7	35.7	35.8	35.8	35.5
C8	26.2	26.4	26.4	26.2	26.2	26.4	26.4
C9	27.7	27.9	27.9	27.8	27.8	27.9	27.9
C10	49.7	50.1	50.2	50.3	50.3	50.1	50.1
C11	53.8	52.9	53.0	53.0	53.0	53.0	52.9
C13	52.8	53.8	54.0	53.9	53.9	53.9	53.9
C1'	---	129.1	131.4	133.2	144.9	139.6	117.8
C2'	---	120.9	109.4	149.1	123.9	131.0	136.8
C3'	---	103.0	147.3	---	149.6	126.2	---
C4'	---	124.3	146.8	148.2	---	127.7	---
C5'	---	---	108.0	122.8	149.6	136.4	129.9
C6'	---	110.5	122.1	136.1	123.9	120.8	---
C7'	---	123.2	---	---	---	149.9	---
		127.8 **(C2'a)**	100.9 **(CH_2)**			146.5 **(C8'a)**	
		135.3 **(C5'a)**				128.6 **(C4'a)**	

Table 3-26 ^{1}H and ^{13}C chemical shifts of 5-heterocyclic derivatives of cytisine **123e** – **126e** [$CDCl_3$, 500 MHz for ^{1}H NMR; 125 MHz for ^{13}C NMR]

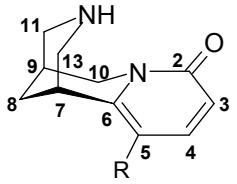

R	H cytisine **27**	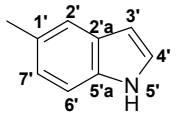	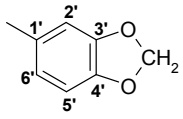	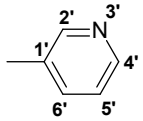	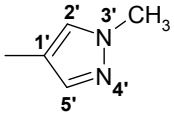
		123e	**124e**	**125e**	**126e**
H3	6.10	6.49	6.45	6.52	6.46
H4	7.00	7.28	7.17	7.18	7.22
H7	2.62	3.14	3.08	2.97	3.13
$H8_A$	1.65	1.81	1.84	1.86	1.88
$H8_B$		1.93	1.91	1.94	
H9	2.03	2.30	2.30	2.35	2.31
H10α	3.57	3.97	3.93	3.95	3.95
H10β	3.77	4.23	4.18	4.21	4.17
$H11_A$	2.70 – 2.75	3.08	2.82	3.14	3.08
$H11_B$		2.93	2.72	2.93	2.98
$H13_A$	2.70 – 2.75	2.87	3.08	2.79	2.93
$H13_B$		2.64	2.92	2.71	2.87
H2'	---	7.44	6.65	8.49	7.26
H3'	---	6.53	---	---	---
H4'	---	7.26	---	8.58	---
H5'	---	8.53 **(NH)**	6.80	7.33	7.38
H6'	---	6.98	6.63	7.55	---
	5.72 **(H5)**	7.39 **(H7')**	5.97 **($C\underline{H}_2$)**	---	3.91 **($C\underline{H}_3$)**
C2	163.7	163.2	163.1	163.0	163.1
C3	116.8	115.7	116.0	116.7	116.3
C4	138.8	142.2	141.5	141.0	142.0
C5	105.1	120.5	118.8	115.3	109.4
C6	150.9	147.6	147.8	148.1	148.2
C7	35.5	31.6	31.6	31.6	31.8
C8	26.2	26.4	26.4	26.2	26.3
C9	27.7	27.4	27.4	27.2	27.3
C10	49.7	50.4	50.4	50.4	50.4
C11	53.8	52.2	52.1	51.8	52.4
C13	52.8	52.9	52.9	52.7	52.9
C1'	---	129.8	132.0	134.3	118.5
C2'	---	121.7	110.2	148.8	139.1
C3'	---	102.6	147.7	---	---
C4'	---	125.1	146.9	150.5	---
C5'	---	135.0 **(C5'a)**	108.4	123.5	129.1
C6'	---	111.1	123.1	137.2	---
C7'	---	123.9	---	---	---
	---	128.0 **(C2'a)**	101.2 **($\underline{C}H_2$)**	---	39.1 **($\underline{C}H_3$)**

In the HSQC experiment of **127e** (Figure 3-25), the carbons C2'a and C5'a were identified by comparison with literature data[286] for the corresponding carbons in the unsubstituted indole (Figure 3-23/A). Assignments of C1' (δ 129.13 ppm) and C3 (δ 128.90 ppm) were achieved when ^{13}C chemical shifts for **117e** and its 5-counterpart **123e** were compared. In both spectra, quaternary carbon signals at δ 129.1 (C1' in **117e**) and 129.8 ppm (C1' in **123e**) were present, whereas the signal at δ 128.9 ppm (substituted C3 of **117e**) was replaced in the spectrum of 5-(5'-indolyl)-cytisine **123e** in favour of a signal at δ 115.7 ppm (unsubstituted C3 of **123e**). Vice versa, in the spectrum of **117e** the ^{13}C chemical shift of the methine carbon C5 was located at δ 105.1 ppm, while in the spectrum of **123e** the substituted C5 signal was at δ 120.5 ppm. This comparison, as well as the complete assignment of ^{1}H and ^{13}C chemical shifts for **117e** allowed a straightforward assignment of all ^{1}H and ^{13}C chemical shifts for 5-(5'-indolyl)-cytisine **123e**.

The assignment of ^{13}C chemical shifts of the indolyl moieties of both isomers were verified by the literature[286] comparison (Figure 3-23). Shift differences in the spectra of **117e** and **123e** agree well with the above mentioned diagnostical tools for differentiating the 3- and 5-isomers (Figure 3-22).

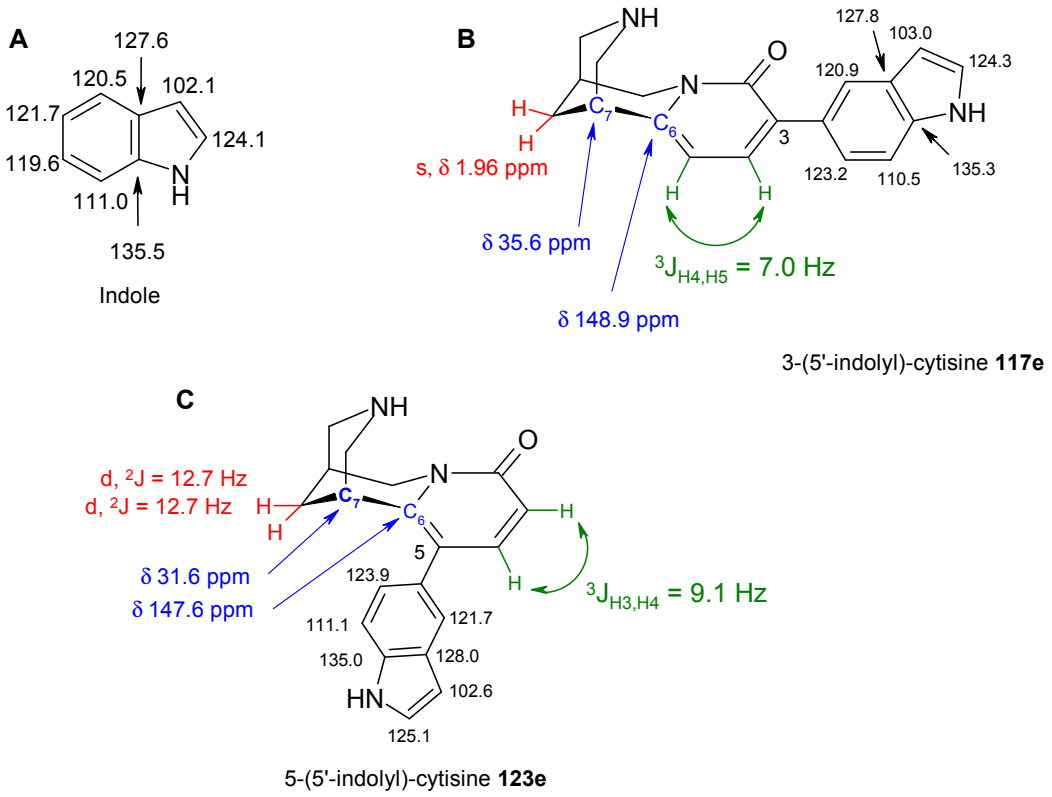

Figure 3-23 Comparison of ^{13}C chemical shifts of unsubstituted indole (A, Ref. 286) and indole moiety bound to cytisine in positions 3 (B) and 5 (C). Also the diagnostical tools to distinguish the isomers **117e** and **123e** are pictured.

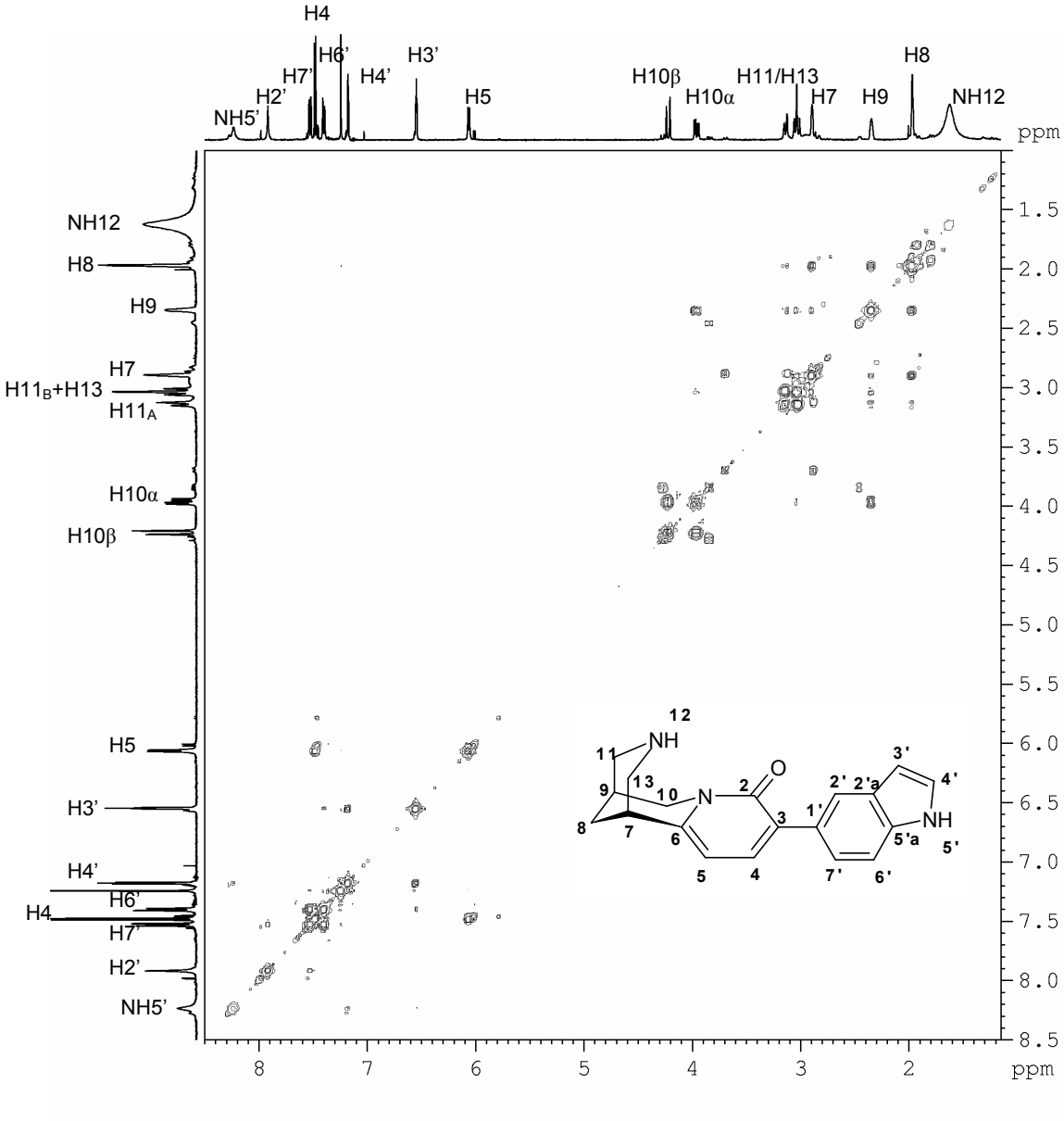

Figure 3-24 2D COSY contour plot of 3-(5'-indolyl)-cytisine **117e** ($CDCl_3$, 500 MHz)

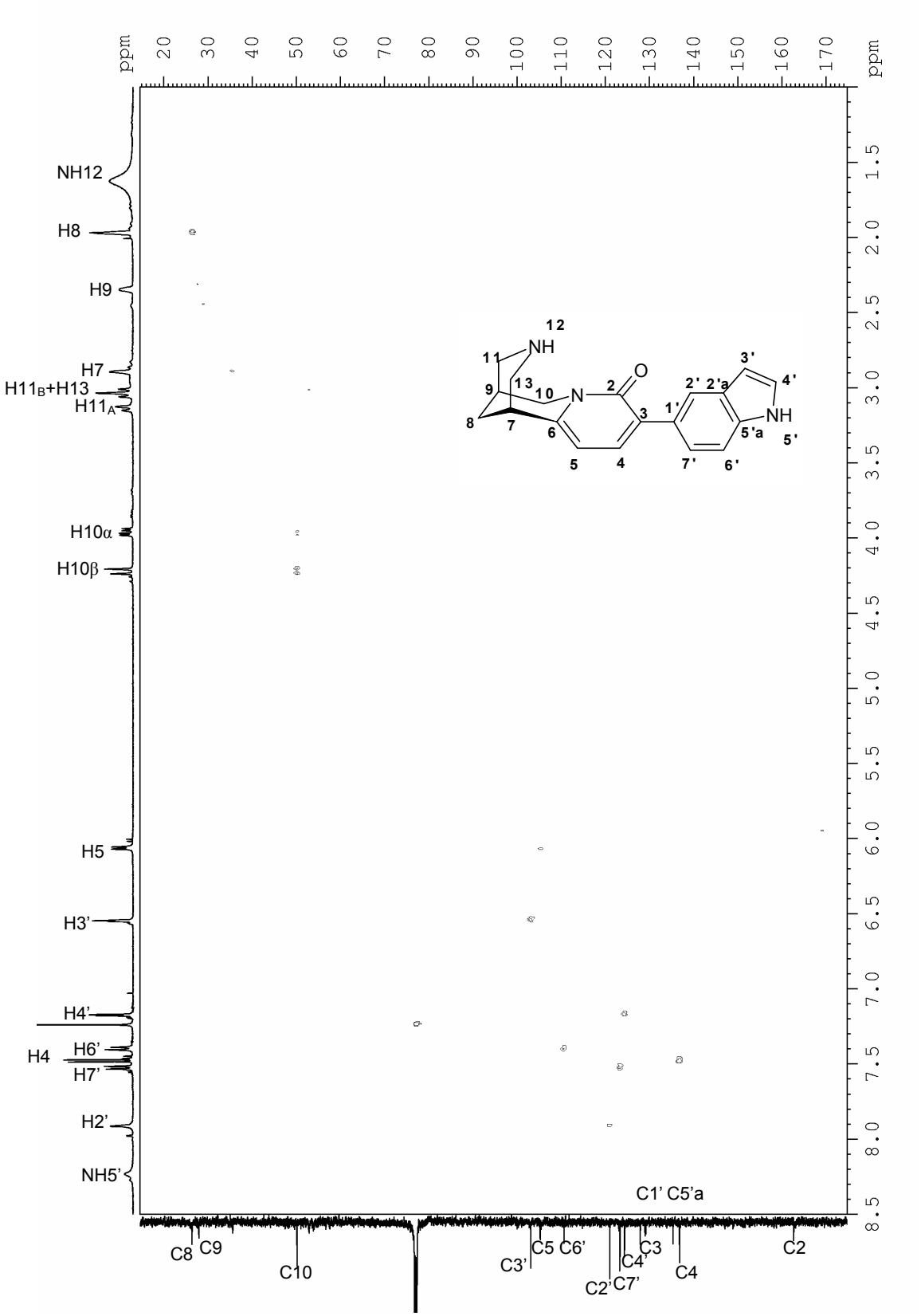

Figure 3-25 2D HSQC contour plot of 3-(5'-indolyl)-cytisine **117e** [$CDCl_3$, 500 MHz for ^{1}H NMR; 125 MHz for ^{13}C NMR]

3.3.3.5.2 3- and 5-(3',4'-Methylenedioxyphenyl)-cytisine **118e** & **124e**

In the set of the 3',4'-methylenedioxyphenyl-cytisines **118e** and **124e**, the ^{1}H and ^{13}C chemical shift assignments were first completed for the 5-isomer **124e**. Herein, the cytisine moiety could be easily assigned by comparison with previous assignments, since the 5-substituent of any type was found not to influence the chemical shifts of the cytisine moiety (Table 3-26). The aromatic protons of **124e** were assigned with the aid of the 2D COSY spectrum (Figure 3-26). The proton at δ 6.45 ppm was assigned to H3. H3 displayed a cross signal to the doublet at δ 7.17 ppm, this was therefore assigned to H4. The doublet at δ 6.65 ppm except of its meta coupling (^{4}J = 1.8 Hz) showed no cross signal and was assigned to H2'. The doublet of doublet at δ 6.63 ppm was assigned to H6', due to its meta coupling (^{4}J = 1.8 Hz towards H2'). The significant cross peak for H6' and a doublet at δ 6.80 ppm proved this signal to be H5'.

The HSQC spectrum of **124e** assigned peaks to the carbons bonded with protons (Figure 3-27). The quaternary carbons C3' and C4' had nearly identical chemical shifts (δ 146.9 and 147.7 ppm) and could not be unambiguously assigned. The substitution of C5 caused a downfield shift of $\Delta\ \delta$ 14.6 ppm compared to the ^{13}C chemical shift of an unsubstituted C5 in the cytisine spectrum (δ 104.2 ppm). The remaining ^{13}C chemical shift at δ 132.0 ppm was assigned to the quaternary carbon C1'.

The assignment of ^{1}H and ^{13}C chemical shifts of 3-(3',4'-methylenedioxy-phenyl) derivative **118e** (Table 3-24 and 3-25) was completed with the information obtained from the assignment of **124e** and the known NMR spectral differences between the 3- and 5 isomers.

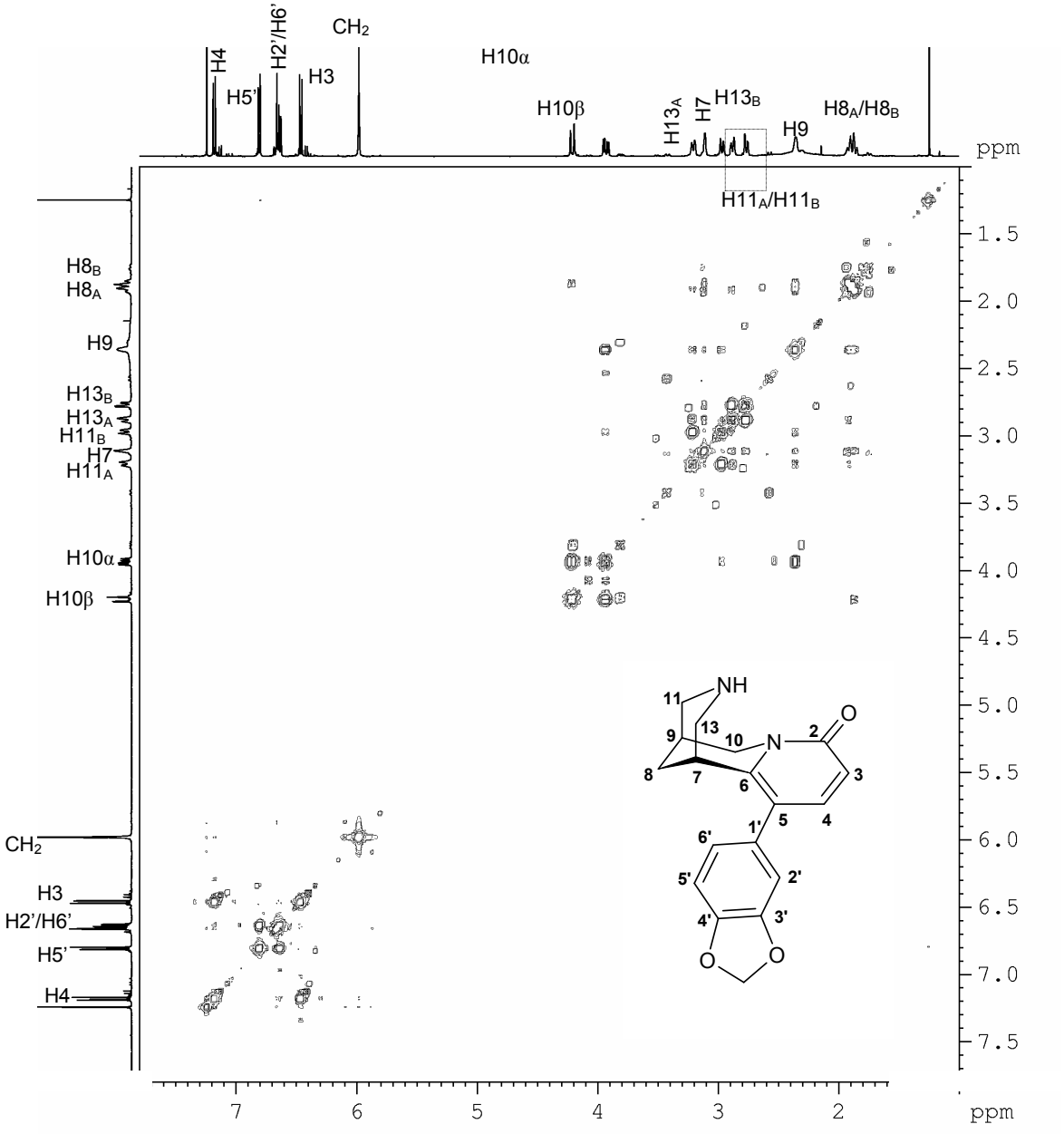

Figure 3-26 2D COSY contour plot of 5-(3',4'-methylenedioxyphenyl)-cytisine **124e** ($CDCl_3$, 500 MHz)

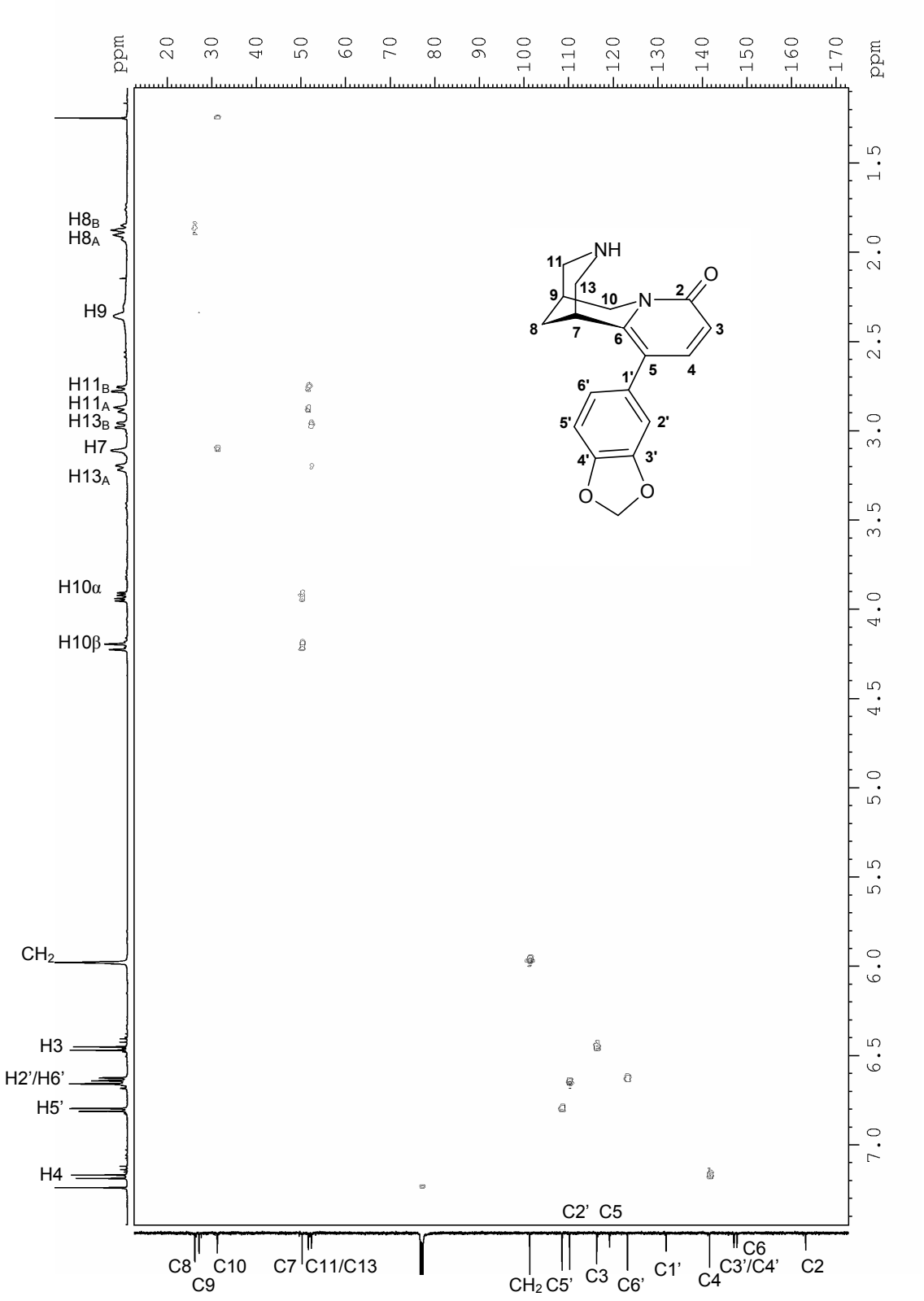

Figure 3-27 2D HSQC contour plot of 5-(3',4'-methylenedioxyphenyl)-cytisine **124e** [$CDCl_3$, 500 MHz (^{1}H NMR); 125 MHz (^{13}C NMR)]

3.3.3.5.3 3- and 5-(3'-Pyridyl)-cytisine **119e** & **125e**

The protons' chemical shifts for the cytisine moiety of the 3-(3'-pyridyl)-cytisine **119e** (Table 3-24) were feasible by comparing them with those of 3-phenyl derivative **93e** and the assignment was verified with further information obtained from the COSY experiment (Figure 3-28). A comparison of ^{1}H signals of the cytisine partial structures of **93e** and **119e** revealed no significant differences (Table 3-13 and 3-24). The pyridyl moiety in **119e** was easily assigned from the COSY mapping (Figure 3-28). Proton H2' and H4' both are attached to a carbon with nitrogen as a neighbour and were expected to be shifted downfield. Therefore, the doublet at δ 8.78 ppm with a vicinal coupling constant of ^{4}J = 1.6 Hz was assigned to H2'. This proton correlated to the doublet of doublet of doublet (ddd) at δ 8.16 ppm, which also showed a coupling of ^{4}J = 1.6 Hz and was identified as H6'. The H6' proton showed one further coupling to the more upfield shifted "ddd" signal at δ 7.29 ppm, which was assigned to H5'. The H4' proton was recognised as a doublet of doublet at δ 8.49 ppm, due to its cross signals to H5' and H6' and its respective coupling constants of ^{3}J = 4.7 Hz (to H5') and ^{4}J = 1.6 Hz (to H6').

Thus, the COSY spectrum revealed a complete ^{1}H shift data set and the HSQC spectrum (Figure 3-29) identified the ^{13}C chemical shifts of carbons attached to protons. The signals at δ 161.9 and 151.5 ppm were assigned to the carbonyl C2 and the quaternary C6. The two remaining signals at δ 133.2 and 123.9 ppm were attributed to C1' and C3, respectively. The ^{13}C chemical shift for carbon 3 in pyridine (equivalent to C1') is reported to be δ 123.6 ppm.[286] As the deshielding of the carbon nucleus by aryl substitution causes a downfield shift, the signal at δ 133.2 ppm had to be assigned to C1'. The remaining signal at δ 123.9 ppm was then attributed to C3. Hence, the C3 suffered downfield shifting by $\Delta\ \delta$ 7.1 ppm through the introduction of the pyridyl moiety.

The complete assignment of the ^{1}H and ^{13}C chemical shifts of **119e**, additivity rules and the estimated chemical shifts allowed a fast assignment of the ^{1}H and ^{13}C NMR spectral data for 5-(3'-pyridyl)-cytisine **125e** (Table 3-26).

3.3.3.5.4 3-(4'-Pyridyl)-cytisine **120e**

The ^{1}H chemical shifts of the cytisine moiety in **120e** (Table 3-24) were clearly assigned through an analogy with 3-(3'-pyridyl)-cytisine **119e**. The 4-pyridyl moiety is a symmetrical residue that possesses two sets of equivalent protons – "ortho" (H3' and H5') and "meta" (H2' and H6') protons with regard to the nitrogen. The most shifted downfield doublet of doublet

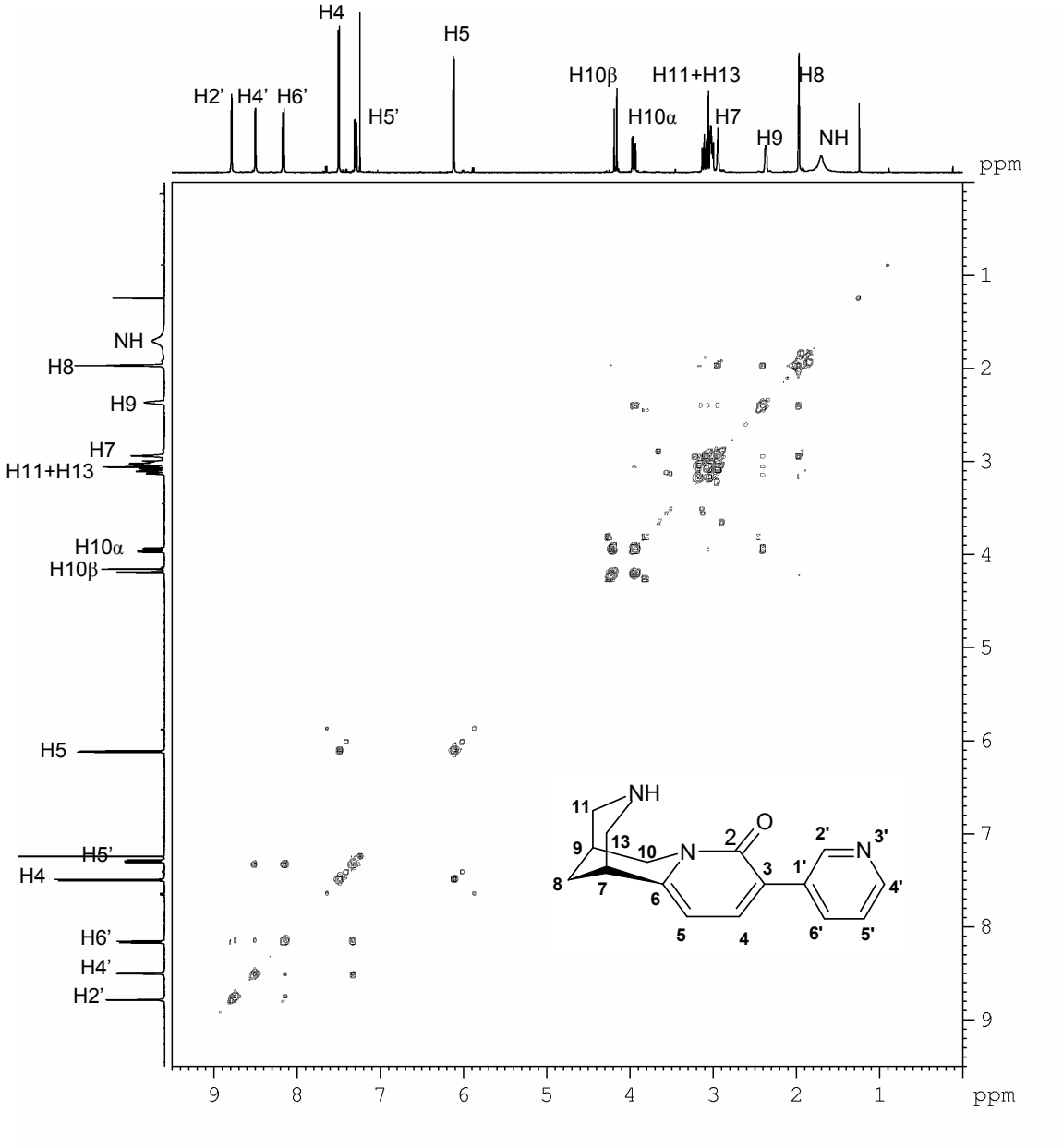

Figure 3-28 2D COSY contour plot of 3-(3'-pyridyl)-cytisine **119e** ($CDCl_3$, 500 MHz)

was assigned to the pair of "ortho" protons (δ 8.57 ppm). This signal displayed a cross peak to the doublet of doublet at δ 7.67 ppm, this being assigned to H2' and H6'.

The HSQC chemical shift map of **120e** identified the equivalent carbons C3'/C5' (δ 149.6 ppm) as well as C2'/C6' (δ 123.9 ppm). The quaternary C1' was located at δ 144.9 ppm and the C3 was due to the downfield shift of the pyridyl substitution assigned to the ^{13}C peak at δ 122.8 ppm (Table 3-25).

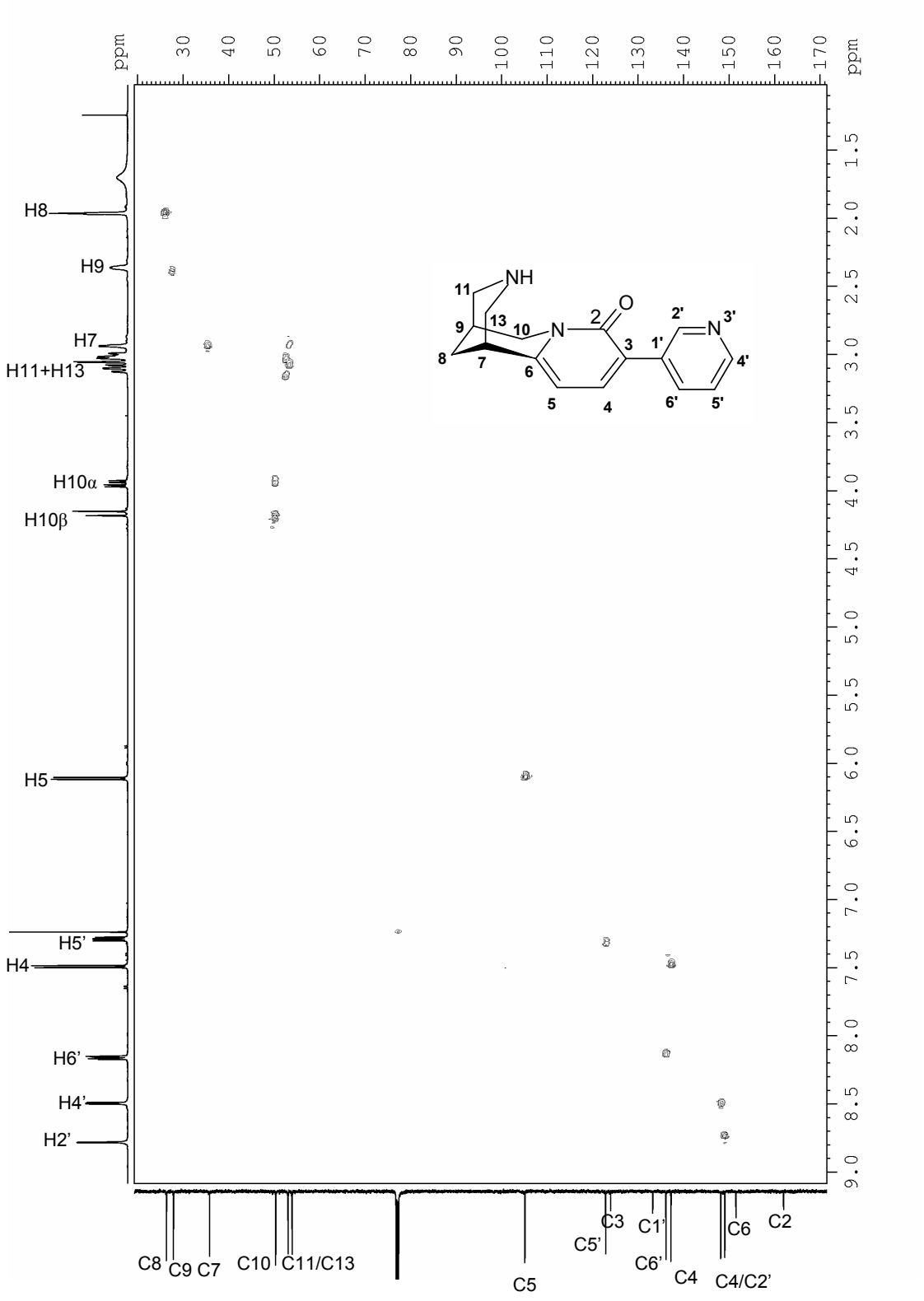

Figure 3-29 2D HSQC contour plot of 3-(3'-pyridyl)-cytisine **119e** [$CDCl_3$, 500 MHz (^{1}H NMR); 125 MHz (^{13}C NMR)]

3.3.3.5.5 3-(Quinolin-8'-yl)-cytisine **121e**

The ^{1}H and ^{13}C signals of the cytisine moiety in **121e** were assigned with the aid of previous findings (i.e. assignments of **117e** – **120e**, Table 3-24 and 3-25). The assignment of the quinoline moiety was facilitated by comparison of experimental and literature data for the unsubstituted quinoline[286] and verified with information obtained from the COSY map (Figure 3-30). The most deshielded signal at δ 8.86 ppm was identified as H7' and this provided a starting point for the assignment of the remaining quinoline protons. A cross-peak between H7' and a doublet of doublet at δ 8.15 ppm approved this "dd" to be H5'. The H7' proton also displayed a cross peak to the doublet of doublet at δ 7.35 ppm (^{4}J = 4.1 Hz) and it was therefore assigned to H6'. The correlation between H5' and H6' was observed as ^{3}J = 8.2 Hz. The triplet at δ 7.56 ppm (^{3}J = 7.3 Hz) was attributed to H3'. This signal showed cross-peaks to the two "dd" signals located at δ 7.78 and 7.85 ppm, which were identified as H4' and H2', respectively.

The one-bond ^{1}H-^{13}C correlations detected in the HSQC spectrum allowed assignments of ^{13}C signals to the carbons linked to protons (Figure 3-31). The quaternary carbons C4'a (δ 128.6 ppm) and C8'a (δ 146.5 ppm) were identified with regard to the literature data of the corresponding carbons in the unsubstituted quinoline (δ 128.0 and 148.1 ppm, respectively)[286] The two remaining signals were assigned to carbons C1' (δ 139.6 ppm) and C3 (δ 136.5 ppm) on the basis of calculated chemical shifts and chemical shifts of unsubstituted C1' (δ 129.2 ppm) in quinoline and C3 (δ 116.8 ppm) in cytisine **27**. However, the unambiguous differentiation of these two carbons would have required further NMR experiments, such as a 2D HMBC correlation map.

3.3.3.5.6 3- and 5-(1-Methyl-1*H*-pyrazol-4'-yl)-cytisine **122e** & **126e**

The assignment of the ^{1}H and ^{13}C chemical shifts of the cytisine moieties in **122e** and **126e** (Tables 3-24, 3-25 and 3-26) was consequently achieved following those of 3- and 5-(hetero)aryl substituted analogues (e.g. **93e**, **103e**, **119e** or **125e**).

Two singlets shifted most downfield at δ 8.29 / 7.80 ppm in the ^{1}H spectrum of **122e** and at δ 7.38 / 7.26 ppm in the spectrum of the 5-analogue **126e** were assigned to H5' and H2' of the 1-methyl-1*H*-pyrazol-4'-yl moiety. The HSQC spectrum located four methine carbons at δ 136.8/139.1 ppm (C2') and δ 129.9/129.1 ppm (C5') for **122e** and **126e**, respectively.

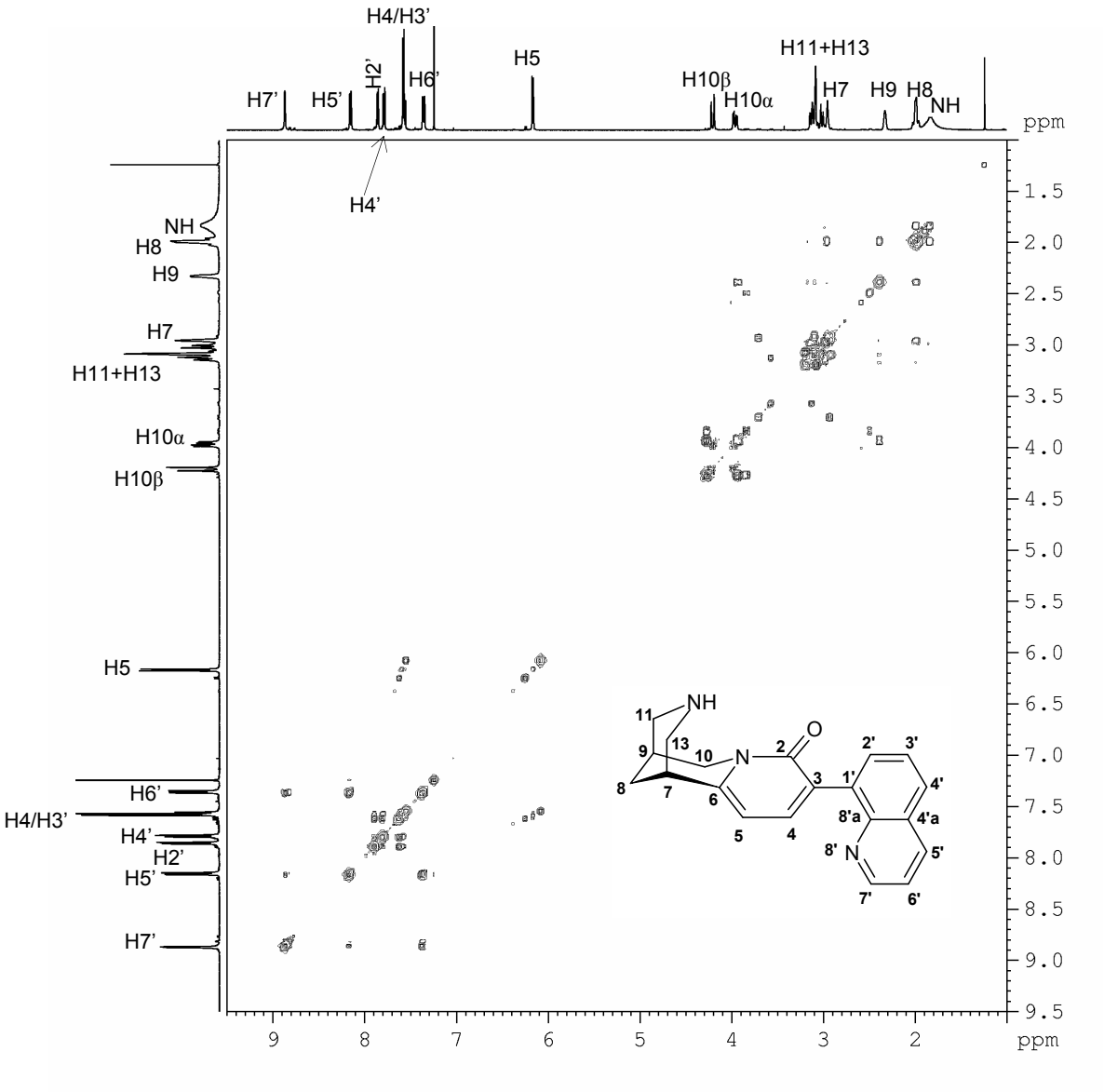

Figure 3-30 2D COSY contour plot of 3-(quinolin-8'-yl)-cytisine **121e** ($CDCl_3$, 500 MHz)

Interestingly, the substitution of position 3 with 1-methyl-1*H*-pyrazol-4'-yl led to a significant upfield shift ($\Delta\ \delta$ 6.4 ppm) of the ^{13}C signal of C4. Upfield shift of C4 has been observed when position 5 was substituted with both aryl and heteroaryl moiety, but never with the 3-substitution. The $\Delta\ \delta$ is remarkable as well, since the 5-substitution caused a shift of no more than 3.4 ppm.

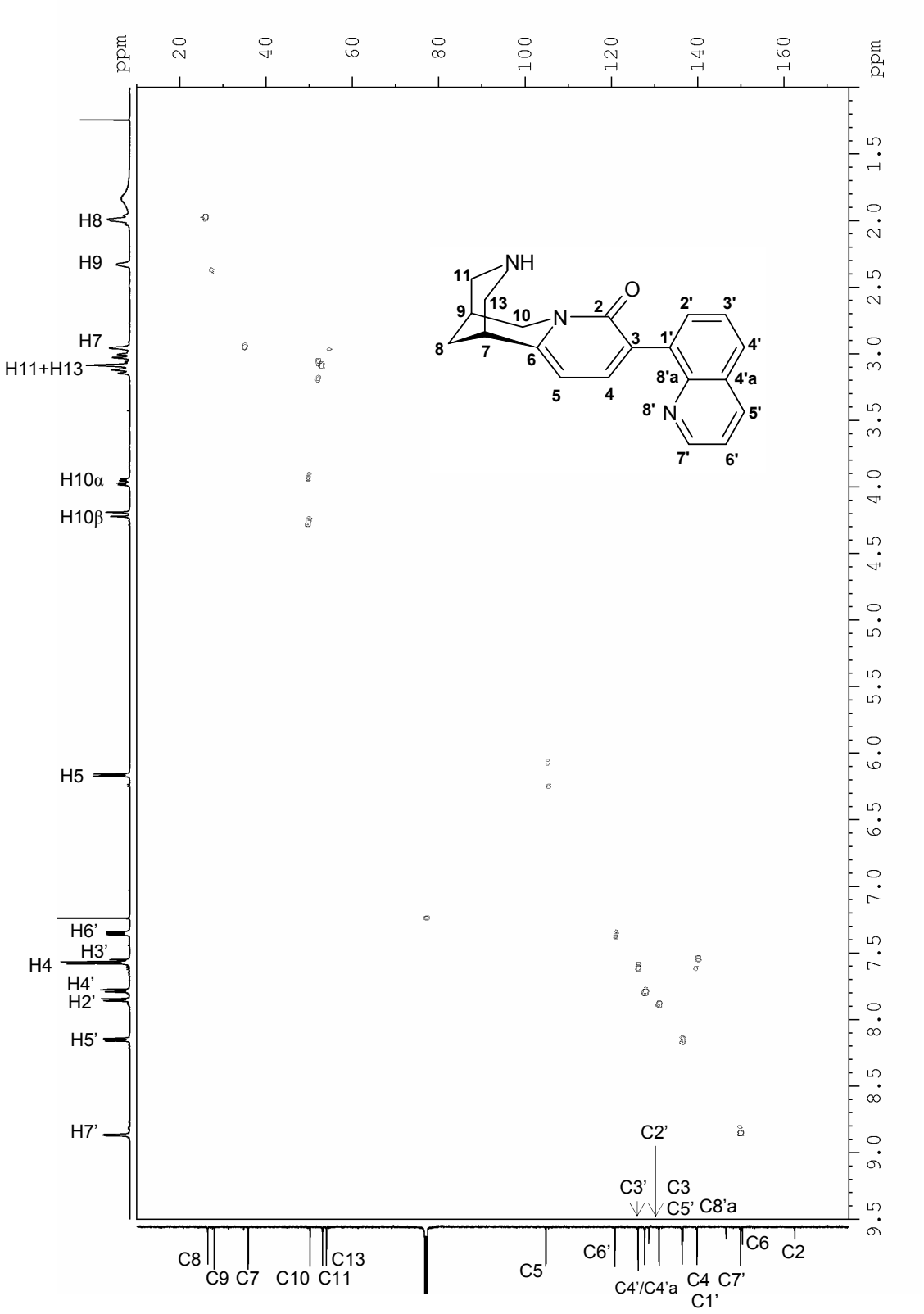

Figure 3-31 2D HSQC contour plot of 3-(quinolin-8'-yl)-cytisine **121e** [$CDCl_3$, 500 MHz (^{1}H NMR); 125 MHz (^{13}C NMR)]

3.3.3.6 Disubstituted Analogues of Cytisine

The ^{1}H and ^{13}C signals assignment of the disubstituted cytisine derivatives, 5-bromo-3-phenyl-cytisine **128e** and 5-bromo-3-(3'-pyridyl)-cytisine **129e**, is listed in the Table 3-27 and it was easily completed with the aid of previous assignments, especially those of 3-phenylcytisine **93e** and 3-(3'-pyridyl)-cytisine **119e**.

The position of the substituents could be proved with the analysis of all previously gathered information. For example, in the structure of **128e** the proton H2' was located at δ 7.65 ppm, which compares well with the chemical shift of H2' in **93e** (δ 7.69 ppm). Thus, both signals were deshielded by the adjacent carbonyl group. Furthermore, the ^{13}C chemical shift of C5 (δ 98.8 ppm) compared to the chemical shift of the unsubstituted C5 in **93e** (δ 104.9 ppm) gave an additivity increment of -6.1 ppm that compares well to the literature value of bromine's SCS (-5.4 ppm)[286].

Similarly, the ^{1}H chemical shifts of the pyridyl moiety in **129e** were found to correlate greatly with the chemical shifts of the corresponding protons in **119e**. The carbon C5 was located in **129e** at δ 98.7 ppm, which represented an upfield shift of -6.3 ppm when compared to the ^{13}C chemical shift of the unsubstituted C5 in **119e** (δ 105.0 ppm).

Due to the substitution of position 5, the H8 protons of both derivatives **128e** and **129e** appeared as two separated broad doublets with vicinal coupling of ^{2}J = 12.9 Hz (**128e**) and 13.2 Hz (**129e**). The signals of H11 and H13 were also separated doublets each with the mutual coupling of ^{2}J = 12.3 Hz (for **128e**) and ^{2}J = 12.0 Hz (for **129e**).

Table 3-27 ^{1}H and ^{13}C chemical shifts of disubstituted derivatives of cytisine **128e** and **129e** [$CDCl_3$; 500 MHz (^{1}H NMR); 125 MHz (^{13}C NMR)]

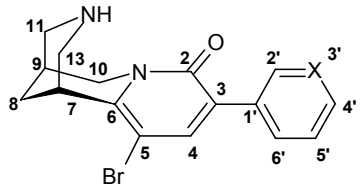

X = C **128e**
X = N **129e**

	3-Ph-5-Br-cyt **128e** δ [ppm]	3-(3'pyridyl)-5-Br-cyt **129e** δ [ppm]		3-Ph-5-Br-cyt **128e** δ [ppm]	3-(3'-pyridyl)-5-Br-cyt **129e** δ [ppm]
H3	---	---	**C2**	161.2	161.0
H4	7.60	7.67	**C3**	128.6	125.3
H5	---	---	**C4**	140.4	140.6
H7	3.36	3.42	**C5**	98.8	98.7
$H8_A$	1.98	2.02	**C6**	147.0	149.1
$H8_B$	1.94	1.97	**C7**	34.9	35.0
H9	2.34	2.39	**C8**	26.4	26.4
H10α	3.96	4.00	**C9**	27.6	27.5
H10β	4.13	4.16	**C10**	50.3	50.4
$H11_A$	3.08	3.12	**C11**	51.3	51.4
$H11_B$	2.99	3.03	**C13**	52.7	52.7
$H13_A$	3.18	3.25	**C1'**	136.0	131.9
$H13_B$	2.96	2.98	**C2'**	128.6	148.8
H2'	7.65	8.81	**C3'**	128.1	N
H3'	7.37	N	**C4'**	127.8	148.3
H4'	7.30	8.55	**C5'**	128.1	122.9
H5'	7.37	7.33	**C6'**	128.6	136.1
H6'	7.65	8.13			

3.4 *In Vitro* Pharmacology of Novel nAChR Ligands based on Cytisine

In order to evaluate the impact of the substituents at positions 3 or 5 on the binding affinity of cytisine **27**, all novel ligands were investigated in radioligand binding studies at several nAChR subtypes.

For determination of $\alpha4\beta2^*$ affinity, rat brain membranes and [^{3}H]epibatidine were employed. Ki values for inhibition of [^{3}H]MLA binding ($\alpha7^*$ binding site) was measured also in rat brain membranes. Affinity for the ganglionic $\alpha3\beta4^*$ nACh receptor was determined in assays performed with calf adrenals and the radioligand [^{3}H]epibatidine. *Torpedo californica* electroplax provided tissues rich of $(\alpha1)_2\beta1\gamma\delta$ receptor and the binding studies were completed with [^{3}H]epibatidine.

The receptor subtypes are designated with an asterix, following the IUPHAR recommendation to indicate the receptor subtype with an asterix, if a native tissue is used, where the definite subtype composition is not exactly known.

The radioligand binding studies were performed by Aliaa Abdelrahman (research group of Dr. D. Gündisch).

3.4.1 Structure-Activity Relationship of 3-Phenyl Analogues

3.4.1.1 Results of the Radioligand Binding Studies

$\alpha4\beta2^*$ nAChRs (Table 3-28)

Cytisine **27** possesses picomolar affinity for $\alpha4\beta2^*$ nAChR (K_i = 0.122 nM). The introduction of a phenyl moiety into position 3 reduced the affinity of the parent alkaloid more than 1000-fold (K_i = 128 nM for **93e**). The bulkier m-biphenyl substituent (**100e**) showed the same effect (K_i = 200 nM).

Meta-substitution of the phenyl moiety exerted various effects on $\alpha4\beta2^*$ binding, but none of the 3-arylated cytisine ligands exhibited higher binding to $\alpha4\beta2^*$ nAChR than the parent alkaloid **27**. The affinity of **94e** – **100e** was found to be influenced by both steric and electrostatic effects produced by substituents in the meta-position of the phenyl ring. While a substitution of the meta-position with bulky electron withdrawing chlorine resulted in an approximately 1630-times less potent ligand **98e** (K_i = 199 nM), the small electron withdrawing fluorine (compound **99e**) in the same position caused only 45-fold decrease of the affinity (K_i = 5.7 nM) compared to cytisine **27**. Strong electron withdrawing trifluoromethyl

Table 3-28 Binding affinity values (K_i) for 3-aryl derivatives of cytisine **93e** – **100e** at α4β2*, α7*, α3β4* and $(\alpha 1)_2\beta 1\gamma\delta$ nACh receptor subtypes

Structure	No.	**α4β2*** [^{3}H]epi rat brain Ki [nM][a]	**α7*** [^{3}H]MLA rat brain Ki [nM][b]	**α3β4*** [^{3}H]epi calf adrenals Ki [nM][a]	**$(\alpha 1)_2\beta 1\gamma\delta$** [^{3}H]epi Torp. calif. electroplax Ki [nM][a]
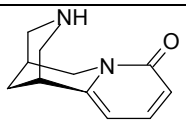	**27**	0.122	250	19	1,300
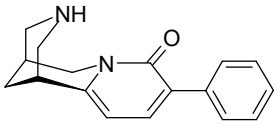	**93e**	128	> 10,000	> 10,000	> 10,000
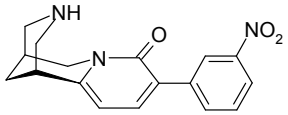	**94e**	23	> 10,000	> 2,000	> 10,000
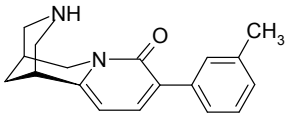	**95e**	28	> 10,000	>10,000	> 10,000
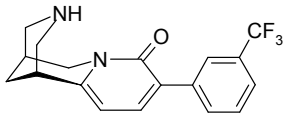	**96e**	8.3	> 10,000	3,700	> 10,000
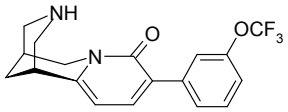	**97e**	67	> 10,000	> 10,000	> 10,000
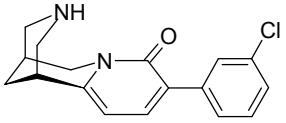	**98e**	199	> 10,000	> 10,000	> 10,000
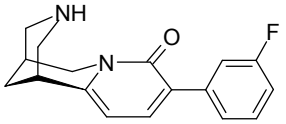	**99e**	5.7	> 10,000	1,200	> 10,000
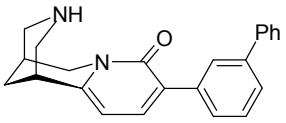	**100e**	200	> 10,000	>10,000	> 10,000

a) values are the mean from at least n = 3 to 5 independent assays
b) preliminary results

group has the same impact on the binding affinity and the compound **96e** shows nearly the same K_i value (K_i = 8.3 nM). Substitution of the phenyl ring with larger electron withdrawing nitro (compound **94e**) and trifluoromethoxy (compound **97e**) groups resulted in less potent ligands (K_i = 23 and 67 nM, respectively), when compared to compounds **96e** and **99e**.

The role of the electron withdrawing properties is obvious from the binding affinities of 3-(m-tolyl)-cytisine **95e** (K_i = 28 nM) and the corresponding trifluoromethyl analogue **96e** (K_i = 8.3 nM). The size of the methyl and the trifluoromethyl moiety is nearly identical, but the methyl group as an electron donating substituent led to a 3-fold decrease in affinity compared to substitution with trifluoromethyl, which possesses strong electron withdrawing properties.

α7* nAChR (Table 3-28)

The binding affinity of cytisine **27** to α7* nAChR (K_i = 250 nM) was decreased via introduction of m-substituted phenyl moieties into position 3. The ligands **93e** – **100e** displayed K_i values > 10,000 nM.

$\alpha3\beta4$* nAChR (Table 3-28)

The introduction of a phenyl moiety into position 3 decreased the cytisine's **27** binding to the ganglionic nACh receptors (K_i = 19 nM). The ligands **93e** – **100e** displayed K_i > 1,200 nM, whereas the ligands featuring an electron withdrawing group, i.e. 3-(3'-trifluoromethylphenyl)-cytisine **96e** (K_i = 3,700 nM) and 3-(3'-fluorophenyl)-cytisine **99e** (K_i = 1,200 nM) displaced [^{3}H]epibatidine from the $\alpha3\beta4$* binding sites in calf adrenals with highest affinities. Thus, the most potent $\alpha4\beta2$* ligands possess the highest affinity for $\alpha3\beta4$* nACh receptor.

$(\alpha1)_2\beta1\gamma\delta$ nAChR (Table 3-28)

Cytisine **27** binds to the $(\alpha1)_2\beta1\gamma\delta$ subtype with K_i = 1,300 nM. Substitution of the position 3 in the cytisine backbone with various meta-substituted phenyl moieties (**93e** – **100e**) resulted in K_i values >10,000 nM.

3.4.1.2 Discussion

According to the Sheridan model of the nicotinic pharmacophore[108], cytisine **27** binds to the nAChR via two "bridges" – the bispidine nitrogen is responsible for π-cation interaction and the pyridone oxygen (acting as hydrogen bond acceptor – HBA) builds hydrogen bonds with amino acids of the receptor's binding domain.

Previous SAR studies revealed that a substitution of the cytisine's secondary amine caused dramatic loss of $\alpha4\beta2$* affinity[118,122,123], but halogenation of the α-position to the carbonyl group (position 3) improved the binding affinity and the 3-bromo analogue **40** displayed the

highest affinity (K_i = 0.010 nM).[118,183] These results suggested, that next to the carbonyl oxygen accepting the hydrogen bond there is a region that accommodates the halogen substitution, but it was difficult to state how bulk-tolerant this region is.

The results presented herein reveal that the introduction of a bulky aryl moiety into the position 3 of cytisine **27** decreases the affinity of this highly $\alpha4\beta2$* potent ligand (K_i = 0.122 nM). 3-Phenyl-cytisine **93e** and 3-(m-biphenyl)-cytisine **100e** displayed more than 1000-fold lower affinity (K_i = 128 and 200 nM, respectively) than the parent alkaloid **27**. On the other hand, the addition of electron withdrawing fluoro, trifluoromethyl or nitro group to the phenyl moiety led to ligands **99e**, **96e** and **94e** which showed higher affinity (K_i = 5.7 – 23 nM) than the parent 3-phenyl-cytisine **93e** (K_i = 128 nM).

Binding affinities of "all-carbon" analogues of cytisine **57** (Figure 3-32) support this hypothesis, since increasing the size of the substituents in the position that parallels the position 3 in cytisine **27** diminished affinity (e.g. K_i > 500 nM for phenyl analogue **57j**, Figure 3-32).[185] However, the results presented by Coe *et al*[185] also showed that while the introduction of an amino moiety (electron donating group) did not improve the affinity (K_i > 500 nM for **57m**), the introduction of an electron withdrawing substituent (e.g. trifluoromethyl **57k** or methoxy **57l**) increased the binding to $\alpha4\beta2$ nAChR subtype (K_i = 200 and 370 nM, respectively) (Figure 3-32).

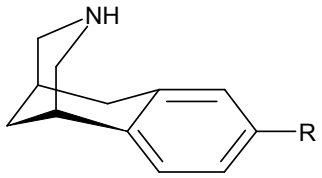

57a	R = H	K_i = 34 nM (h$\alpha4\beta2$, HEK293 cells)
57k	R =4-PhCF_3	K_i = 200 nM (h$\alpha4\beta2$, HEK293 cells)
57l	R =4-PhOMe	K_i = 370 nM (h$\alpha4\beta2$, HEK293 cells)
57j	R = Ph	K_i > 500 nM (h$\alpha4\beta2$, HEK293 cells)
57m	R =3-PhNH_2	K_i > 500 nM (h$\alpha4\beta2$, HEK293 cells)

Figure 3-32 Binding affinities of 3-aryl substituted "all-carbon" derivatives of cytisine **57** [Ref.185]

Thus, the position 3 of the cytisine backbone seems to possess dimensional limits, however the substituent's volume itself is not the crucial factor for the $\alpha4\beta2$ affinity. Increasing the size of the substituent via an addition of an electron-withdrawing group (e.g. phenyl **93e** $\rightarrow$ trifluoromethylphenyl **96e**) leads to an improvement of the binding affinity (e.g. K_i = 128 nM $\rightarrow$ K_i = 8.3 nM).

Another example is the comparison of the binding affinities of nitro analogues **94e**, **57f** and **58** (Figure 3-33). A nitro group directly bound to the cytisine backbone results in only 3-times lower affinity than cytisine **27** (K_i = 0.122 nM) and 3-nitrocytisine **58** retains picomolar K_i

value (K_i = 0.42 nM).[183] Introducing a phenyl ring between the cytisine and the nitro moiety further decreases the $\alpha4\beta2$* affinity (K_i = 23 nM for **94e**). The nitro group directly bound to the "all-carbon" cytisine scaffold provides ligands **57f** with low nanomolar binding affinity, even if the HBA carbonyl group is missing.[185]

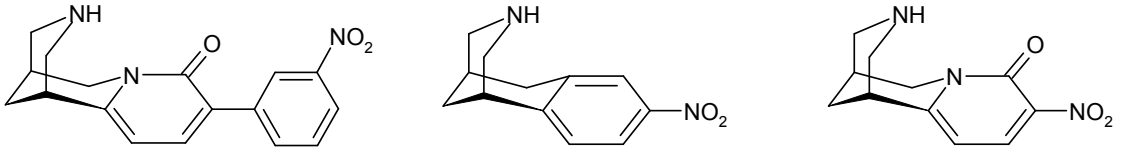

94e
K_i = 23 nM ($\alpha4\beta2$, rat brain)

57f
K_i = 4.9 nM ($\alpha4\beta2$, HEK293 cells)

58
K_i = 0.42 nM ($\alpha4\beta2$, rat brain)

Figure 3-33 Structures and K_i values of nitro derivatives of cytisine [Ref. 183, 185]

These collective findings suggest that small electron-withdrawing groups in the position 3 of the cytisine **27** core play an important role in the $\alpha4\beta2$* receptor recognition.

The introduction of phenyl moiety into position 3 led to cytisine derivative **93e** with dramatically decreased affinity (K_i > 10,000 nM) for $\alpha3\beta4$* nACh receptor compared to the lead **27** (K_i = 19 nM). An electron withdrawing substitution (CF_3 and F) in the meta-position of phenyl moiety provided ligands **96e** and **99e** with micromolar $\alpha3\beta4$* affinity (K_i = 1,200 – 3,700 nM), whereas ligands with other meta-substituents (i.e. CH_3, OCF_3, Ph, Cl) showed lower inhibition of [^{3}H]epibatidine binding in calf adrenals preparation (K_i > 10,000 nM). Thus, the bulk tolerating region next to the carbonyl group seems to be more limited for the $\alpha3\beta4$* than for $\alpha4\beta2$* affinity.

The substitution of position 3 with aryl moieties was found to be detrimental for $\alpha7$* and $(\alpha1)_2\beta1\gamma\delta$ affinity as all ligands in the series under consideration showed lower inhibition of [^{3}H]MLA and [^{3}H]epibatidine binding in rat brain membranes and crude membrane fraction of *Torpedo californica* electroplax (K_i > 10,000 nM).

3.4.2 Structure-Activity Relationship of 5-Phenyl Analogues

3.4.2.1 Results of the Radioligand Binding Studies

$\alpha4\beta2$* nAChR (Table 3-29)

The introduction of a phenyl moiety into the position 5 of the cytisine **27** (K_i = 0.122 nM) decreased the binding affinity (K_i = 45 nM for **103e**). The introduction of m-substituted phenyl moieties resulted in analogues with various $\alpha4\beta2$* affinities. Both electron donating (CH_3 in **105e**) and electron withdrawing (CF_3 and OCF_3 in **106e** and **107e**, respectively) substituents modified the affinity of 5-phenyl-cytisine **103e** (K_i = 45 nM) very slightly (K_i = 23 – 55 nM). Surprisingly, the K_i value of 300 nM makes the 5-(3'-fluoro-phenyl) analogue **109e** the less potent ligand in the series of 5-aryl derivatives. The biphenyl analogue **110e** displayed affinity of K_i = 190 nM. The introduction of m-nitrophenyl moiety into position 5 resulted in a ligand **104e** that displaced [^{3}H]epibatidine from the rat brain with a high affinity (K_i = 3.7 nM).

$\alpha7$* nAChR (Table 3-29)

Cytisine **27** binds to the $\alpha7$* nACh receptor with K_i = 250 nM. Substitution of the position 5 in the cytisine backbone with various meta-substituted phenyl moieties (compounds **103e** – **110e**) resulted in K_i values > 10,000 nM.

$\alpha3\beta4$* nAChR (Table 3-29)

All 5-arylated cytisine analogues **103e** – **110e** possessed K_i > 10,000 nM, with an exception of **104e**. The 5-(3'-nitrophenyl) derivative **104e** inhibited [^{3}H]epibatidine binding in calf adrenals with a K_i value of 481 nM.

$(\alpha1)_2\beta1\gamma\delta$ nAChR (Table 3-29)

All compounds in the series of 5-phenyl cytisine analogues **103e** – **110e** displayed K_i > 10,000 nM when tested in radioligand binding assays employing a crude membrane fraction of *Torpedo californica* electroplax

Table 3-29 Binding affinity values (K_i) for 5-aryl derivatives of cytisine **103e** – **110e** at α4β2*, α7*, α3β4* and $(\alpha1)_2\beta1\gamma\delta$ nACh receptor subtypes

Structure	No.	**α4β2*** [^{3}H]epi rat brain Ki [nM][a]	**α7*** [^{3}H]MLA rat brain Ki [nM][b]	**α3β4*** [^{3}H]epi calf adrenals Ki [nM][a]	**$(\alpha1)_2\beta1\gamma\delta$** [^{3}H]epi Torp. calif. electroplax Ki [nM][a]
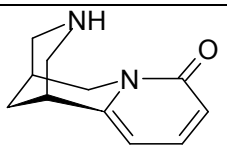	**27**	0.122	250	19	1,300
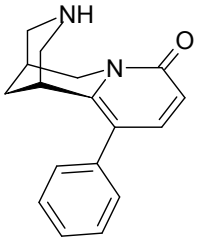	**103e**	45	> 10,000	> 10,000	> 10,000
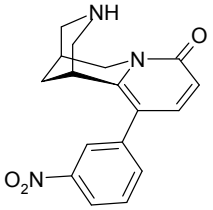	**104e**	3.7	> 10,000	481	> 10,000
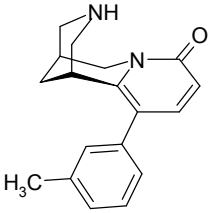	**105e**	24	> 10,000	>10,000	> 10,000
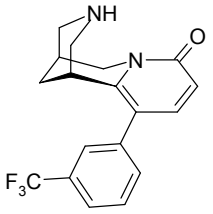	**106e**	55	> 10,000	> 10,000	> 10,000
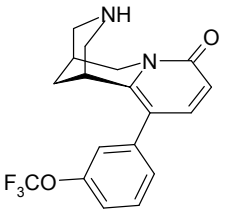	**107e**	23	> 10,000	> 10,000	> 10,000

Continued on page 139

Continued from page 138

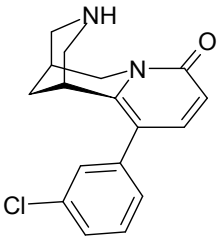	**108e**	170[b]	> 10,000	> 10,000	> 10,000
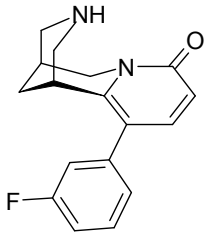	**109e**	300	> 10,000	> 2,000	> 10,000
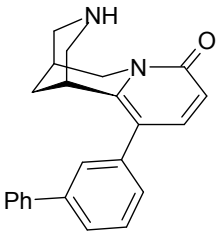	**110e**	190	> 10,000	>10,000	> 10,000

a) values are the mean from at least n = 3 to 5 independent assays
b) preliminary results

3.4.2.2 Discussion

Previous studies[118,183] with 5-halogenated cytisine derivatives suggested that the position 5 is more bulk-tolerant than the position 3 but does not favour substituents with high electronegativity. Results presented herein confirm the bulk-tolerating properties of position 5. The introduction of a phenyl moiety into the position 5 of cytisine **27** caused reduction of binding affinity, but the 5-phenyl-cytisine **103e** (K_i = 45 nM) was 3-times more potent than its corresponding 3-phenyl analogue **93e** (K_i = 128 nM). The derivative **110e** possessing 3-biphenyl moiety in the position 5 shows binding affinity (K_i = 190 nM) very similar to that of the corresponding 3-substituted analogue **100e** (K_i = 200 nM). Thus, the 3- and 5-substituted counterparts seem to become equipotent with the increasing size of the substituents.

The second hypothesis regarding the negative impact of the high electronegativity was confirmed with the ligand **109e** that possesses fluorine in the meta-position of the phenyl moiety and shows the lowest affinity (K_i = 300 nM) in the series of 5-arylated cytisine analogues **103e** – **110e**. Thus, although the high electronegativity and electron withdrawing

effect is preferred for position 3, the same effect in position 5 is detrimental for α4β2* affinity. Substituents such as methyl (entry **105e**), trifluoromethyl (entry **106e**) or trifluoromethoxy (entry **107e**) do not significantly alter the α4β2* binding affinity (K_i = 23 – 55 nM) when compared to 5-phenyl-cytisine **93e** (K_i = 45 nM).

5-(3'-Nitro-phenyl) analogue **104e** exhibits the highest affinity in the series under consideration (K_i = 3.7 nM) and represents an 18-fold increase of the affinity in comparison to 5-nitro-cytisine **59** (K_i = 65.6 nM)[183]. It could be hypothesised that **104e** binds to α4β2* nACh receptor in a new fashion. The π-cation interaction between the basic nitrogen and electron rich aromatic acid residues of the binding domain remains, but the HBA function in the ligand **104e** is presented not by the carbonyl oxygen, but by the oxygen in the nitro group. The low nanomolar affinity of 5-nitro "all-carbon" analogue of cytisine **57h** supports the presumption of the new binding mode, since the compound **57h**, although missing the "conventional" HBA functionality (pyridone's oxygen in cytisine **27**), is able to inhibit [^{3}H]nicotine binding in cells expressing α4β2* nAChRs (K_i = 14 nM).[185] Figure 3-34 illustrates a very simplified version of the new binding mode. In order to follow and prove this theory, one needs to synthesise and evaluate ligands bearing nitro group at various distances from bispidine's nitrogen and avoid of any other HBA functionality.

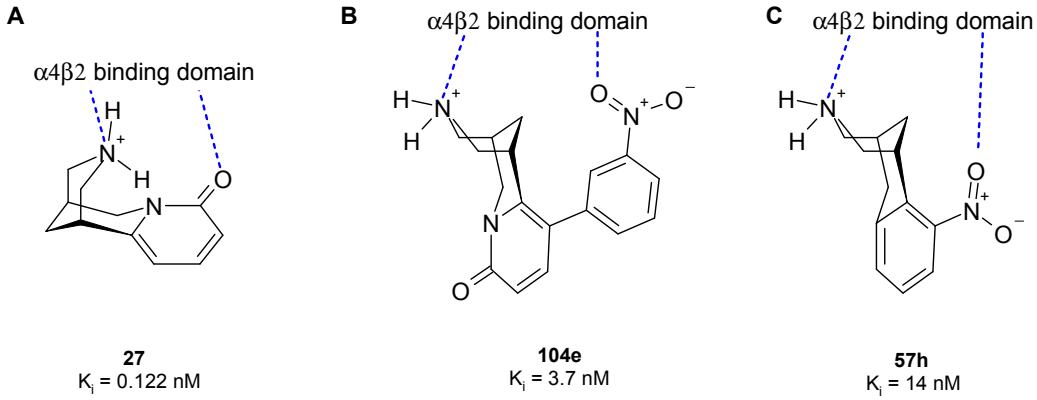

27
K_i = 0.122 nM

104e
K_i = 3.7 nM

57h
K_i = 14 nM

Figure 3-34 Binding mode of cytisine **27** (A). A simplified version of the proposed new binding mode for the nitro analogues **104e** and **57h** (B and C). [K_i values for **57h** from Ref. 185]

3.4.3 Structure-Activity Relationship of Heterocyclic Analogues

3.4.3.1 Results of the Radioligand Binding Studies

3.4.3.1.1 3-Heterocyclic Cytisine Analogues

$\alpha4\beta2$* nAChR (Table 3-30)

The introduction of various heteroaromatic moieties into position 3 resulted in compounds that inhibited [^{3}H]epibatidine binding in rat brain membrane preparations (Table 5-3). Compound **117e**, substituted with the 5'-indolyl moiety, had the lowest affinity (K_i = 853 nM) not only in the series under consideration but also among all novel cytisine derivatives. The introduction of the 3'-pyridyl and 4'-pyridyl residues into position 3 led to highly potent ligands **119e** and **120e** (K_i = 0.91 and 3.9 nM, respectively). The compound **122e**, substituted with a 4'-(1-methyl-1*H*-pyrazole) moiety showed K_i value of 0.177 nM and thus is the analogue with highest $\alpha4\beta2$* affinity. The addition of bulkier 3,4-methylenedioxyphenyl and quinolin-8-yl moieties led to analogues **118e** and **121e** with similar affinity (K_i = 110 and 95 nM, respectively).

$\alpha7$* nAChR (Table 3-30)

The 3-heteroaryl cytisine derivatives **117e** – **122e** showed K_i values > 10,000 nM.

$\alpha3\beta4$* nAChR (Table 3-30)

In the $\alpha3\beta4$* binding assays, the 3-heteroaryl derivatives of cytisine **117e** – **122e** exhibit diverse structure-affinity patterns. The 3-(N-methyl-1*H*-pyrazol-4'-yl)-cytisine **122e** possesses affinity (K_i = 33 nM) comparable to the affinity of the parent alkaloid **27** (K_i = 19 nM), whereas the 3-(3'-pyridyl) and 3-(4'-pyridyl) analogues **119e** and **120e** possess 3- and 11-fold lower affinity than cytisine **27** (K_i = 119 and 436 nM, respectively). The remaining 3-heteroaryl cytisine derivatives **117e**, **118e** and **121e** show K_i > 10,000 nM.

$(\alpha1)_2\beta1\gamma\delta$ nAChR (Table 3-30)

Substitution of the position 3 in cytisine **27** with heteroaryl moieties led to ligands **117e** – **122e** with decreased affinity for muscle nACh receptor (K_i > 5,000 nM).

Table 3-30 Binding affinity values (K_i) for 3-heteroaryl derivatives of cytisine **117e** – **122e** at $\alpha4\beta2^*$, $\alpha7^*$, $\alpha3\beta4^*$ and $(\alpha1)_2\beta1\gamma\delta$ nACh receptor subtypes

Structure	No.	**α4β2*** [^{3}H]epi rat brain Ki [nM][a]	**α7*** [^{3}H]MLA rat brain Ki [nM][b]	**α3β4*** [^{3}H]epi calf adrenals Ki [nM][a]	**$(\alpha1)_2\beta1\gamma\delta$** [^{3}H]epi Torp. calif. electroplax Ki [nM][a]
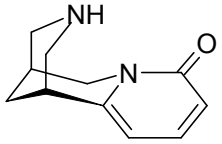	**27**	0.122	250	19	1,300
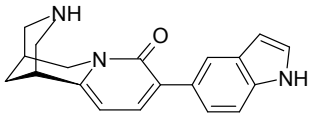	**117e**	853	> 10,000	> 10,000	> 10,000
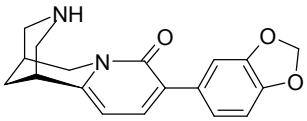	**118e**	110	> 10,000	> 10,000	> 10,000
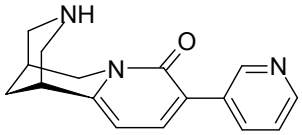	**119e**	0.91	> 10,000	119	> 10,000
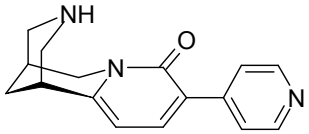	**120e**	3.9	> 10,000	436	> 10,000
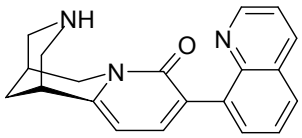	**121e**	95	> 10,000	> 10,000	> 10,000
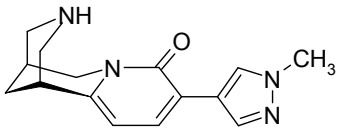	**122e**	0.177	> 10,000	33	> 5,000

a) values are the mean from at least n = 3 to 5 independent assays
b) preliminary results

3.4.3.1.2 5-Heterocyclic Cytisine Analogues

$\alpha4\beta2$* nAChR (Table 3-31)

Four cytisine analogues **122e** – **126e** bearing heterocyclic substituent in position 5 exhibited binding affinities for the $\alpha4\beta2$* subtype in the low nanomolar range (K_i = 2.2 – 96 nM). The N-methyl-1*H*-pyrazole cytisine analogue **126e** had the highest affinity (K_i = 2.2 nM) whereas the 3',4'-methylenedioxyphenyl analogue **124e** showed the lowest affinity (K_i = 96 nM) of these four derivatives. 5-(5'-indolyl)- and 5-(3'-pyridyl) derivatives **123e** and **125e** displayed similar binding affinities (K_i = 20.4 and 10.9 nM, respectively).

$\alpha7$* nAChR (Table 3-31)

All compounds in the series of 5-heteroaryl cytisine analogues **123e** – **126e** showed K_i > 10,000 nM when tested in radioligand binding assays employing rat brain membranes and [^{3}H]MLA.

$\alpha3\beta4$* nAChR (Table 3-31)

The addition of a heterocyclic moiety into position 5 provided ligands **123e** – **126e** with various affinity for the $\alpha3\beta4$* receptor. Two analogues, namely **125e** (K_i = 4,300 nM) and **126e** (K_i = 656 nM) inhibited the [^{3}H]epibatidine binding in the calf adrenals preparation stronger than another two analogues **123e** and **124e** (K_i > 10,000 nM).

$(\alpha1)_2\beta1\gamma\delta$ nAChRs (Table 3-31)

Cytisine derivatives **123e** – **126e** bearing heteroaryl moiety in position 5 exhibit K_i > 10,000 nM when evaluated in radioligand binding assays employing [^{3}H]epibatidine and *Torpedo californica* electroplax.

3.4.3.2 Discussion

The trend observed with bulkier substituents in the series of aryl substituted analogues **93e** – **100e** and **103e** – **110e** has been confirmed also in the series of heterocyclic derivatives **117e** – **126e**. The increasing bulkiness of the substituent (i.e. 5'-indolyl, quinolin-8'-yl and 3',4'-methylenedioxyphenyl) hinders the interaction with $\alpha4\beta2$* receptor and the ligands **117e**, **118e**, **121e** and **124e** displayed lower affinities (K_i = 95 – 853 nM) than the parent alkaloid **27** (K_i = 0.122 nM). The similar affinity of isomeric 3',4'-methylenedioxyphenyl derivatives **118e** and **124e** (K_i = 110 and 96 nM) resembles the pattern observed with biphenyl derivatives **100e** and **110e** (K_i = 200 and 190 nM, respectively), i.e. with the increasing size of the substituent the isomeric ligands become equipotent.

Table 3-31 Binding affinity values (K_i) for 5-heteroaryl derivatives of cytisine **123e** – **126e** at α4β2*, α7*, α3β4* and $(\alpha 1)_2\beta 1\gamma\delta$ nACh receptor subtypes

Structure	No.	**α4β2*** [^{3}H]epi rat brain Ki [nM][a]	**α7*** [^{3}H]MLA rat brain Ki [nM][b]	**α3β4*** [^{3}H]epi calf adrenals Ki [nM][a]	**$(\alpha 1)_2\beta 1\gamma\delta$** [^{3}H]epi Torp. calif. electroplax Ki [nM][a]
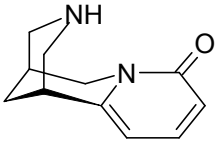	**27**	0.122	250	19	1,300
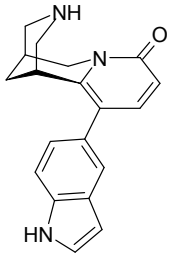	**123e**	20.4	> 10,000	> 10,000	> 10,000
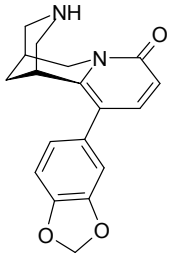	**124e**	96	> 10,000	> 10,000	> 10,000
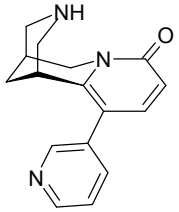	**125e**	10.9	> 10,000	4,300	> 10,000
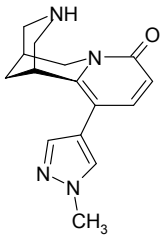	**126e**	2.2	> 10,000	656	> 10,000

a) values are the mean from at least n = 3 to 5 independent assays
b) preliminary results

The introduction of a smaller N-bearing heterocycle instead of the indolic or the quinolinic moiety into the position 3 resulted in compounds with affinities in the picomolar range. The compounds **119e** (3'-pyridyl analogue) and **122e** (N-methyl-1*H*-pyrazol-4'-yl analogue) turned out to be the most potent ligands in the series under consideration (K_i = 0.91 and 0.177 nM, respectively), whereas the affinity of **122e** compares well with the lead alkaloid **27** (K_i = 0.122 nM). Incorporation of the 3'-pyridyl and N-methyl-1*H*-pyrazol-4'-yl moieties into the position 5 resulted in 12-fold reduction of affinity compared to their 3-substituted counterparts. However, the 5-substituted analogues **125e** and **126e** retain low nanomolar affinity (K_i = 10.9 and 2.2 nM, respectively).

Substitution or replacement of 3'-pyridyl moiety decreased the $\alpha4\beta2$* binding affinity. 4-Pyridyl residue in the position 3 resulted in a compound **120e** with 4-fold reduced affinity (K_i = 3.9 nM) when compared to 3'-pyridyl analogue **119e**, indicating the importance of nitrogen's position to the pharmacophoric elements. Fluorine substitution of the 3'-pyridyl moiety also had a negative impact on the affinity towards $\alpha4\beta2$ nAChR (K_i = 24 nM for (3-(2-fluoropyridin-5-yl)-cytisine).[125]

Comparison of the structure-activity patterns for $\alpha4\beta2$* nAChR with respect to aryl and heteroaryl substitution in the position 3 indicates that the two series have the same structural requirements for the size of the substituent but different requirements when the position 3 bears smaller moiety. By increasing the size of the substituent the binding affinity diminishes, regardless of the (hetero)aryl character of the substituent. However, the incorporation of small heteroaryl moieties into the cytisine molecule is accepted much better than the introduction of differently substituted phenyl moieties.

The introduction of different substituents into the position 5 influenced the $\alpha4\beta2$* binding affinity in a different, less destructive manner. Herein, the bulk tolerating region also possesses dimensional limits but the substitution in general reduced the binding affinity to a smaller degree. The high binding affinity of 5-(5'-indolyl)-cytisine **123e** to the rat brain [^{3}H]epibatidine binding sites (K_i = 20.4 nM) supports this hypothesis, as the corresponding 3-isomer **117e** showed a 40-fold lower affinity (K_i = 853 nM). Additionally, one can not exclude, that the introduction of different substituents (e.g. 3-nitrophenyl, indol) leads to a new binding mode between the ligands and the $\alpha4\beta2$* nACh receptor. Oxygen of the nitro group or indolic nitrogen could overtake or support (via HBA and/or π-π interaction) the role of the so far recognised pharmacophoric elements of cytisine **27**.

3-(N-Methyl-1*H*-pyrazol-4'-yl)-cytisine **122e** with K_i = 33 nM has been identified as the most $\alpha3\beta4$* potent ligand in this series. The 3'- and 4'-pyridyl moieties in position 3 resulted in a decrease of the $\alpha3\beta4$*affinity (K_i = 119 and 436 nM for **119e** and **120e**, respectively). The

introduction of bulkier heterocyclic cores such as 5'-indolyl; 3',4'-methylenedioxyphenyl or 8'-quinolinyl caused more significant reduction of the α3β4* affinity (K_i > 10,000 nM).

Position 5 seems to be even less bulk-tolerating, as 5-(3'-pyridyl)-cytisine **125e** (K_i = 4,300 nM) possesses a 36-fold lower affinity compared to the 3-counterpart **119e** (K_i = 119 nM). Similarly, N-methyl-1*H*-pyrazol-4'-yl in position 5 resulted in ligand **126e** with a 20-fold reduced affinity (K_i = 656 nM) compared to the 3-isomer **122e** (K_i = 33 nM).

Although the ligands with highest α4β2* affinity showed also the highest binding to α3β4* nAChR, the cytisine's **27** selectivity (K_i (α4β2*)/K_i (α3β4*) ≈ 155) for the brain binding sites may be improved with the heteroaryl substitution of position 5. The 5-(5'-indolyl)-cytisine **123e** with a ratio of K_i (α4β2*)/K_i (α3β4*) ≈ 490 was identified as the most α4β2* selective ligand. Another two 5-heteroaryl derivatives of cytisine, namely 5-(3'-pyridyl) and 5-(N-methyl-1*H*-pyrazol-4'-yl) analogues **125e** and **126e** also showed prevalence for the central [^{3}H]epibatidine bindings sides over the peripheral α3β4* subtype (K_i (α4β2*)/K_i (α3β4*) ≈ 394 and 298, respectively).

3.4.4 Structure-Activity Relationship of Disubstituted Analogues

3.4.4.1 Results of the Radioligand Binding Studies

α4β2* nAChR (Table 3-32)

5-Bromo-3-phenyl-cytisine **128e** and 5-bromo-3-(3'-pyridyl)-cytisine **129e** displaced [^{3}H]epibatidine from rat brain membranes with similar affinities (K_i = 131 and 92 nM, respectively). Hence, the disubstitution of cytisine scaffold resulted in 1073- and 754-fold reduction of α4β2* affinity compared to the parent alkaloid **27** (K_i = 0.122 nM).

α7* nAChR (Table 3-32)

The cytisine analogues **128e** – **129e** displayed K_i > 10,000 nM when tested in radioligand binding assays employing rat brain membranes and [^{3}H]MLA.

α3β4* nAChR (Table 3-32)

Cytisine derivatives **128e** – **129e** featuring two-fold substitution on the pyridone moiety exhibited for the α3β4* nAChRs K_i values > 2,000 nM .

Table 3-32 Binding affinity values (K_i) for disubstituted derivatives of cytisine **128e** and **129e** at $\alpha4\beta2^*$, $\alpha7^*$, $\alpha3\beta4^*$ and $(\alpha1)_2\beta1\gamma\delta$ nACh receptor subtypes

Structure	No.	**α4β2*** [^{3}H]epi rat brain Ki [nM][a]	**α7*** [^{3}H]MLA rat brain Ki [nM][b]	**α3β4*** [^{3}H]epi calf adrenals Ki [nM][a]	**$(\alpha1)_2\beta1\gamma\delta$** [^{3}H]epi Torp. calif. electroplax Ki [nM][a]
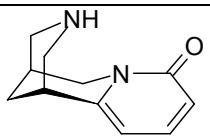	**27**	0.122	250	19	1,300
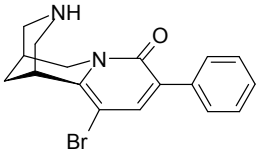	**128e**	131	> 10,000	> 5,000	> 10,000
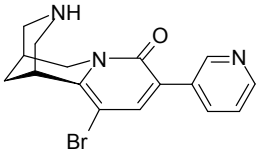	**129e**	92	> 10,000	> 2,000	> 10,000

a) values are the mean from at least n = 3 to 5 independent assays
b) preliminary results

$(\alpha1)_2\beta1\gamma\delta$ nAChR (Table 3-32)

Disubstitution of cytisine's positions 3 and 5 resulted in a dramatic reduction of binding affinity to muscle nAChRs (K_i > 10,000 nM for both ligands **128e** and **129e**).

3.4.4.2 Discussion

5-Bromo-3-phenyl analogue **128e** (K_i = 131 nM) retains the binding affinity of 3-phenyl-cytisine **93e** (K_i = 128 nM) but comparing compound **128e** to the 5-bromo analogue **43** (K_i = 0.308 nM)[118] its affinity is 425-times decreased. This undoubtedly supports the previous finding about negative impact of 3-phenyl substitution on the receptor recognition. The moderate nanomolar affinity of 5-bromo-3-(3'-pyridyl)-cytisine **129e** (K_i = 92 nM) was somehow expected from the results obtained from dihalogenated analogues, where the enhancing effect of 3-halogenation counterbalanced only partially with the deleterious effect of 5-halogenation.[118,147,148] The dihalogenated analogues of cytisine possess lower affinities (K_i = 0.52 – 10.8 nM) than the monosubstituted analogues.[118] The disubstituted analogue **119e** displaced [^{3}H]epibatidine from rat brain [^{3}H]epibatidine binding sites with a 100-fold

lower affinity than the 3-(3'-pyridyl) analogue **119e** (K_i = 0.91 nM) and with a 300-fold reduced binding affinity compared to 5-bromo-cytisine **43** (K_i = 0.308 nM)[118].

3.5 Summary of Structure-Activity Relationships

SAR for α4β2* nAChR

- position 3 possesses bulk-tolerance limit since a substitution with the phenyl moiety decreased the binding affinity
- the combination of steric and electrostatic properties is crucial for the binding affinity
- the affinity within the 3-aryl analogues improved with the introduction of small electron withdrawing groups into the meta-position of the phenyl ring
- introduction of 3-pyridyl and N-methyl-1*H*-pyrazol-4-yl moieties into position 3 yielded the most potent ligands in the series under consideration
- substitution of position 3 with bulkier heterocyclic moieties not tolerated
- substitution of position 5 significantly improves the subtype selectivity
- introduction of 5-indolyl moiety into position 5 yielded the most selective ligand

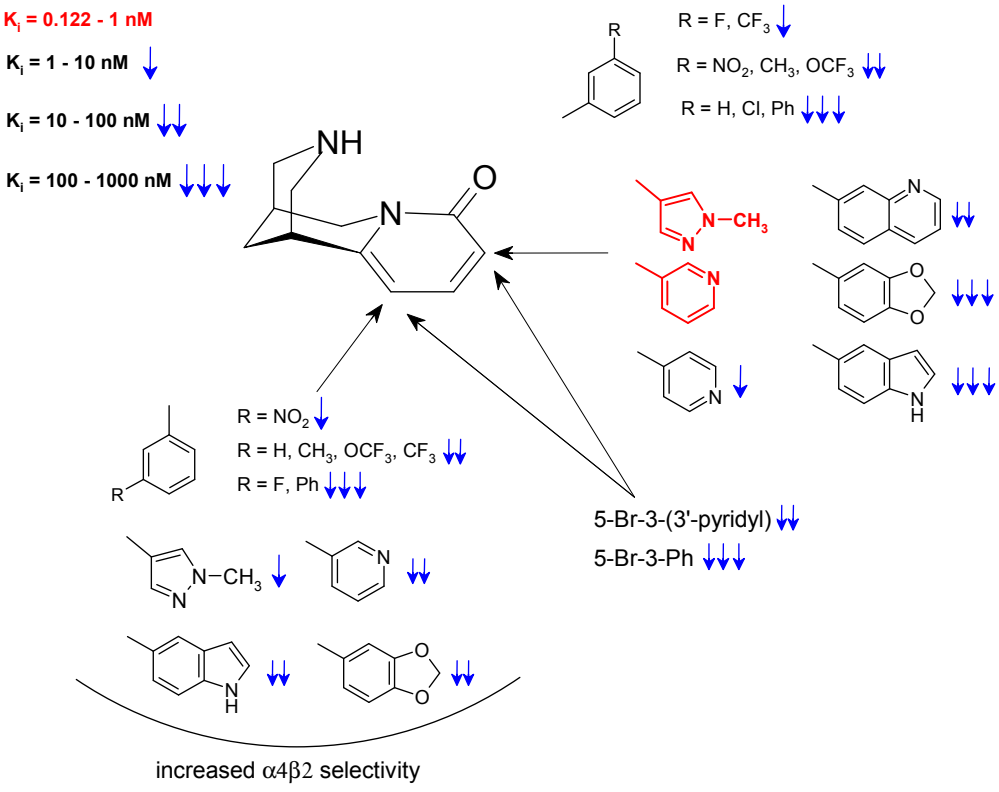

SAR for α3β4* nAChR

- (hetero)aryl substitution of the position 3 reduces the binding affinity
- within the 3-arylated analogues only the analogues with electron-withdrawing groups in the meta-position exhibited affinity in lower micromolar range
- introduction of the N-methyl-1*H*-pyrazol-4-yl moiety into position 3 yielded the most potent ligand
- position 5 does not accomodate bulkier substitution and 5-arylated analogues have better α4β2* selectivity profile than their 3-counterparts

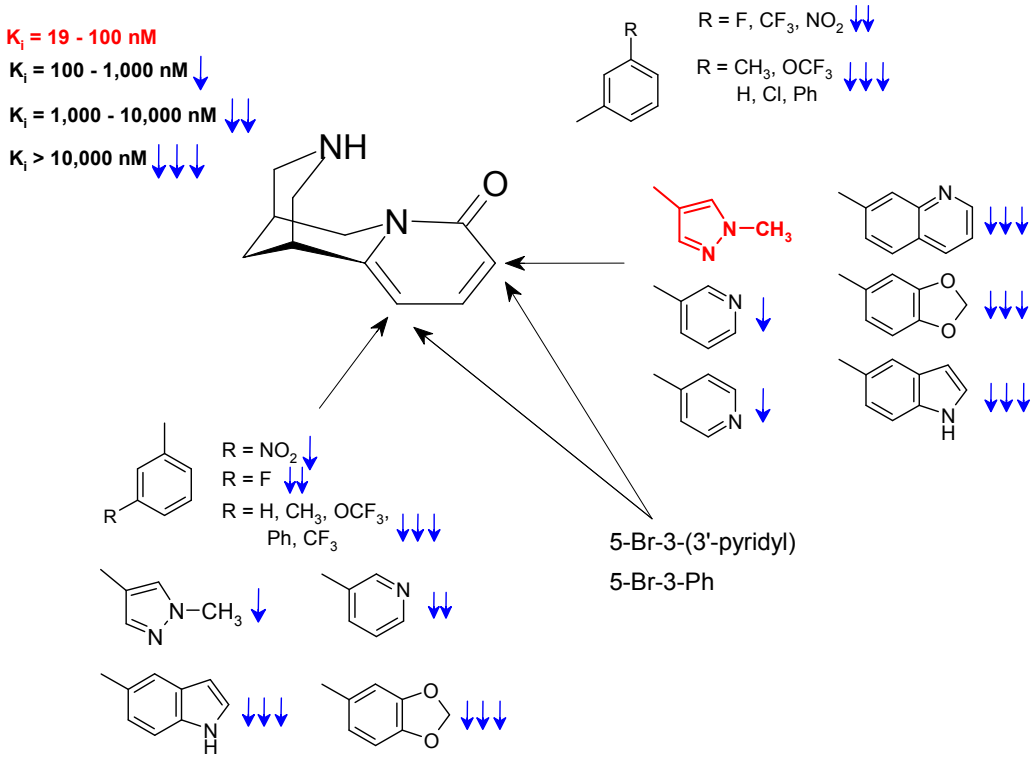

SAR for α7* and $(\alpha 1)_2\beta 1\gamma\delta$ nAChRs

All modification on the cytisine scaffold led to significant decrease of the ligand's binding affinities to the central α7* and neuromuscular $(\alpha 1)_2\beta 1\gamma\delta$ nAChRs (K_i > 10,000 nM).

4 Project II: Development of Novel nAChR Ligands based on Choline

4.1 Choline as a Lead Compound

Choline **4**, a precursor and a metabolite of acetylcholine **1**, possesses micromolar affinity towards $\alpha4\beta2$ nAChR (K_i = 112 µM) and is an effective $\alpha7$ agonist even if it presents very low affinity for the $\alpha7$ nACh receptor (K_i = 2,380 µM).[52]

Choline **4** has been shown to possess cytoprotective properties[53] and a series of choline derivatives has been evaluated as neuroprotective agents. Jonnala *et al*[53] reported that although choline **4** exhibited only about 40% of the full cytoprotective effect of nicotine **10**, its pyrrolidine derivative **132** (Figure 4-1) showed a markedly improved potency and efficacy, thus the authors suggested that the choline structure may serve as a template for the development of novel agents with both $\alpha7$-nicotinic agonist activity and potential neuroprotective ability. The same group synthesized several choline derivatives and identified JAY 2-21-29 (Figure 4-1) as the most effective analogue with potent cytoprotective action.[290]

Simsek and co-workers showed that several 3-pyridyl ether analogues (e.g. **133**, Figure 4-1) of choline displayed nanomolar affinities for [^{3}H]nicotine sensitive binding sites and nociceptive properties.[291] Similar analogues of choline, where the amine function is incorporated in a cyclic carbon skeleton are one of the most potent ligands for $\alpha4\beta2$ nAChRs (e.g. A-85380 **15**).[74a]

The structure of choline **4** can be found in a variety of compounds displaying multifarious pharmacological effects, for example in drugs with antihistaminic and analgesic properties like diphenhydramine **134** and nefopam **135**, which even display affinities in micromolar range for neuronal nAChRs.[292] Aryl ether analogues of choline are known as inhibitors of amine oxidase[293] and are also described as compounds with antibacterial, cholesterol lowering, and germicidal properties.[294] Mono- and poly-substituted pyridyl ether analogues of choline were patented for the use as pesticides.[295]

Nevertheless, the structure of choline has attracted limited interest as a lead compound in the search for nAChR ligands and it was rationale to revisit this structure as a lead for development of novel nAChR ligands.

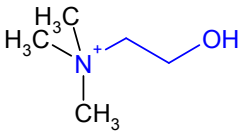

choline **3**
K_i = 112 µM (α4β2, rat brain)
K_i = 2.38 mM (α7, rat brain)

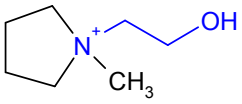

pyrrolidinecholine **132**

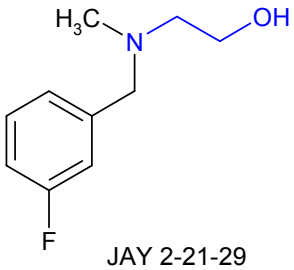

JAY 2-21-29

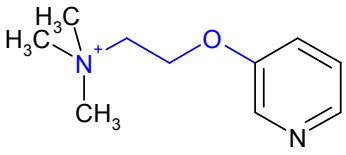

133
K_i = 0.5 nM (α4β2, rat brain)

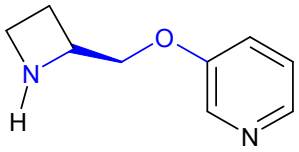

A-85380 **15**
K_i = 0.05 nM (α4β2, rat brain)
K_i = 100 nM (α7, rat brain)

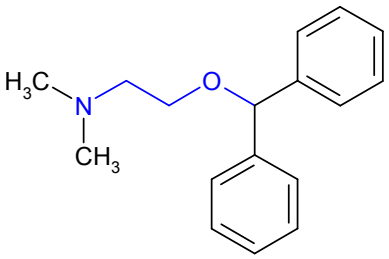

Diphenhydramine **134**
K_i = 4,800 nM (α7, rat brain)
K_i = 5,920 nM (α4β2, rat brain)

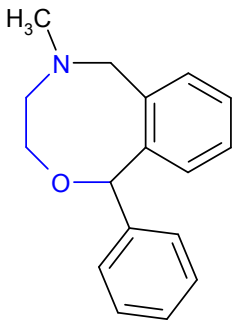

Nefopam **135**
K_i = 23,000 nM (α7, rat brain)
K_i = 8,000 nM (α4β2, rat brain)

Figure 4-1 Structure and binding affinities of choline **3** and of compounds containing choline moiety (highlighted in blue) [Ref. 52, 53, 74a, 290 – 292]

4.2 Syntheses of novel nAChR Ligands based on Choline

4.2.1 Introduction

The introduction of an amide moiety into the structure of phenyl ether of choline yielded a carbamate **5** with high affinity and subtype selectivity for α7 nAChR. In order to evaluate the structure **5** and obtain information about structural requirements and limitations for nAChR affinity, a library of phenylcarbamate analogues was synthesized.

Cabamates are synthesized in various ways. Alkyl halides may be converted to carbamates by treatment with a secondary amine and K_2CO_3 under phase transfer conditions (Scheme 4-1/A).[296] When chloroformates ROCOCl are treated with primary amines, carbamates of type ROCONHR' are obtained. An example of this reaction is the use of benzyl chloroformate to protect the amino group of amino acid and peptides. The $PhCH_2OCO$ group is called the carbobenzoxy group (abbreviated as Cbz) (Scheme 4-1/B).[193]

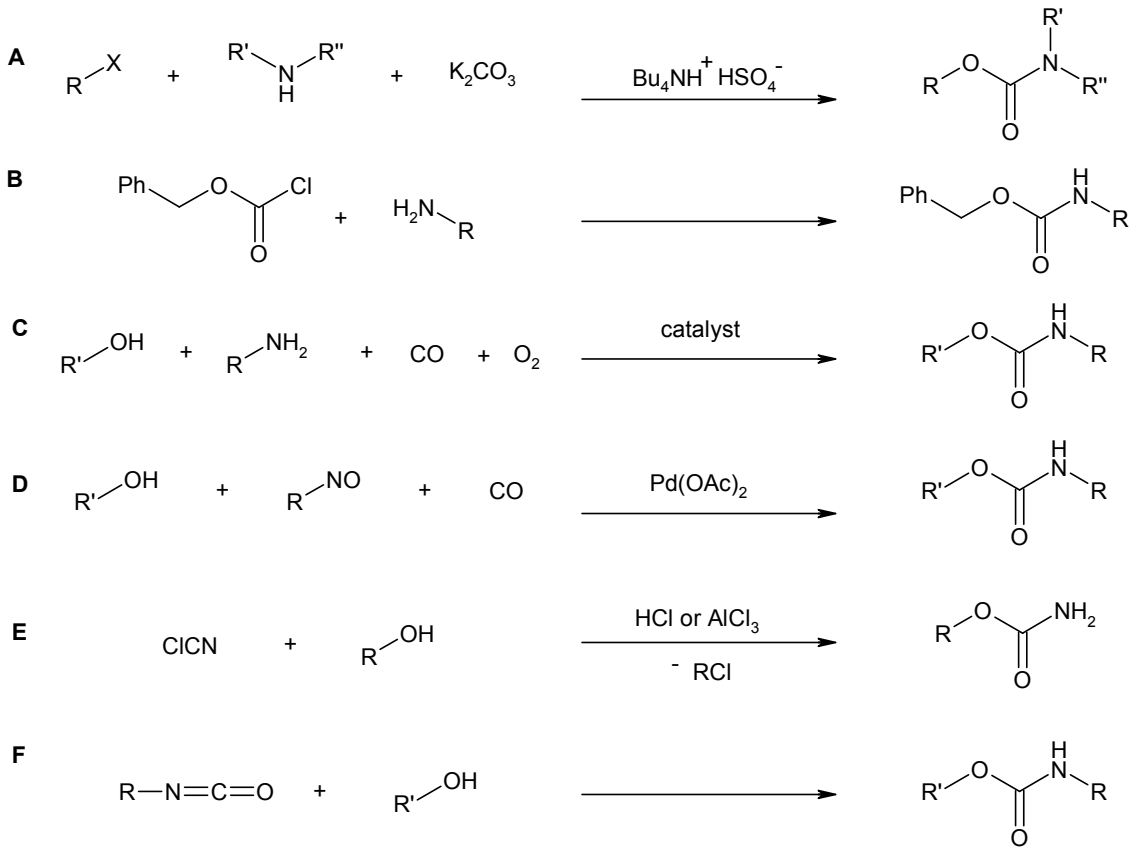

Scheme 4-1 Synthetic routes to carbamate derivatives [Ref. 193, 296 – 300]

Carbamates can be obtained from primary and secondary amines, if these react with CO, O_2 and an alcohol R'OH in the presence of a catalyst (Scheme 4-1/C) [297] or by treatment of nitroso and nitro compounds with CO, R'OH, $Pd(OAc)_2$ and $Cu(OAc)_2$ (Scheme 4-1/D).[298] Cyanogen chloride reacts with alcohols in the presence of an acid catalyst such as dry HCl or $AlCl_3$ to give carbamates (Scheme 4-1/E).[299]

Substituted carbamates are prepared when isocyanates are treated with alcohols (Scheme 4-1/F).[300] This is an excellent reaction, of wide scope and gives good yields. Isothiocyanates similarly give thiocarbamates RNHCSOR', though they react slower than the corresponding isocyanates. The mechanism of this reaction is poorly understood, though the oxygen of the alcohol is certainly attacking the carbon of the isocyanate.[193] The addition of ROH to isocyanates can also be catalysed by metalic compounds[301] or by light[302].

4.2.2 Method/Results

The synthesis of the phenylcarbamate derivatives was carried out according to the Method F (Scheme 4-2). Equimolar amounts of amino alcohols and the appropriate phenylisocyanates were stirred for 1.5 – 4 hours under argon atmosphere. The reaction was carried out in toluene at 50°C, as reflux temperature was found to reduce yields and increased the formation of the byproducts. The solvent was evaporated and the resulting oily residue was purified by flash chromatography on a small amount of silica gel eluting with dichlormethane/methanol mixture. The products were obtained as yellow oils that crystallised on standing (28% – 97%).

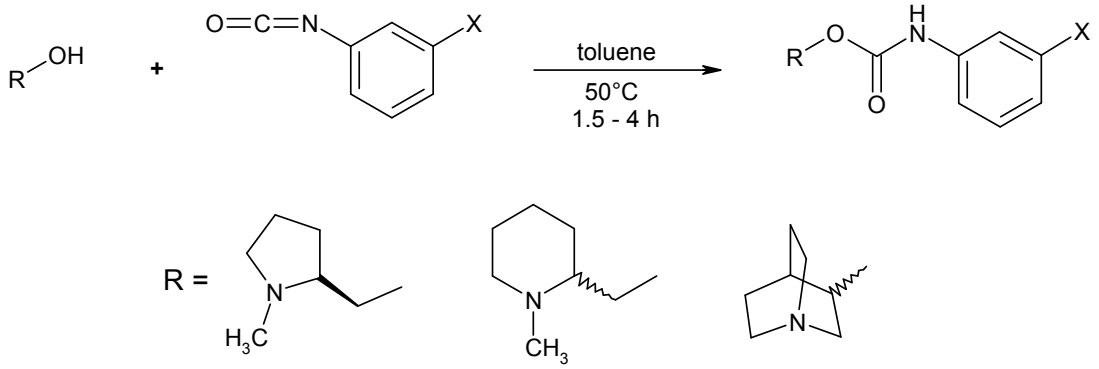

X = CH_3 **136**
X = Br **137**

X = CH_3 **138**
X = Br **139**

X = CH_3 **140**
X = Br **141**

Scheme 4-2 Syntheses of carbamate analogues **136** – **141**

The reaction had to be carried out in a water-free solvent (i.e. dry toluene) under argon atmosphere in order to avoid the decomposition of the isocyanate reactant.[303] Isocyanates are hydrolysed in the presence of water to primary amines and this reaction is catalysed by acids or bases.[193] This may explain why the addition of triethylamine was found to have negative impact on the yields of the syntheses. The primary amine then reacts with isocyanate to give substituted urea derivatives as side-products. Scheme 4-3 shows an unwanted synthesis of 1,3-di-m-tolyl-urea **142** from m-tolylisocyanate **143** in the presence of water. The side-product **142** (M = 240.3 g/mol) crystallised in toluene, thus was easily isolated by filtration and identified via mass spectroscopy ($[M+H]^+$ = 240.2). Interestingly, m-tolylisocyanate always led to the production of side products, whereas this side reaction was not observed when 3-bromopenylisocyanate was employed. Therefore, the yields of methyl analogues **136**, **138** and **140** were significantly lower (28% – 42%) than the yields of the bromo analogues **137**, **139** and **141** (75% – 97%).

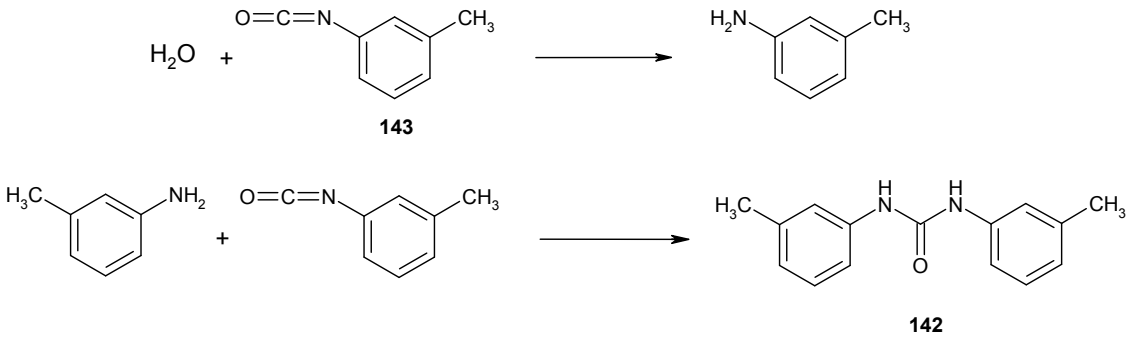

Scheme 4-3 Synthesis of the side-product *1,3-di-m-tolyl-urea* **142**

Compounds **144** and **145** were prepared by the Suzuki coupling reaction under microwave irradiation (Scheme 4-4). Microwave irradiation (60 – 100 W) and standard Suzuki conditions allowed addition of the phenyl and styryl moieties to the phenyl ring of **141** in less than 10 minutes. The reaction mixture was allowed to cool to room temperature and the solvent evaporated under pressure. The oily residue was purified by column chromatography with the dichloromethane/methanol mixture and crystallised from the mixture of diethyl ether/petroleum ether. The coupling products were obtained as yellow crystalline powders (22% – 39%).

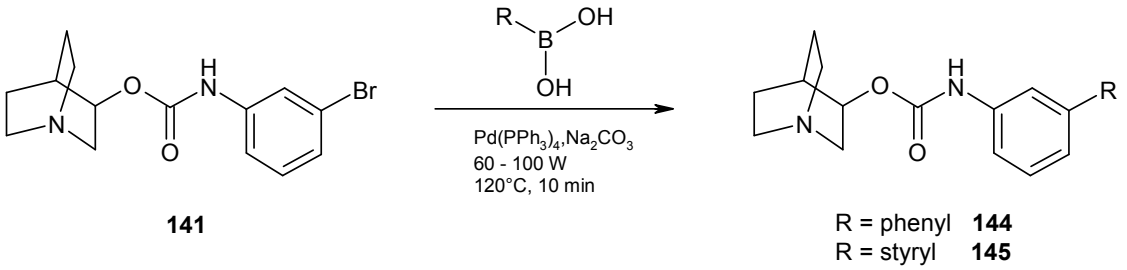

Scheme 4-4 Suzuki cross-coupling reaction under microwave accelerated conditions as a key step in the syntheses of the biaryls **144** and **145**

4.2.3 Discussion

The syntheses of the carbamate derivatives **136** – **141** were carried out under argon atmosphere and in dry solvents. The addition of triethylamine, which is used for the preparation of carbamate derivatives[304], did not positively influence the yield of the desired products **136** – **141**. Reflux temperature led to the reduction of yields and increased the production of byproducts, e.g. **142**.

The azabicyclic carbamate derivative **141**, also claimed as a α7 nAChR ligand in a patent of Astra Laboratories[304], was used as a reactant for synthesis of the phenyl and styryl analogues **144** and **145**. The combination of Suzuki cross-coupling protocol[191] with microwave dielectric heating[229,230] allowed synthesis of the coupling products **144** and **145** in 10 min (22% – 39%).

The low yields are results of several impacts and it has to be pointed out that the Suzuki protocol for addition of the phenyl or styryl moieties to the compound **141** was not optimized, since the reactions yielded sufficient amount of the products **144** and **145** for the biological evaluation. The following should be taken into consideration for the improvement of the reaction's outcome; firstly, the carbamate bond might be instable for the Suzuki protocol under microwave accelerated conditions, although the microwave irradiation (up to 100 W) itself did not hydrolyse the carbamate bond employing DME as used in the Suzuki reaction. The boronic acids are in general weak acids (pKa = 8.6 for phenylboronic acid) and have not been reported to be able to cleave the carbamate bond. However, the combination of a boronic acid and microwave irradiation led to the formation of unwanted byproducts. Low yields of biaryl coupling product could be caused by the hydrolysis of the carbamate bond. Secondly, the applied microwave energy (60 – 100 W) probably led to the decomposition of the catalytic system. Optimization of the experimental protocol for the Suzuki cross-coupling reaction on the cytisine skeleton revealed that the energy of no more than 50 W should be

applied in the cross-coupling reactions employing Pd-catalyst (e.g. $Pd(PPh_3)_4$). Thus, using lower microwave energy could lead to higher yields.

However, the protocol developed in our hands yielded the biphenyl carbamate coupling product **144** in a very fast and simpler way compared to the method described by Naito et al.[305] or Astra Laboratories[304]. In their work, the biphenyl derivative **144** was synthesized using the biphenyl isocyanate, which was obtained by the addition of diphenylphosphoryl azide (DPPA) to the biphenyl-3-carboxylic acid (Figure 4-5/A)[305] or by the addition of phosgene to 3-aminobiphenyl (Figure 4-5/B)[304]. The styryl analogue **145** is a novel nAChR ligand.

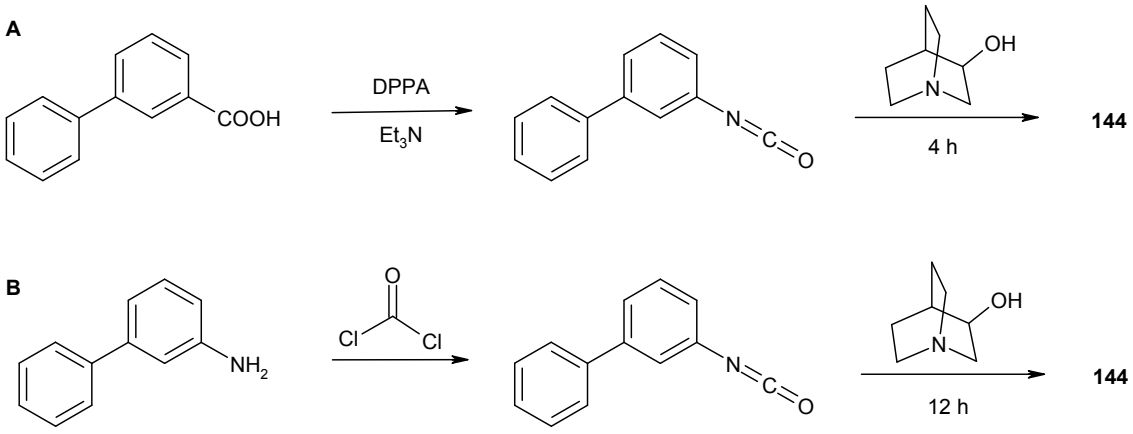

Scheme 4-5 Synthesis of **144** via different routes described by Naito et al. (A) and Astra Laboratories (B) [Ref. 304, 305]

4.3 *In Vitro* Pharmacology of Novel nAChR Ligands based on Choline

Compounds **136** – **141** and **144** – **145** were evaluated for their abilities to compete for [^{3}H]epibatidine and [^{3}MLA] binding sites in rat forebrain ($\alpha4\beta2^*$, $\alpha7^*$), pig adrenals ($\alpha3\beta4^*$) and *Torpedo californica* electroplax membrane fractions ($(\alpha1)_2\beta1\gamma\delta$).

The receptor subtypes are designated with an asterix, following the IUPHAR recommendation to indicate the receptor subtype with an asterix, if native tissue is used, where the definite subtype composition is not exactly known.

The radioligand binding studies were performed by Cristina Tilotta (research group of Dr. D. Gündisch).

4.3.1 Results of the Radioligand Binding Assays

Cyclization of the quaternary amine into a rigid azacyclic structure (N-methyl-pyrrolidine, N-methyl-piperidine and quinuclidine) and subsequent m-substitution provided nAChR ligands with various binding profiles (Table 4-1 and 4-2).

$\alpha4\beta2^*$ and $\alpha7^*$ nAChR

N-Methylpyrrolidine- and N-methylpiperidine analogues **136** – **139** showed micromolar affinity for $\alpha7^*$ (K_i = 10.8 – 31.8 μM) and nanomolar affinity for $\alpha4\beta2^*$ nAChRs (K_i = 175 – 1,248 nM). The $\alpha4\beta2^*$ binding affinity of the unsubstituted N-methylpyrrolidine carbamate **146** (K_i = 1,100 nM) remained unchanged with the methylation of the phenyl ring (K_i = 1,248 nM for **136**) but was improved with a bromo substitution (K_i = 526 nM for **137**). Whereas the unsubstituted N-methylpiperidino derivative **147** did not displace [^{3}H]epibatidine from rat brain membrane preparations, the brominated analogue **139** showed micromolar affinity (K_i = 3,770 nM) and the methyl analogue **138** nanomolar affinity (K_i = 175 nM) with a prevalence for the $\alpha4\beta2^*$ nAChR ($K_i(\alpha4\beta2)$ / $K_i(\alpha7) \approx 181$).

The quinuclidine analogue **149** like the phenylcarbamate **5** exhibited remarkable affinity for $\alpha7^*$ (K_i = 44 and 39 nM, respectively) versus $\alpha4\beta2^*$ (K_i = 3,084 and 835 nM). The substitution of the phenyl moiety, especially with bulky aryl residues reduced the affinity for $\alpha7^*$ (K_i = 273 – 1,135 nM), which can be strongly observed in the styryl analogue **145** (K_i = 6,100 nM).

Table 4-1 Binding affinity values (K_i) for phenylcarbamate derivatives of choline at α4β2*, α7*, α3β4* and $(\alpha1)_2\beta1\gamma\delta$ nACh receptor subtypes

Structure	No.	**α4β2*** [^{3}H]epi rat brain Ki [nM][a]	**α7*** [^{3}H]MLA rat brain Ki [nM][a]	**α3β4*** [^{3}H]epi pig adrenal Ki [nM][a]	**$(\alpha1)_2\beta1\gamma\delta$** [^{3}H]epi Torp. calif. electroplax Ki [nM][a]
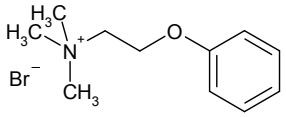	**4**§	22.3	196	135	697
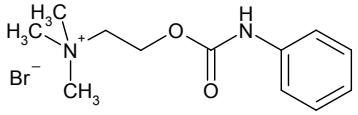	**5**§	835	38.9	2,200	> 20,000
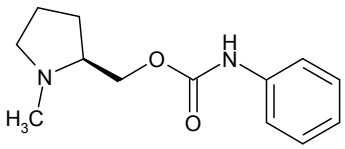	**146**§	1,100	5,853	2,582	> 20,000
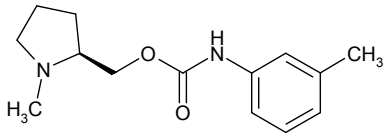	**136**	1,248	14,108	6,000	n.d.
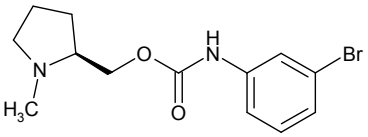	**137**	526	10,810	6,146	n.d.
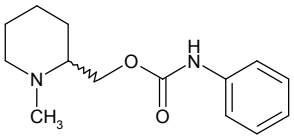	**147**§	> 20,000	15,000	6,100	> 20,000
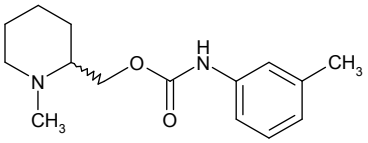	**138**	175	31,800	14,392	> 20,000
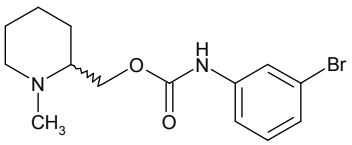	**139**	3,770	27,000	6,357	n.d.

§) synthesized by Matthias Ändra (research group of Dr. D. Gündisch)
a) values are the mean from at least n = 3 to 5 independent assays

Table 4-2 Binding affinity values (K_i) for quinuclidine phenylcarbamate derivatives at α4β2*, α7*, α3β4* and $(\alpha1)_2\beta1\gamma\delta$ nACh receptor subtypes

Structure	No.	**α4β2*** [^{3}H]epi rat brain Ki [nM][a]	**α7*** [^{3}H]MLA rat brain Ki [nM][a]	**α3β4*** [^{3}H]epi pig adrenal Ki [nM][a]	**$(\alpha1)_2\beta1\gamma\delta$** [^{3}H]epi Torp. calif. electroplax Ki [nM][a]
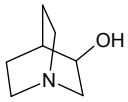	**148**	5,924	7,761	14,604	n.d.
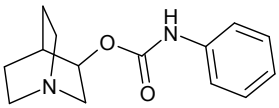	**149**[§]	3,084	44	1,627	> 20,000
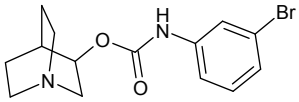	**141**	2,988	273	715	n.d.
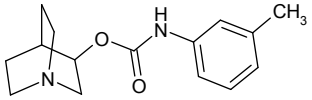	**142**	2,695	321	1,478	n.d.
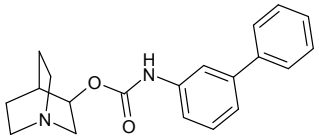	**144**	7,772	1,135	1,448	n.d.
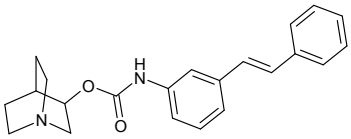	**145**	5,350	6,100	5,976	n.d.

[§]) synthesized by Matthias Ändra (research group of Dr. D. Gündisch)
a) values are the mean from at least n = 3 to 5 independent assays

α3β4* nAChR

The phenylcarbamate derivatives **136** – **141** and **144** – **145** were also investigated for their affinities towards the α3β4* subtype and with an exception of **141** (K_i = 715 nM) all analogues showed K_i values in the micromolar range (K_i = 1,448 – 14,392 nM). Compared with the pyrrolidine and piperidine series a higher affinity for α3β4* is observed in the series of the quinuclidine derivatives.

$(\alpha1)_2\beta1\gamma\delta$ nAChR

Several analogues were tested for their affinity for the $(\alpha1)_2\beta1\gamma\delta$ nAChR and the evaluated derivatives showed low binding to the muscle type nAChR (K_i > 20,000 nM).

4.3.2 Discussion

The phenylether of choline **4** was transformed into a α7 nAChR selective compound with nanomolar affinity when converting it into the corresponding carbamate analogue.[55,292] Cyclization of the quaternary nitrogen provided nAChR ligands with an interesting pharmacological profile.

Methyl-pyrrolidine and methyl-piperidine derivatives showed K_i values in the higher nanomolar and lower micromolar range for α4β2* and lower affinity for α7* subtype. The subtype selectivity profile of the analogues **136** – **139** (α4β2* > α3β4* > α7*) is consistent with the affinity rank order of most nAChR ligands. Cyclization of the quaternary nitrogen into a quinuclidine core provided ligand **149** with a high α7* affinity (K_i = 44 nM). Methylation or bromination of the phenyl moiety in **149** decreased the α7* affinity (K_i = 273 – 321 nM), as did the introduction of bulkier phenyl or styryl moieties (K_i = 1,135 – 6,100 nM)

3-Quinuclidinole **148**, which can be considered as a rigid choline derivative was also tested for the ability to recognise various nAChR subtypes and it displayed K_i values in the micromolar range for α4β2* (K_i = 5,924 nM) and α7* (K_i = 7,761 nM) nAChRs, suggesting that the spatial distance between the nitrogen and oxygen in the structure of 3-quinuclidinole **148** is compatible with the pharmacophore elements.

In summary, carbamates bearing pyrrolidine (**136**-**137**) or piperidine (**138**-**139**) moiety have been shown to possess lower affinity for α7* nAChR than the analogues in the quinuclidine series (**140** – **141** and **144** – **145**), although the same structural elements are present (a protonable basic nitrogen, a carbamate moiety and a π-electron system). Furthermore, in contrast to the quinuclidine analogues, the pyrrolidine and piperidine analogues exhibited higher affinities for α4β2* nAChR. Thus, the quinuclidine core linked via a carbamate bond to the π-electron system provides a template for high affinity ligands with α7-subtype selectivity. Similar results were obtained with the exploration of the quinuclidine scaffold, which has become popular for construction of ligands, especially for the interaction with the α7 receptor subtype.[306] However, the carbamate moiety as a link between the pharmacophoric elements does not show a predisposition for an α7-selective ligand. When in combination with other azacyclic cores, such as N-methylpyrrolidine or N-methylpiperidine, it provides ligands with prevalance for α4β2 nAChRs.

5 Summary

Nicotinic acetylcholine receptors (nAChRs) are ligand-gated ion channel receptors composed of five polypeptide subunits. There are many different nAChR subtypes constructed from a variety of different subunit combinations, resulting into diverse roles of nAChRs in the central and peripheral nervous system. The CNS nicotinic mechanism is known to be involved in a normal human cognitive and behavioural functioning and the nAChRs have been implicated with a number of human pathologies (e.g. Alzheimer's or Parkinson's disease, schizophrenia, addiction or depression). Ongoing investigation of the molecular structure, function and distribution of nAChR has opened up a new era for the potential clinical application of nAChR drugs in the treatment of a various CNS disorders. Moreover, one cannot forget that activation of neuronal nAChRs produces antinociception in a variety of preclinical pain models. This activity suggests that compounds targeting neuronal nAChRs may represent a new class of analgesic agents.

For this to be achieved, new nAChR ligands are being synthesized and tested for their activity in order to get more information about the structure requirements for an interaction with various nAChR subtypes. The new findings might provide important information regarding the selectivity. This will be of importance, since the *in vivo* profile of the hitherto existing agents tested in clinical trials is mostly accompanied by side effects.

The presented Ph.D. thesis was focused on synthesis and biological evaluation of novel nicotinic acetylcholine receptor ligands based on cytisine **27** (Project I, main project) and choline **3** (Project II).

Project I: Development of Novel nAChRs Ligands based on Cytisine

The quinolizidine alkaloid cytisine **27** has been recognised as nAChR partial agonist with selectivity and subnanomolar affinity for $\alpha4\beta2$ nAChR (K_i = 0.122 nM). The knowledge of the structure-activity relationship for this lead compound is very limited, due to the emerging trend of pharmaceutical companies to minimise the amount of biological data in the patent literature. Hardly anything is known about the impact of a bulkier substituent in position 3 and/or 5 on the cytisine affinity. Therefore, a library of 3- and/or 5-(hetero)aryl analogues of cytisine was synthesized and evaluated for the affinity towards several nAChR subtypes.

Chemistry

- Numerous isolation experiments were carried out and the total amount of approximately 15 g of cytisine **27** (0.11% – 0.48% yields with regard to the amount of the plant material) was isolated from natural sources (*Laburnum anagyroides* and *watereri, Fabaceae*). In order to improve purity of the isolated alkaloid **27**, preparative HPLC was used instead of crystallization.
- The intermediates 3-bromo-, 5-bromo- and 3,5-dibromo-N-*t*BOC-cytisine **81** – **83** were synthesized like previously reported, however, the isomers were separated and purified with preparative HPLC and obtained in high purity. The column chromatography purification, performed according to the published procedures, was ineffective (difficult separation of the isomers, low yields).
- The key step of the new synthetic route was palladium-mediated Suzuki cross-coupling of either N-protected 3- or 5-bromocytisine **81** or **82** with different aryl- and heteroarylboronic acids under microwave-accelerated conditions.

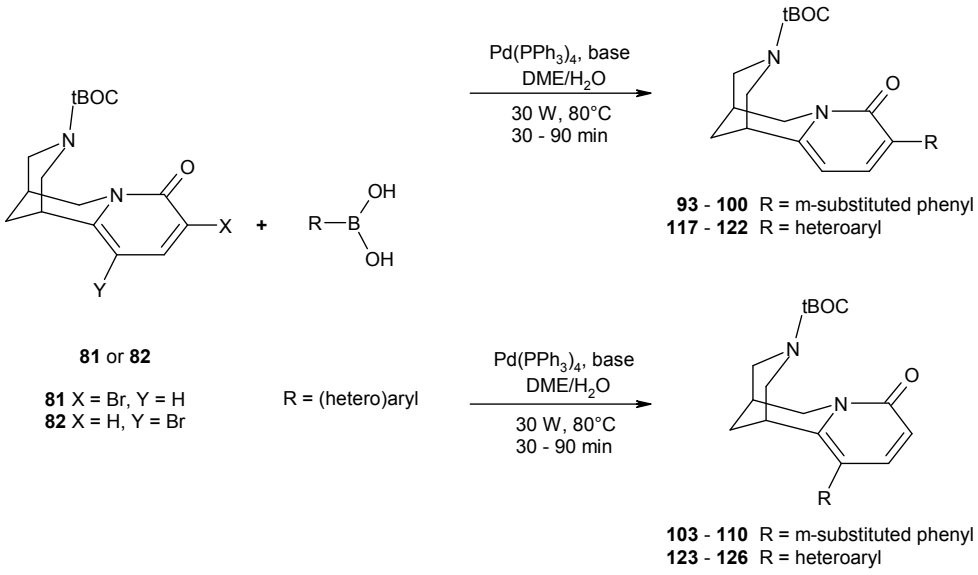

- Microwave heating has demonstrated clear advantages over the conventional heating procedures (faster reactions, higher yields, less side products) and allowed incorporation of (hetero)aryl moieties into position 3 or 5 in 30-90 minutes.
- The purification of the coupling products was efficiently performed with preparative high performance liquid chromatography.
- Selective Suzuki cross-coupling reaction was carried out with 3,5-dibromo-N-*t*BOCcytisine **83**. Employing carefully selected condition allowed coupling reaction only in position 3, while the bromine in position 5 was not attacked. In this way

obtained 3-phenyl-5-bromo- and 3-(3'-pyridyl)-5-bromo analogues **128** and **129** are novel disubstituted cytisine derivatives.

- The N-*t*BOC protecting group was quantitatively hydrolysed in an aqueous solution of the compound employing the microwave dielectric heating. This fast, efficient and clean (no reagents, water as a solvent) cleavage of the *t*BOC protecting group via microwave-mediated thermal fission of carbon dioxide and isobutene has not been described so far.

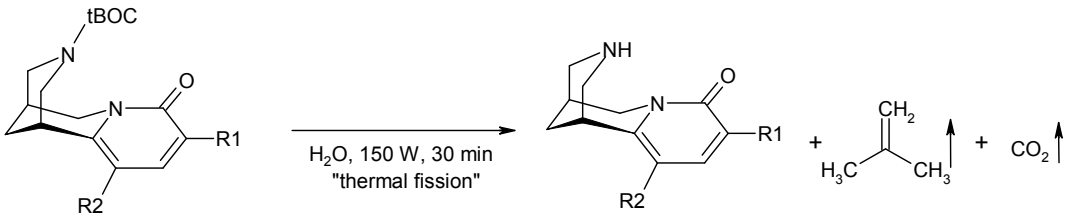

- Detailed 1D and 2D NMR studies of cytisine **27** were performed and the ^{1}H (in green) and ^{13}C (in blue) chemical shifts of the cytisine were unambiguously assigned.

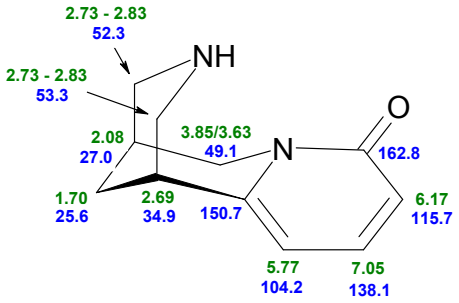

- Detailed 1D and 2D NMR studies of 3-phenyl and 5-phenyl cytisine derivatives **93e** and **103e** afforded identification of "diagnostical tools", which are very useful for differentiation of the 3- and 5-isomers.

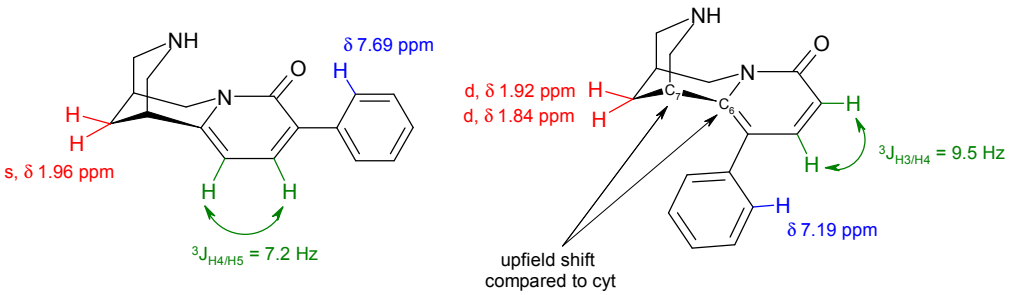

3-phenyl-cytisine **93e** 5-phenyl-cytisine **103e**

In total, three known (**93e**, **99e** and **103e**) and twenty five novel pyridone-modified analogues of cytisine featuring a (hetero)aryl substituent in the position 3 or 5 were synthesized. The known ligands were re-synthesized in a new improved synthetic route (Suzuki reaction instead of Stille reaction) and in order to gain information about their pharmacological behaviour.

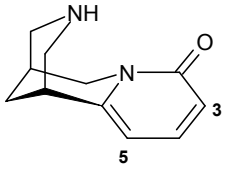

Substituents introduced into the position 3 or 5 of cytisine

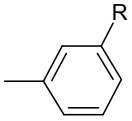

R = H, NO_2, CH_3, CF_3, OCF_3, Cl, F, Ph

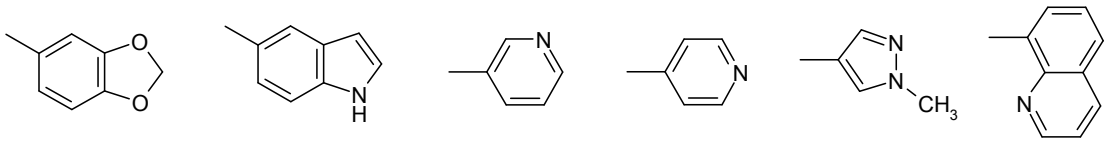

Pharmacology

All nAChRs ligands have been tested in radioligand binding studies for their affinity towards $\alpha4\beta2^*$, $\alpha7^*$, $\alpha3\beta4^*$ and $(\alpha1)_2\beta1\gamma\delta$ nAChR subtypes in order to understand what structure elements contribute to the subtype selectivity. The affinities of novel ligands are always compared to the affinity of the lead compound, i.e. cytisine **27** (K_i = 0.122 nM).

- The introduction of m-substituted phenyl moieties into position 3 decreased the affinity for the $\alpha4\beta2^*$ nACh receptor (K_i = 5.7 – 200 nM), whereas the degree of the affinity reduction depended on the nature of the meta-substituent (F < CF_3 < NO_2 ≈ CH_3 < OCF_3 < H < Cl < Ph). The results suggest that small electron-withdrawing groups on the phenyl moiety are preferred.
- The $\alpha4\beta2^*$ affinities of 5-aryl derivatives were decreased (K_i = 3.7 – 300 nM), however the meta-substitution of the phenyl ring influenced the $\alpha4\beta2^*$ binding affinity in a different manner when compared to the corresponding series of 3-arylated analogues (NO_2 < OCF_3 ≈ CH_3 < H < CF_3 < Ph < F).

- The introduction of heterocyclic moieties into the position 3 of cytisine resulted in a ligand with a lowest α4β2* affinity (5-(5'-indolyl)-cytisine **123e**, K_i = 853 nM) as well as in ligands with two highest α4β2* affinities (**119e** and **122e**)

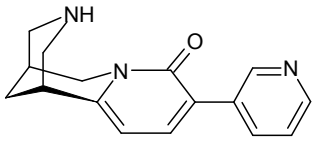

119e
K_i = 0.91 nM

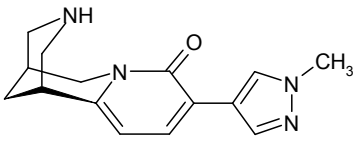

122e
K_i = 0.177 nM

- Ligand **122e** shows the highest affinity also for α3β4* nAChR (K_i = 33 nM) but retains subtype selectivity for α4β2* subtype (α4β2*/α3β4*/α7*/$(\alpha 1)_2\beta 1\gamma\delta$ = 1 : 186 : > 55,000 : 28,000).
- The substitution of position 5 significantly improves the subtype selectivity since the α3β4* nAChR seems to possess smaller dimensional limit for the position 5 than the α4β2* receptor subtype. 5-Aryl and heteroaryl analogues of cytisine show better selectivity profile than their 3-counterparts.
- The introduction of 5-indolyl moiety into position 5 yielded the most selective ligand **123e** (α4β2*/α3β4*/α7*/$(\alpha 1)_2\beta 1\gamma\delta$ = 1 : 490 : >490 : 490).
- The high binding data for 5-(3'-nitrophenyl)-cytisine **104e** (K_i = 3.7 nM) and 5-(5'-indol)-cytisine **113e** (K_i = 20.4 nM) suggest the posibility of new binding mode between these ligands and the α4β2* nACh receptor (e.g. additional π-π interaction between the ligand and the receptor).
- All 3-and 5- substituted cytisine derivatives showed low affinity for the α7* and $(\alpha 1)_2\beta 1\gamma\delta$ nAChR subtype (K_i > 10,000 nM).
- Disubstitution of the cytisine skeleton in positions 3 and 5 led to ligands **128e** and **129e** with decreased affinity for the nAChR subtypes tested (α4β2*, α7*, α3β4* and muscle type).

The putative hydrophobic region next to the HBA functionality of cytisine (carbonyl group) is indeed not bulk-tolerant, but rather the electrostatic than the steric properties of the aryl moiety ultimately influence the α4β2* affinity, i.e. 3-trifluoromethyl-phenyl analogues displays higher affinity than the 3-phenyl analogue. Thus, for the prediction of the binding affinities for cytisine derivatives one always has to consider the combination of substituent's steric and electrostatic characteristics. The combined findings suggest that small electron-withdrawing

groups are preferred for the position 3. The introduction of a smaller N-bearing heterocycle into the position 3 resulted in compounds with affinities in picomolar range.

The position 5 is more bulk-tolerant than the position 3 with regard to the α4β2* affinity, but less bulk-tolerant for the α4β3* affinity. Additionally, the position 5 does not favour substituents with high electronegativity. These results allow development of α4β2*-selective ligands via appropriate substitution of the position 5 (e.g. with bulky indole moiety).

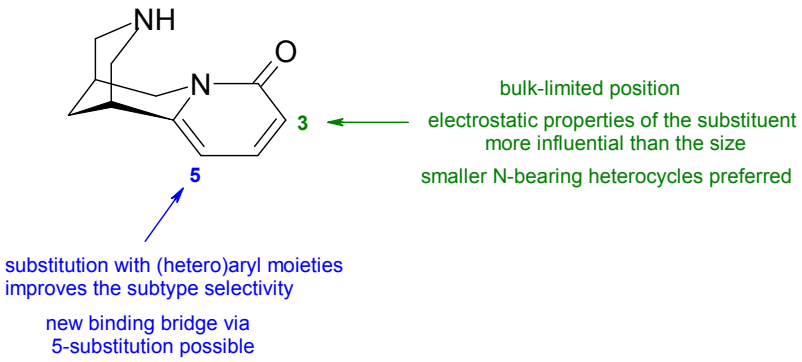

These results provide valuable information regarding the requirements of the α4β2 nAChR subtype for a cytisine-derived ligand with high affinity and selectivity and greatly extend the knowledge of SAR for cytisine as a lead compound.

Project II: Development of Novel nAChRs Ligands based on Choline

The vast majority of the nAChR ligands are compounds selective for α4β2 subtype. Only limited amount of synthetic α7 agents, next to the naturally occurring toxins with high α7 affinity, have been reported in the literature, e.g. GTS-21 **13** and AR-R17779 **26**.

Choline **3**, a precursor and a metabolite of acetylcholine **1**, possesses micromolar affinity for α4β2 receptor (K_i = 112 μM) and is an effective agonist of α7 nAChRs even if it presents very low affinity for this subtype (K_i = 2,380 μM). However, despite its pharmacological profile and cytoprotective properties, the structure of choline **3** has attracted limited interest as lead compound in the search for nAChR ligands. Therefore, it was rationale to revisiting this structure as a lead for development of novel nAChRs ligands.

Addition of amide moiety into a phenylether of choline **4** (potent ganglion stimulant) resulted into a phenylcarbamate derivative **5**, that exhibited nanomolar α7-affinity combined with high selectivity for this receptor subtype. In order to explore the requirements of the α7 nACh receptor for a selective and potent ligand and answer the question whether a carbamate bond between nAChR pharmacophoric elements always results into an α7-selective ligand, a

library of phenylcarbamate analogues was synthesized. In the target phenylcarbamate derivatives, the quaternary nitrogen was incorporated into various azacyclic systems (N-methylpyrrolidine, N-methylpiperidine and quinuclidine) with the intention to improve BBB permeability. Additional substitution at the phenyl moiety should give deeper insight into the structure-activity relationship.

Chemistry

- The target phenylcarbamates were synthesized via the addition of corresponding azacyclic alcohol to the m-substituted phenylisocyanate.

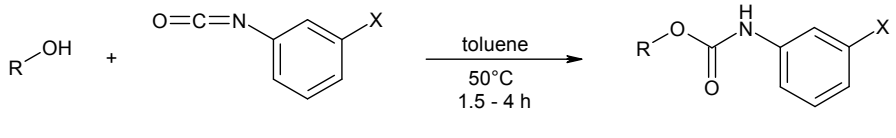

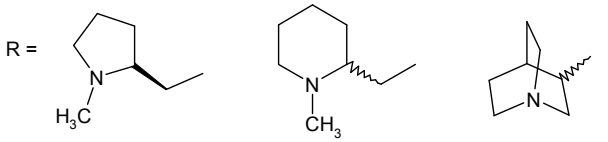

136 X = CH_3
137 X = Br

138 X = CH_3
139 X = Br

140 X = CH_3
141 X = Br

- In order to avoid hydrolyses of the isocyanates, the reactions were carried out under argon atmosphere in dry solvent (toluene).
- The biaryl analogues **144** and **145** were successfully synthesized by employing the Suzuki protocol. Microwave dielectric heating was used instead of the conventional heating and allowed the addition of the phenyl and styryl moieties to the quinuclidine derivative **141** in 10 min.

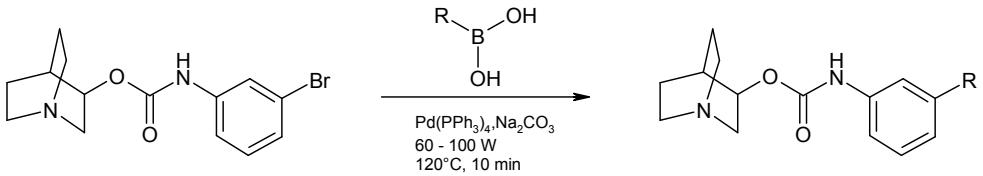

141

144 R = phenyl
145 R = styryl

Pharmacology

- Incorporation of the quaternary nitrogen into a pyrrolidine skeleton decreased the α7* binding while enhancing the α4β2* binding. The ligand's affinity to the [^{3}H]epibatidine binding sites in rat brain membranes is supported by meta-substitution of the phenyl moiety with bromine.

- Expansion of the pyrrolidine ring to piperidine leads to a notable reduction of the affinity for α4β2* and loss of the affinity for α7* nAChR subtype.
- Quinuclidinole analogues exhibit remarkable selectivity for α7* receptor over α4β2* nAChR. Substitution in the position 3 of the phenyl moiety caused a reduction of binding affinity with the rank-order H < Br ≈ CH_3 < Ph < styryl.

The carbamates bearing pyrrolidine **136 – 137** or piperidine **138** – **139** moiety had been shown to possess a prevalance for the α4β2* nAChR subtype while the corresponding analogues in the quinuclidine series **140** – **141** revealed a higher binding to the α7* subtype. Thus, the carbamate bond as a link between the protonable nitrogen and π-electron system does not necessarily provide an α7-selective ligand. The 3-quinuclidinole core seems to possess favourite distance between the oxygen and nitrogen and in combination with carbamate moiety and π-electron system it provides a template for development of selective and potent α7 ligands.

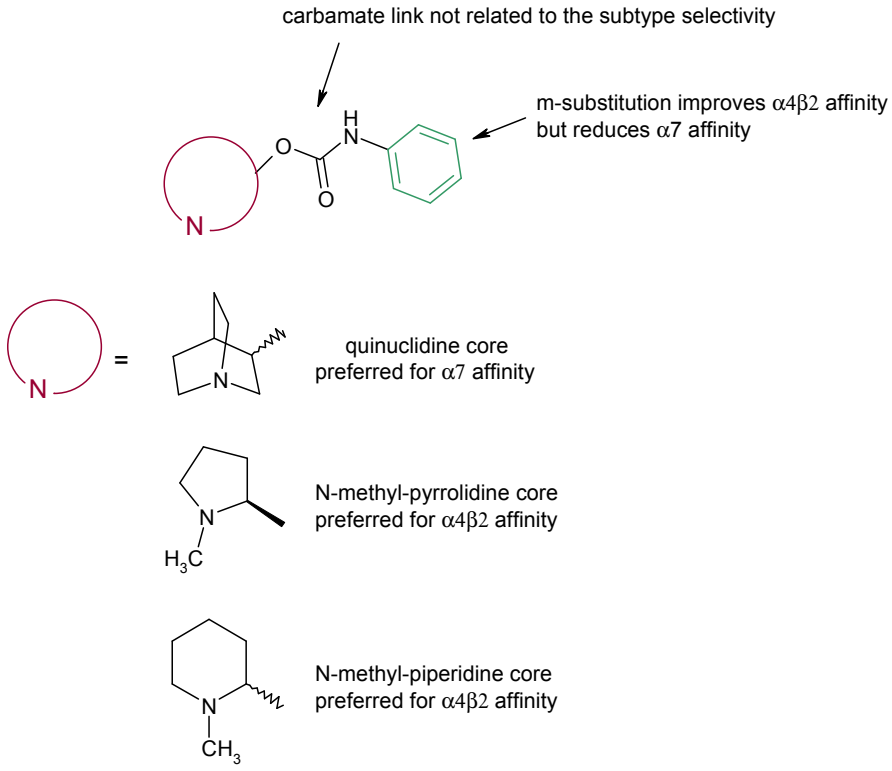

Concluding Remarks

It has been long accepted that targeting nAChRs represent a pathway for the treatment of various CNS-related and non CNS-related disorders (e.g. Alzheimer's and Parkinson's disease, schizophrenia, depression, inflammation, pain). Advances in medicinal chemistry, molecular biology and behavioural pharmacology have resulted in a better understanding of the role of nAChRs in the pathological processes as well as in a development of various structurally different nicotinic ligands, whereas several agents have entered clinical trials.

The presented thesis was focused on development of novel nAChR ligands based on cytisine and choline. The synthesized compounds enrich the nAChR pharmacopoeia and the collective findings of biological evaluation greatly extend the knowledge of structure-activity relationship for the leads cytisine and choline.

It has been shown that bulky aryl substituents attached to the cytisine skeleton decrease the affinity of the lead to the $\alpha4\beta2$ nACh receptor, while smaller nitrogen bearing heteroaryls in the position 3 afford ligands with picomolar affinity. Substitution of the position 5 in cytisine leads to an improved selectivity for central nicotinic receptor over nAChRs in the peripheral nervous system and this makes the 5-substituted analogues very interesting. Since the partial agonist behaviour of cytisine provides pharmacological profile required for the treatment of smoking cessation, it is almost essential in the future to test the activities of these ligands. Cytisine has been recently evaluated as an antidepressive drug and several novel derivatives presented herein are currently under investigation in a depression test system at Yale University in New Haven, USA.

Carbamates bearing N-methyl-pyrrolidine or N-methyl-piperidine moiety have been shown to possess lower affinity for $\alpha7^*$ nAChR than their analogues in the quinuclidine series, although the same structural elements are present (a protonable basic nitrogen, a carbamate moiety and a π-electron system). However, the carbamate bond as a link between a quinuclidine core and the π-electron system provides a template for high affinity ligands with $\alpha7$-subtype selectivity, whereas replacement of the quinuclidine moiety by other azacyclic cores, such as N-methylpyrrolidine or N-methylpiperidine, provides ligands with prevalance for $\alpha4\beta2$ nAChRs. Since the carbamate bond is easily hydrolyzed and does not show a predisposition for a $\alpha7$-selective ligand, it might be replaced by e.g. an amide bond. A library of compounds, in which various azacyclic cores are linked to a π-electron system via an amide bond, would offer new and interesting nAChRs ligands.

6 Experimental Procedures

6.1 General Information

Ultraturrax Homogenization

The homogenization was completed with *ULTRA-TURRAX T50 DPX* homogenizator (Janke&Kunkel, IKA Labortechnik, Germany).

Microwave

Microwave irradiation was carried out using the *CEM*-Discover microwave synthesis system (CEM GmbH, Kamp-Lintfort, Germany).

Solid Phase Extraction

SPE was performed on Solid Phase Extraction *BAKERBOND* spe^{TM} Columns (KMF Laborchemie Handels GmbH, St. Augustin, Germany).

High Performance Liquid Chromatography

The chromatographic system consisted of WellChrom Pump K-120 (*Knauer* GmbH, Germany), Injection & Switching Valves (*Knauer* GmbH, Germany), Preparative HPLC-Pump K-1800 (*Knauer* GmbH, Germany), Fast scanning Spectro-Photometer K-2600 (*Knauer* GmbH, Germany) and Electric Valve Drive (*Knauer* GmbH, Germany). The column used was Eurospher 100 C 18, 10 µm, 250 mm × 20 mm (ID) from Knauer GmbH, Germany. The mobile phase was a mixture of MeOH (HPLC Grade Methanol, Merck KgaA, Darmstadt, Germany) and deionised H_2O. The flow rate of the mobile phase was 20 mL/min and the input of 10 mL was used. The chromatograms were scanned at 254 nm and collected to reaction flasks.

Lyophilization

Lyophilization of water was carried out using the *Alpha 1-4 LSC* (Martin Christ Gefriertrocknungsanlagen GmbH, Osterode, Germany).

Column Chromatography

Column chromatography was carried out on Merck silica gel 60 (70 – 230 mesh). The solvents were evaporated with *Vacuubrand* CVC 2 rotary evaporator (Vacuubrand GmbH & Co KG, Wertheim, Germany).

NMR Spectroscopy

^{1}H- and ^{13}C-NMR spectra (1D and 2D) were measured at 500 MHz and 125 MHz on a Bruker "*Avance 500*" spectrometer at the Institute for Pharmaceutical Chemistry, Poppelsdorf, University of Bonn. $CDCl_3$ was used as a solvent and the chemical shift of the remaining protons of the deuterated solvent served as internal standard: δ ^{1}H 7.24 ppm, δ ^{13}C 77 ppm. The assignment was done with the aid of 2D NMR chemical shift maps (COSY, HSQC, HMBC) as well as with the aid of substituent chemical shifts. The coupling constants are given in Hertz (Hz) and the chemical shifts in part per million (ppm). The signal multiplicities are given as follows: s = singlet, d = doublet, t = triplet, q = quartet, sex = sextet, m = multiplet, br = broad, ovl = overlapping, p = pseudo.

Mass Spectroscopy

The mass spectra (EI with high resolution) were measured on an "*MS-50 A.E.I.*" or "*MAT 95 XL, Thermoquest*" at the Kekulé Institute for Organic Chemistry and Biochemistry, Endenich, University of Bonn.

InfraRed Spectroscopy

Infrared spectra were determined on *Perkin-Elmer* 1600 Series FTIR (Perkin-Elmer, Wellesley, MA, USA) spectrophotometer at the Institute for Pharmaceutical Chemistry, Poppelsdorf, University of Bonn.

Elemental microanalysis

Elemental microanalyses were performed on a *VarioEL* apparatus (Elemetar AnalysenSysteme, GmbH, Hanau, Germany) at the Institute for Pharmaceutical Chemistry, Endenich, University of Bonn.

Melting Point

Melting points were determined on a Büchi B-545 melting point apparatus and are uncorrected. For some derivatives the melting point was not determined due to the little amount of the product.

Thin Layer Chromatography

The purity of the compounds was checked on TLC chromatography (Kieselgel 60 F_{254}, Merck, Darmstadt, Germany) using CH_2Cl_2/MeOH/EDMA 99:1:1 v/v/v as a mobile phase.

For the reverse phase TLC the RP-18 F_{254}s plates (Merck, Darmstadt, Germany) and a mixture MeOH/$H_2$0 80:20 v/v were utilised.

Chemical substances

Commercially obtained chemical substances (purity > 97%) were directly used in the chemical reactions. Commercially obtained solvents with the purity <97% were purified via destillation. The boronic acids were obtained from Acros Organics (provided by KMF Laborchemie Handels GmbH, Sankt Augustin, Germany) or Aldrich-Sigma Chemie GmbH, Taufkirchen, Germany in 95% – 98% purity.

Numbering

The alternative numbering used in the thesis for the name and assignment of the ^{1}H and ^{13}C NMR chemical shifts is not consistent with the IUPAC numbering. The IUPAC name of each compound is listed at the end of the spectroscopic characterisation.

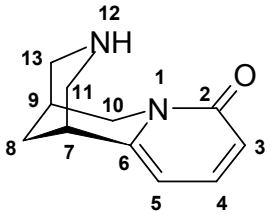

alternative numbering
trivial name: cytisine **27**

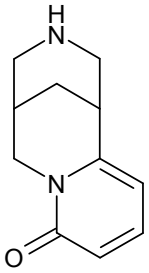

another often used figure of cytisine **27**

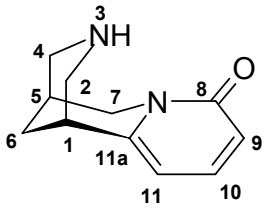

IUPAC numbering
IUPAC name: 1,2,3,4,5,6-Hexahydro-1,5-methano-pyrido[1,2-a][1,5]diazocin-8-one

Intermediates

N-*t*BOC-cytisine **76**, 3-bromo-N-*t*BOC-cytisine **81**, 5-bromo-N-*t*BOC-cytisine **82** and 3,5-dibromo-N-*t*BOC-cytisine **83** were synthesized as previously desribed[124] and were used in following synthetic steps.

6.2 Cytisine **27**

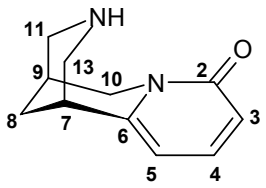

The seeds of *Laburnum anagyroides* and *Laburnum watereri* were collected each year in the Köln-Bonn area in the months September-October. The plant material was air-dried at least for 3 months and ground to a powder consistence.

The plant material was extracted with CH_2Cl_2/MeOH/aq.NH_3 through homogenization by Ultra-turrax for 8 hours (Table 6-1). The evaporated solvent were replaced, exactly the same amounts of each solvent were added to the homogenate during the extraction. The homogenate was centrifuged (2,000 × min, 40 min) and the supernatant collected. The dark green solution was concentrated under reduced pressure to the final volume of 500 mL and extracted with 1M HCl (3 × 100 mL). The aqueous acid solution was rendered alkaline with 26% NH_4OH (pH 11-12) and the free base extracted with CH_2Cl_2 (10 × 100 mL). The organic layers were collected and the solvent evaporated *in vacuo*. The dark green/brownish residue was chromatographed on silica gel column with $CHCl_3$/MeOH 6:1 v/v. The alkaloid **27** was recrystallised from perchlorethylene or directly used in the next step (N-*t*BOC-cytisine **76**, Method B).

Table 6-1 Experimental conditions for the extraction of cytisine **27**

Extraction No.	Amount of the plant material	Solvents*			Cytisine 27	Yields
		CH_2Cl_2	MeOH	aq.NH_3		
1	350 g (seeds only)	500 mL	140 mL	60 mL	0.95 g	0.27%
2	600 g (seeds only)	840 mL	240 mL	90 mL	2.90 g	0.48%
3	1,000 g	2.5 L	1 L	250 mL	1.15 g	0.11%
4	1,000 g	2.5 L	1 L	250 mL	1.83 g	0.18%
5	500 mg	1.3 L	500 mL	125 mL	0.64 g	0.13%
6	1,000 g	2.5 L	1 L	250 mL	1.36 g	0.14%

* The same amount of solvents added through the 8 hours of homogenization.

M.p.: 155-156 °C

^{1}H NMR (500 MHz, $CDCl_3$) δ [ppm] 7.05 (dd, ^{3}J = 9.1 Hz, ^{3}J = 6.9 Hz, 1 H, H4); 6.17 (d, ^{3}J = 9.1 Hz, 1 H, H3); 5.77 (d, ^{3}J = 6.9 Hz, 1 H, H5); 3.77 (d, ^{2}J = 15.4 Hz, 1 H, H10β); 3.57 (dd, ^{2}J = 6.6 Hz, ^{3}J = 15.7 Hz, 1 H, H10α); 2.70 – 2.75 (m, 4 H, H11+H13); 2.62 (s br, 1 H, H7); 2.03 (s br, 1 H, H9); 1.65 (s br, 2 H, H8)

^{13}C NMR (125 MHz, $CDCl_3$) δ [ppm] 162.8 (C=O, C2); 150.7 (C6); 138.1 (C4); 115.7 (C3); 104.2 (C5); 53.3 (C13); 52.3 (C11); 49.1 (C10); 34.9 (C7); 27.0 (C9); 25.6 (C8)

^{1}H NMR (500 MHz, CD_3OD) δ [ppm] 7.49 (dd, ^{3}J = 9.1 Hz, ^{3}J = 6.9 Hz, 1 H, H4); 6.44 (dd, ^{3}J = 9.1 Hz, ^{4}J = 1.6 Hz, 1 H, H3); 6.30 (dd, ^{3}J = 6.9 Hz, ^{4}J = 1.6 Hz, 1 H, H5); 4.09 (d, ^{2}J = 15.5 Hz, 1 H, H10α); 3.92 (dd, ^{2}J = 6.6 Hz, ^{3}J = 15.5 Hz, 1 H, H10β); 2.99 – 3.11 (m, 5 H, H11+H13+H7); 2.39 (s br, 1 H, H9); 2.04 (d, ^{2}J = 12.9 Hz, 1 H, $H8_A$); 1.98 (d, ^{2}J = 12.9 Hz 1 H, $H8_B$)

^{13}C NMR (125 MHz, CD_3OD) δ [ppm] 165.8 (C=O, C2); 153.3 (C6); 141.3 (C4); 117.0 (C3); 108.0 (C5); 54.4 (C13); 53.4 (C11); 51.3 (C10); 36.6 (C7); 29.0 (C9); 26.9 (C8)

IUPAC 1,2,3,4,5,6-hexahydro-1,5-methano-pyrido[1,2-a][1,5]diazocin-8-one

6.3 Synthesis of Intermediates

6.3.1 N-*t*BOC-cytisine **76**

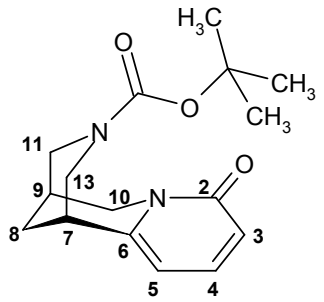

Method A

Cytisine **27** (500 mg, 2.63 mmol), di-*t*-butyldicarbonate (688 mg, 3.15 mmol, 1.2 eq) and Na_2CO_3 (334 mg, 3.15 mmol, 1.2 eq) were stirred in 25 mL CH_2Cl_2 and 6 mL H_2O at 60°C for 2 hours. The reaction mixture was allowed to cool to room temperature and 10 mL of concentrated NaCl solution was added. The organic layer was dried over Mg_2SO_4 and the

solvent evaporated. The product was recrystallised from petroleum ether and obtained as off-white crystalline powder (590 mg – 690 mg, 77% – 90%).

Method B

The dark brownish oily residue obtained from column chromatography in the isolation step was dissolved in 50 mL of CH_2Cl_2. Di-*t*-butyldicarbonate (2 g, 9.0 mmol), Na_2CO_3 (954 mg, 9.0 mmol) and 10 mL H_2O were added. The reaction mixture was stirred at 60°C. The reaction was monitored by TLC (CH_2Cl_2/MeOH 9:1 v/v) and reagents (di-*t*-butyldicarbonate, Na_2CO_3) were added until the cytisine spot disappeared. The mixture was allowed to cool to room temperature, washed with 30 mL of concentrated NaCl solution and the organic layer evaporated under reduced pressure. The yellow residue was dissolved in 150 mL of MeOH/H_2O 60:40 v/v and the product was purified with HPLC.

HPLC Method

Mobile phase: 0 – 10' MeOH/H_2O 60:40 v/v
10' – 15' gradient to 100% MeOH
15' – 25' 100% MeOH

Input: 10 mL

Flow rate: 20 mL/min

Run time: 25 min

Detection: UV at λ = 254 nm

Retention time: $t_{r(N\text{-}tBOC\text{-}cytisine)}$ = 6.9 min

The collected aqueous layer were concentrated under reduced pressure and dried via lyophilization for at least 24 hours. N-*t*BOC-cytisine **76** was obtained as white crystalline powder and was directly used in the bromination step. The yields are calculated over the whole isolation/protection procedure and are listed in the Table 6-2.

Table 6-2 Amount of cytisine **27** calculated from the amount of N-*t*BOC-cytisine **76**. Yields calculated as the ratio of cytisine **27** quantity to the amount of plant material (1,000 g)

Extraction No.	Amount of the plant material	Solvents*			N-*t*BOC-cytisine **76**	Cytisine **27**	Yields
		CH_2Cl_2	MeOH	aq.NH_3			
7	1,000 g	2.5 L	1 L	250 mL	1.80 g	~ 1.18 g	0.12%
8	1,000 g	2.5 L	1 L	250 mL	1.76 g	~ 1.15 g	0.11%
9	1,000 g	2.5 L	1 L	250 mL	2.70 g	~ 1.77 g	0.17%
10	1,000 g	2.5 L	1 L	250 mL	2.30 g	~ 1.51 g	0.15%
11	1,000 g	2.5 L	1 L	250 mL	2.06 g	~ 1.35 g	0.13%

* The same amount of solvents added through the 8 hours of homogenization.

^{1}H NMR (500 MHz, $CDCl_3$) δ [ppm] 7.24 (dd, ^{3}J = 9.1 Hz, ^{3}J = 6.3 Hz, 1 H, H4); 6.41 (d, ^{3}J = 9.1 Hz, 1 H, H3); 6.03 (s br, 1 H, H5); 4.14 (d, ^{2}J = 15.4 Hz, 1 H, H10β); 4.00 – 4.19 (m ovl., 2 H, H13); 3.79 (dd, ^{2}J = 6.6 Hz, ^{3}J = 15.7 Hz, 1 H, H10α); 2.94 – 3.05 (m, 3 H, H7+H11); 2.38 (s br, 1 H, H9); 1.93 (d, 1 H, $H8_A$); 1.87 (d, 1 H, $H8_B$); 1.30 (s, 9 H, *t*BOC-group)

^{13}C NMR (125 MHz, $CDCl_3$) δ [ppm] 163.4 (C=O, C2); 154.5 (C=O; *t*BOC); 148.7 (C6); 138.9 (C4); 117.1 (C3); 105.8 (C5); 80.3 (C(CH_3), *t*BOC); 51.6 (C13); 50.5 (C11); 48.9 (C10); 34.8 (C7); 28.0 (C(CH_3), *t*BOC); 27.5 (C9); 26.1 (C8)

IUPAC 8-oxo-1,5,6,8-tetrahydro-2H,4H-1,5-methano-pyrido[1,2-a][1,5]diazocine-3-carboxylic acid tert-butyl ester

6.3.2 3-Bromo-N-*t*BOC-cytisine **81** and 5-Bromo-N-*t*BOC-cytisine **82**

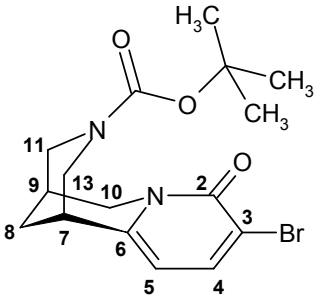

81

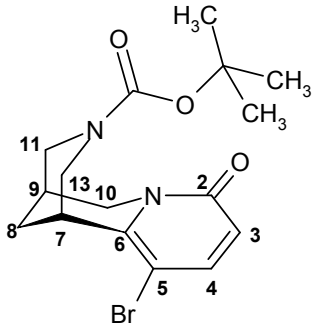

82

N-*t*BOC-cytisine **76** (1 g, 3.44 mmol) and N-bromosuccinimide (613 mg, 3.44 mmol, 1 eq) were stirred in 30 mL CH_2Cl_2 at 60°C for 2 hours. The reaction mixture was allowed to cool to room temperature and the solvent evaporated *in vacuo*. The oily residue was dissolved in 150 mL of MeOH/H_2O 60:40 v/v and the isomers were separated and purified with HPLC.

HPLC method

Mobile phase: MeOH/H_2O 60:40 v/v

Input: 10 mL

Flow rate: 20 mL/min

Run time: 20 min

Detection: UV at λ = 254 nm

Retention time: $t_{r\ (3\text{-Br-N-}t\text{BOC-cyt})}$ = 8.85 min
$t_{r\ (5\text{-Br-N-}t\text{BOC-cyt})}$ = 11.55 min

The collected aqueous layers were concentrated under reduced pressure and products dried via lyophilization for at least 24 hours. The products were obtained as white crystalline powders in 38.0% – 51.9% (**81**) and 28.1% – 42.2% (**82**) yields (Table 6-3).

Table 6-3 Yields of 3-bromo and 5-bromo-N-*t*BOC-cytisine isomers **81** and **82**

Experiment No.	3-Br-N-*t*BOC-cytisine **81**	**Yields**	5-Br-N-*t*BOC-cytisine **82**	**Yields**
1	540 mg	43.0%	422 mg	33.6%
2	543 mg	43.2%	353 mg	28.1%
3	652 mg	51.9%	384 mg	30.6%
4	646 mg	51.4%	530 mg	42.2%
5	477 mg	38.0%	460 mg	36.6%
6	507 mg	40.4%	286 mg	22.8%
7	517 mg	41.2%	395 mg	31.5%
8	504 mg	40.1%	354 mg	28.2%

3-Bromo-N-*t*BOC-cytisine **81**

^{1}H NMR (500 MHz, $CDCl_3$) δ [ppm] 7.64 (d, ^{3}J = 7.6 Hz, 1 H, H4); 5.96 (s br, 1 H, H5); 4.23 (d, ^{2}J = 15.8 Hz, 1 H, H10β); 4.06 – 4.35 (m ovl., 2 H, H13); 3.85 (dd, ^{2}J = 6.3 Hz, ^{3}J = 15.5 Hz, 1 H, H10α); 2.99 – 3.06 (m, 3 H, H7 + H11); 2.40 (s br, 1 H, H9); 1.94 (t, ^{2}J = 13.2 Hz, 2 H, H8); 1.30 (s, 9 H, *t*BOC)

^{13}C NMR (125 MHz, $CDCl_3$) δ [ppm] 159.4 (C=O, C2); 154.4 (C=O, *t*BOC); 148.5 (C6); 140.8 (C4); 112.5 (C3); 105.7 (C5); 80.6 (<u>C</u>(CH_3), *t*BOC); 51.4 (C13); 50.2 (C11); 49.2 (C10); 34.7 (C7); 28.0 (C(<u>C</u>H_3), *t*BOC); 27.4 (C9); 26.0 (C8)

IUPAC 9-bromo-8-oxo-1,5,6,8-tetrahydro-2H,4H-1,5-methano-pyrido[1,2-a][1,5]diazocine-3-carboxylic acid tert-butyl ester

5-Bromo-N-*t*BOC-cytisine **82**

^{1}H NMR (500 MHz, $CDCl_3$) δ [ppm] 7.42 (d, ^{3}J = 9.8 Hz, 1 H, H4); 6.38 (d, ^{3}J = 9.5 Hz, 1 H, H3); 4.36 (s br, 2 H, H13); 4.16 (d, ^{2}J = 15.5 Hz, 1 H, H10β); 3.82 (dd, ^{3}J = 6.0 Hz, ^{2}J = 15.5 Hz, 1 H, H10α); 3.42 (s br, 1 H, H7); 2.90 – 3.06 (m, 2 H, H11); 2.40 (s br, 1 H, H9); 1.97 (s, 2 H, H8); 1.29 (s, 9 H, *t*BOC)

^{13}C NMR (125 MHz, $CDCl_3$) δ [ppm] 162.3 (C=O, C2); 154.4 (C=O, *t*BOC); 145.9 (C6); 142.4 (C4); 118.2 (C3); 99.3 (C5); 80.5 (C(CH$_3$), *t*BOC); 50.2 (C13); 48.9 (C11); 47.2 (C10); 34.2 (C7); 28.0 (C(CH$_3$), *t*BOC); 27.4 (C9); 26.3 (C8)

IUPAC 11-bromo-8-oxo-1,5,6,8-tetrahydro-2H,4H-1,5-methano-pyrido[1,2-a][1,5]diazocine-3-carboxylic acid tert-butyl ester

6.3.3 3,5-Dibromo-N-*t*BOC-cytisine **83**

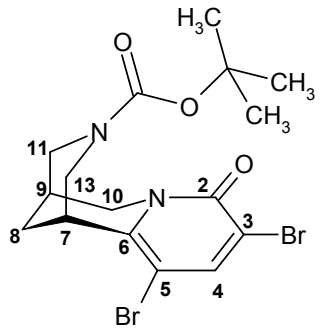

N-*t*BOC-cytisine **76** (600 mg, 2.0 mmol) and N-bromosuccinimide (700 mg, 4.0 mmol, 2 eq) were stirred in 25 mL CH_2Cl_2 at 60°C for 2 hours. The reaction mixture was allowed to cool to room temperature and the solvent evaporated *in vacuo*. The oily residue was dissolved in 100 mL of MeOH/H_2O 60:40 v/v and the product was separated and purified with HPLC.

HPLC method

Mobile phase: isocratic MeOH/H_2O 60:40 v/v
Input: 10 mL
Flow rate: 20 mL/min
Run time: 25 min
Detection: UV at λ = 254 nm
Retention time: $t_{r\ (3,5\text{-diBr-N-tBOC-cyt})}$ = 16.9 min

The collected aqueous layers were concentrated under reduced pressure and the product dried via lyophilization for at least 24 hours. The product was obtained as white crystalline powder (376 mg, 42%).

^{1}H NMR (500 MHz, $CDCl_3$) δ [ppm] 7.83 (s, 1 H, H4); 4.33 (s br, 2 H, H13); 4.22 (d, ^{2}J = 15.8 Hz, 1 H, H10β); 3.85 (dd, ^{3}J = 7.0 Hz, ^{2}J = 16.1 Hz, 1 H, H10α); 3.39 (s br, 1 H, H7);

2.87 – 3.10 (m, 2 H, H11); 2.39 (s br, 1 H, H9); 1.99 (t, ^2J = 14.1 Hz, 2 H, H8); 1.29 (s, 9 H, *t*BOC)

^{13}C NMR (125 MHz, $CDCl_3$) δ [ppm] 158.6 (C=O, C2); 154.2 (C=O, *t*BOC); 145.5 (C6); 143.8 (C4); 113.2 (C3); 98.3 (C5); 80.7 (C(CH_3), *t*BOC); 51.4 (C13); 48.9 (C11); 47.9 (C10); 34.2 (C7); 28.0 (C(CH_3), *t*BOC); 27.3 (C9); 26.2 (C8)

IUPAC 9,11-dibromo-8-oxo-1,5,6,8-tetrahydro-2H,4H-1,5-methano-pyrido[1,2-a][1,5] diazocine-3-carboxylic acid tert-butyl ester

6.4 Synthesis of Novel nAChR Ligands Based on Cytisine

6.4.1 General Procedures

Suzuki cross-coupling reaction

The appropriate bromo-N-*t*BOC-cytisine isomer (**81** - **83**, 0.27 mmol), boronic acid or ester (0.41 mmol; 1.5 eq), base (0.6 mmol, 2.2 eq), DME (3 mL) or DMF (3 mL) and H_2O (1 mL) were placed in a 10-mL microwave glass tube. The solution was washed with argon for 10 min. After the addition of $Pd(PPh_3)_4$ (0.027 mmol, 0.1 eq) the reaction vessel was sealed with a septum and placed into the microwave cavity. Microwave irradiation of 30 W was used, the temperature being ramped from room temperature to 80°C. Once 80°C was reached, the reaction mixture was held for 30 or 60 min. Then the mixture was allowed to cool to room temperature, the reaction vessel was opened and the solvent evaporated under pressure. The brown residue was extracted on SPE C-18 column eluting with mixture MeOH/H_2O 70:30 or 60:40 v/v. The aqueous solution was concentrated *in vacuo* and the *t*BOC-protected product was purified by HPLC.

HPLC method

The ratios of MeOH/H_2O 80:20 (v/v), 70:30 (v/v), 60:40 (v/v), 55:45 (v/v), 50:50 (v/v) were used for 25 min. In the following 5 min gradient to 100% MeOH was run and the system was washed with MeOH for 15 min. The flow rate of the mobile phase was 20 mL/min and the input of 10 mL was used. The chromatograms were scanned at 254 nm and collected to reaction flasks. The retention time given for each compound is the retention time of the N-*t*BOC-protected analogue. The fraction containing the desired product was concentrated *in vacuo* using a rotary evaporator.

Deprotection - Method A

To the concentrated aqueous solution (approximately 15 mL) of the *t*BOC-protected product was added 1M HCl (15 mL) and the mixture was stirred at reflux for 24 hours. The reaction mixture was allowed to cool to room temperature and $NaHCO_3$ was added. Free base was extracted with $CHCl_3$, the organic solvent was evaporated and the desired product dried *in vacuo.*

Deprotection - Method B

The concentrated aqueous solution of the *t*BOC-protected product (approximately 70 mL) was put into a 80-mL microwave glass tube, sealed and placed into a microwave cavity. Microwave irradiation of 150 W was used, the temperature being ramped from room temperature to 150°C. Once 150°C was reached, the reaction mixture was held for 30 min. Then the mixture was allowed to cool to room temperature, the reaction vessel was opened and the solvent evaporated by lyophilization for at least 24 hours.

6.4.2 3-Phenyl-cytisine **93e**

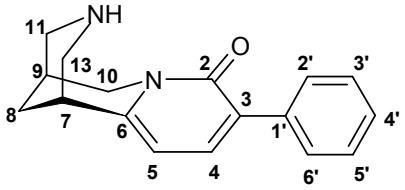

The Suzuki reaction was performed according to the general method with 3-bromo-N-*t*BOC-cytisine **81** (100 mg, 0.27 mmol), phenylboronic acid (50 mg, 0.41 mmol), Na_2CO_3 (64 mg, 0.6 mmol), $Pd(PPh_3)_4$ (30 mg, 0.027 mmol), DME and H_2O. The reaction time was 30 min. For the SPE purification, a mixture of MeOH/H_2O 70:30 v/v (100 mL) was used. The HPLC separation was completed with MeOH/H_2O 60:40 v/v. Deprotection by Method B. The final product obtained as white crystalline powder (42 mg, 0.15 mmol, 58.4%).

M.p.: 139.8 – 140.6 °C
HPLC: t_r = 16.73 min

^{1}H NMR (500 MHz, $CDCl_3$) δ [ppm] 7.69 (dt, ^4J = 1.3 Hz, ^3J = 7.2 Hz, 2 H, H2' + H6'); 7.46 (d, ^3J = 7.2 Hz, 1 H, H4), 7.38 (t, ^3J = 7.2 Hz, 2 H, H3' + H5'); 7.29 (tt, ^4J = 1.3 Hz, ^3J = 7.2 Hz, 1 H, H4'), 6.09 (d, ^3J = 7.2 Hz, 1 H, H5); 4.19 (d, ^2J = 15.5 Hz, 1 H, H10β); 3.96 (dd, ^2J = 6.3 Hz, ^3J = 15.5 Hz, 1 H, H10α); 3.03 (d, ^2J = 12.3 Hz, 1 H, $H11_A$); 3.07 (dd, ^3J = 2.2 Hz, ^2J =

12.3 Hz, 1 H, $H13_A$); 3.02 (d br, ^2J = 12.3 Hz, 2 H, $H11_B$ + $H13_B$); 2.91 (s br, 1 H, H7); 2.34 (s br, 1 H, H9); 1.96 (s br, 2 H, H8)

^{13}C NMR (125 MHz, $CDCl_3$) δ [ppm] 162.1 (C=O, C2); 150.3 (C6); 137.4 (C4); 137.0 (C1'); 128.6 (C2' + C6'); 128.0 (C3' + C5'); 127.4 (C3); 127.2 (C4'); 105.0 (C5); 54.0 (C13); 53.0 (C11); 50.2 (C10); 35.7 (C7); 27.9 (C9); 26.3 (C8)

MS (EI) m/z 266.2 (100), 223.1 (65), 210.1 (20), 185.1 (25), 167.1 (10), 149.1 (10), 133.1 (10), 115.1 (10), 97.1 (10)

HRMS for $C_{17}H_{18}N_2O$ calc. 266.1419
found 266.1426

IUPAC 9-phenyl-1,2,3,4,5,6-hexahydro-1,5-methano-pyridino[1,2-a]diazocin-8-one

6.4.3 3-(3'-Nitro-phenyl)-cytisine **94e**

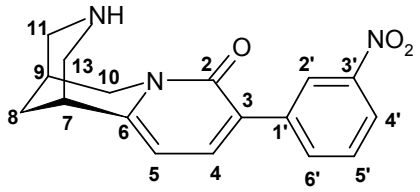

The Suzuki reaction was performed according to the general method with 3-bromo-N-*t*BOC-cytisine **81** (100 mg, 0.27 mmol), 3-nitrophenylboronic acid (68 mg, 0.41 mmol), Na_2CO_3 (64 mg, 0.6 mmol), $Pd(PPh_3)_4$ (30 mg, 0.027 mmol), DME and H_2O. The reaction time was 30 min. For the SPE purification, a mixture of MeOH/H_2O 70:30 v/v (100 mL) was used. The HPLC separation was completed with MeOH/H_2O 60:40 v/v. Deprotection by Method A. The final product obtained as yellow crystalline powder (70 mg, 0.22 mmol, 83%).

M.p.: 209.3 – 209.8 °C
HPLC: t_r = 17.18 min

^{1}H NMR (500 MHz, $CDCl_3$) δ [ppm] 8.53 (t, ^4J = 1.9 Hz, 1 H, H2'); 8.10 – 8.13 (m, ovl., 2 H, H4' + H6'); 7.54 (d, ^3J = 7.3 Hz, 1 H, H4); 7.52 (t, ^3J = 8.0 Hz, 1 H, H5'); 6.13 (d, ^3J = 7.3 Hz, 1 H, H5); 4.17 (d, ^2J = 15.7 Hz, 1 H, H10β); 3.95 (dd, ^3J = 6.6 Hz, ^2J = 15.7 Hz, 1 H, H10α); 2.98 – 3.14 (m, 4 H, H11 + H13); 2.95 (s br, 1 H, H7); 2.38 (s br, 1 H, H9); 1.97 (s, 2 H, H8); 1.87 (s br, NH)

^{13}C NMR (125 MHz, $CDCl_3$) δ [ppm] 161.7 (C=O); 152.0 (C6); 148.2 (C3'); 139.0 (C1'); 137.6 (C4); 134.7 (C6'); 128.9 (C5'); 124.7 (C3); 123.3 (C2'); 121.9 (C4'); 105.0 (C5); 53.8 (C13); 52.9 (C11); 50.3 (C10); 35.7 (C7); 27.7 (C9); 26.1 (C8)

MS (EI) m/z 311.2 (90), 268.1 (100), 255.1 (20), 230.1 (15), 82.1 (25), 44.0 (10)

HRMS for $C_{17}H_{17}N_3O_3$ calc. 311.1269
found 311.1267

IUPAC 9-(3-nitro-phenyl)-1,2,3,4,5,6-hexahydro-1,5-methano-pyridino[1,2-a]diazocin-8-one

6.4.4 3-(3'-Methyl-phenyl)-cytisine **95e**

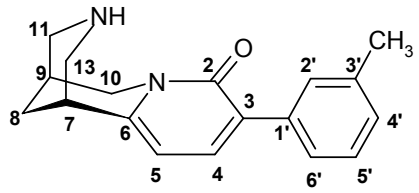

The Suzuki reaction was performed according to the general method with 3-bromo-N-*t*BOC-cytisine **81** (100 mg, 0.27 mmol), m-tolylboronic acid (55 mg, 0.41 mmol), Na_2CO_3 (64 mg, 0.6 mmol), $Pd(PPh_3)_4$ (30 mg, 0.027 mmol), DME and H_2O. The reaction time was 30 min. For the SPE purification, a mixture of MeOH/H_2O 70:30 v/v (100 mL) was used. The HPLC separation was completed with MeOH/H_2O 65:35 v/v. Deprotection by Method A. The final product obtained as off-white crystalline powder (49 mg, 0.16 mmol, 65%).

M.p.: n.d.
HPLC: t_r = 16.27 min

^{1}H NMR (500 MHz, $CDCl_3$) δ [ppm] 7.52 (s br, 1 H, H2'); 7.43 (d, ^{3}J = 7.3 Hz, 2 H, H4 + H6'); 7.26 (t, ^{3}J = 7.3 Hz, 1 H, H5'); 7.09 (d, ^{3}J = 7.3 Hz, 1 H, H4'); 6.06 (d, ^{3}J = 7.0 Hz, 1 H, H5); 4.18 (d, ^{2}J = 15.6 Hz, 1 H, H10β); 3.94 (dd, ^{3}J = 6.6 Hz, ^{2}J = 15.6 Hz, 1 H, H10α), 2.91 (s br, 1 H, H7); 3.00 – 3.11 (m, 4 H, H11 + H13); 2.35 (s, 3 H, CH_3); 2.34 (s, 1 H, H9); 1.97 (s, 2 H, H8)

^{13}C NMR (125 MHz, $CDCl_3$) δ [ppm] 162.2 (C=O); 150.0 (C6); 137.5 (C1'); 137.3 (C3'); 137.0 (C4); 129.3 (C2'); 128.1 (C4'); 128.0 (C5'); 127.6 (C3); 125.7 (C6'); 105.0 (C5); 53.9 (C13); 52.8 (C11); 50.1 (C10); 35.6 (C7); 27.8 (C9); 26.3 (C8); 21.5 ($\underline{C}H_3$)

MS (EI) m/z 280.2 (80), 237.1 (100), 224.1 (25), 199.1 (20), 82.1 (10), 44.0 (40)

HRMS for $C_{18}H_{20}N_2O$ calc. 280.1576
found 280.1579

IUPAC 9-m-tolyl-1,2,3,4,5,6-hexahydro-1,5-methano-pyridino[1,2-a]diazocin-8-one

6.4.5 3-(3'-Trifluoromethyl-phenyl)-cytisine **96e**

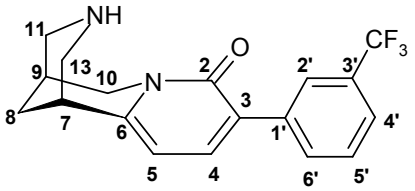

The Suzuki reaction was performed according to the general method with 3-bromo-N-*t*BOC-cytisine **81** (100 mg, 0.27 mmol), 3-trifluoromethylphenylboronic acid (77 mg, 0.41 mmol), Na_2CO_3 (64 mg, 0.6 mmol), $Pd(PPh_3)_4$ (30 mg, 0.027 mmol), DME and H_2O. The reaction time was 30 min. For the SPE purification, a mixture of MeOH/H_2O 70:30 v/v (100 mL) was used. The HPLC separation was completed with MeOH/H_2O 65:35 v/v. Deprotection by Method A. The final product obtained as off-white crystalline powder (47 mg, 0.14 mmol, 52%).

M.p.: 140.9 – 143.0 °C
HPLC: t_r = 19.28 min

^{1}H NMR (500 MHz, $CDCl_3$) δ [ppm] 7.95 (s, 1 H, H2'); 7.91 (d, ^3J = 7.8 Hz, 1 H, H6'); 7.52 (d, ^3J = 7.8 Hz, 1 H, H4'); 7.49 (d, ^3J = 7.0 Hz, 1 H, H4); 7.47 (t, ^3J = 7.8 Hz, 1 H, H5'); 6.11 (d, ^3J = 7.0 Hz, 1 H, H5); 4.16 (d, ^2J = 15.6 Hz, 1 H, H10β); 3.95 (dd, ^3J = 6.3 Hz, ^2J = 15.6 Hz, 1 H, H10α); 2.99 – 3.13 (m, 4 H, H11 + H13); 2.94 (s br, 1 H, H7); 2.35 (s br, 1 H, H9); 1.96 (s, 2 H, H8)

^{13}C NMR (125 MHz, $CDCl_3$) δ [ppm] 161.9 (C=O, C2); 151.4 (C6); 138.1 (C1'); 137.4 (C4); 131.9 (C6'); 130.4 (q, $^2J_{C,F}$ = 31.7 Hz, C3'); 128.4 (C5'); 125.8 (C3); 125.3 (q, $^3J_{C,F}$ = 3.7 Hz, C4'); 123.8 (q, $^3J_{C,F}$ = 3.7 Hz, C2'); 123.2 (q, $^1J_{C,F}$ = 272.5 Hz, $\underline{C}F_3$), 104.9 (C5); 54.0 (C13); 53.0 (C11); 50.3 (C10); 35.7 (C7); 27.8 (C9); 26.2 (C8)

MS (EI) m/z 334.2 (85), 291.1 (100), 270.0 (25), 253.1 (35), 82.1 (30), 44.0 (90)

HRMS for $C_{18}H_{17}F_3N_2O$ calc. 334.1293
found 334.1294

IUPAC 9-(3-trifluoromethyl-phenyl)-1,2,3,4,5,6-hexahydro-1,5-methano-pyridino[1,2-a]-diazocin-8-one

6.4.6 3-(3'-Trifluoromethoxy-phenyl)-cytisine **97e**

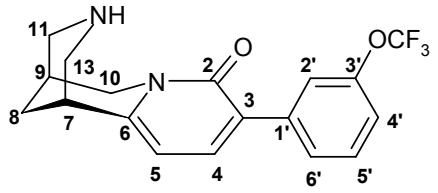

The Suzuki reaction was performed according to the general method with 3-bromo-N-*t*BOC-cytisine **81** (100 mg, 0.27 mmol), 3-trifluoromethoxyphenylboronic acid (62 mg, 0.41 mmol), Na_2CO_3 (64 mg, 0.6 mmol), $Pd(PPh_3)_4$ (30 mg, 0.027 mmol), DME and H_2O. The reaction time was 30 min. For the SPE purification, a mixture of MeOH/H_2O 70:30 v/v (100 mL) was used. The HPLC separation was completed with MeOH/H_2O 65:35 v/v. Deprotection by Method A. The final product obtained as off-white crystalline powder (61 mg, 0.17 mmol, 64%).

M.p.: n.d.
HPLC: t_r = 21.28 min

^{1}H NMR (500 MHz, $CDCl_3$) δ [ppm] 7.63 (ddd, ^4J = 1.3 Hz, ^4J = 1.6 Hz, ^3J = 8.0 Hz, 1 H, H6'); 7.58 (s br, 1 H, H2'); 7.45 (d, ^3J = 7.3 Hz, 1 H, H4); 7.38 (t, ^3J = 8.0 Hz, 1 H, H5'); 7.11 (dquint, ^4J = 1.3 Hz, ^3J = 8.0 Hz, 1 H, H4'); 6.07 (d, ^3J = 7.3 Hz, 1 H, H5); 4.17 (d, ^2J = 15.5 Hz, 1 H, H10β); 3.93 (dd, ^3J = 6.6 Hz, ^2J = 15.5 Hz, 1 H, H10α); 2.95 – 3.12 (m, 4 H, H11 + H13); 2.91 (s br, 1 H, H7); 2.35 (s br, 1 H, H9); 1.95 (s br, 2 H, H8)

^{13}C NMR (125 MHz, $CDCl_3$) δ [ppm] 161.8 (C=O, C2); 151.1 (C6); 149.0 (q, $^3J_{C,F}$ = 1.5 Hz, C3'); 139.3 (C1'); 137.3 (C4); 129.2 (C5'); 126.9 (C6'); 125.6 (C3); 121.5 (q, $^1J_{C,F}$ = 257.0 Hz, $\underline{C}F_3$); 121.1 (C4'); 119.5 (C2'); 105.0 (C5); 53.7 (C13); 52.8 (C11); 50.2 (C10); 35.6 (C7); 27.7 (C9); 26.1 (C8)

MS (EI) m/z 350.2 (100), 307.1 (100), 294.1 (20), 269.1 (30), 82.0 (20), 44.0 (50)

HRMS for $C_{18}H_{17}F_3N_2O_2$ calc. 350.1242
found 350.1244

IUPAC 9-(3-trifluoromethoxy-phenyl)-1,2,3,4,5,6-hexahydro-1,5-methano-pyridino[1,2-a] diazocin-8-one

6.4.7 3-(3'-Chloro-phenyl)-cytisine **98e**

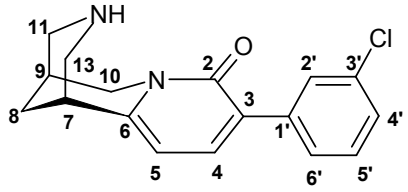

The Suzuki reaction was performed according to the general method with 3-bromo-N-*t*BOC-cytisine **81** (100 mg, 0.27 mmol), 3-chlorophenylboronic acid (63 mg, 0.41 mmol), Na_2CO_3 (64 mg, 0.6 mmol), $Pd(PPh_3)_4$ (30 mg, 0.027 mmol), DME and H_2O. The reaction time was 30 min. For the SPE purification, a mixture of MeOH/H_2O 70:30 v/v (100 mL) was used. The HPLC separation was completed with MeOH/H_2O 65:45 v/v. Deprotection by Method B. The final product obtained as white crystalline powder (38 mg, 0.13 mmol, 47%).

M.p.: 190.6 – 190.9 °C
HPLC: t_r = 20.39 min

^{1}H NMR (500 MHz, $CDCl_3$) δ [ppm] 7.69 (t, ^4J = 1.6 Hz, 1 H, H2'); 7.58 (dt, ^4J = 1.6 Hz, ^3J = 7.9 Hz, 1 H, H4'); 7.44 (d, ^3J = 7.3 Hz, 1 H, H4); 7.29 (t, ^3J = 7.9 Hz, 1 H, H5'); 7.23 (dd, ^4J = 1.6 Hz, ^3J = 7.9 Hz, 1 H, H6'); 6.08 (d, ^3J = 7.3 Hz, 1 H, H5); 4.16 (d, ^2J = 15.6 Hz, 1 H, H10β); 3.94 (dd, ^3J = 6.0 Hz, ^2J = 15.6 Hz, 1 H, H10α); 3.11 (d, ^2J = 12.0 Hz, 1 H, $H11_A$); 3.06 (dd, ^3J = 2.2 Hz, ^2J = 12.0 Hz, 1 H, $H13_A$); 3.00 (d, ^2J = 12.0 Hz, 2 H, $H11_B$ + $H13_B$); 2.92 (s br, 1 H, H7); 2.35 (s br, 1 H, H9); 1.96 (s br, 2 H, H8)

^{13}C NMR (125 MHz, $CDCl_3$) δ [ppm] 161.8 (C=O, C2); 151.0 (C6); 139.1 (C1'); 137.3 (C4); 133.9 (C3'); 129.2 (C5'); 128.6 (C2'); 127.2 (C4'); 126.7 (C6'); 125.9 (C3); 105.0 (C5); 53.9 (C13); 53.0 (C11); 50.2 (C10); 35.7 (C7); 27.8 (C9); 26.2 (C8)

MS (EI) m/z 300.1 (100), 257.1 (95), 244.0 (30), 219.0 (40), 192.1 (5), 150.0 (10), 82.1 (10), 68.1 (5)

HRMS for $C_{17}H_{17}ClN_2O$ calc. 300.1029
found 300.1025

IUPAC 9-(3-chloro-phenyl)-1,2,3,4,5,6-hexahydro-1,5-methano-pyridino[1,2-a]diazocin-8-one

6.4.8 3-(3'-Fluoro-phenyl)-cytisine **99e**

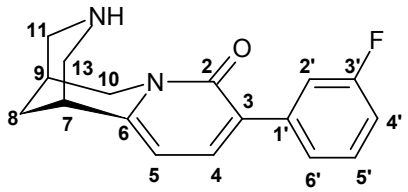

The Suzuki reaction was performed according to the general method with 3-bromo-N-*t*BOC-cytisine **81** (100 mg, 0.27 mmol), 3-fluorophenylboronic acid (56 mg, 0.41 mmol), Na_2CO_3 (64 mg, 0.6 mmol), $Pd(PPh_3)_4$ (30 mg, 0.027 mmol), DME and H_2O. The reaction time was 30 min. For the SPE purification, a mixture of MeOH/H_2O 70:30 v/v (100 mL) was used. The HPLC separation was completed with MeOH/H_2O 65:35 v/v. Deprotection by Method A. The final product obtained as off-white crystalline powder (35 mg, 0.12 mmol, 46%).

M.p.: 138.9 – 140.0 °C
HPLC: t_r = 13.7 min

^{1}H NMR (500 MHz, $CDCl_3$) δ [ppm] 7.45 (d, ^3J = 7.2 Hz, 1 H, H4); 7.43 (d br, ^3J = 8.2 Hz, 2 H, H2' + H6'); 7.32 (dt, ^4J = 6.3 Hz, ^3J = 8.5 Hz, 1 H, H5'); 6.96 (tdd, ^4J = 0.9 Hz, ^4J = 2.5 Hz, ^3J = 8.5 Hz, 1 H, H4'); 6.08 (d, ^3J = 7.2 Hz, 1 H, H5); 4.17 (d, ^2J = 15.6 Hz, 1 H, H10β); 3.93 (dd, ^3J = 6.0 Hz, ^2J = 15.6 Hz, 1 H, H10α); 3.12 (d, ^2J = 12.0 Hz, 1 H, $H11_A$); 3.06 (dd, ^3J = 2.2 Hz, ^2J = 12.0 Hz, 1 H, $H13_A$); 3.01 (d, ^2J = 12.0 Hz, 1 H, $H11_B$); 2.98 (d, ^2J = 13.0 Hz, 1 H, $H13_B$); 2.92 (s br, 1 H, H7); 2.36 (s br, 1 H, H9); 2.26 (s br, NH); 1.96 (s br, 2 H, H8)

^{13}C NMR (125 MHz, $CDCl_3$) δ [pm] 163.6 (d, $^1J_{C,F}$ = 244.1 Hz, C3'); 161.9 (C=O, C2); 150.7 (C6); 139.4 (d, $^3J_{C,F}$ = 8.2 Hz, C1'); 137.3 (C4); 129.4 (d, $^3J_{C,F}$ = 8.5 Hz, C5'); 126.0 (d, $^4J_{C,F}$ = 2.3 Hz, C3); 124.1 (d, $^4J_{C,F}$ = 2.7 Hz, C6'); 115.6 (d, $^2J_{C,F}$ = 22.4 Hz, C4'); 114.1 (d, $^2J_{C,F}$ = 21.2 Hz, C2'); 105.0 (C5); 53.6 (C13); 52.7 (C11); 50.1 (C10); 35.5 (C7); 27.7 (C9); 26.1 (C8)

MS (EI) m/z 284.2 (100), 241.2 (100), 228.1 (30), 203.1 (40), 149.1 (25), 82.1 (20), 44.0 (50)

HRMS for $C_{17}H_{17}FN_2O$ calc. 284.1325
found 284.1324

IUPAC 9-(3-fluoro-phenyl)-1,2,3,4,5,6-hexahydro-1,5-methano-pyridino[1,2-a]diazocin-8-one

6.4.9 3-(Biphenyl-3'-yl)-cytisine **100e**

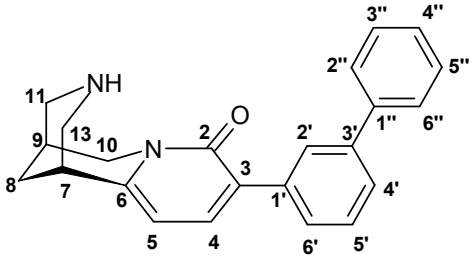

The Suzuki reaction was performed according to the general method with 3-bromo-*t*BOC-cytisine **81** (100 mg, 0.27 mmol), 3-biphenylboronic acid (80 mg, 0.41 mmol), Na_2CO_3 (64 mg, 0.6 mmol), $Pd(PPh_3)_4$ (30 mg, 0.027 mmol), DME and H_2O. The reaction time was 30 min. For the SPE purification mixture of MeOH/H_2O 80:20 v/v (100 mL) was used. The HPLC separation was completed with MeOH/H_2O 65:35 v/v for 15 min, then a gradient to the final mixture of MeOH/H_2O 80:20 v/v was run for 15 min. Deprotection by Method A. The final product obtained as off-white crystalline powder (33 mg, 0.1 mmol, 36%).

M.p.: 95.2 – 97 °C
HPLC: t_r = 27.29 min

^{1}H NMR (500 MHz, $CDCl_3$) δ [ppm] 7.91 (t, ^{4}J = 1.6 Hz, 1 H, H2'); 7.69 (ddd, ^{4}J = 1.3 Hz, ^{4}J = 1.6 Hz, ^{3}J = 8.0 Hz, 1 H, H6'); 7.62 (dt, ^{4}J = 1.3 Hz, ^{3}J = 8.2 Hz, 2 H, H2'' + H6''); 7.51 (d, ^{3}J = 7.3 Hz, 1 H, H4; dd, ovl., 1 H, H4'); 7.44 (d, ^{3}J = 8.0 Hz, 1 H, H5'); 7.40 (tt, ^{4}J = 1.9 Hz, ^{3}J =

7.0 Hz, 2 H, H3'' + H5''); 7.31 (tt, ^4J = 1.3 Hz, ^3J = 7.0 Hz, 1 H, H4'); 6.09 (d, ^3J = 7.3 Hz, 1 H, H5); 4.19 (d, ^2J = 15.6 Hz, 1 H, H10β); 3.97 (dd, ^3J = 5.7 Hz, ^2J = 15.6 Hz, 1 H, H10α); 3.00 – 3.13 (m, 4 H, H11 + H13); 2.93 (s br, 1 H, H7); 2.35 (s br, 1 H, H9); 1.97 (s br, 2 H, H8)

^{13}C NMR (125 MHz, $CDCl_3$) δ [ppm] 162.1 (C=O, C2), 150.4 (C6), 141.4 (C3'), 141.0 (C1''), 137.6 (C4), 137.8 (C1'), 129.1 (C3), 128.5*, 128.1*, 127.8*, 127.4*, 127.1*, 126.8*, 126.6*, 125.5*, 105.3 (C5), 53.9 (C13), 53.0 (C11), 50.2 (C10), 35.3 (C7), 27.5 (C9), 26.3 (C8)

MS (EI) m/z 342.2 (100), 299.2 (65), 262.1 (60), 183.1 (35), 108.0 (10)

HRMS for $C_{23}H_{22}N_2O$ calc. 342.1732
found 342.1734

IUPAC 9-biphenyl-3-yl-1,2,3,4,5,6-hexahydro-1,5-methano-pyridino[1,2-a]diazocin-8-one

6.4.10 5-Phenyl-cytisine **103e**

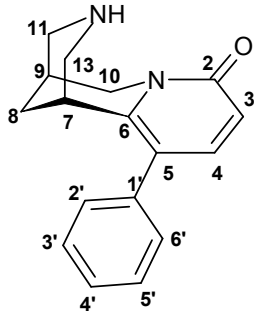

The Suzuki reaction was performed according to the general method with 5-bromo-N-*t*BOC-cytisine **82** (100 mg, 0.27 mmol), phenylboronic acid (50 mg, 0.41 mmol), Na_2CO_3 (64 mg, 0.6 mmol), $Pd(PPh_3)_4$ (30 mg, 0.027 mmol), DME and H_2O. The reaction time was 60 min. For the SPE purification, a mixture of MeOH/H_2O 70:30 v/v (100 mL) was used. The HPLC separation was completed with MeOH/H_2O 60:40 v/v. Deprotection by Method B. The final product obtained as white crystalline powder (28 mg, 0.1 mmol, 39%).

M.p.: 91 °C
HPLC: t_r = 17.32 min

^{1}H NMR (500 MHz, $CDCl_3$) δ [ppm] 7.37 (tt, ^{4}J = 1.3 Hz, ^{3}J = 7.3, 2 H, H3' + H5'); 7.31 (tt, ^{4}J = 1.6 Hz, ^{3}J = 7.3 Hz, 1 H, H4'); 7.21 (d, ^{3}J = 9.5 Hz, 1 H, H4); 7.18 (tt, ^{4}J = 1.6 Hz, ^{3}J = 7.3 Hz, 2 H, H2' + H6'); 6.49 (d, ^{3}J = 9.5 Hz, 1 H, H3), 4.19 (d, ^{2}J = 15.6 Hz, 1 H, H10β); 3.95 (dd, ^{3}J = 6.9 Hz, ^{2}J = 15.6 Hz; 1 H, H10α); 3.12 (d, ^{2}J = 12.0 Hz, 1 H, $H11_A$); 3.04 (s br, 1 H, H7); 2.92 (d, ^{2}J = 12.0 Hz, 1 H, $H11_B$); 2.81 (d, ^{2}J = 12.0 Hz, 1 H, $H13_A$); 2.69 (dd, ^{3}J = 2.5 Hz, ^{2}J = 12.0 Hz, 1 H, $H13_B$), 2.30 (s br, 1 H, H9); 1.92 (d, ^{2}J = 13.0 Hz, 1 H, $H8_A$); 1.84 (d, ^{2}J = 13.0 Hz, 1 H, $H8_B$)

^{13}C NMR (125 MHz, $CDCl_3$) δ [ppm] 163.1 (C=O); 147.5 (C6); 141.4 (C4); 138.5 (C1'); 129.8 (C2' + C6'); 128.6 (C3' + C5'); 127.4 (C4'); 119.3 (C5); 116.1 (C3); 53.0 (C13); 52.2 (C11); 50.4 (C10); 31.6 (C7); 27.4 (C9); 26.4 (C8)

MS (EI) m/z 266.2 (100), 223.1 (100), 210.1 (30), 185.1 (20), 167.1 (10), 149.1 (10), 133.1 (10), 82.1 (10)

HRMS for $C_{17}H_{18}N_2O$ calc. 266.1419
found 266.1416

IUPAC 11-phenyl-1,2,3,4,5,6-hexahydro-1,5-methano-pyridino[1,2-a]diazocin-8-one

6.4.11 5-(3'-Nitro-phenyl)-cytisine **104e**

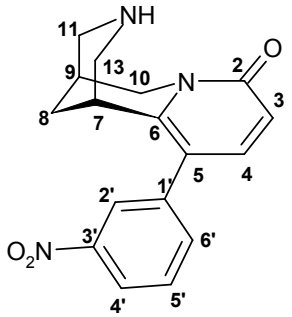

The Suzuki reaction was performed according to the general method with 5-bromo-N-*t*BOC-cytisine **82** (100 mg, 0.27 mmol), 3-nitrophenylboronic acid (68 mg, 0.41 mmol), Na_2CO_3 (64 mg, 0.6 mmol), $Pd(PPh_3)_4$ (30 mg, 0.027 mmol), DME and H_2O. The reaction time was 30 min. For the SPE purification, a mixture of MeOH/H_2O 70:30 v/v (100 mL) was used. The HPLC separation was completed with MeOH/H_2O 60:40 v/v. Deprotection by Method A. The final product obtained as yellow crystalline powder (52 mg, 0.17 mmol, 62%).

M.p.: 175.6 – 177.2 °C
HPLC: t_r = 16.7 min

^{1}H NMR (500 MHz, $CDCl_3$) δ [ppm] 8.19 – 8.21 (m, 1 H, H4'); 8.09 – 8.11 (m, 1 H, H2'); 7.55 – 7.60 (m, 2 H, H5' + H6'); 7.18 (d, ^{3}J = 9.3 Hz, 1 H, H4); 6.52 (d, ^{3}J = 9.3 Hz, 1 H, H3); 4.19 (d, ^{2}J = 15.5 Hz, 1 H, H10β); 3.96 (dd, ^{2}J = 6.6 Hz, ^{3}J = 15.5 Hz, 1 H, H10α); 3.10 (d, ^{2}J = 9.1 Hz, 1 H, $H11_A$); 2.93 (s br, 2 H, H7 + $H11_B$); 2.74 (d br, ^{2}J = 9.1 Hz, 2 H, H13); 2.35 (s br, 1 H, H9); 1.94 (s br, 1 H, $H8_A$); 1.87 (s br, 1 H, $H8_B$)

^{13}C NMR (125 MHz, $CDCl_3$) δ [ppm] 163.0 (C=O, C2); 148.4 (C3'); 148.1 (C6); 141.0 (C4); 140.0 (C1'); 135.5 (C6'); 129.2 (C5'); 124.2 (C2'); 121.9 (C4'); 117.2 (C5); 116.3 (C3); 52.9 (C13); 52.0 (C11); 50.5 (C10); 32.1 (C7); 27.7 (C9); 26.3 (C8)

MS (EI) m/z 311.2 (65), 268.1 (100), 255.1 (20), 230.1 (15), 183.1 (10), 167.1 (10), 149.1 (10), 82.1 (15), 68.1 (10)

HRMS for $C_{17}H_{17}N_3O_3$ calc. 311.1270
found 311.1269

IUPAC 11-(3-nitro-phenyl)-1,2,3,4,5,6-hexahydro-1,5-methano-pyridino[1,2-a]diazocin-8-one

6.4.12 5-(3'-Methyl-phenyl)-cytisine **105e**

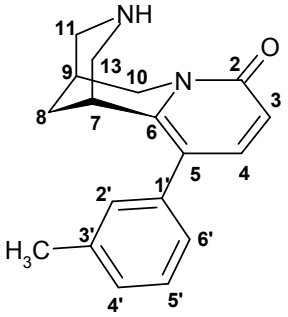

The Suzuki reaction was performed according to the general method with 5-bromo-N-*t*BOC-cytisine **82** (100 mg, 0.27 mmol), m-tolylboronic acid (55 mg, 0.41 mmol), Na_2CO_3 (64 mg, 0.6 mmol), $Pd(PPh_3)_4$ (30 mg, 0.027 mmol), DME and H_2O. The reaction time was 30 min. For the SPE purification, a mixture of MeOH/H_2O 70:30 v/v (100 mL) was used. The HPLC

separation was completed with MeOH/H_2O 65:35 v/v. Deprotection by Method A. The final product obtained as off-white crystalline powder (44 mg, 0.16 mmol, 58%).

M.p.: n.d.
HPLC: t_r = 16.17 min

^{1}H NMR (500 MHz, $CDCl_3$) δ [ppm] 7.25 (t, ^{3}J = 7.5 Hz, 1 H, H5'); 7.19 (d, ^{3}J = 9.2 Hz, 1 H, H4); 7.12 (d br, ^{3}J = 7.5 Hz, 1 H, H4'); 6.99 (d br, ^{3}J = 7.5 Hz, 1 H, H6'; s br, ovl., 1 H, H2'); 6.47 (d, ^{3}J = 9.2 Hz, 1 H, H3); 4.19 (d, ^{2}J = 15.5 Hz, 1 H, H10β); 3.93 (ddd, ^{4}J = 0.9 Hz, ^{3}J = 6.9 Hz, ^{2}J = 15.5 Hz, 1 H, H10α); 3.07 (s br, 1 H, H7); 3.04 (d, ^{2}J = 12.3 Hz, $H11_A$); 2.91 (d, ^{2}J = 12.3 Hz, 1 H, $H11_B$); 2.81 (d, ^{2}J = 12.3 Hz, 1 H, $H13_A$); 2.68 (dd, ^{3}J = 2.5 Hz, ^{2}J = 12.3 Hz, 1 H, $H13_B$); 2.35 (s, 3 H, CH_3); 2.29 (s br, 1 H, H9); 1.92 (d br, ^{2}J = 13.0 Hz, 1 H, $H8_A$); 1.83 (d br, ^{2}J = 13.0 Hz, 1 H, $H8_B$)

^{13}C NMR (125 MHz, $CDCl_3$) δ [ppm] 163.1 (C=O, C2); 147.4 (C6); 141.4 (C4); 138.4 (C1'); 138.3 (C3'); 130.4 (C2'); 128.4 (C5'); 128.1 (C4'); 126.8 (C6'); 119.5 (C5); 116.0 (C3); 53.0 (C13); 52.2 (C11); 50.4 (C10); 31.6 (C7); 27.4 (C9); 26.4 (C8); 21.4 ($\underline{C}H_3$)

MS (EI) m/z 280.2 (80), 237.1 (100), 224.1 (25), 199.1 (20), 82.1 (10), 44.0 (30)

HRMS for $C_{18}H_{20}N_2O$ calc. 280.1576
found 280.1577

IUPAC 11-m-tolyl-1,2,3,4,5,6-hexahydro-1,5-methano-pyridino[1,2-a]diazocin-8-one

6.4.13 5-(3'-Trifluoromethyl-phenyl)-cytisine **106e**

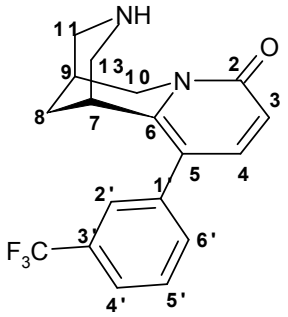

The Suzuki reaction was performed according to the general method with 5-bromo-N-*t*BOC-cytisine **82** (100 mg, 0.27 mmol), 3-trifluoromethylphenylboronic acid (77 mg, 0.41 mmol), Na_2CO_3 (64 mg, 0.6 mmol), $Pd(PPh_3)_4$ (30 mg, 0.027 mmol), DME and H_2O. The reaction

time was 30 min. For the SPE purification mixture of MeOH/H_2O 70:30 v/v (100 mL) was used. The HPLC separation was completed with MeOH/H_2O 65:35 v/v. Deprotection by Method A. The final product obtained as off-white crystalline powder (58 mg, 0.17 mmol, 64%).

M.p.: 155.2 – 157.0 °C
HPLC: t_r = 17.05 min

^{1}H NMR (500 MHz, $CDCl_3$) δ [ppm] 7.58 (d, ^3J = 7.9 Hz, 1 H, H6'); 7.50 (t, ^3J = 7.9 Hz, 1 H, H5'); 7.46 (s, 1 H, H2'); 7.39 (d, ^3J = 7.9 Hz, 1 H, H4'); 7.17 (d, ^3J = 9.2 Hz, 1 H, H4), 6.49 (d, ^3J = 9.2 Hz, 1 H, H3); 4.18 (d, ^2J = 15.7 Hz, 1 H, H10β); 3.94 (dd, ^3J = 6.0 Hz, ^2J = 15.7 Hz, 1 H, H10α); 3.06 (d, ^2J = 12.3 Hz, 1 H, $H11_A$); 2.93 (s br, 1 H, H7); 2.90 (d, ^2J = 12.3 Hz, 1 H, $H11_B$); 2.75 (d, ^2J = 12.3 Hz, 1 H, $H13_A$); 2.69 (dd, ^3J = 2.5 Hz, ^2J = 12.3 Hz, 1 H, $H13_B$); 2.31 (s br, 1 H, H9); 1.93 (d br, ^2J = 12.9 Hz, 1 H, $H8_A$), 1.82 (d br, ^2J = 12.9 Hz, 1 H, $H8_B$)

^{13}C NMR (125 MHz, $CDCl_3$) δ [ppm] 163.0 (C=O, C2); 148.0 (C6); 140.8 (C4); 139.3 (C1'); 133.2 (C6'); 130.9 (q, $^2J_{C,F}$ = 32.2 Hz, C3'); 129.2 (C5'); 126.5 (q, $^3J_{C,F}$ = 3.7 Hz, C2'); 124.9 (q, $^1J_{C,F}$ = 272.5 Hz, $\underline{C}F_3$), 124.3 (q, $^3J_{C,F}$ = 3.7 Hz; C4'); 117.6 (C5); 116.4 (C3); 53.0 (C13); 52.1 (C11); 50.5 (C10); 31.7 (C7); 27.3 (C9); 26.3 (C8)

MS (EI) m/z 334.2 (80), 291.1 (100), 253.1 (20), 196.1 (5), 183.1 (5), 167.1 (10), 149.1 (10), 97.1 (5), 82.1 (10)

HRMS for $C_{18}H_{17}F_3N_2O$ calc. 334.1293
found 334.1295

IUPAC 11-(3-trifluoromethyl-phenyl)-1,2,3,4,5,6-hexahydro-1,5-methano-pyridino[1,2-a]diazocin-8-one

6.4.14 5-(3'-Trifluoromethoxy-phenyl)-cytisine **107e**

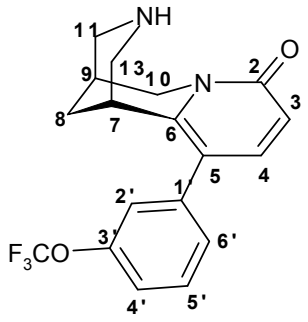

The Suzuki reaction was performed according to the general method with 5-bromo-*t*BOC-cytisine **82** (100 mg, 0.27 mmol), 3-trifluoromethoxyphenylboronic acid (62 mg, 0.41 mmol), K_3PO_4 (60 mg, 0.6 mmol), $Pd(PPh_3)_4$ (30 mg, 0.027 mmol), DME and H_2O. The reaction time was 60 min. For the SPE purification, a mixture of MeOH/H_2O 70:30 v/v (100 mL) was used. The HPLC separation was done with MeOH/H_2O 65:35 v/v. Deprotection by Method B. The final product obtained as off-white crystalline powder (26 mg, 0.07 mmol, 27%).

M.p.: n.d.
HPLC: t_r = 21.12 min

^{1}H NMR (500 MHz, $CDCl_3$) δ [ppm] 7.41 (t, ^3J = 8.0 Hz, 1 H, H5'); 7.20 (ddd, ^4J = 1.3 Hz, ^4J = 2.5 Hz, ^3J = 8.0 Hz, 1 H, H4'); 7.19 (d, ^3J = 9.2 Hz, 1 H, H4); 7.15 (dt, ^4J = 1.3 Hz, ^3J = 8.0 Hz, 1 H, H6'); 7.08 (d, ^4J = 2.5 Hz, 1 H, H2'); 6.50 (d, ^3J = 9.2 Hz, 1 H, H5); 4.26 (d, ^2J = 15.7 Hz, 1 H, H10β); 3.95 (dd, ^3J = 6.9 Hz, ^2J = 15.7 H, 1 H, H10α); 3.39 (d, ^2J = 12.3 Hz, 1 H, $H11_A$); 3.11 (s br, 1 H, H7); 3.07 (d, ^2J = 12.3 Hz, 1 H, $H11_B$); 2.92 (d, ^2J = 12.3 Hz, 1 H, $H13_A$); 2.82 (dd, ^3J = 2.5 Hz, ^2J = 12.3 Hz, 1 H, $H13_B$); 2.46 (s br, 1 H, H9); 1.91 (s br, 2 H, H8)

^{13}C NMR (125 MHz, $CDCl_3$) δ [ppm] 163.2 (C=O, C2), 149.3 (q, ^3J = 1.5 Hz, C3'), 148.3 (C6), 140.0 (C1'), 141.1 (C4), 130.2 (C5'), 128.2 (C6'), 122.3 (C4'), 120.0 (C2'), 119.4 (q, J = 257.6 Hz, $\underline{C}F_3$), 117.0 (C3), 116.4 (C5), 51.2 (C13), 50.4 (C11), 49.8 (C10), 30.5 (C7), 26.4 (C9), 25.5 (C8)

MS (EI) m/z 350.2 (60), 307.1 (100), 294.1 (25), 269.1 (20), 82.0 (30), 44.0 (50)

HRMS for $C_{18}H_{17}F_3N_2O_2$ calc. 350.1242
found 350.1252

IUPAC 11-(3-trifluoromethoxy-phenyl)-1,2,3,4,5,6-hexahydro-1,5-methano-pyridino[1,2-a]diazocin-8-one

6.4.15 5-(3'-Chloro-phenyl)-cytisine **108e**

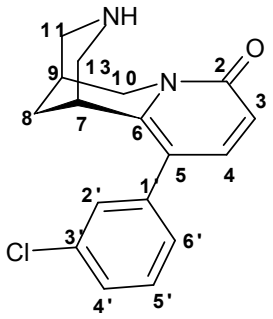

The Suzuki reaction was performed according to the general method with 5-bromo-N-*t*BOC-cytisine **82** (100 mg, 0.27 mmol), 3-chlorophenylboronic acid (63 mg, 0.41 mmol), K_3PO_4 (60 mg, 0.6 mmol), $Pd(PPh_3)_4$ (30 mg, 0.027 mmol), DME and H_2O. The reaction time was 60 min. For the SPE purification, a mixture of MeOH/H_2O 70:30 v/v (100 mL) was used. The HPLC separation was done with MeOH/H_2O 65:45 v/v. Additional flash chromatography on silica gel done with CH_2Cl_2/MeOH/EDMA 99:1:1 v/v/v and the purification was completed with HPLC (MeOH/H_2O 65:35 v/v for 25 min). Deprotection by Method B. The final product obtained as white crystalline powder (18 mg, 0.06 mmol, 22%).

M.p.: 80.6 – 81 °C
HPLC: 20.52 min

^{1}H NMR (500 MHz, $CDCl_3$) δ [ppm] 7.32 (m, ovl., 2 H, H2' + H4'); 7.21 (t, ^3J = 8.3 Hz, 1 H, H5'); 7.17 (d, ^3J = 9.2 Hz, 1 H, H4); 7.09 (dd, ^4J = 1.6 Hz; ^3J = 8.3 Hz, 1 H, H6'); 6.49 (d, ^3J = 9.2 Hz, 1 H, H3); 4.21 (d, ^2J = 15.6 Hz, 1 H, H10β); 3.95 (dd, ^3J = 6.1 Hz, ^2J = 15.6 Hz, 1 H, H10α); 3.17 (d, ^2J = 12.6 Hz, 1 H, $H11_A$); 3.04 (s br, 1 H, H7); 2.95 (d, ^2J = 12.6 Hz, 1 H, $H13_A$); 2.81 (dd, ^3J = 2.2 Hz, ^2J = 12.6 Hz, 1 H, $H13_B$); 2.73 (d, ^2J = 12.6 Hz, 1 H, $H11_B$); 2.34 (s br, 1 H, H9); 1.93 (s br, 2 H, H8)

^{13}C NMR (125 MHz, $CDCl_3$) not available due to the small amount of the sample

MS (EI) m/z 300.1 (100), 257.1 (95), 244.0 (30), 219.0 (40), 192.1 (5), 150.0 (10), 82.1 (10), 68.1 (5)

HRMS for $C_{17}H_{17}ClN_2O$ calc. 300.1029
found 300.1025

IUPAC 11-(3-chloro-phenyl)-1,2,3,4,5,6-hexahydro-1,5-methano-pyridino[1,2-a]diazocin-8-one

6.4.16 5-(3'-Fluoro-phenyl)-cytisine **109e**

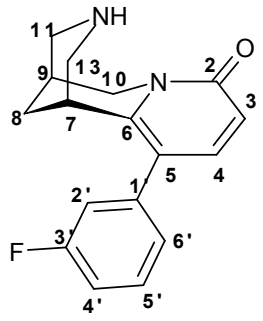

The Suzuki reaction was performed according to the general method with 5-bromo-N-*t*BOC-cytisine **82** (100 mg, 0.27 mmol), 3-fluorophenylboronic acid (56 mg, 0.41 mmol), Na_2CO_3 (64 mg, 0.6 mmol), $Pd(PPh_3)_4$ (30 mg, 0.027 mmol), DME and H_2O. The reaction time was 30 min. For the SPE purification, a mixture of MeOH/H_2O 70:30 v/v (100 mL) was used. HPLC separation was completed with MeOH/H_2O 65:35 v/v. Deprotection by Method A. The final product obtained as off-white crystalline powder (62 mg, 0.22 mmol, 81%).

M.p.: n.d.
HPLC: t_r = 12.32 min

^{1}H NMR (500 MHz, $CDCl_3$) δ [ppm] 7.32 (td, ^4J = 6.0 Hz, ^3J = 7.9 Hz, 1 H, H5'); 7.16 (d, ^3J = 9.2 Hz, 1 H, H4); 7.01 (tdd, ^4J = 0.9 Hz, ^4J = 2.5 Hz, ^3J = 8.5 Hz, 1 H, H4'); 6.96 (dt, ^4J = 1.4 Hz, ^3J = 7.9 Hz, 1 H, H6'); 6.90 (dt, ^4J = 1.4 Hz, ^3J = 7.9 Hz, 1 H, H2'); 6.47 (d, ^3J = 9.2 Hz, 1 H, H3); 4.17 (d, ^2J = 15.7 Hz, 1 H, H10β); 3.92 (dd, ^3J = 6.8 Hz, ^2J = 15.7 Hz, 1 H, H10α); 3.03 (d, ^2J = 11.3 Hz, 1 H, $H11_A$); 3.07 (s br, 1 H, H7), 2.93 (s br, 1 H, $H11_B$); 2.79 (d br, ^2J = 11.0 Hz, 1 H, $H13_B$); 2.71 (d br, ^2J = 11.0 Hz, 1 H, $H13_B$); 2.31 (s br, 1 H, H9); 1.91 (s br, 2 H, $H8_A$ + NH); 1.84 (d br, ^2J = 12.6 Hz, 1 H, $H8_B$)

^{13}C NMR (125 MHz, $CDCl_3$) δ [ppm] 163.6 ($^1J_{C,F}$ = 247.6 Hz; C3'); 163.0 (C=O, C2); 147.6 (C6); 140.9 (C4); 140.6 ($^3J_{C,F}$ = 7.7 Hz, C1'); 130.1 ($^3J_{C,F}$ = 8.5 Hz, C5'); 125.6 ($^4J_{C,F}$ = 2.8 Hz,

C6'); 118.0 ($^4J_{C,F}$ = 1.7 Hz, C5); 116.8 ($^2J_{C,F}$ = 21.0 Hz, C2'); 116.2 (C3), 114.4 ($^2J_{C,F}$ = 21.0 Hz, C4'); 52.8 (C13); 52.1 (C11); 50.4 (C10), 31.6 (C7); 27.3 (C9); 26.2 (C8)

MS (EI) m/z 284.1 (95), 241.0 (100), 228.0 (30), 203.0 (20), 149.0 (20), 133.0 (15), 82.1 (10), 57.1 (10)

HRMS for $C_{17}H_{17}FN_2O$ calc. 284.1325
found 284.1334

IUPAC 11-(3-fluoro-phenyl)-1,2,3,4,5,6-hexahydro-1,5-methano-pyridino[1,2-a]diazocin-8-one

6.4.17 5-(Biphenyl-3'-yl)-cytisine **110e**

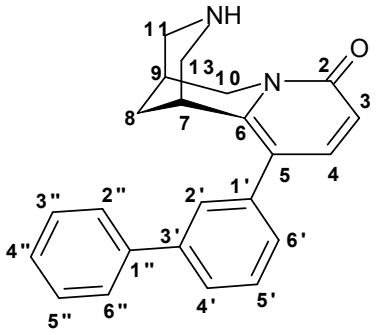

The Suzuki reaction was performed according to the general method with 5-bromo-N-*t*BOC-cytisine **82** (100 mg, 0.27 mmol), 3-biphenylboronic acid (80 mg, 0.41 mmol), Na_2CO_3 (64 mg, 0.6 mmol), $Pd(PPh_3)_4$ (30 mg, 0.027 mmol), DME and H_2O. The reaction time was 30 min. For the SPE purification, a mixture of MeOH/H_2O 80:20 v/v (100 mL) was used. The HPLC separation was done with MeOH/H_2O 65:35 v/v for 15 min, subsequently a gradient to the final mixture of MeOH/H_2O 80:20 v/v was run for 15 min. Deprotection by Method A. The final product obtained as off-white crystalline powder (58 mg, 0.17 mmol, 62%).

M.p.: 168.5 – 169.8 °C
HPLC: t_r = 27.65 min

^{1}H NMR (500 MHz, $CDCl_3$) δ [ppm] 7.55 – 7.58 (m, 3 H, H2'+H2''+H6''); 7.41 – 7.46 (m, 4 H, H3''+H5''+H5'+H6'); 7.35 (tt, ^4J = 1.6 Hz, ^3J = 7.6 Hz, 1 H, H4''); 7.26 (d, ^3J = 9.1 Hz, 1 H, H4); 7.17 (dt, ^4J = 1.6 Hz, ^3J = 7.6 Hz, 1 H, H4'); 6.51 (d, ^3J = 9.1 Hz, 1 H, H3); 4.22 (d, ^2J = 15.4 Hz, 1 H, H10$_\beta$); 3.96 (dd, ^3J = 6.6 Hz, ^2J = 15.4 Hz, 1 H, H10α); 3.09 (s, 1 H, H7); 3.07

(d, ^2J = 12.3 Hz, 1 H, $H11_A$); 2.91 (d, ^2J = 12.3 Hz, 1 H, $H11_B$); 2.85 (d, ^2J = 12.3 Hz, 1 H, $H13_A$); 2.72 (dd, ^3J = 2.5 Hz, ^2J = 12.3 Hz, 1 H, $H13_B$), 2.30 (s, 1 H, H9); 1.94 (d br, ^2J = 12.9 Hz, 1 H, $H8_A$); 1.84 (d br, ^2J = 12.9 Hz, 1 H, $H8_B$); 1.23 (br s, 1 H, NH)

^{13}C NMR (125 MHz, $CDCl_3$) δ [ppm] 163.1 (C=O); 147.7 (C6); 141.6 (C1''); 141.3 (C4); 140.6 (C3'); 139.0 (C1'); 129.1*; 128.6*; 128.9*; 128.6*; 128.5*; 127.1*; 127.6*; 126.1*; 119.1 (C5); 116.1 (C3); 53.0 (C13); 52.3 (C11); 50.5 (C10); 31.4 (C7); 27.4 (C9); 26.4 (C8)

MS (EI) m/z 342.2 (100), 299.2 (90), 262.1 (50), 201.20 (20), 183.1 (30), 170.1 (20), 149.0 (20)

HRMS for $C_{23}H_{22}N_2O$ calc. 342.1732
found 342.1734

IUPAC 11-biphenyl-3-yl-1,2,3,4,5,6-hexahydro-1,5-methano-pyridino[1,2-a]diazocin-8-one

6.4.18 3-(1*H*-Indol-5'-yl)-cytisine **117e**

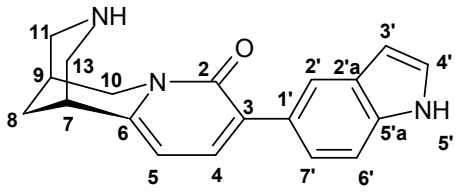

The Suzuki reaction was performed according to the general method with 3-bromo-N-*t*BOC-cytisine **81** (100 mg, 0.27 mmol), 5-indolylboronic acid (65 mg, 0.41 mmol), Na_2CO_3 (64 mg, 0.6 mmol), $Pd(PPh_3)_4$ (30 mg, 0.027 mmol), DME and H_2O. The reaction time was 30 min. For the SPE purification, a mixture of MeOH/H_2O 60:40 v/v (100 mL) was used. The HPLC separation was completed with MeOH/H_2O 60:40 v/v. Deprotection by Method B. The final product obtained as yellowish crystalline powder (31 mg, 0.1 mmol, 37%).

M.p.: 139.0 – 141.1 °C
HPLC: t_r = 16.12 min

* the assignment of the biphenyl moiety could not be completed

^{1}H NMR (500 MHz, $CDCl_3$) δ [ppm] 8.28 (s br, 1 H, indolic NH); 7.92 (s br, 1 H, H2'); 7.52 (dd, ^{4}J = 1.6 Hz, ^{3}J = 8.5 Hz, 1 H, H7'); 7.47 (d, ^{3}J = 7.0 Hz, 1 H, H4); 7.38 (d, ^{3}J = 8.5 Hz, 1 H, H6'); 7.16 (pseudo t, ^{3}J = 2.8 Hz, 1 H, H4'); 6.54 (tt, ^{4}J = 0.9 Hz, ^{3}J = 2.2 Hz, 1 H, H3'); 6.06 (d, ^{3}J = 7.0 Hz, 1 H, H5); 4.22 (d, ^{2}J = 15.6 Hz, 1 H, H10β); 3.96 (dd, ^{3}J = 6.3 Hz, ^{2}J = 15.6 Hz, 1 H, H10α); 3.12 (d, ^{2}J = 12.6 Hz, 1 H, $H11_A$); 3.00 – 3.06 (m, 3 H, $H11_B$ + H13); 2.89 (s br, 1 H, H7); 2.34 (s br, 1 H, H9); 1.96 (s br, 2 H, H8)

^{13}C NMR (125 MHz, $CDCl_3$) δ [ppm] 162.6 (C=O); 148.9 (C6); 136.7 (C4); 135.3 (C5a); 129.1 (C1'); 128.9 (C3); 127.8 (C2a); 124.3 (C4'); 123.2 (C7'); 120.9 (C2'); 110.5 (C6'); 105.1 (C5); 103.0 (C3'); 53.8 (C13); 52.9 (C11); 50.1 (C10); 35.6 (C7); 27.9 (C9); 26.4 (C8)

MS (EI) m/z 305.2 (100), 261.1 (70), 249.2 (20), 233.2 (20), 44.0 (10)

HRMS for $C_{19}H_{19}N_3O$ calc. 305.1528
found 305.1531

IUPAC 9-(1*H*-Indol-5-yl)-1,2,3,4,5,6-hexahydro-1,5-methano-pyridino[1,2-a]diazocin-8-one

6.4.19 3-(3',4'-Methylenedioxy-phenyl)-cytisine **118e**

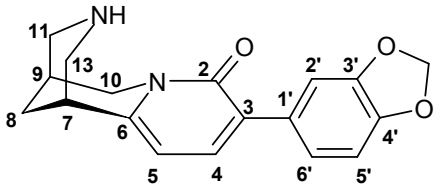

The Suzuki reaction was performed according to the general method with 3-bromo-N-*t*BOC-cytisine **81** (100 mg, 0.27 mmol), 3,4-methylenedioxyphenylboronic acid (68 mg, 0.41 mmol), Na_2CO_3 (64 mg, 0.6 mmol), $Pd(PPh_3)_4$ (30 mg, 0.027 mmol), DME and H_2O. The reaction time was 30 min. For the SPE purification, a mixture of MeOH/H_2O 70:30 v/v (100 mL) was used. The HPLC separation was completed with MeOH/H_2O 60:40 v/v. Deprotection by Method B. The final product obtained as off-white crystalline powder (30 mg, 0.1 mmol, 36%).

M.p.: 259.1 – 261.6 °C
HPLC: t_r = 18.99 min

^{1}H NMR (500 MHz, $CDCl_3$) δ [ppm] 7.38 (d, ^3J = 7.3 Hz, 1 H, H4); 7.26 (d, ^4J = 1.6 Hz, 1 H, H2'); 7.12 (dd, ^4J = 1.6 Hz, ^3J = 8.2, 1 H, H6'); 6.81 (d, ^3J = 8.2 Hz, 1 H, H5'); 6.05 (d, ^3J = 7.3 Hz, 1 H, H5); 5.94 (s, 2 H, CH_2); 4.16 (d, ^2J = 15.7 Hz, 1 H, H10β); 3.93 (dd, ^3J = 6.6 Hz, ^2J = 15.7 Hz, 1 H, H10α); 3.11 (d, ^2J = 12.0 Hz, 1 H, $H11_A$); 3.06 (dd, ^3J = 2.2 Hz, ^2J = 12.0 Hz, 1 H, $H13_A$); 3.00 (d br; ^2J = 12.0 Hz, 2 H, $H11_B$ + $H13_B$); 2.90 (s br, 1 H, H7); 2.34 (s br, 1 H, H9); 1.95 (s br, 2 H, H8)

^{13}C NMR (125 MHz, $CDCl_3$) δ [ppm] 162.1 (C=O, C2); 149.9 (C6); 147.3 (C3'); 146.8 (C4'); 136.4 (C4); 131.4 (C1'); 127.1 (C3); 122.1 (C6'); 109.4 (C2'); 108.0 (C5'); 104.9 (C5); 100.9 ($\underline{C}H_2$); 54.0 (C13); 53.0 (C11); 50.2 (C10); 35.7 (C7); 27.9 (C9); 26.4 (C8)

MS (EI) m/z 310.1 (100), 267.0 (70), 254.0 (20), 229.0 (25), 180.0 (5), 155.0 (10), 140.0 (10)

HRMS for $C_{18}H_{18}N_2O_3$ calc. 310.1317
found 310.1324

IUPAC 9-(benzo[1,3]dioxol-5-yl)-1,2,3,4,5,6-hexahydro-1,5-methano-pyridino[1,2-a]diazocin-8-one

6.4.20 3-(Pyridin-3'-yl)-cytisine **119e**

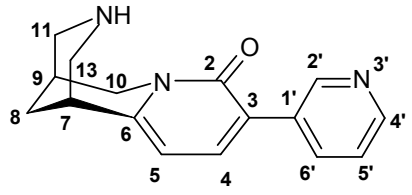

The Suzuki reaction was performed according to the general method with 3-bromo-N-*t*BOC-cytisine **81** (100 mg, 0.27 mmol), 3-pyridineboronic acid (49 mg, 0.41 mmol), K_3PO_4 (126 mg, 0.6 mmol), $Pd(PPh_3)_4$ (30 mg, 0.027 mmol), DME and H_2O. The reaction time was 60 min. For the SPE purification, a mixture of MeOH/H_2O 60:40 v/v (100 mL) was used. The HPLC separation was completed with MeOH/H_2O 50:50 v/v. Deprotection by Method B. The final product obtained as yellow crystalline powder (48 mg, 0.18 mmol, 66%).

M.p.: 79.8 – 81.6 °C
HPLC: t_r = 16.05 min

^{1}H NMR (500 MHz, $CDCl_3$) δ [ppm] 8.78 (d, ^4J = 1.6 Hz, 1 H, H2'); 8.49 (dd, ^4J = 1.6 Hz, ^3J = 4.7 Hz, 1 H, H4'); 8.16 (ddd, ^4J = 1.6 Hz, ^4J = 2.2 Hz, ^3J = 7.9 Hz, 1 H, H6'); 7.49 (d, ^3J = 7.3 Hz, 1 H, H4); 7.29 (ddd, ^5J = 0.9 Hz, ^3J = 4.7 Hz, ^3J = 7.9 Hz, 1 H, H5'); 6.11 (d, ^3J = 7.3 Hz, 1 H, H5); 4.16 (d, ^2J = 15.6 Hz, 1 H, H10β); 3.94 (dd, ^3J = 6.9 Hz, ^2J = 15.6 Hz, 1 H, H10α); 3.11 (d, ^2J = 12.0 Hz, 1 H, $H11_A$); 3.06 (dd, ^3J = 2.2 Hz, ^2J = 12.0 Hz, 1 H, $H13_A$); 2.99 – 3.03 (m, 2 H, H 11_B + $H13_B$); 2.95 (s br, 1 H, H7); 2.36 (s br, 1 H, H9); 1.96 (s br, 2 H, H8)

^{13}C NMR (125 MHz, $CDCl_3$) δ [ppm] 161.9 (C=O, C2); 151.5 (C6); 149.1 (C2'); 148.2 (C4'); 137.2 (C4); 136.1 (C6'); 133.2 (C1'); 123.9 (C3); 122.8 (C5'); 105.0 (C5); 53.9 (C13); 53.0 (C11); 50.3 (C10); 35.7 (C7); 27.8 (C9); 26.2 (C8)

MS (EI) m/z 267.1 (100), 223.1 (100), 211.1 (20), 186.1 (25), 82.1 (5)

HRMS for $C_{16}H_{17}N_3O$ calc. 267.1371
found 267.1376

IUPAC 9-pyridin-3-yl -1,2,3,4,5,6-hexahydro-1,5-methano-pyridino[1,2-a]diazocin-8-one

6.4.21 3-(Pyridin-4'-yl)-cytisine **120e**

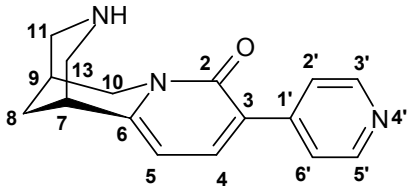

The Suzuki reaction was performed according to the general method with 3-bromo-N-*t*BOC-cytisine **81** (100 mg, 0.27 mmol), 4-pyridineboronic acid (49 mg, 0.41 mmol), K_3PO_4 (126 mg, 0.6 mmol), $Pd(PPh_3)_4$ (30 mg, 0.027 mmol), DME and H_2O. The reaction time was 90 min. For the SPE purification, a mixture of MeOH/H_2O 60:40 v/v (100 mL) was used. The HPLC separation was completed with MeOH/H_2O 50:50 v/v. Deprotection by Method B. The final product obtained as yellow crystalline powder (45 mg, 0.17 mmol, 62%).

M.p.: n.d.
HPLC: t_r = 17.8 min

^{1}H NMR (500 MHz, $CDCl_3$) δ [ppm] 8.57 (dd, ^4J = 1.6 Hz, ^3J = 6.1 Hz, 2 H, H3' + H5'); 7.67 (dd, ^4J = 1.6 Hz, ^3J = 6.1 Hz, 2 H, H2' + H6'); 7.57 (d, ^3J = 7.4, 1 H, H4); 6.13 (d, ^3J = 7.4 Hz, 1 H, H5); 4.16 (d, ^2J = 15.8 Hz, 1 H, H10β); 3.95 (dd, ^3J = 6.6 Hz, ^2J = 15.8 Hz, 1 H, H10α); 3.11 (dd, ^3J = 2.5 Hz, ^2J = 12.3 Hz, 1 H, $H11_A$); 3.07 (dd, ^3J = 2.5 Hz, ^2J = 12.3 Hz, 1 H, $H13_A$); 3.04 (d, ^2J = 12.3 Hz, 1 H, $H13_B$); 3.00 (ddd, ^4J = 1.2 Hz, ^3J = 2.5 Hz, ^2J = 12.3 Hz, 1 H, $H11_B$); 2.94 (s br, 1 H, H7), 2.36 (s br, 1 H, H9), 1.96 (s br, 2 H, H8)

^{13}C NMR (125 MHz, $CDCl_3$) δ [ppm] 161.5 (C=O, C2); 152.6 (C6); 149.6 (C3' + C5'); 144.9 (C1'); 137.8 (C4); 123.9 (C2' + C6'); 122.8 (C3); 104.9 (C5); 53.9 (C13), 53.0 (C11), 50.3 (C10), 35.8 (C7), 27.8 (C9), 26.2 (C8)

MS (EI) m/z 267.1 (100), 223.1 (100), 211.1 (25), 186.1 (40), 149.1 (10), 133.6 (10), 117.1 (10), 82.1 (10)

HRMS for $C_{16}H_{17}N_3O$ calc. 267.1371
found 267.1379

IUPAC 9-pyridin-4-yl-1,2,3,4,5,6-hexahydro-1,5-methano-pyridino[1,2-a]diazocin-8-one

6.4.22 3-Quinolin-8'-yl-cytisine **121e**

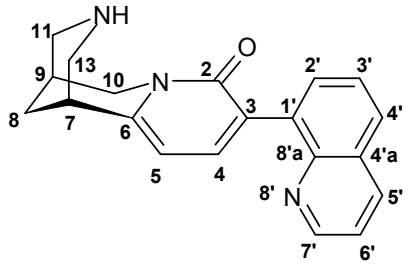

The Suzuki reaction was performed according to the general method with 3-bromo-N-*t*BOC-cytisine **81** (50 mg, 0.13 mmol), 8-quinolineboronic acid (35 mg, 0.2 mmol), K_3PO_4 (60 mg, 0.3 mmol), $Pd(PPh_3)_4$ (15 mg, 0.013 mmol), DME and H_2O. The reaction time was 30 min. For the SPE purification, a mixture of MeOH/H_2O 70:30 v/v (100 mL) was used. The HPLC separation was completed with MeOH/H_2O 60:40 v/v. Deprotection by Method B. The final product obtained as off-white crystalline powder (37 mg, 0.12 mmol, 44%).

M.p.: 207.1 – 209.7 °C
HPLC: t_r = 18.43 min

^{1}H NMR (500 MHz, $CDCl_3$) δ [ppm] 8.86 (dd, ^4J = 1.9 Hz, ^3J = 4.1 Hz, 1 H, H7'); 8.15 (dd, ^4J = 1.9 Hz, ^3J = 8.2 Hz, 1 H, H5'); 7.85 (dd, ^4J = 1.3 Hz, ^3J = 7.3 Hz, 1 H, H2'); 7.78 (dd, ^4J = 1.3 Hz, ^3J = 7.3 Hz, 1 H, H4'); 7.58 (d, ^3J = 7.3 Hz, 1 H, H4); 7.56 (t, ^3J = 7.3 Hz, 1 H, H3'); 7.35 (dd, ^3J = 4.1 Hz, ^3J = 8.2 Hz, 1 H, H6'); 6.16 (d, ^3J = 7.3 Hz, 1 H, H5); 4.21 (d, ^2J = 15.7 Hz, 1 H, H10β); 3.96 (dd, ^3J = 6.3 Hz, ^2J = 15.7 Hz, 1 H, H10α); 3.13 (d, ^2J = 12.3 Hz, 1 H, $H13_A$); 3.08 (s br, 2 H, H11); 3.02 (d, ^2J = 12.3 Hz, 1 H, $H13_B$); 2.95 (s br, 1 H, H7); 2.33 (s br, 1 H, H9), 1.96 (t, ^2J = 13.2 Hz, 2 H, H8), 1.83 (br s, NH)

^{13}C NMR (125 MHz, $CDCl_3$) δ [ppm] 162.5 (C=O, C2); 150.4 (C6); 149.9 (C7'); 146.5 (C8'a); 139.8 (C4); 139.6 (C1'); 136.5 (C3); 136.4 (C5'); 131.0 (C2'); 128.6 (C4'a); 127.7 (C4'); 126.2 (C3'); 120.8 (C6'); 104.8 (C5); 53.9 (C13); 53.0 (C11); 50.1 (C10); 35.8 (C7); 27.9 (C9); 26.4 (C8)

MS (EI) m/z 317.2 (100), 273.1 (50), 261.1 (40), 245.1 (20), 231.1 (10), 167.1 (15)

HRMS for $C_{20}H_{19}N_3O$ calc. 317.1528
found 317.1532

IUPAC 9-quinolin-8-yl-1,2,3,4,5,6-hexahydro-1,5-methano-pyridino[1,2-a]diazocin-8-one

6.4.23 3-(1-Methyl-1*H*-pyrazol-4'-yl)-cytisine **122e**

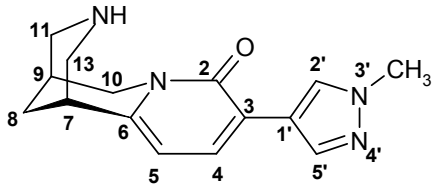

The Suzuki reaction was performed according to the general method with 3-bromo-N-*t*BOC-cytisine **81** (100 mg, 0.27 mmol), 1-methyl-4-(4,4,5,5-tetramethyl-1,3,2-dioxaborolan-2-yl)-1*H*-pyrazole (84 mg, 0.41 mmol), K_3PO_4 (126 mg, 0.6 mmol), $Pd(PPh_3)_4$ (30 mg, 0.027 mmol), DME and H_2O. The reaction time was 30 min. For the SPE purification, a mixture of MeOH/H_2O 60:40 v/v (100 mL) was used. The HPLC separation was completed with

MeOH/H_2O 50:50 v/v. Deprotection by Method B. The final product obtained as yellow crystalline powder (51 mg, 0.19 mmol, 70%).

M.p.: 113.4 °C
HPLC: t_r = 15.32 min

^{1}H NMR (500 MHz, $CDCl_3$) δ [ppm] 8.29 (s, 1 H, H5'); 7.80 (s, 1 H, H2'); 7.56 (d, ^3J = 7.3 Hz, 1 H, H4); 6.05 (d, ^3J = 7.3 Hz, 1 H, H5); 4.18 (d, ^2J = 15.7 Hz, 1 H, H10β); 3.94 (dd, ^3J = 6.6 Hz, ^2J = 15.7 Hz, 1 H, H10α); 3.90 (s, 3 H, C$\underline{H}_3$); 3.09 (d, ^2J = 12.0 Hz, 1 H, $H11_A$); 3.03 (dd, ^3J = 2.2 Hz, ^2J = 12.0 Hz, 1 H, $H13_A$); 2.99 (d, ^2J = 12.0 Hz, 1 H, $H13_B$); 2.96 (d, ^2J = 12.0 Hz, 1 H, $H11_B$); 2.90 (s br, 1 H, H7), 2.33 (s br, 1 H, H9), 1.94 (s br, 2 H, H8)

^{13}C NMR (125 MHz, $CDCl_3$) δ [ppm] 161.2 (C=O, C2); 148.0 (C6); 136.8 (C2'); 132.4 (C4); 129.9 (C5'); 119.8 (C3); 117.8 (C1'); 105.1 (C5); 53.9 (C13); 52.9 (C11); 50.1 (C10); 38.9 ($\underline{C}H_3$); 35.5 (C7); 27.9 (C9); 26.4 (C8)

MS (EI) m/z 270.1 (100), 227.1 (60), 214.1 (10), 189.1 (20), 135.1 (5), 82.1 (5)

HRMS for $C_{15}H_{18}N_4O$ calc. 270.1481
found 270.1480

IUPAC 9-(1-Methyl-1*H*-pyrazol-4-yl)-1,2,3,4,5,6-hexahydro-1,5-methano-pyridino[1,2-a]diazocin-8-one

6.4.24 5-(1*H*-Indol-5'-yl)-cytisine **123e**

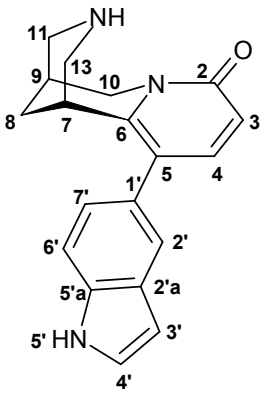

The Suzuki reaction was performed according to the general method with 5-bromo-N-*t*BOC-cytisine **82** (100 mg, 0.27 mmol), 5-indolylboronic acid (65 mg, 0.41 mmol), Na_2CO_3 (64 mg, 0.6 mmol), $Pd(PPh_3)_4$ (30 mg, 0.027 mmol), DME and H_2O. The reaction time was 30 min. For the SPE purification, a mixture of MeOH/H_2O 70:30 v/v (100 mL) was used. The HPLC separation was completed with MeOH/H_2O 60:40 v/v. Deprotection by Method B. The final product obtained as yellowish crystalline powder (21 mg, 0.07 mmol, 26%).

M.p.: 176.5 – 177.5 °C
HPLC: t_r = 15.55 min

^{1}H NMR (500 MHz, $CDCl_3$) δ [ppm] 8.53 (s br, 1 H, 5'-NH); 7.44 (t, ^4J = 0.9 Hz, 1 H, H2'); 7.39 (dt, ^4J = 0.9 Hz, ^3J = 7.0 Hz, 1 H, H7'); 7.28 (d, ^3J = 9.1 Hz, 1 H, H4); 7.26 (t, ^3J = 2.8 Hz, 1 H, H4'); 6.98 (dd, ^3J = 1.6 Hz, ^3J = 7.0 Hz, 1 H, H6'); 6.53 (tt, ^4J = 0.9 Hz, ^3J = 2.8 Hz, 1 H, H3'); 6.49 (d, ^3J = 9.1 Hz, 1 H, H3); 4.23 (d, ^2J = 15.7 Hz, 1 H, H10β); 3.97 (dd, ^3J = 6.9 Hz, ^2J = 15.7 Hz, 1 H, H10α); 3.14 (s br, 1 H, H7); 3.08 (d, ^2J = 12.3 Hz, 1 H, $H11_A$); 2.93 (d, ^2J = 12.3 Hz, 1 H, $H11_B$); 2.87 (d, ^2J = 12.3 Hz, 1 H, $H13_A$); 2.64 (dd, ^3J = 2.5 Hz, ^2J = 12.3 Hz, 1 H, $H13_B$); 2.30 (s br, 1 H, H9); 1.93 (d br, ^2J = 12.7 Hz, 1 H, $H8_A$); 1.81 (d br, ^2J = 12.7 Hz, 1 H, $H8_B$)

^{13}C NMR (125 MHz, $CDCl_3$) δ [ppm] 163.2 (C=O, C2); 147.6 (C6); 142.2 (C4); 135.0 (C5'a); 129.8 (C1'); 128.0 (C2'a); 125.1 (C4'); 123.9 (C7'); 121.7 (C2'); 120.5 (C5); 115.7 (C3); 111.1 (C6'); 102.6 (C3'); 52.9 (C13); 52.2 (C11); 50.4 (C10); 31.6 (C7); 27.4 (C9); 26.4 (C8)

MS (EI) m/z 305.1 (100), 262.1 (70), 249.1 (25), 235.0 (20), 221.0 (15), 206.1 (10), 154.1 (10)

HRMS for $C_{19}H_{19}N_3O$ calc. 305.1528
found 305.1533

IUPAC 11-(1H-indol-5-yl)-1,2,3,4,5,6-hexahydro-1,5-methano-pyridino[1,2-a]diazocin-8-one

6.4.25 5-(3',4'-Methylenedioxy-phenyl)-cytisine **124e**

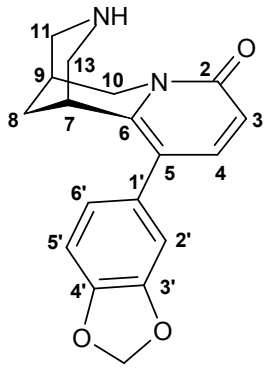

The Suzuki reaction performed according to the general method with 5-bromo-N-*t*BOC-cytisine **82** (100 mg, 0.27 mmol), 3,4-methylenedioxyphenylboronic acid (68 mg, 0.41 mmol), $Ba(OH)_2*8H_2O$ (185 mg, 0.6 mmol), $Pd(PPh_3)_4$ (30 mg, 0.027 mmol), DME and H_2O. The reaction time was 60 min. For the SPE purification, a mixture of MeOH/H_2O 70:30 v/v (100 mL) was used. The HPLC separation was completed with MeOH/H_2O 60:40 v/v. Deprotection by Method B. The final product obtained as off-white crystalline powder (21 mg, 0.07 mmol, 25%).

M.p.: 94.5 – 96.5 °C
HPLC: t_r = 18.68 min

^{1}H NMR (500 MHz, $CDCl_3$) δ [ppm] 7.17 (d, ^3J = 9.3 Hz, 1 H, H4); 6.80 (d, ^3J = 7.9 Hz, 1 H, H5'); 6.65 (d, ^4J = 1.8 Hz, 1 H, H2'); 6.63 (dd, ^4J = 1.8 Hz, ^3J = 7.9 Hz, 1 H, H6'); 6.45 (d, ^3J = 9.3 Hz, 1 H, H3); 5.97 (s, 2 H, CH_2); 4.18 (d, ^2J = 15.7 Hz, 1 H, H10β); 3.93 (dd, ^3J = 6.6 Hz, ^2J = 15.7 Hz, 1 H, H10α); 3.08 (d, ^2J = 12.0 Hz, 1 H, $H11_A$; s br, ovl., 1 H, H7); 2.92 (d, ^2J = 12.0 Hz, 1 H, $H11_B$); 2.82 (d, ^2J = 12.0 Hz, 1 H, $H13_A$); 2.72 (dd, ^3J = 2.2 Hz, ^2J = 12.0 Hz, 1 H, $H13_B$); 2.30 (s br, 1 H, H9); 1.95 (d br, ^2J = 12.9 Hz, 1 H, $H8_A$); 1.84 (d br, ^2J = 12.9 Hz, 1 H, $H8_B$)

^{13}C NMR (125 MHz, $CDCl_3$) δ [ppm] 163.1 (C=O, C2); 147.8 (C6); 147.7 (C3'); 146.9 (C4'); 141.5 (C4); 132.0 (C1'); 123.1 (C6'); 118.8 (C5); 116.0 (C3); 110.2 (C2'); 108.4 (C5'); 101.2 ($\underline{C}H_2$), 52.9 (C13); 52.1 (C11); 50.4 (C10); 31.6 (C7); 27.4 (C9); 26.4 (C8)

MS (EI) m/z 310.1 (100), 267.0 (70), 254.0 (20), 229.0 (25), 155.0 (10), 82.0 (10)

HRMS for $C_{18}H_{18}N_2O_3$ calc. 310.1317
found 310.1318

IUPAC 11-(benzo[1,3]dioxol-5-yl)-1,2,3,4,5,6-hexahydro-1,5-methano-pyridino[1,2-a]diazocin-8-one

6.4.26 5-(Pyridin-3'-yl)-cytisine **125e**

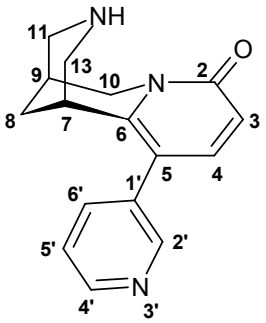

The Suzuki reaction was performed according to the general method with 5-bromo-N-*t*BOC-cytisine **82** (100 mg, 0.27 mmol), 3-pyridineboronic acid (49 mg, 0.41 mmol), $Ba(OH)_2$*$8H_2O$ (185 mg, 0.6 mmol), $Pd(PPh_3)_4$ (30 mg, 0.027 mmol), DMF and H_2O. The reaction time was 90 min. For the SPE purification, a mixture of MeOH/H_2O 60:40 v/v (100 mL) was used. The HPLC separation was competed with MeOH/H_2O 50:50 v/v. Deprotection by Method B. The final product obtained as yellow crystalline powder (23 mg, 0.09 mmol, 32%).

M.p.: 70.4 – 72.0 °C
HPLC: t_r = 14.52 min

^{1}H NMR (500 MHz, $CDCl_3$) δ [ppm] 8.58 (dd, ^4J = 1.6 Hz, ^3J = 5.0 Hz, 1 H, H4'); 8.49 (d, ^4J = 1.9 Hz, 1 H, H2'); 7.55 (dt, ^4J = 1.9 Hz, ^3J = 7.9 Hz, 1 H, H6'); 7.33 (ddd, ^5J = 0.6 Hz, ^3J = 5.0 Hz, ^3J = 7.9 Hz, 1 H, H5'); 7.18 (d, ^3J = 9.2 Hz, 1 H, H4); 6.52 (d, ^3J = 9.2 Hz, 1 H, H3); 4.21 (d, ^2J = 15.6 Hz, 1 H, H10β); 3.95 (dd, ^3J = 6.6 Hz, ^2J = 15.6 Hz, 1 H, H10α); 3.14 (d, ^2J = 12.0 Hz, 1 H, $H11_A$); 2.97 (s br, 1 H, H7); 2.93 (d, ^2J = 12.0 Hz, 1 H, $H11_B$); 2.79 (d, ^2J =

12.0 Hz, 1 H, H13$_A$); 2.71 (dd, ^{3}J = 2.5 Hz, ^{2}J = 12.0 Hz, 1 H, H13$_B$); 2.35 (s br, 1 H, H9), 1.94 (d, ^{2}J = 13.0 Hz, 1 H, H8$_A$), 1.86 (d, ^{2}J = 13.0 Hz, 1 H, H8$_B$)

^{13}C NMR (125 MHz, CDCl$_3$) δ [ppm] 163.0 (C=O, C2); 150.5 (C6); 148.8 (C2'); 148.1 (C6); 141.0 (C4); 137.2 (C6'); 134.3 (C1'); 123.5 (C5'); 116.7 (C3); 115.3 (C5), 52.7 (C13); 51.8 (C11); 50.4 (C10); 31.6 (C7); 27.2 (C9); 26.2 (C8)

MS (EI) m/z 267.1 (100), 224.1 (95), 211.1 (20), 186.1 (15), 156.1 (10), 82.0 (5)

HRMS for $C_{16}H_{17}N_3O$ calc. 267.1371
found 267.1377

IUPAC 11-pyridin-3-yl -1,2,3,4,5,6-hexahydro-1,5-methano-pyridino[1,2-a]diazocin-8-one

6.4.27 5-(1-Methyl-1*H*-pyrazol-4'-yl)-cytisine **126e**

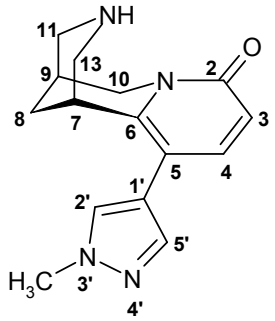

The Suzuki reaction was performed according to the general method with 5-bromo-N-*t*BOC-cytisine **82** (100 mg, 0.27 mmol), 1-methyl-4-(4,4,5,5-tetramethyl-1,3,2-dioxaborolan-2-yl)-1H-pyrazole (84 mg, 0.41 mmol), Ba(OH)$_2$*8H$_2$O (185 mg, 0.6 mmol), Pd(PPh$_3$)$_4$ (30 mg, 0.027 mmol), DME and H$_2$O. The reaction time was 60 min. For the SPE purification, a mixture of MeOH/H$_2$O 60:40 (100 mL) was used. The HPLC separation was completed with MeOH/H$_2$O 50:50 v/v. Deprotection by Method B. The final product obtained as yellow crystalline powder (14 mg, 0.05 mmol, 19%).

M.p.: n.d.
HPLC: t_r = 12.65 min

^{1}H NMR (500 MHz, $CDCl_3$) δ [ppm] 7.38 (s, 1 H, H5'); 7.26 (s, 1 H, H2'); 7.22 (d, ^3J = 9.1 Hz, 1 H, H4); 6.46 (d, ^3J = 9.1 Hz, 1 H, H3); 4.17 (d, ^2J = 15.7 Hz, 1 H, H10β); 3.95 (dd, ^3J = 6.9 Hz, ^2J = 15.7 Hz, 1 H, H10α); 3.91 (s, 3 H, CH_3); 3.13 (s br, 1 H, H7); 3.08 (d, ^2J =12.3 Hz, 1 H, $H11_A$); 2.98 (d, ^2J = 12.3 Hz, 1 H, $H11_B$); 2.93 (d, ^2J = 12.3 Hz, 1 H, $H13_A$); 2.87 (dd, ^3J = 2.5 Hz, ^2J = 12.3 Hz, 1 H, $H13_B$); 2.31 (s, 1 H, H9); 1.88 (s, 2 H, H8)

^{13}C NMR (125 MHz, $CDCl_3$) δ [ppm] 163.1 (C=O, C2); 148.2 (C6); 142.0 (C4); 139.1 (C2'); 129.1 (C5'); 118.5 (C1'); 116.3 (C3); 109.4 (C5); 52.9 (C13); 52.4 (C11); 50.4 (C10); 39.1 ($\underline{C}H_3$); 31.8 (C7); 27.3 (C9); 26.3 (C8)

MS (EI) m/z 270.1 (100), 227.1 (68), 214.1 (25), 200.1 (15), 189.1 (30), 146.0 (20), 119.1 (10), 82.0 (10)

HRMS for $C_{15}H_{18}N_4O$ calc. 270.1481
found 270.1482

IUPAC 11-(1-methyl-1*H*-pyrazol-4-yl)-1,2,3,4,5,6-hexahydro-1,5-methano-pyridino[1,2-a]diazocin-8-one

6.4.28 5-Bromo-3-phenyl-cytisine **128e**

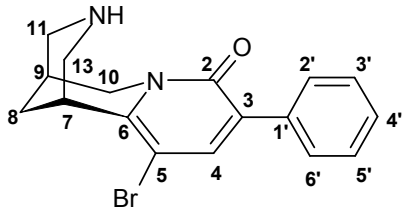

The Suzuki reaction was performed according to the general method with 3,5-dibromo-N-*t*BOC-cytisine **83** (121 mg, 0.27 mmol), 3-phenylboronic acid (50 mg, 0.41 mmol), Na_2CO_3 (64 mg, 0.6 mmol), $Pd(PPh_3)_4$ (30 mg, 0.027 mmol), DME and H_2O. The reaction time was 30 min. For the SPE purification, a mixture of MeOH/H_2O 80:20 v/v (100 mL) was used. The HPLC separation was completed with MeOH/H_2O 70:30 v/v. Deprotection by Method A. The final product obtained as off-white crystalline powder (38 mg, 0.11 mmol, 33%).

M.p.: 126.1 – 127.0 °C
HPLC: t_r = 25.23 min

^{1}H NMR (500 MHz, $CDCl_3$) δ [ppm] 7.65 (d, ^3J = 7.2 Hz, 2 H, H2'+H4'); 7.60 (s, 1 H, H4); 7.37 (t, ^3J = 7.2 Hz, 2 H, H3' + H5'); 7.30 (tt, ^4J = 1.3 Hz, ^3J = 7.2 Hz, 1 H, H4'); 4.13 (d, ^2J = 15.5 Hz, 1 H, H10β); 3.96 (dd, ^3J = 6.6 Hz, ^2J = 15.5 Hz, 1 H, H10α); 3.36 (s br, 1 H, H7); 3.18 (d, ^2J = 12.3 Hz, 1 H, $H13_A$); 3.08 (d, ^2J =12.3 Hz, 1 H, $H11_A$); 2.99 (d, ^2J = 12.3 Hz, 1 H, $H11_B$); 2.96 (d, ^2J = 12.3 Hz, 1 H, $H13_B$); 2.34 (s br, 1 H, H9); 1.98 (d br, ^2J = 12.9 Hz, 1 H, $H8_A$); 1.94 (d br, ^2J = 12.9 Hz, 1 H, $H8_B$)

^{13}C NMR (125 MHz, $CDCl_3$) δ [ppm] 161.2 (C=O, C2); 147.0 (C6); 140.4 (C4); 136.0 (C1'); 128.6 (C3); 128.6 (C2' + C6'); 128.1 (C3' + C5'); 127.8 (C4'); 98.8 (C5); 52.7 (C13); 51.3 (C11); 50.3 (C10); 34.9 (C7); 27.6 (C9); 26.4 (C8)

MS (EI) m/z 344.1 (100), 302.0 (80), 277.1 (20), 263.0 (40), 162.1 (40), 82.1 (20), 57.1 (10)

HRMS for $C_{17}H_{17}BrN_2O$ calc. 344.0524
found 344.0529

IUPAC 11-bromo-9-phenyl-1,2,3,4,5,6-hexahydro-1,5-methano-pyridino[1,2-a]diazocin-8-one

6.4.29 5-Bromo-3-(pyridin-3'-yl)-cytisine **129e**

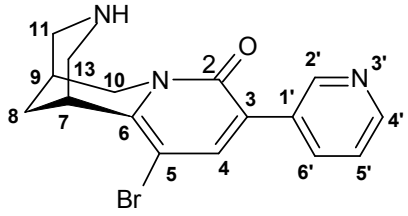

The Suzuki reaction was performed according to the general method with 3,5-dibromo-N-*t*BOC-cytisine **83** (121 mg, 0.27 mmol), 3-pyridineboronic acid (49 mg, 0.41 mmol), K_3PO_4 (60 mg, 0.6 mmol), $Pd(PPh_3)_4$ (30 mg, 0.027 mmol), DME and H_2O. The reaction time was 60 min. For the SPE purification, a mixture of MeOH/H_2O 70:30 v/v (100 mL) was used. The HPLC separation was completed with MeOH/H_2O 70:30 v/v. Deprotection by Method B. The final product obtained as yellow crystalline powder (39 mg, 0.11 mmol, 41%).

M.p.: 87.6 – 92.3 °C
HPLC: t_r = 26.98 min

^{1}H NMR (500 MHz, $CDCl_3$) δ [ppm] 8.81 (d, ^{4}J = 1.6 Hz, 1 H, H2'); 8.55 (dd, ^{4}J = 2.0 Hz, ^{3}J = 5.1 Hz, 1 H, H4'); 8.13 (dt, ^{4}J = 2.0 Hz, ^{3}J = 8.0 Hz, 1 H, H6'); 7.67 (s, 1 H, H4); 7.33 (dd, ^{3}J = 5.1 Hz, ^{3}J =8.0 Hz, 1 H, H5'); 4.16 (d, ^{2}J = 15.8 Hz, 1 H, H10β); 4.00 (dd, ^{3}J = 6.6 Hz, ^{2}J = 15.8 Hz, 1 H, H10α); 3.42 (s br, 1 H, H7); 3.25 (d, ^{2}J = 12.0 Hz, 1 H, $H13_A$); 3.12 (d, ^{2}J =12.0 Hz, 1 H, $H11_A$); 3.03 (d, ^{2}J = 12.0 Hz, 1 H, $H11_B$); 2.98 (dd, ^{3}J = 2.2 Hz, ^{2}J = 12.0 Hz, 1 H, $H13_B$); 2.39 (s br, 1 H, H9); 2.02 (d br, ^{2}J = 13.2 Hz, 1 H, $H8_A$); 1.96 (d br, ^{2}J = 13.2 Hz, 1 H, $H8_B$)

^{13}C NMR (125 MHz, $CDCl_3$) δ [ppm] 161.0 (C=O, C2); 149.1 (C6); 148.8 (C2'); 148.3 (C4'); 140.6 (C4); 136.1 (C6'); 131.9 (C1'); 125.3 (C3); 122.9 (C5'); 98.7 (C5); 52.7 (C13); 51.4 (C11); 50.4 (C10); 35.0 (C7); 27.5 (C9); 26.4 (C8)

MS (EI) m/z 347.0/345.0 (90), 303.0 (100), 289.0 (20), 264.0 (40), 223.1 (10), 194.1 (10), 168.1 (5), 82.0 (10)

HRMS for $C_{16}H_{16}BrN_3O$ calc. 345.0477
found 345.0475

IUPAC 11-bromo-9-pyridin-3-yl-1,2,3,4,5,6-hexahydro-1,5-methano-pyridino[1,2-a]diazocin-8-one

6.5 Synthesis of Novel nAChR Ligands Based on Choline

6.5.1 General Procedure for the Synthesis of Phenylcarbamates

Equimolar amounts of the amino alcohol and appropriate phenylisocyanate were stirred in toluene (10 mL) under argon atmosphere at 50 °C for 1.5 – 4 hours. The solvent was evaporated and the resulting oily residue was purified by flash chromatography on a small amount of silica gel (max. 50 mg) eluting with CH_2Cl_2/MeOH (95:5).

6.5.2 (3-Methyl-phenyl)-carbamic (S)-(-)-1-methyl-pyrrolidin-2-yl-methyl ester **136**

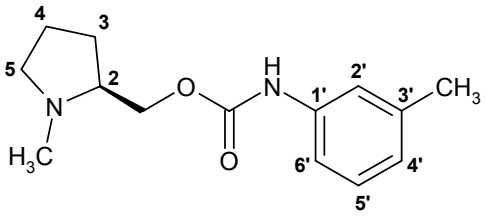

The synthesis was performed according to the general method with (S)-(-)-1-methyl-2-pyrrolidinylmethanol (0.24 mL, 2 mmol) and m-tolylisocyanate (0.26 mL, 2 mmol). The final product was obtained as a colourless oil (206 mg, 0.83 mmol, 42%).

M.p.: 62.1-62.3 °C

$[\alpha]_D^{20}$ + 1.3295° (c 0.02, MeOH)

IR (KBr): 1565, 1710, 2799, 2855, 3053 cm^{-1}

^{1}H NMR (500 MHz, $CDCl_3$) δ 7.21 (s, 1 H, H2'); 7.11 – 7.17 (m, 2 H, H5' + H6'); 6.84 (d, ^3J = 6.9 Hz, 1 H, H4'); 6.67 (s, 1 H, NH); 4.22 (dd, ^3J = 4.4 Hz, ^2J = 11.0 Hz, 1 H, CH_{2A}); 4.05 (dd, ^3J = 4.7 Hz, ^2J = 11.4 Hz, 1 H, CH_{2B}); 3.08 (dt, ^3J = 1.9 Hz, ^3J = 8.2 Hz, 1 H, H2); 2.43 – 2.48 (m, 1 H, $H5_A$); 2.40 (s, 3 H, CH_3); 2.30 (s, 3 H, N-CH_3); 2.20 – 2.26 (dt, ^3J = 7.6 Hz, ^3J = 9.5 Hz, 1 H, $H5_B$); 1.88 – 1.93 (m, 1 H, $H4_A$); 1.64 – 1.81 (m, 3 H, H3 + $H4_B$)

^{13}C NMR (125 MHz, $CDCl_3$) δ 153.5 (C=O); 139.0 (C1'); 137.8 (C3'); 128.8 (C5'); 124.2 (C4'); 119.2 (C2'); 115.6 (C6'); 66.0 (CH_2); 64.2 (C2); 57.5 (C5); 41.2 (N-CH_3); 27.9 (C3); 22.7 (C4); 21.5 (CH_3)

MS (EI) m/z 248.1 (20) [M], 97 (20), 84 (100)

Anal. calcd. for $C_{14}H_{20}N_2O_2$ (248.33) C, 67.71; H, 8.05; N, 11.28

Found C, 67.21; H, 8.12; N, 10.65

6.5.3 (3-Bromo-phenyl)-carbamic (S)-(-)-1-methyl-pyrrolidin-2-yl-methyl ester **137**

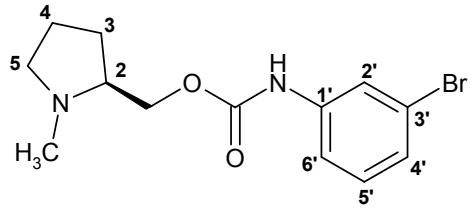

The synthesis was performed according to the general method with (S)-(-)-1-methyl-2-pyrrolidinylmethanol (0.24 mL, 2 mmol) and m-bromophenylisocyanate (0.25 mL, 2 mmol). The final product was obtained as a colourless oil, which crystallised on standing (610 mg, 1.94 mmol, 97%).

M.p.: 49.0 – 49.6 °C
IR (KBr): 2942, 2857, 1714, 1596 cm^{-1}
$[\alpha]_D^{20}$ + 1.3295° (c 0.02, MeOH)

^{1}H NMR (500 MHz, $CDCl_3$) δ 7.62 (s, 1 H, H2'); 7.23 (s br, 1 H, H6'); 7.10 – 7.16 (m, 2 H, H4' + H5'); 6.78 (br s, 1 H, NH); 4.22 (dd, J = 4.4 Hz, J = 11.0 Hz, 1 H, CH_{2A}); 4.10 (dd, J = 4.4 Hz, J = 11.0 Hz, 1 H, CH_{2B}); 3.07 (dt, J = 1.9 Hz, J = 7.9 Hz, 1 H, H2); 2.42 – 2.47 (m, 1 H, $H5_A$); 2.39 (s, 3 H, N-CH_3); 2.20 – 2.25 (dt, J = 7.3 Hz, J = 9.5 Hz, 1 H, $H5_B$); 1.82 – 1.93 (m, 1 H, $H4_A$); 1.63 – 1.82 (m, 3 H, H3 + $H4_B$)

^{13}C NMR (125 MHz, $CDCl_3$) δ 153.2 (C=O); 139.2 (C1'); 130.3 (C5'); 126.3 (C4'); 122.7 (C3'); 121.4 (C2'); 117.0 /C6'); 66.3 (CH_2); 64.1 (C2); 57.5 (C5); 41.1 (CH_3); 27.8 (C3); 22.7 (C4)

MS (EI) m/z 312.1 (20) [M-H^+], 198.9 (10), 97 (20), 84.0 (100)

Anal. calc. for $C_{13}H_{17}BrN_2O_2$ (313.202) C, 49.85; H, 5.47; N, 8.94
Found C, 49.01; H, 5.57; N, 8.54

6.5.4 (3-Methyl-phenyl)-carbamic 1-methyl-piperidin-2-yl-methyl ester **138**

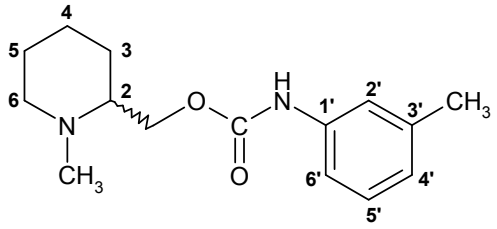

The synthesis was performed according to the general method with 2-hydroxymethyl-N-methylpiperidine (0.26 mL, 2 mmol) and m-tolylisocyanate (0.26 mL, 2 mmol). The final product was obtained as a yellowish oil, which crystallised on standing (210 mg, 0.6 mmol, 30%).

M.p.: 73.5 – 75.5 °C
IR (KBr): 2937, 2852, 2803, 1732 cm^{-1}

^{1}H NMR (500 MHz, $CDCl_3$) δ 7.23 (s, 1 H, H2'); 7.15 – 7.19 (m, 2 H, H5' + H6'); 6.87 (d, ^{3}J = 6.9 Hz, 1 H, H4'); 6.81 (s, 1 H, NH); 4.25 (dd, ^{3}J = 4.1 Hz, ^{2}J = 11.7 Hz, 1 H, CH_{2A}); 4.23 (dd, ^{3}J = 3.2 Hz, ^{2}J = 11.7 Hz, 1 H, CH_{2B}); 2.88 – 2.93 (m, 1 H, H2); 2.34 (s, 3 H, N-CH_3); 2.32 (s, 3 H, CH_3); 2.08 – 2.13 (m, 2 H, H6); 1.75 – 1.82 (m, 1 H, $H3_A$); 1.50 – 1.69 (m, 4 H, H4 + H5); 1.24 – 1.34 (m, 1 H, $H3_B$)

^{13}C NMR (125 MHz, $CDCl_3$) δ 153.6 (C=O); 139.0 (C1'); 137.8 (C3'); 128.9 (C5'); 124.2 (C4'); 119.1 (C2'); 115.6 (C6'); 66.2 (CH_2); 62.9 (C2); 57.4 (C6); 43.2 (N-CH_3); 29.2 (C3); 25.8 (C5); 24.2 (C4); 21.5 (CH_3)

MS (EI) m/z 262.2 (38) [M], 134 (10), 98.1 (100), 77 (10)

Anal. calcd. for $C_{15}H_{22}N_2O_2$ (262.353)		C, 68.67; H, 8.45; N, 10.67
	Found	C, 68.78; H: 8.47; N, 10.13

6.5.5 (3-Bromo-phenyl)-carbamic 1-methyl-piperidin-2-yl-methyl ester **139**

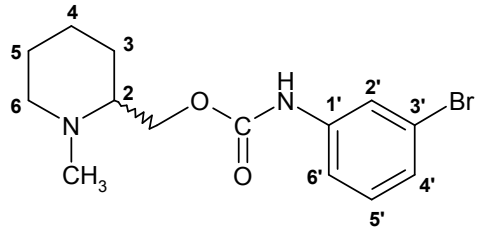

The synthesis was performed according to the general method with 2-hydroxymethyl-N-methylpiperidine (0.26 mL, 2 mmol) and m-bromophenylisocyanate (0.25 mL, 2 mmol). The final product was obtained as yellowish oil, which crystallised on standing (555.2 mg, 1.7 mmol, 85%).

M.p.: 67.3 – 68.1 °C

IR (KBr): 2936, 2856, 2794, 1729, 1705, 1533 cm^{-1}

^{1}H NMR (500 MHz, $CDCl_3$) δ 7.66 (s, 1 H, H2'); 7.26 (d, ^3J = 7.8 Hz, 1 H, H6'); 7.12 – 7.20 (m, 2 H, H4' + H5'); 7.04 (s, 1 H, NH); 4.28 (dd, ^3J = 3.8 Hz, ^2J = 11.7 Hz, 1 H, CH_{2A}); 4.20 (dd, ^3J = 3.2 Hz, J = 11.7 Hz, 1 H, CH_{2B}); 2.91 (d, ^3J = 11.7 Hz, 1 H, H2); 2.35 (s, 3 H, N-CH_3); 2.06 – 2.12 (m, 2 H, H6); 1.76 – 1.80 (m, 1 H, $H3_A$); 1.51 – 1.68 (m, 4 H, H4 + H5); 1.25 – 1.35 (m, 1 H, $H3_B$)

^{13}C NMR (125 MHz, $CDCl_3$) δ 153.2 (C=O); 139.3 (C1'); 130.2 (C5'); 126.3 (C4'); 122.7 (C3'); 121.3 (C2'); 116.9 (C6'); 66.3 (CH_2); 62.8 (C2); 57.3 (C6); 43.0 (N-CH_3); 29.1 (C6); 25.6 (C5); 24.1 (C4)

MS (EI) m/z 326.1 (10) [M^+], 196.9 (10), 98 (100)

Anal. calcd. for $C_{14}H_{19}Br\,N_2O_2$ (327.218) C, 51.39; H, 5.85; N, 8.56

Found C, 50.81; H, 6.00; N, 8.12

6.5.6 m-Tolyl-carbamic acid 1-aza-bicyclo[2.2.2]oct-3-yl ester **140**

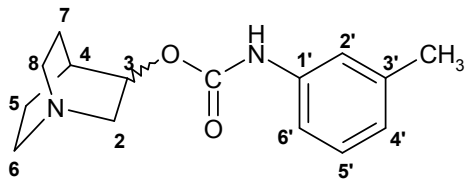

The synthesis was performed according to the general method with 3-quinuclidinole (254 mg, 2 mmol) and m-tolylisocyanate (0.26 mL, 2 mmol). The resulting oily residue was purified by column chromatography eluting with CH_2Cl_2/MeOH (90:10→90:50 v/v) and crystallised from diethyl ether. The final product was obtained as white crystalline powder (150 mg, 0.57 mmol, 28%).

M.p.: 150.1 – 150.4 °C
IR (KBr): 2938, 2866, 2780, 1710, 1598, 1559 cm^{-1}

^{1}H NMR (500 MHz, $CDCl_3$) δ 7.29 (s, 1 H, H2'); 7.26 (d, ^3J = 8.2 Hz, 1 H, H6'); 7.18 (t, ^3J = 7.6 Hz, 1 H, H5'); 6.88 (d, ^3J = 7.6 Hz, 1 H, H4'); 4.84 – 4.85 (m, 1 H, $H3_A$); 3.34 (qui, J = 1.7 Hz, 1 H, $H3_B$); 3.25 (ddd, J = 2.4 Hz, J = 8.4 Hz, J = 14.7 Hz, 1 H, H2); 2.77 – 2.95 (m, 5 H, H2 + H6 +H8); 2.34 (s, 3 H, CH_3); 2.10 – 2.14 (m, 1 H, H4); 1.98 – 2.06 (m, 1 H, H5 or H7); 1.78 – 1.85 (m, 1 H, H5 or H7); 1.66 – 1.72 (m, 1 H, H5 or H7); 1.52 – 1.58 (m, 1 H, H5 or H7)

^{13}C NMR (125 MHz, $CDCl_3$): δ 156.0 (C=O); 140.3 (C1'); 140.0 (C3'); 130.0 (C5'); 125.1 (C4'); 120.8 (C2'); 117.3 (C6'); 72.5 (C3); 56.4 (C2); 48.3 (C8); 47.3 (C6); 26.8 (C4); 25.1 (C7); 21.9 (C5); 20.4 (CH_3)

MS (EI) m/z 260.2 (25) [M], 147.1 (10), 134.0 (32), 122.0 (40), 105.0 (100), 82 (18), 77 (25)

Anal. calcd. for $C_{15}H_{20}N_2O_2$ (260.34) C, 68.20; H, 7.74; N, 10.76
Found C, 68.37; H, 7.72; N, 10.98

6.5.7 3-Bromo-carbamic acid 1-aza-bicyclo[2.2.2]oct-3-yl ester **141**

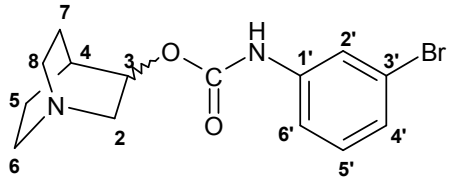

The synthesis was performed according to the general method with 3-quinuclidinole (254 mg, 2 mmol) and 3-bromophenylisocyanate (0.25 mL, 2 mmol). The oily residue was crystallised from diethyl ether to yield the final product as white crystals (488 mg, 1.5 mmol, 75%).

M.p.: 162.2 – 162.4 °C
IR (KBr): 3163, 2943, 2866, 1722, 1595 cm^{-1}

^{1}H NMR (500 MHz, $CDCl_3$ + TMS) δ 7.65 (s, 1 H, H2'); 7.26 (s, 1 H, H6'); 7.13 – 7.20 (m, 2 H, H4' + H5'); 7.08 (s, 1 H, NH); 4.80 – 4.91 (m, 1 H, H3); 3.27 (ddd, J = 1.9 Hz, J = 8.4 Hz, J = 14.5 Hz, 1 H, $H2_A$); 2.73 – 2.96 (m, 5 H, $H2_B$ + H6 + H8); 2.09 – 2.18 (s, 1 H, H4); 1.81 – 1.87 (m, 1 H, H5 or H7); 1.68 – 1.75 (m, 1 H, H5 or H7); 1.55 – 1.61 (m, 1 H, H5 or H7); 1.40 – 1.46 (m, 1 H, H5 or H7)

^{13}C NMR (125 MHz, $CDCl_3$ + TMS) δ 153.1 (C=O); 139.4 (C1'); 130.3 (C5'); 126.3 (C4'); 122.8 (C3'); 121.6 (C2'); 117.0 (C6'); 72.5 (C3); 55.4 (C2); 47.3 (C8); 46.5 (C6); 25.4 (C4); 24.5 (C7); 19.5 (C5)

MS (EI) m/z 324.1 (40) [M-H^+], 126.1 (100), 109.0 (28), 82.0 (22)

Anal. calc. for $C_{14}H_{17}BrN_2O_2$ (325.21) C, 51.70; H, 5.27; N, 8.61
Found C, 51.05; H, 5.22; N: 8.60

6.5.8 Biphenyl-3-yl-carbamic acid 1-aza-bicyclo[2.2.2]oct-3-yl ester **144**

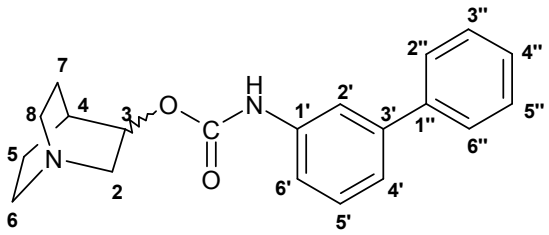

3-Bromo-carbamic acid 1-aza-bicyclo-[2.2.2]oct-3-yl ester **141** (325 mg, 1 mmol), phenylboronic acid (244 mg, 2 mmol), tetrakis-(triphenylphosphin)-palladium(0) (58 mg, 0.05 mmol), Na_2CO_3 (233 mg, 2.2 mmol), toluene (5 mL) and a magnetic stir bar were placed in a 10-mL microwave glass tube. The vessel was sealed with a septum and placed into the microwave cavity. Enhanced microwave irradiation of 100 W was used, the temperature being ramped from room temperature to 120°C. Once 120°C was reached, the reaction mixture was held for 20 min. Then, the mixture was allowed to cool to room temperature, the reaction vessel was opened and the solvent was evaporated under pressure. The oily residue was purified by column chromatography on silica gel eluting with CH_2Cl_2/MeOH (80:20). The final product was crystallised from the mixture of diethyl ether/petroleum ether and obtained as a yellow crystalline powder (37.7 mg, 0.11 mmol, 22.7%).

M.p.: 201 – 202 °C
IR (KBr) 3189, 2934, 2868, 1716 cm^{-1}

^{1}H NMR (500 MHz, DMSO-*d*$_6$) δ 9.66 (s, 1 H, NH); 7.79 (s, 1 H, H2'); 7.58 (dt, ^4J = 1.4 Hz, ^3J = 7.1 Hz, 2 H, H2''+H6''); 7.43 – 7.47 (m, 3 H, H6'+H3''+H5''); 7.36 (tt, ^4J = 1.4 Hz, ^3J = 7.1 Hz, 1 H, H4''); 7.35 (t, ^3J = 7.7 Hz, 1 H, H5'); 7.25 (dt, ^4J = 1.5 Hz, ^3J = 8.2 Hz, 1 H, H4'); 4.68 – 4.71 (m, 1 H, H3); 3.15 (ddd, J = 1.8 Hz, J = 7.9 Hz, J = 14.5 Hz, 1 H, $H2_A$); 2.57 – 2.72 (m, 5 H, $H2_B$ + H6 + H8); 1.98 (sx, J = 3.2 Hz, 1 H, H4); 1.78 – 1.83 (m, 1 H, H5 or H7); 1.59 – 1.65 (m, 1 H, H5 or H7); 1.47 – 1.54 (m, 1 H, H5 or H7), 1.33 – 1.39 (m, 1 H, H5 or H7)

^{13}C NMR (125 MHz, DMSO-*d*$_6$) δ 153.6 (C=O); 140.9 (C3'); 140.4 (C1'); 139.9 (C1''); 129.4 C5'); 129.1 (C3'' + C5'); 127.6 (C4''); 126.7 (C2'' + C6''), 120.9 (C4'); 117.4 (C2'); 116.6 (C6'); 71.4 (C3); 55.3 (C2); 47.1 (C8); 46.1 (C6); 25.4 (C4); 24.4 (C7); 19.3 (C5)

MS (EI) m/z 322.2 (10) [M+]

Anal. calcd. for $C_{20}H_{22}N_2O_2$ (322.41): C, 74.50; H, 6.88; N, 8.69.
Found: C, 74.28; H, 6.48; N, 8.15.

6.5.9 3-(Styryl)-phenyl]carbamic acid 1-aza-bicyclo-[2.2.2]oct-3-yl ester **145**

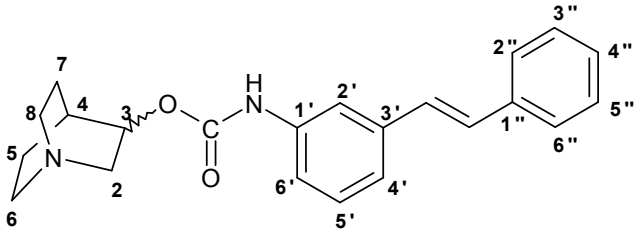

3-Bromo-carbamic acid 1-aza-bicyclo[2.2.2]oct-3-yl ester **141** (325 mg, 1mmol), styrylboronic acid (300 mg, 2mmol), tetrakis-(triphenylphosphin)-palladium(0) (115.5 mg, 0.1 mmol), Na_2CO_3 (233 mg, 2.2mmol), toluene (5mL) and a magnetic stir bar were placed in a 10-mL microwave glass tube. The vessel was sealed with a septum and placed into the microwave cavity. Microwave irradiation of 60 W was used, the temperature being ramped from room temperature to 120 °C. Once 120 °C was reached, the reaction mixture was held for 10 min. Then the mixture was allowed to cool to room temperature, the reaction vessel was opened and the solvent was evaporated under pressure. The oily residue was purified by column chromatography on silica gel eluting with CH_2Cl_2/MeOH (90:10). The final product was crystallised from the mixture of diethyl ether/petroleum ether and obtained as a yellow crystalline powder (101.1 mg, 0.2 mmol, 39%).

M.p.: 174 – 175 °C
IR (KBr): 3021, 2945, 2771, 2661, 2589, 1728, 1589, 1547, 1224, 960 cm^{-1}

^{1}H NMR (500 MHz, DMSO-*d*$_6$) δ 9.81 (s, 1 H, NH); 7.70 (s, 1 H, H2'); 7.59 (d, ^3J = 7.1 Hz, 2 H, H2'' + H6''); 7.44 (d, J = 7.3 Hz, 1 H, H6'); 7.37 (t, ^3J = 7.4 Hz, 3 H, H3'' + H5'' + H5'); 7.26 – 7.29 (m, 2 H, H4' + H4''); 7.20 (d, ^3J = 16.6 Hz, 1 H, -C<u>H</u>=); 7.13 (d, ^3J = 16.6 Hz, 1 H,-C<u>H</u>=); 4.93 – 5.00 (m, 1 H, H3); 3.68 (ddd, J = 2.1 Hz, J = 8.4 Hz, J = 13.7 Hz, 1 H, $H2_A$); 3.15 – 3.25 (m, 5 H, $H2_B$ + H6 + H8); 2.28 (sx, J = 2.9 Hz, 1 H, H4); 1.73 – 1.91 (m, 4 H, H5 + H7)

^{13}C NMR (125 MHz, DMSO-*d*$_6$) δ 153.0 (C=O); 139.3 (C1'); 137.7 (C3'); 136.9 (C1''); 129.2, 128.8 (C3'' + C5''); 128.7 (-<u>C</u>H=); 128.5 (C5'); 127.9 (C4''); 126.7 (C2'' + C6''); 121.2 (C4');

118.03 (C6'); 116.5 (C2'); 67.6 (C3); 53.1 (C2); 45.9 (C8); 45.1 (C6); 24.0 (C4); 20.2 (C7); 16.9 (C5)

MS (EI) m/z 348.2 (100) [M^+]

Anal. calcd. for $C_{22}H_{24}N_2O_2$ (348.45): C, 75.83; H, 6.94; N, 8.04
Found C, 75.68; H, 6.96; N, 8.23

6.6 In Vitro Evaluation of Novel nAChRs Ligands

6.6.1 General Information

Instruments

Filter:	Whatman GF/B, Brandell, Gaithersburg, MD, USA
Harvester:	Brandell M48, M24, Gaithersburg, MD, USA
Homogenizator:	RW 16 basic, IKA Labortechnik, Germany
Liquid Scintillation Counter:	Tricarb® 2900 TR, canberra packard/Perkin Elmer, Dreieich, Germany
pH Meter:	WTW, pH – 197, with pH-Electrode SenTix41, IKA Labortechnik, Germany
Photometer:	Beckman DU®, 530 Life Science, Germany
Pipettes:	Eppendorf research and Eppendorf Multipipette plus
Ultraturrax:	T25 basic, IKA Labortechnik, Germany
Vortex:	MS2, Minishaker, IKA Labortechnik, Germany
Centrifuge:	Beckman Avanti™, J-20 XP, Beckman Coulter, USA

Chemicals

Calcium Chloride Dihydrate ($CaCl_2$)	C 3306, Sigma-Aldrich Chemie GmbH, München, Germany
Dimethylsulfoxide (DMSO)	Merck KG, Darmstadt, Germany
Ethanol p.a.	Merck KG, Darmstadt, Germany
N-[2-Hydroxyethyl]piperazine-N'[2-ethansulfonic] acid (HEPES)	H 3375, Sigma-Aldrich Chemie GmbH, München, Germany
Magnesium Chloride Hexahydrate ($MgCl_2$)	M 2670, Sigma-Aldrich Chemie GmbH, München, Germany

Methyllycaconitine Citrate (MLA)	M 168, Sigma-Aldrich Chemie GmbH, München, Germany
Natrium Chloride (NaCl)	S 7653, Sigma-Aldrich Chemie GmbH, München, Germany
(S)-(-)-Nicotine Hydrogentartrate	N 5260, Sigma-Aldrich Chemie GmbH, München, Germany
Potassium Chloride (KCl)	P 9541, Sigma-Aldrich Chemie GmbH, München, Germany
D-(+)-Saccharose	84097, Fluka Biochemika, Sigma-Aldrich Chemie GmbH, Taufkirchen, Germany
Tris[Hydroxymethyl]aminomethane (TRIS base)	T 1503, Sigma-Aldrich Chemie GmbH, München, Germany
Tris[Hydroxymethyl]aminomethane Hydrochlorid (TRIS*HCl)	T 3253, Sigma-Aldrich Chemie GmbH, München, Germany
Water Elga Pure Lab ultra	ELGA, Ransbach-Baumbach, Germany
Ultima Gold™	Perkin Elmer and Analytical Science, MA, USA

is a mixture of:

Ethoxylated Alkylphenol 10% – 20%
Bis(2-ethylhexyl) hydrogen phosphate 10% – 20%
Docusate Sodium ≤ 2.5%
Triethyl Phosphate ≤ 2.5%
Diisopropyl Naphtalene Isomers 60% – 80%
2,5 – Diphenyloxazole ≤ 2.5%
1,4 – Bis(4-methyl-alpha-styryl) benzene ≤ 2.5%

Radioligands

(±)-[^{3}H]Epibatidine ([^{3}H]Epi) (S.A.: 33.3 – 66.6 Ci/mmol)	Perkin Elmer Life Sciences Products, Köln, Germany
[^{3}H]Methyllycaconitine ([^{3}H]MLA) (S.A.: 20 Ci/mmol)	TOCRIS Cookson Ltd., Avonmouth, Bristol, England

Tissues

frozen *Torpedo californica* Electroplax	Marinus Inc., Long Beach, CA, USA
frozen Sprague-Dawley rat brains	Pel-Freez Biologicals, rogers, AR, USA
Calf adrenals	local slaughterhouse, Köln, Germany

Buffer Solutions

HSS-Buffer (HEPES Salt Solution, incubation assay buffer, buffer for membrane preparation)

15.0 nM HEPES
120.0 nM NaCl
5.4 mM KCl
0.8 mM $MgCl_2*6H_2O$
1.8 mM $CaCl_2*2H_2O$
adjusted with concentrated NaOH-solution to pH 7.4

TRIS-Buffer (rinse buffer)

42.0 mM TRIS*HCl
8.0 mM TRIS-Base

Saccharose/TRIS-Buffer (for membrane preparation)

320.0 mM D-(+)-Saccharose
25.0 mM TRIS*HCl

6.6.2 Membrane Preparation

Preparation of rat brains

Frozen rat brains were thawed slowly before the preparation of the P2 rat brain membrane fraction (30 – 60 min on ice, afterwards at room temperature). A single cut just behind the inferior colliculi was done to exclude the cerebellum and medulla. After the determination of the wet weight (1.32 g on average), the brains were pressed into a pulp using a syringe and homogenised in saccharose buffer with a glass teflon homogenizator (Potter, 10 seconds). The tissue was then centrifuged (1,000 × g, 20 min, 4°C), the supernatant (S1) aspirated with a Pasteur pipette and stored on ice. The P1 pellet was re-suspended in saccharose buffer and the centrifugation was repeated. The supernatant S1' was collected and added to the supernatant S1. The combined supernatants were centrifuged (25,000 × g, 20 min, 4°C), the supernatant S2 was removed and the pellet P2 collected and diluted with HSS-buffer. The buffer volume added was calculated on the basis of the wet weight in a ratio 1:2.

The final pellet was stored in aliquots at -80°C. On the day of the experiment, the P2 membrane fraction was thawed, diluted with HSS-buffer (30-fold volume), homogenised and centrifuged (35,000 × g, 10 min, 4°C). The collected pellet was suspended in HSS-buffer and used in the radioligand binding experiments.

Preparation of calf adrenals

Frozen calf adrenals (-80°C) were placed on ice for 30 – 60 min and allowed to thaw slowly before they were cut into small pieces. After determination of the wet weight (4-6 g), the tissue was homogenised in HSS-buffer (Ultraturrax at 750 rpm). The homogenate was centrifuged (30,000 × g, 10 min, 4°C), the pellets collected and washed. This procedure was repeated five times. The buffer volume used to re-suspend the pellets was calculated on the basis of the wet weight in a ratio 1:6.5.

The prepared tissues were stored in aliquots at -80°C. One hour before the experiments the tissues were slowly thawed, homogenised in HSS-buffer and centrifuged (25,000 × g, 20 min, 4°C). The pellets were re-suspended in fresh HSS-buffer and used for radioligand binding assays.

Preparation of Torpedo californica electroplax

Frozen samples of *Torpedo californica* electric organ (-80°C) were placed on ice for 30 – 60 min and allowed to thaw slowly before the membrane preparation. The tissue was homogenised in an ice-cold HSS-buffer (Ultraturrax at 750 rpm) and centrifuged (30,000 × g, 10 min, 4°C). The pellets were collected, washed four times with HSS-buffer through re-homogenization and centrifugation at the same settings. The remaining pellets were collected, re-suspended in HSS and stored in aliquots at -80°C.

One hour before the experiments the tissues were slowly thawed, homogenised in HSS-buffer and centrifuged (25,000 × g, 20 min, 4°C). The pellets were re-suspended in fresh HSS-buffer and used for radioligand binding assays.

6.6.3 Radioligand Binding Studies

Competition assay using (±)-[^{3}H]epibatidine ([^{3}H]Epi) and rat brain P2-fraction ($\alpha4\beta2$ nAChR)*

A dilution row of 6 – 9 concentrations of the test compound was prepared. Each assay sample, with a total volume of 500 µL contained 100 µL of the membrane protein (60µg), 100 µL of (±)-[^{3}H]epibatidine (0.5 nM), 100 µL of HSS-buffer and 200 µL of the test compound. Non-specific binding was determined in the presence of 300 µM (-)-nicotine tartrate salt. The samples were homogenised and incubated for 90 min at 22°C. The incubation was terminated by vacuum filtration through glass fibre filters pre-soaked in 1% poly(ethyleneimine). The filter were rinsed three times with TRIS-buffer, punched out and

transferred into 4 mL scintillation vials. The scintillation vials were filled with scintillation cocktail (2 mL) and the radioactivity was measured using a liquid scintillation counter.

Assays were carried out in duplicate, triplicates or quadruplicates.

Competition assay using [^{3}H]methyllycaconitine ([^{3}H]MLA) and rat brain P2-fraction (α7 nAChR)*

A dilution row of 6 – 9 concentrations of the test compound was prepared. Each assay sample, with a total volume of 250 µL contained 50 µL of the test compound, 100 µL of [^{3}H]MLA and 100 µL of the P2-membrane protein fraction (60 – 70 µg). Non-specific binding was determined in the presence of 1 µM MLA. The samples were homogenised and incubated for 120 min at 22°C. The incubation was terminated by vacuum filtration through glass fibre filters pre-soaked in 1% poly(ethyleneimine). The filters were rinsed three times with TRIS-buffer, punched out and transferred into 4 mL scintillation vials. The scintillation vials were filled with scintillation cocktail (2 mL) and the radioactivity was measured using a liquid scintillation counter.

Assays were carried out in duplicates, triplicates or quadruplicates.

Competition assay using (±)-[^{3}H]epibatidine ([^{3}H]Epi) and calf adrenals membrane fraction ($\alpha3\beta4$ nAChR)*

A dilution row of 6 – 9 concentrations of the test compound was prepared. Each assay sample, with a total volume of 500 µL contained 200 µL of the test compound, 100 µL of (±)-[^{3}H]epibatidine, 100 µL of the calf adrenal membrane protein fraction (60 – 70 µg) and 100 µM of HSS-buffer. Non-specific binding was determined in the presence of 300 µM (-)-nicotine tartrate salt. The samples were homogenised and incubated for 90 min at 22°C. The incubation was terminated by vacuum filtration through glass fibre filters pre-soaked in 1% poly(ethyleneimine). The filters were rinsed three times with TRIS-buffer, punched out and transferred into 4 mL scintillation vials. The scintillation vials were filled with scintillation cocktail (2 mL) and the radioactivity was measured using a liquid scintillation counter.

Assays were carried out in duplicates, triplicates or quadruplicates

Competition assay using (±)-[^{3}H]epibatidine ([^{3}H]Epi) and Torpedo californica electroplax ($(\alpha 1)_2\beta 1\gamma\delta$ nAChR)

A dilution row of 6 – 9 concentrations of the test compound was prepared. Each assay sample, with a total volume of 500 µL contained 200 µL of the test compound, 100 µL of (±)-[^{3}H]epibatidine and 100 µL of the Torpedo californica electroplax fraction (60 – 70 µg). Non-specific binding was determined in the presence of 300 µM (-)-nicotine tartrate salt. The samples were homogenised and incubated for 90 min at 22°C. The incubation was terminated by vacuum filtration through glass fibre filters pre-soaked in 1% poly(ethyleneimine). The filters were rinsed three times with TRIS-buffer, punched out and transferred into 4 mL scintillation vials. The scintillation vials were filled with scintillation cocktail (2 mL) and the radioactivity was measured using a liquid scintillation counter.

Assays were carried out in duplicates, triplicate or quadruplicates.

7 Abreviations

ACh	acetylcholine
AChBP	acetylcholine binding protein
AD	Alzheimer's disease
ADNFLE	Autosomal Dominant Nocturnal Frontal Lobe Epilepsy
BBB	blood-brain barrier
9-BBN	9-borabicyclo[3.3.1]nonane
α-Bgt	α -Bungarotoxin
*t*BOC	*tert*-butoxycarbonyl
br	broad
$CDCl_3$	deuterated chloroform
CD_3OD	deuterated methanol
CNS	Central Nervous System
COSY	Correlated Spectroscopy
d	doublet
dba	dibenzylideneacetone
DEPT	Distortionless Enhancement by Polarization Transfer
DHβE	dihydro-β-erythroidine
DMA	N,N-dimethylacetamide
DME	1,2-dimethoxyethane
DMF	dimethylformamide
DMCC	N,N-dimethylcarbamoylcholine
DMSO	dimethylsulfoxide
DMPP	N,N-dimethylphenylpiperazine
DPPA	diphenylphosphoryl azide
dppf	1,1'-bis(diphenylphosphino)ferrocene
$GABA_A$	γ-aminobutyric acid receptor type A
GHz	gigahertz
GTS-21	3-(2,4-dimethoxybenzylidene)-anabaseine
h	hour(s)
HBA	hydrogen bond acceptor
HBD	hydrogen bond donor
[^{3}H]α-Bgt	tritium labelled α-bungarotoxin
(±)-[^{3}H]Epi	tritium labelled (±)-epibatidine
[^{3}H]MLA	tritium labelled methyllycaconitine
HEK	human embryonic kidney cells
HMBC	Heteronuclear Multiple Bond Correlation

HMPA	hexamethylphosphoric triamide
HPLC	High Performance Liquid Chromatography
HRMS	High Resolution Mass Spectroscopy
HSQC	Heteronuclear Single Quantum Coherence
5-HT	5-hydroxytryptamine (serotonine)
Hz	Hertz
INADEQUATE	Incredible Natural Abundance Double Quantum Transfer Experiment
IR	infrared spectrum/spectroscopy
J	coupling constant
K_d	dissociation constant
K_i	inhibition constant
LSC	liquid scintillation counter
M	molar
m	multiplet
mAChR	muscarinic acetylcholine receptor
MAOS	Microwave-Assisted Organic Synthesis
MCC	N-methylcarbamoylcholine
Me	Methyl-
MeCN	acetonitrile
MeOH	methanole
mg	milligram
min	minutes
MLA	methyllycaconitine
mM	milimolar
mmol	millimol
μM	micromolar
M.p.	Melting point
MS	mass spectroscopy
n	number of experiments
nAChR	nicotinic acetylcholine receptor
NBS	N-bromosuccinimide
nM	nanomolar
NMP	N-methylpyrrolidinone
NMR	Nuclear Magnetic Resonance
ovl.	overlapping
PET	Positron Emission Tomography
PD	Parkinson’s Disease

pM	picomolar
RP	reverse phase
q	quartet
s	singlet
SAR	structure-activity relationship
SCS	substituent-induced chemical shift
SEM	standard error of the mean
sex	sextet
SFD	single-frequency decoupling
SH-SY5Y	human neuroblastoma cell line
S_N	nuclephilic substitution
SPE	solid phase extraction
t	triplet
TBAB	tetrabutylammonium bromide
Tf	triflate
TFA	trifluoroacetic acid
THF	tetrahydrofuran
TLC	thin layer chromatography
UV	ultraviolet spectroscopy
VMAT-2	vesicular monoamine transporter-2

8 References

1. Sharples D.G.V.; Wonnacott S. Neuronal Nicotinic Receptors. *Tocris Reviews* No. 19, 2001

2. Lloyd G.K.; Williams M. Neuronal Nicotinic Acetylcholine Receptors as Novel Drug Targets. *JPET* 292, 461 – 467 (2000)

3. Karlin A. Emerging structure of the nicotinic acetylcholine receptors. *Nature Reviews Neuroscience* 3, 102 – 114 (2000)

4. Le Novere N.; Changeux J.P. Molecular evolution of the nicotinic acetylcholine receptor: an example of multigene family in excitable cell. *J Mol Evol* 40, 155 – 172 (1995)

5. Hogg R.C.; Raggenbass M.; Bertrand D. Nicotinic acetylcholine receptors: from structure to brain function. *Rev Physiol Biochem Pharmacol* 147, 1 – 46 (2003)

6. Unwin N. Refined structure of the nicotinic acetylcholine receptor at 4Å resolution. J Mol Biol 346, 967 – 989 (2005)

7. Raftery M.A.; Vandlen R.L.; Reed K.L.; Lee T. Characterization of *Torpedo californica* acetylcholine receptor: its subunit composition and ligand-binding properties. *Cold Spring Harb Symp Quant Biol* 40, 193 – 202 (1976)

8. Mishina M.; Takai T.; Imoto K.; Noda M.; Takahashi T.; Numa S.; Methfessel C.; Sakmann B. Molecular distinction between fetal and adult forms of muscle acetylcholine receptor. *Nature* 321, 406 – 411 (1986)

9. Lindstrom J. The structures of neuronal nicotinic receptors. *In:* Clementi, F.; Fornasari D.; Gotti, C. (Eds.), Handbook of Experimental Pharmacology Vol. Neuronal Nicotinic receptors. Springer, Berlin, pp. 101 - 162

10. Anand R.; Conroy W.G.; Schoepfer R.; Whiting P.; Lindstrom J. Neuronal nicotinic acetylcholine receptor expressed in Xenopus ocytes have a pentametric quartenary structure. *J Biol Chem* 266,11192 – 11198 (1991)

11. Groot-Kormelik P.J.; Luyten W.H.; Colquhoun D.; Sivilotti L.G. Formation of functional alpha3beta4alpha5 human neuronal nicotinic receptors in Xenopus oocytes: a reporter mutation approach. *Br J Pharmacol* 134, 789 – 796 (2001)

12. Gotti, C.; Fornasari, D.; Clementi, F. Human neuronal nicotinic receptors. *Prog Neurobiol* 53, 199-237 (1997)

13. **a)** Middleton R.E.; Cohen J.B. Mapping of the acetylcholine binding site of the nicotinic acetylcholine receptor:[^{3}H]nicotine as an agonist photoaffinity label. *Biochemistry* 30, 6987 - 6997 (1991)

b) Oswald R.E.; Changeux J.P. Crosslinking of alpha-bungarotoxin to the acetylcholine receptor from Torpedo marmorata by ultraviolet light irradiation. *FEBS Lett* 139, 225 - 229 (1982)

c) Reynolds J.A.; Karlin A. Molecular weight in detergent solution of acetylcholine receptor from Torpedo californica. *Biochemistry* 17, 2035 - 2038 (1978)

14. Ortells M.O.; Barrantes G.E.; Wood C.; Lunt G.G.; Barrantes F. *J Protein Eng* 10, 511 – 517 (1997)

15. **a)** Chiara D.C.; Xie Y.; Cohen J.B. Structure of the agonist-binding sites of the Torpedo nicotinic acetylcholine receptor: affinity-labeling and mutational analyses identify gamma Tyr-111/delta Arg-113 as antagonist affinity determinants. *Biochemistry* 38, 6689 – 6698 (1999)

b) Galzi J.L.; Revah F.; Black D.; Goeldner M.; Hirth C.; Changeux J.P. Identification of novel amino acid alpha-tyrosine 93 2ithin the cholinergic ligand-binding sites of the acetylcholine receptor by photoaffinity labelling. Additional evidence for a three-loop model of the cholinergic ligand-binding sites. *J Biol Chem* 265, 10430 - 10437 (1990)

c) Wang D.; Chiara D.C.; Xie Y.; Cohen J.B. Probing the structure of the nicotinic acetylcholine receptor with 4-benzoylcholine, a novel photoaffinity competitive antagonist, *J Biol Chem* 275, 28666 – 28674 (2000)

16. Brejc K.; van Dijk W.J.; Klaasen R.V.; Schuurmans M.; van der Oost J.; Smit A.B.; Sixma T.K. Crystal structure of an Ach-binding protein reveals the ligand-binding domain of the nicotinic receptors. *Nature* 411, 269 – 276 (2001)

17. **a)** Dougherty D.A. Cation-pi interaction in chemistry and biology: a new view of benzene, Phe, Tyr and Trp. *Science* 271, 163 – 168 (1996)
b) Zhong et al. From ab initio quantum mechanics to molecular neurobiology: a cation-pi binding site in the nicotinic receptor. *Proc Natl Acad Sci* USA 95, 12088 – 12093 (1998)

18. **a)** Dursun S.M.; Reveley M.A. Differential effects of transdermal nicotine on microstructured analyses of tics in Tourette's syndrome: an open study. *Psychol Med* 27, 483 – 487 (1997)
b) McConville B.J.; Sandberg P.R.; Fogelson M.H.; King J.; Cirino P.; Parker K.W.; Norman A.B. The effects of nicotine plus haloperidol compared to nicotine only and placebo nicotine only in reducing tic severity and frequency in Tourette's disorder. *Biol Psychiatry* 31, 832 – 840 (1992)

19. **a)** Sanberg P.R; McConville B.J.; Fogelson M.H.; Manderscheid P.Z.; Parker K.W.; Blythe M.M.; Klykylo W.M.; Norman A.B. Nicotine potentiates the effect of haloperidol in animals and in patients with Tourette syndrome. *Biomed Pharmacother* 43, 19 - 23 (1989)
b) Silver A.A.; Shytle R.D.; Philipp M.K.; Wilkinson B.J.; McConville B.; Sandberg P.R. Transdermal nicotine and haloperidol in Tourette's disorder: a double-blind placebo-controlled study. *J Clin Psychiatry* 60, 707 - 714 (2001)

20. **a)** Gotti C.; Clementi F. Neuronal nicotinic recetors: from structure to pathology. *Progress Neurobiol* 74, 363 – 396 (2004)
b) Lohr J.B.; Flynn K. Smoking and schizophrenia. *Schizophr Res* 8, 93 - 102 (1992)

21. Goff D.C.; Henderson D.C.; Amico E. Cigarette smoking in schizophrenia: relationship to psychopathology and medication side effects. *Am J Psychiatry* 149, 1189 - 1194 (1992)

22. Freedman R.; Hall M.; Adler L.E.; Leonard S. Evidence in post-mortem brain tissue for decreased number of hippocampal nicotinic receptors in schizophrenia. *Biol Psychiatry* 38, 22 – 33 (1995)

23. **a)** Berkowic S.; Curtis L.; Bertrand D. Neuronal nicotinic receptor channel dysfunction in human epilepsy syndrome, In *Neuronal Nicotinic receptors: Pharmacology and Therapeutic Opportunities* (Arneric S.P.; Brioni J.D. eds) pp 287 – 306, Wiley-Liss, New York (1998)
b) Hirose S.; Iwata H.; Akiyoshi H.; Kobayashi K.; Ito M.; Wada K.; Kaneko S.; Mitsudome A. A novel mutation of CHRNA4 responsible for autosomal dominant nocturnal frontal lobe epilepsy. *Neurology* 53, 1749 – 1753 (1999)
c) McLellan A.; Phillips H.A.; Rittey C.; Kirkpatrick M.; Mulley J.C.; Goudie D.; Stephenson J.B.; Tolmie J.; Scheffer I.E.; Berkovic S.F.; Zuberi S.M. Phenotypic comparison of two Scottish families with mutation in different genes causing autosomal dominant noctrurnal front lobe epilepsy. *Epilepsia* 44, 613 – 617 (2003)
d) De Fusco M.; Becchetti A.; Patrignani A.; Annesi G.; Gambardella A.; Quattrone A.; Ballabio A.; Wanke E.; Casari G. The nicotinic receptor beta2 subunit is mutant in nocturnal frontal lobe epilepsy. *Nat Genet* 26, 275 – 276 (2000)

24. Sutor B.; Zolles G. Neuronal nicotinic acetylcholine receptors and autosomal dominant nocturnal front lobe epilepsy: a critical review. *Pflugers Arch* 442, 642 – 651 (2001)

25. Gahring L.C.; Persiyanov K.; Dunn D.; Weiss R.; Meyer E.L.; Rogers S.W. Mouse-strain-specific nicotinic acetylcholine receptor expression by inhibitory interneurons anda strocytes in the dorsal hippocampus. *J Comp Neurol* 468, 334 – 346 (2004)

26. Breslau N. Psychiatric comorbidity of smoking and nicotine dependence. *Behav Genet* 25, 95 – 103 (1995)

27. Pomerleau O.F.; Downey K.K.; Stelson F.W.; Pomerleau C.S. Cigarette smoking in adult patients diagnosed with attention deficit hyperactivity disorder. *J Subst Abuse* 7, 373 – 378 (1995)

28. Delacourte A.; Defossez A. Alzheimer's disease: Tau proteins, the promoting factors of microtubule assembly, are major components of paired helical filaments. *J Neurol Sci* 76, 173-186 (1986)

29. Coyle J.T.; Price D.L.; DeLong M.R. Alzheiner's disease: a disorder of cortical cholinergic innervation. *Science* 219, 1184 – 1190 (1983)

30. **a)** Sihver W.; Gillberg P.G.; Svensson A.L.; Nordberg A. Autoradiographic comparison of [^{3}H](-)nicotine, [^{3}H]cytisine and [^{3}H]epibatidine binding in relation to vesicular acetylcholine transport sites in the temporal cortex in Alzheimer disease. *Neuroscience* 94, 685 – 696 (1999)
b) Warpman U.; Nordberg A. Epibatidine and ABT-418 reveal selective losses of alpha4beta2 nicotinic receptors in Alzheimer brains. *Neuroreport* 6, 2419 - 2423 (1995)

31. **a)** Allen Y.S.; Devanathan P.H.; Owen G.P. Neurotoxicity of beta-amyloid protein: cytochemical changes and apoptotic cell death investigated in organotypic cultures. *Clin Exp Pharmacol Physiol* 22, 370 – 371 (1995)
b) Forloni G. Neurotoxicity of beta-amyloid and prion peptides. *Curr Opin Neurol* 9, 492 – 500 (1996)
c) McKee A.C.; Kowall N.W.; Schumacher J.S.; Beal M.F. The neurotoxicity of amyloid beta protein in aged primates. *Amyloid* 5, 1 – 9 (1998)

32. **a)** Quik M.; Jeyarasasingam G. Nicotinic receptors and Parkinson's disease. *Eur J Pharmacol* 393, 223 – 230 (2000)
b) Lichtensteiger W.; Hefti F.; Felix D.; Huwyler T.; Melamed E.; Schlumpf M. Stimulation of nigrostriatal dopamine neurones by nicotine. *Neuropharmacology* 21, 963 – 968 (1982)

33. Kita T.; Okamoto M.; Nakashima T. Nicotine-induced sensitization to ambulatory stimulant effect produced by daily administration into the ventral tegmental area and the nucleus accumbens in rats. *Life Sci* 50, 583 – 590 (1992)

34. Mihailescu S.; Palomero-Rivero M.; Meade-Huerta P.; Maza-Flores A.; Drucker-Colin R. Effects of nicotine and mecamylamine on rat dorsal raphe neurons. *Eur J Pharmacol* 360, 31 – 36 (1998)

35. Tanner C.M.; Goldman S.M.; Aston D.A.; Ottman R.; ellenberg J.; Mayeux R.; Langston J.W. Smoking and Parkinson's disease in twins. *Neurology* 58, 581 – 588 (2002)

36. Brioni, J. D.; Decker, M. W.; Sullivan, J. P.; Arneric, S. P. The pharmacology of (-)-nicotine and novel cholinergic modulators. *Adv Pharmacol* 37, 153-214 (1997)

37. Sullivan J.P.; Briggs C.A.; Donelly-Roberts D.; Brioni J.D.; Radek R.J.; McKenna D.G.; Campbell J.E.; Arneric S.P.; Decker M.W. (+)-Epibatidine can diffetentially evoke responses mediated by putative subtypes of nicotinic acetylcholine receptors (nAChR) ligands in the rat tail-flick assay. *Med Chem Res* 4, 502 – 516 (1994)

38. **a)** Thatte U. ABT-594. *Curr Opin CPNS Drugs* 2, 227 – 234 (2000)
b) Sorbera L.A.; Revel L.; Leeson P.A.; Castaner J. ABT-594, Treatment of neuropathic pain, nicotinic agonist. *Drugs Fut* 26, 927 – 934 (2001)

39. Boyce S.; Webb J.K.; Shepheard S.L.; Russell M.G.N.; Hill R.G.; Rupniak N.M.J. Analgesic and toxic effects of ABT-594 resemble epibatidine and nicotine in rats. *Pain* 85, 443 – 450 (2000)

40. Taylor A.L.; Bettcher D.W. WHO Framework Convention on Tobacco
Control: a global ''good'' for public health. *Bull World Health Organ* 78, 920 – 929 (2000)

41. **a)** Di Ciara G. Role of dopamine in the behavioural actions o nicotine related to addiction. *Eur J Pharmacol* 393, 295 – 314 (2000)
b) Dani J.A.; De Biasi M. Cellular mechanisms of nicotine addiction. *Pharmacol Biochem Behav* 70, 439 – 446 (2001)

42. Carey J.; Ariniello L.; McComb M. Brain Facts. A primer on the brain and nervous system. *The Society for Neuroscience* 2002

43. **a)** Cryan J.F.; Gasparinia F.; van Heekeb G.; Markou A. Non-nicotinic neuropharmacological strategies for nicotine dependence: beyond bupropion *Drug Disc Today* 8, 1025 - 1034 (2003)
b) Domino E.F. Round table on nicotinic receptors in addiction: summary report. *Eur J Pharmacol* 393, 315 – 320 (2000)

44. **a)** Hogg R.C.; Bertrand D. Nicotinic acetylcholine receptors as drug targets. *Curr Drug Targets – CNS & Neurological Disorders* 3, 123 – 130 (2004)
b) Youdim M.B.H.; Buccafusco J.J. CNS targets for multi-functional drugs treatment of Alzheimer's and Parkinson's diseases. *J Neural Transm* 2005 (early view)
c) Newhouse P.; Singh A.; Potter A. Nicotine and nicotinic receptor involvement in neupsychiatric disorders. *Curr Topics Med Chem* 4, 267 – 282 (2004)
d) Jain K.K. Modulators of nicotinic acetylcholine receptors as analgesics. *Curr Opin Inv Drugs* 5, 76 – 81 (2004)
e) Decker M.W.; Rueter L.E.; Bitner R.S. Nicotinic acetylcholine receptor agonists: a potential new class of analgesics. *Curr Topics Med Chem*,4, 369 – 384 (2004)
f) Toma L.; Barlocco D.; Gelain A. Neuronal nicotinic acetylcholine receptor agonists. *Expert Opin Ther Patents* 14, 1029 – 1040 (2004)
g) Suto M.J.; Zacharias N. Neuronal nicotinic acetylcholine receptors as drug targets. *Expert Opin Ther Targets* 8, 61 – 64 (2004)
h) Bunnelle W.H.; Decker M.W. Neuronal nicotinic acetylcholine receptor ligands as potential analgesics. *Expert Opin Ther Patents* 13, 1003 – 1021 (2003)
i) Foulds J.; Burke M.; Steinberg M.; Williams J.M.; Ziedonis D.M. Advances in pharmacotherapy for tobacco dependence. *Expert Opin Emerg Drugs* 9, 39 – 53 (2004)

45. **a)** Bunnelle W.H.; Dart M.J.; Schrimpf M.R. Design of ligands for the nicotinic acetylcholine receptors, the quest for selectivity. *Curr Topics Med Chem* 4, 299 – 334 (2004)
b) Glennon R.A.; Dukat M. Central nicotinic ligands and pharmacophores. *Pharm Acta Helv* 74, 103 – 114 (2000)
c) Breining S.R. Recent developments in the synthesis of nicotinic acetylcholine receptors ligands. *Curr Top Med Chem* 4, 609 - 629 (2004)

46. Schmitt J.D. Exploring the nature of molecular recognition in nicotinic acetylcholine receptors. *Curr Med Chem* 7, 749 – 800 (2000)

47. Papke R.L.; Bencherif M.; Lippiello P. An evaluation of neuronal nicotinic acetylcholine receptor activation by quartenary nitrogen compounds indicates that choline is selective for the alpha 7 subtype. *Neurosci Lett* 213, 201 – 201 (1996)

48. Marks M.J.; Stitzel J.A.; Romm E.; Wehner J.M.; Collins C. Nicotinic binding sites in rat and mouse brain: comparison of acetylcholine, nicotine and α-bungarotoxin. *Mol Pharmacol* 30, 427 – 436 (1986)

49. Jensen A.A.; Mikkelsen I.; Frølund B.; Bräuner-Osborne H.; Falch E.; Krogsgaard-Larsen P. Carbamoylcholine homologs: Novel and potent agonists at the neuronal nicotinic acetylcholine receptors. *Mol Pharmacol* 64, 865 – 875 (2003)

50. Boksa P.; Quik M.; Mitchell J.B.; Collier B.; O'Neil W.; Quirion R. Pharmacological activity of N-methyl-carbamylcholine, a novel acetylcholine receptor agonist with selectivity for nicotinic receptors. *Eur J Pharmacol* 173, 93 – 108 (1989)

51. Abood L.G.; Grassi S. [^{3}H]Methylcarbamylcholine, a new radioligand for studying brain nicotinic receptors. *Biochem Pharmacol* 35, 4199 – 4202 (1986)

52. Alkondon M.; Pereira E.F.R.; Cortes W.S.; Maelicke A.; Albuquerque E. Choline is a selective agonist of alpha7 nicotinic acetylcholine receptors in the rat brain neurons. *Eur J Neurosci* 9, 2734 – 2742 (1997)

53. Jonnala R.R.; Graham J.H.; Terry A.V.; Beach J.W.; Young J.A.; Buccafusco J.J. Relative levels of cytoprotection produced by analog of choline and the role α7-nicotinic acetylcholine receptor. *Synapse* 47, 262 – 269 (2003)

54. Renshaw R.R.; Armstrong W.D. Basis for the physiological activity of onium compounds. *J Biol Chem* 103, 187 – 189 (1933)

55. Andrä M.; Tilotta C.M.; Gündisch D. *Drugs Fut.* 27(Suppl. A), P113 (2002)

56. Dukat M.; Fiedler W.; Dumas D.; Damaj I.; Martin B.R.; Rosecrans J.A.; James J.R.; Glennon R.A. Pyrrolidine-modified and 6-substituted analogs of nicotine: a structure-affinity investigation. *Eur J Med Chem* 31, 875 – 888 (1996)

57. Bencherif M.; Byrd G.; Caldwell W.S.; Hayes J.R.; Lippiello P.M. Pharmacological characterization of RJR-2403: A nicotinic agonist with potential therapeutic benefit in the treatment of Alzheimer's disease. *CNS Drug Rev* 3, 325 – 345 (1997)

58. **a)** Bencherif M.; Caldwell W.S.; Dull W.S.; Lippiello P.M.; Crooks P.A.; Bhatti B.S.; Deo N.M.; Ravard A. Preparation of 2-azabicyclo[2.2.1]hept-5-ene and 2-azabicyclo[2.2.2]oct-5-ene compounds for use in pharmaceutical composition for prevention and treatment of central nervous system disorders. *WO96/36637* (1996)
b) Crooks P.A.; Caldwell W.S.; Dull G.M.; Bhatti B.S. Pharmaceutical composition for prevention and treatment of central nervous system disorders. *WO96/20929* (1996)

59. Gatto G.J.; Bohme G.A.; Caldwell W.S.; Letchworth S.R.; Traina V.M.; Obinu M.C.; Laville M.; Reibaud M.; Pradier L.; Dunbar G.; Bencherif M. TC-1734: An orally active neuronal nicotinic acetylcholine receptor modulator with antidepressant, neuroprotective and long-lasting cognitive effects. *CNS Drug Rev* 10, 147 – 166 (2004)

60. **a)** Lippiello P.M.; Fernandes K.G. The binding of L-[^{3}H]nicotine to a single class of high affinity sites in rat brain membranes. *Mol Pharmacol* 29, 448-454 (1986)
b) Boksa P.; Quirion R. [^{3}H]-N-methyl-carbamylcholine, a new radioligand specific for nicotinic acetylcholine receptors in brain. *Eur J Pharmacol* 139, 323 – 333 (139)

61. Garcha H.S.; Thomas P.; Spivak C.E.; Wonnacott S.; Stolerman I.P. Behavioural and ligand-binding studies in rtas with 1-acetyl-4-methylpiperazine, a novel nicotinic agonist. *Psychopharmacology* 110, 347 – 354 (1993)

62. **a)** Manetti D.; Bartolini A.; Borea P.A.; Bellucci C.; Dei S.; Ghelardini C.; Gualtieri F.; Romanelli M.N.; Scapecchi S.; Teodori E.; Varani K. Hybridized and isosteric analogues of N^1-acetyl-N^4-dimethylpiperazinium iodide (ADMP) and N^1-phenyl-N^4-dimethylpiperazinium iodide (DMPP) with central nicotinic action. *Bioorg Med Chem* 7, 457 – 465 (1999)
b) Romanelli M.N.; Manetti D.; Scapecchi S.; Borea P.A.; Dei S.; Bartolini A.; Ghelardini C.; Gualtieri F.; Guandalini L.; Varani K. Structure-activity relationships of a unique nicotinic ligand: N^1-dimethyl-N^4-phenylpiperazinium iodide (DMPP). *J Med Chem* 44, 3946 – 3946 (2001)

63. **a)** Wang D.X.; Booth H.; Lerner-Marmarosh N.; Osdene T.S.; Abood L. Structure-activity relationships for nicotine analogs comparing to competition for [^{3}H]-nicotine binding and psychotropic potency. *Drug Dev Res* 45, 10 – 16 (1998)
b) Glennon R.A.; Maarouf A.; Fahmy S.M.; Fan F.; Yousif M.; Shafik R.; Dukat M. Structure activity relationships of simple nicotine analogs. *Med Chem Res* 2, 546 – 551 (1993)
c) Glassco W.; May E.L.; Damaj M.I.; Martin B.R. In vivo and in vitro activity of some N-substituted (±)nornicotine analogs. *Med Chem Res* 4, 273 – 282 (1994)
d) Lin N.-H.; Carrera J.G.M.; Anderson D.J. Synthesis and evaluation of nicotine analogs as neuronal nicotinic acetylcholine receptor ligands. *J Med Chem* 37, 3542 – 3553 (1994)
e) Kim K.H.; Lin N.-H.; Anderson D.A. Quantitative structure activity relationships of nicotine analogues as neuronal nicotinic acetylcholine receptor ligands. *Bioorg Med Chem Lett* 4, 2211 – 2217 (1996)

64. Kem W.R.; Mahnir V.M.; Papke R.L.; Lingle C.J. Anabaseine is a potent agonist on muscle and neuronal alpha-bungarotoxin-sensitive nicotinic receptors. *J Phar Exp Ther* 283, 979 – 992 (1997)

65. Kem W.R. Anabaseine as a molecular model for design of α7 nicotinic receptor agonist drugs. In *Perspectives in molecular toxicology*; Ménez, A. Ed. John Wiley Sons: New York, pp 297 – 314 (2002)

66. **a)** De Fiebre C.M.; Meyer E.M.; Henry J.C.; Muraskin S.I.; Kem W.R.; Papke R.L. Characterization of a series of anabaseine-derived compounds reveals that the 3-(4)-dimethylaminocinnamylidine derivative is a selective agonist at neuronal nicotinic $\alpha 7/^{125}$I-α-bungarotoxin receptor subtypes. *Mol Pharmacol* 47, 164 – 171 (1995)
b) Meyer E.M.; Kuryatov A.; Gerzanich V.; Lindstrom J.; PapkeR.L. Analysis of 3-(4-hydroxy-4-2-methoxybenzilidine)anabaseine. Selectivity and activity at human and rat alpha-7 nicotinic receptors. *J Pharmacol Exp Ther* 287, 918 – 925 (1998)
c) Meyer E.M.; Tay E.T.; Zoltewicz J.A.; Meyers C.; King M.A.; Papke R.L.; De Fiebre C.M. Neuroprotective and memory-related actions of novel alpha-7 nicotinic agents with different mixed agonist/antagonist properties. *J Pharmacol Exp Ther* 284, 1026 – 1034 (1998)

67. Cosford N.D.P.; Bleicher L.; Herbaut A.; McCallum J.S.; Vernier J.-M.; Dawson H.; Whitten J.P.; Adams P.; Chavez-Noriega L.; Correa L.D.; Crona J.H.; Mahaffy L.S.; Menzaghi F.; Rao T.S.; Reid R.; Sacaan A.I.; Santori E.; Stauderman K.A.; Whelan K.; Lloyd G.K.; McDonald I.A. (S)-(-)-5-Ethynyl-3-(1-methyl-2-pyrrolidinyl)pyridine maleate (SIB-1508Y): A novel antiparkinsonian agent with selectivity for neuronal nicotinic acetylcholine receptors. *J Med Chem* 39, 3235 – 3237 (1996)

68. Cosford N.D.P.; Bleicher L.; Vernier J.-M.; Chavez-Noriega L.; Rao T.S.; Siegel R.S.; Suto C.; Washburn M.; McDonald I.A. Recombinant human receptors and functional assays in the discovery of altinicline (SIB-1508Y), a novel acetylcholine-gated ion channel (nAChR) agonist. *Pharm Acta Helv* 74, 125 – 130 (2000)

69. Dukat M.; Dowd M.; Damaj M.I.; Martin B.; El-Zahabi M.A.; Glennon R.A. Synthesis, receptor binding and QSAR studies on 6-substituted nicotine derivatives as cholinergic ligands. *Eur J Med Chem* 34, 31 - 40 (1999)

70. Ramunno A.; Dukat M.; Lee M.; Young R.; El-Zahabi M.; Damaj M.I.; Martin B.; Glennon R.A. 6-(2-Phenylethyl)nicotine: A novel nicotinic cholinergic receptor ligand. *Bioorg Med Chem Lett* 15, 3237 – 3240 (2005)

71. **a)** Garvey D.S.; Wasicak J.T.; Decker M.W.; Brioni J.D.; Buckley M.J.; Sullivan J.P.; Carrera G.M.; Holladay M.W.; Arneric S.P.; Williams M. Novel isoxazoles which interact with brain cholinergic channel receptors have instrictic cognitive enhancing and anxiolytic activities. *J Med Chem* 37, 1055 – 1059 (1994)
b) Lin N.-H.; He Y.; Arneric S.P.; Sullivan J.P. Synthesis and structure-activity relationships of 2'-(R)- and (S) pyrrolidine-modified analogs of the cholinergic channel activator, ABT-418. *Bioorg Med Chem Lett* 5, 1141 – 1146 (1995)

72. Arneric S.P.; Anderson D.J.; Bannon A.W.; Briggs C.A.; Buccafusco J.J.; Brioni J.D.; Decker M.W.; Donnelly-Roberts D.; Gopalakrishnan M.; Holladay M.W.; Kyncl J.; marsh K.C.; Pauly J.; Radek R.J.; Rodrigues D.; Sullivan J.P. Preclinical pharmacology of ABT-418: A prototypical cholinergic channel activator for the potential treatment of Alzheimer's disease. *CNS Drug Rev* 1, 1 – 26 (1995)

73. Williams M.; Davis R.E. Alzheimer's disease and related dementias: prospects for treatment. *Exp Opin Invest Drugs* 6, 735 – 757 (1997)

74. **a)** Abreo M.A.; Lin N.H.; Garvey D.S.; Gunn D.E.; Hettinger A.M.; wasicak J.T.; Pavlik P.A.; Martin Y.C.; Donnelly-Roberts D.L.; Anderson D.J.; Campbell J.E.; Piattoni-Kaplan M.; Sullivan J.P.; Williams M.; Arneric S.P.; Holladay M.W. Novel 3-pyridyl ethers with subnanomolar affinity for central nicotinic acetylcholine receptors. *J Med Chem* 39, 817 – 825 (1996)
b) Lin N.-H.; Gunn D.E.; Ryther K.B.; Garvey D.S.; Donnelly-Roberts D.; Decker M.W.; Brioni J.D.; Buckley M.J.; Rodrigues D.; Marsh K.G.; Anderson D.J.; Buccafusco J.J.; Prendergast M.A.; Sullivan J.P.; Williams M.; Arneric S.P.; Holladay M.W. Structure-activity studies on 2-methyl-3-(2(S)-pyrrolidinylmethoxy)pyridine (ABT-089): An orally bioavailable 3-pyridylether nicotinic acetylchoine receptor ligand with cognition-enhancing properties. *J Med Chem* 40, 385 – 390 (1997)

75. Sullivan J.P.; Donnelly-Roberts D.L.; Briggs C.A.; Anderson D.J.; Gopalakrishnan M.; Piattoni-Kaplan M.; Campbell J.E.; McKenna D.G.; Molinari E.; Hettinger A.-M.; Garvey D.S.; Wasicak J.T.; Holladay M.W.; Williams M.; Arneric S.P. A-85380 [3-(2(S)-azetidinylmethoxy)pyridine]: *In vitro* pharmacological properties of a novel, high affinity α4β2 nicotinic acetylcholine receptor ligand. *Neuropharmacology* 35, 725 – 734 (1996)

76. Holladay M.W.; Wasicak J.T.; Lin N.-H.; He Y.; Ryther K.B.; Bannon M.J.; Kim D.J.B.; Decker M.W.; Anderson D.J.; Campbell J.E.; Kuntzweiler T.A.; Donnelly-Roberts D.L.; Piattoni-Kaplan M.; Briggs C.A.; Williams M.; Arneric S.P. Identification and structure-activity relationships of (R)-5-(2-azetidinylmethoxy)-2-chloropyridine (ABT-594), a potent, orally active non-opiate analgesic agent acting via neuronal acetylcholine receptors. *J Med Chem* 41, 407 – 412 (1998)

77. Donnelly-Roberts D.L.; Puttfarcken P.S.; Kuntzweiler T.A.; Briggs C.A.; Anderson D.J.; Campbell J.E.; Piattoni-Kaplan M.; McKenna D.G.; Wasicak J.T.; Holladay M.W.; Williams M.; Arneric S.P. ABT-594 [(R)-5-(2-azetidinylmethoxy)-2-chloropyridine]: A novel, orally effective analgesic acting via neuronal nicotinic acetylcholine receptors: I. *In vitro* characterization. *J Pharm Exp Ther* 285, 777 – 786 (1998)

78. **a)** Badio B.; Shi D.; Garraffo M.; Daly J.W. Antinociceptive effects of the alkaloid epibatidine: Further studies on involvement of nicotinic receptors. *Drug Dev Res* 36, 46 – 59 (1995)

b) Damaj M.I.; Glassco W.; Dukat M.; May E.L.; Glennon R.A.; Martin B.R. Pharmacology of novel nicotinic analogs. *Drug Dev Res* 38, 177 - 187 (1996)

c) Carroll F.I.; Liang F.; Navarro H.A.; Brieaddy L.E.; Abraham P.; Damaj M.I., Martin B.R. Synthesis, nicotinic acetylcholine receptor binding and antinociceptive properties of 2-exo-2-(2'-substituted 5'-pyridinyl)-7-azabicyclo[2.2.1]heptanes: Epibatidine analogues. *J Med Chem* 44, 2229 – 2237 (2001)

79. Spande T.F.; Garraffo H.M.; Edwards M.W.; Yeh H.J.C.; Panel L.; Daly J.W. Epibatidine: A novel (chloropyridyl)azabicycloheptane with potent analgesic activity from an Ecuadorian poison frog. *J Am Chem Soc* 114, 3475 – 3478 (1992)

80. Carroll F.I. Epibatidine structure-activity relationship. *Bioorg Med Chem Lett* 14, 1889 – 1896 (2004)

81. **a)** Li T.; Qian C.; Eckman J.; Huang D.F.; Shen T.Y. The analgesic effect of epibatidine and isomers. *Bioorg Med Chem Lett* 3, 2759 - 2764 (1993)

b) Horti A.G.; Scheffel U.; Kimes A.S.; Musachio J.L.; Ravert H.T.; Mathews W.B.; Zhan Y.; Finley P.A.; London E.D.; Dannals R.F. Synthesis and Evaluation of *N*-[^{11}C]Methylated Analogues of Epibatidine as Tracers for Positron Emission Tomographic Studies of Nicotinic Acetylcholine Receptors. *J Med Chem* 41, 4199 - 4206 (1998)

82. **a)** Carroll F.I.; Lee J.R.; Navarro H.A.; Brieaddy L. E.; Abraham P.; Damaj M.I., Martin B.R. Synthesis, nicotinic acetylcholine receptor binding and antinociceptive properties of 2-exo-2-(2'-substituted-3'-phenyl- 5'-pyridinyl)-7-azabicyclo[2.2.1] heptanes: Novel nicotinic antagonist *J Med Chem* 44, 4039 – 4041 (2001)

b) Carroll F.I.; Lee J.R.; Navarro H.A.; Ma W.; Brieaddy E.; Abraham P.; Damaj M.I., Martin B.R. Synthesis, Nicotinic Acetylcholine receptor binding and antinociceptive properties of 2-exo-2-(2',3'-disubstituted 5'-pyridinyl)-7-azabicyclo[2.2.1]heptanes: Epibatidine analogues. *J Med Chem* 45, 4755 – 4761 (2002)

c) Carroll F.I.; Ware R.; Brieaddy L.E.; Navarro H.A.; Damaj M.I., Martin B.R. Synthesis, nicotinic acetylcholine receptor binding, and antinociceptive properties of 2'-fluoro-3'-(substituted phenyl)deschloroepibatidine analogues. Novel nicotinic antagonist *J Med Chem* 47, 4588 – 4594 (2004)

d) Carroll F.I.; Ma W.; Yokota Y.; Lee J.R.; Brieaddy L.E.; Navarro H.A.; Damaj M.I., Martin B.R. Synthesis, nicotinic acetylcholine receptor binding and antinociceptive properties of 3'-substituted deschloroepibatidine analogues.Novel nicotinic antagonist *J Med Chem* 48, 1221 – 1228 (2005)

83. Badio B.; Garaffo H.M.; Plummer C.V.; Padgett W.L.; Daly J.W. Synthesis and nicotinic activity of epiboxidine: an isoxazole analogue of epibatidine. *Eur J Pharmacol* 321, 189 – 194 (1997)

84. Che C.; Petit G.; Kotzyba-Hibert F.; Bertrand S.; Bertrand D.; Grutter T.; Goeldner M. Syntheses and biological properties of cysteine-reactive epibatidine derivatives. *Bioorg Med Chem Lett* 13, 1001- 1004 (2003)

85. **a)** Krow G.R.; Cheung O.H.; Hu Z.; Huang Q.; Hutchinson J.; Liu N.; Nguyen K.T.; Ulrich S.; Yuan J.; Xiao Y.; Wypij D.M.; Zuo F.; Carroll P.J. Nitrogen bridge homoepibatidines. *syn*-6- and *syn*-5(6-chloro-3-pyridyl)isoquinuclidines. *Tetrahedron* 55, 7747 – 7756 (1999)
b) Malpass J.R.; Hemmings D.A.; Wallis A.L.; Fletcher S.R.; Patel S. Synthesis and nicotinic acetylcholine-binding properties of epibatidine homologues: homoepibatidine and dihomoepibatidine. *J Chem Soc Perkin Trans* 1, 1044 - 1051 (2001)
c) Zhang C.; Gyermek L.; Trudell M.L. Synthesis of optically pure epibatidine analogs: (1*R*, 2*R*, 5*S*)-2β-(2-chloro-5-pyridinyl)-8-azabicyclo[3.2.1]octane and (1*R*, 2*S*, 5*S*)-2α-(2-chloro-5-pyridinyl)-8-azabicyclo[3.2.1]octane from (-)-cocaine *Tetrahedron Lett* 38, 5619 - 5622 (1997)

86. **a)** Wei Z.-L., Petukhov P.A.; Xiao Y.; Tuckmantel W.; George C.; Kellar K.J.; Kozikowski A.P. Synthesis, Nicotinic Acetylcholine Receptor Binding Affinities, and Molecular Modeling of Constrained Epibatidine Analogues. *J Med Chem* 46, 921 - 924 (2003)
b) Abe H.; Arai Y.; Aoyagi S.; Kibayashi C. Synthesis of conformationally constrained spirodihydrofuropyridine analogues of epibatidine. *Tetrahedron Lett* 44, 2971 - 2973 (2003)
c) Lennox J.R.; Turner S.C.; Rapoport H. Enantiospecific Synthesis of Annulated Nicotine Analogues from D-Glutamic Acid. 7-Azabicyclo[2.2.1]heptano[2.3-*c*]pyridines *J Org Chem* 66, 7078 – 7083 (2001)

87. **a)** Carmichael W.W.; Biggs D.F.; Gorham P.R.; Toxicology and pharmacological action of Anabaena flos-aquae toxin. *Science* 187, 384 – 544 (1975)
b) Spivak C.E.; Witkop B.; Albuquerque E.X.; Anatoxin-a: A novel, potent agonist at the nicotinic receptor. *Mol Pharmacol* 18, 384 – 394 (1980)

88. Wonnacot S.; Jackman S.; Swanson K.L.; Rapoport H.; Albuquerque E.D. Nicotinic pharmacology of anatoxin analogs. II. Side chain structure-activity relationships at neuronal nicotinic ligand binding sites. *J Pharmacol Exp Ther* 259, 387 – 391 (1991)

89. Gündisch D.; Harms K.; Schwarz S.; Seitz G.; Stubbs M.T.; Wegge T. Synthesis and evaluation of diazine containing bioisosteres of (-)-ferruginine as ligands for nicotinic acetylcholine receptors. *Bioorg Med Chem* 9, 2683 – 2691 (2001)

90. Thomas P.; Stephens M.; Wilkie G.; Amar M.; Lunt G.G.; Whiting P.; Gallagher T.; Pereira E.; Alkodon M.; Albuquerque E.X.; Wonacott S. (+)-Anatoxin-a is a potent agonist at neuronal nicotinic acetylcholine receptors. *J Neurochem* 60, 2308 – 2311 (1993)

91. **a)** Thomas P.; Brough P.A.; Gallagher T.; Wonacott S. Alkyl-modified side chain variants of anatoxin-a: A series of potent nicotinic agonists. *Drug Dev Res* 31, 147 – 156 (1994)
b) Hernandez A.; Rapoport H. Conformationally constrained analogs of anatoxin. Chirospecific synthesis of s-trans carbonyl ring-fused analogs. *J Org Chem* 59, 1058 – 1066 (1994)

92. Gündisch D.; Kämpchen T.; Schwarz S.; Seitz G.; Siegl J.; Wegge T. Syntheses and evaluation of pyridazine and pyrimidine containing bioisosteres of (±)-pyrido[3.4-b]homotropane and pyrido-[3.4-b]tropane as novel nAChR ligands. *Bioorg Med Chem* 10, 1-9 (2002)

93. **a)** Reavill C.; Walther B.; Stolerman I.P.; Testa B. Behavioural and pharmacokinetic studies on nicotine, cytisine and lobeline. *Neuropharmacology* 29, 619 – 624 (1990)

b) Decker M.W.; Brioni J.D.; Bannon A.W.; Arneric S.P. Diversity of neuronal nicotinic acetylcholine receptors: lessons from behaviour and implications for CNS therapeutics. *Life Science* 56, 545 – 570 (1995)

94. Damaj M.I.; Patrick G.S.; Creasy K.R.; Martin B.R. Pharmacology of lobeline, a nicotinic receptor ligand. *J Phar Exp Ther* 282, 410 – 419 (1997)

95. Miller D.K.; Crooks P.A.; Dwoskin L.P. Lobeline inhibits nicotine-evoked [^{3}H]dopamine overflow from rat striatal slices and nicotine-evoked $^{86}Rb^{+}$ efflux from thalamic synaptosomes. *Neuropharmacology* 39, 2654 – 2662 (2000)

96. **a)** Barlow R.B.; Johnson O. Relations between structure and nicotine-like activity: X-ray crystal structure analysis of (-)-cytisine and (-)-lobeline hydrochlorid and a comparison with (-)-nicotine and other nicotine-like compounds. *Br J Pharmacol* 98, 799 – 808 (1989)

b) Flammia D.; Dukat M.; Damaj M.I.; Martin B.; Glennon R.A. Lobeline: Structure-affinity investigation of nicotinic acetylcholinergic receptor binding. *J Med Chem* 42, 3726 – 3731 (1999)

97. **a)** Beach J.W.; McCurdy C.R.; Gattu M.; Boss K.L.; Templeton O.E.; Terry A.V. Jr. Synthesis and receptor binding of N-substituted-2-styryl-1,2,3,6-tetrahydropyridines as potential nicotinic agonists. *Med Chem Res* 7, 271 – 281 (1997)

b) Terry A.V. Jr.; Williamson R.; Gattu M.; Beach J.W.; McCurdy C.R.; Sparks J.A.; Pauly J.R. Lobeline and structurally simplified analogs exhibit diferential agonist activity and sensitivity to anatagonist blockade when compared to nicotine. *Neuropharmaco*l 37, 93 – 102 (1998)

98. Zheng G.; Dwoskin L.P.; Deaciuc A.G.; Zhu J.; Jones M.D.; Crooks P.A. Lobelane analogues as novel ligands for the vesicular monoamine transporter-2. *Bioorg Med Chem* 13, 3899 – 3909 (2005)

99. Ward J.M.; Cockcroft V.B.; Lunt G.G.; Smillie F.S.; Wonnacott S. Methyllycaconitine a selective probe for neuronal α-bungarotoxin binding sites. *FEBS* 270, 45 – 48 (1990)

100. Coates P.A.; Blagbrough I.S.; Hardick D.J.; Rowan M.G.; Wonnacott S.; Potter B.V.L. Rapid and efficient isolation of the nicotinic receptor atagonist methyllycaconitine from Delphinium: Assignment of the methylsuccinimide absolute stereochemistry as S. *Tetrahedron Lett* 35, 8701 – 8704 (1994)

101. Hardick D.J.; Cooper G.; Scott-Ward T.; Blagbrough I.S.; Potter B.V.L.; Wonnacott S. Conversion of the sodium channel activator aconitine into a potent α7-selective ligand. *FEBS Lett* 365, 79 – 82 (1995)

102. **a)** Davies A.R.L.; Hardick D.J.; Blagbrough I.S.; Potter B.V.; Wolstenholme A.J.; Wonnacott S. Characterization of the binding of [^{3}H]methyllycaconitine: a new radioligand for labelling α7-type neuronal nicotinic acetylcholine receptors. *Neuropharmacol* 38, 679 – 690 (1999)

b) Navarro H.A.; Zhong D.; Abraham P.; Xu H.; Carroll F.I. Synthesis and pharmacological characterization of [^{125}I]iodomethyllycaconitine ([^{125}I]iodo-MLA). A new ligand for the α7 nicotinic acetylcholine receptor. *J Med Chem* 43, 142 – 145 (2000)

103. Chavez-Noriega L.E.; Crona J.H.; Washburn M.S.; Urrutia A.; Elliott K.J.; Johnson E.C. Pharmacological characterization of recombinant human neuronal nicotinic acetylcholine receptors hα2β2, hα2β4, hα3β2, hα3β4, hα4β4 and hα7 expressed in Xenopus oocytes. *J Pharmacol Exp Ther* 280, 346 – 356 (1997)

104. Mullen G.; Napier J.; Balestra M.; DeCory T.; Hale G.; Macor J.; Mack R.; Loch J.; Wu E.; Kover A.; Verhoest P.; Sampognaro A.; Phillips E.; Zhu Y.; Murray R.; Griffith R.; Blosser J.; Gurley D.; Machulskis A.; Zongrone J.; Rosen A.; Gordon J. (-)-Spiro[1-azabicyclo[2.2.2]octane-3,5'-oxazolidin-2'-one], a conformationaly resticted analogue of acetylcholine, is a highly selective full agonist at the α7 nicotinic acetylcholine receptor. *J Med Chem* 43, 4045 – 4050 (2000)

105. Levin E.D.; Bettegowda C.; Blosser J.; Gordon J. AR-R1779, an alpha7 nicotinic agonist, improves learning and memory in rats. *Behav Pharmacol* 10, 675 – 680 (1999)

106. Grottick A.J.; Higgins G.A. Effect of subtype selective nicotinic compounds on attention as assessed by the five-choice serial reaction time task. *Behav Brain Res* 117, 197 – 208 (2000)

107. Beers W.H.; Reich E. Structure and activity of acetylcholine. *Nature* (London) 225, 917 – 922 (1970)

108. Sheridan R.P.; Nilakantan R.; Dixon J.S., Venkataraghavan R. The ensemble approach to distance geometry: Application to the nicotinic pharmacophore. *J Med Chem* 29, 899 – 906 (1986)

109. Holladay, M. W.; Dart, M. J ; Lynch, J. K. Neuronal nicotinic acetylcholine receptors as targets for drug discovery. *J Med Chem* 40, 4169-4194 (1997)

110. Tønder J.E.; Hansen J.B.; Begtrup M.; Pettersson I.; Rimvall K.; Christensen B.; Ehbar U.; Olesen P.H. Improving the nicotinic pharmacophore with series of (isoxazole)methylene-1-azacyclic compounds: synthesis, structure-activity and molecular modelling. *J Med Chem* 42, 4970 – 4980 (1999)

111. Tønder J.E.; Olesen P.H.; Hansen J.B.; Begtrup M.; Pettersson I. An improved nicotinic pharmacophore and a stereoselective CoMFA-model for nicotinic agonists acting at the central nicotinic acetylcholine receptors. *J Comp-Aided Mol Des* 15, 247 – 258 (2001)

112. Tønder J.E.; Olesen P.H. Agonists at α4β2 nicotinic acetylcholine receptors: Structure-activity relationships and molecular modelling. *Curr Med Chem* 8, 651-674 (2001)

113. **a)** Dukat M.; Damaj M.I.; Glassco W.; Dumas D.; May E.L.; Martin B.R.; Glennon R.A. Epibatidine: A very high affinity nicotine-receptor ligand. *Med Chem Res* 4, 131 – 139 (1994)

114. Koren A.O.; Horti A.G.; Mukhin A.G.; Gündisch D.; Kimes A.S.; Dannals R.F.; London E.D. 2-, 5- and 6-Halo-3-(2(S)-azetidinylmethoxy)pyridines: Synthesis, affinity for nicotinic acetylcholine receptors and molecular modelling. *J Med Chem* 41, 3690 – 3698 (1998)

115. Glennon R.A.; Dukat M. α4β2 nACh receptor pharmacophore models. *Bioorg Med Chem Lett* 14, 1841 – 1844 (2004)

116. Toma L.; Quadrelli P.; Bunnelle W.H.; Anderson D.J.; Meyer M.D.; Cignarella G.; Gelain A.; Barlocco D. 6-Chloropyridazin-3-yl derivatives active as nicotinic agents: synthesis, binding, and modelling studies. *J Med Chem* 45, 4011 – 4017 (2002)

117. a) Glennon R.A.; Dukat M. Musings on $\alpha 4\beta 2$ Nicotinic Acetylcholine (nACh) Receptor Pharmacophore Models. *Curr Topics Med Chem* 4, 631-644 (2004)
b) Glennon R.; Dukat M. Central nicotinic ligands and pharmacophores. *Pharm Acta Helv* 74, 103 – 114 (2000)

118. Imming P.; Klaperski P.; Stubbs M.T.; Seitz G.; Gündisch D. Syntheses and evaluation of halogenated cytisine derivatives and of bioisosteric thiocytisine as potent and selective nAChR ligands. *Eur J Med Chem* 36:375 – 388, 2001

119 . Papke R.L.; Heinemann S.F. Partial agonist properties of cytisine on neuronal nicotinic receptors containing the β2 subunit. *Mol Pharmacol* 45, 142 – 149 (1994)

120. www.tabex.net

121. Coe J.W.; Brooks P.R.; Vetelino M.G.; Wirtz M.C.; Arnold E.P.; Huang J.; sands S.B.; Davis T.I.; Lebel L.A.; Fox C.B.; Shrikhande A.; Heym J.H.; Schaeffer E.; Rolle,a H.; Lu Y.; Mansbach R.S.; Chambers L.K.; Rovetti C.C.; Schulz D.W.; Tingley F.D.; O'Neill B.T. Varenicline: An α4β2 nicotinic receptor partial agonist for smoking cessation. *J Med Chem* 48, 3474 – 3477 (2005)

122. Nicolotti O.; Canu Boido C.; Sparatore F.; Carotti A. Cytisine derivatives as high affinity nAChR ligands: synthesis and comparative molecular field analysis. *Farmaco* 57, 469 – 478 (2002)

123. **a)** Canu Boido C.; Sparatore F. Synthesis and preliminary pharmacological evaluation of some cytisine derivaties. *Farmaco* 54, 438 – 451 (1999)

b) Canu Boido C.; Tasso B.; Boido V.; Sparatore F. Cytisine derivatives as ligands for neuronal nicotine receptors and with various pharmacological activities. *Farmaco* 58, 265 – 277 (2003)

124. O'Neill B. Pyridone-fused azabicyclic- or cytisine derivatives, their preparation and their use in addiction therapy. WO 98/18798, PCT/IB97/01282, US 6,235,734 B1, US 2003/0065173 A1

125. Roger G.; Lagnel B.; Rouden J.; Besret L.; Valette H.; Demphel S.; Gopisetti JM.; Coulon C.; Ottaviani M.; Wrenn L.A.; Letchworth S.R.; Bohme G.A.; Benavides J.; Lasne M.-C.; Bottlaender M.;Dollé F. Synthesis of a [2-pyridinyl-^{18}F]-labelled fluoro derivative of (-)-cytisine as a candidate radioligand for brain nicotinic α4β2 receptor imaging with PET. *Bioorg Med Chem* 11, 5333 – 5343 (2003)

126. Bohlmann F.; Zeisberg R. ^{13}C NMR Spektren von Lupinen-Alkaloiden. *Chem Ber* 108, 1043 – 1051 (1975)

127. Takamatsu S.; Saito K.; Ohmiya S.; Ruangrungsi N.; Murakoshi I. Lupin alkaloids from Sophora exigua. Phytochemistry 30, 3793 – 3795 (1991)

128. Asres K.; Phillipson J.D.; Mascagni P. Alkaloids of Bolusanthus speciosus. Phytochemistry 25, 1449 – 1452 (1986)

129. Husseman and Marmé, Ztschr.Chem. 1, 161 (1865)

130. **a)** Partheil A. Ueber das Cytisin. *Chem Berichte* 23, 3201 – 3204 (1891)
b) Partheil A. Ueber das Cytisin. Zweite Mittheilung. *Chem Berichte* 24, 634 – 640 (1891)

131. Partheil A. Über Cytisin und Ulexin. II. Abhandlung. *Chem Berichte* 232, 161 – 177 (1894)

132. Gerrard A.W. Pharm Jour Trans, 18, 101 (1892)

133. Gorter K. Ueber die Bestandteile der Wurzel von Baptisia tinctoria. *Archiv der Pharm* 321 (1897)

134. **a)** Ing H.R. Cytisine. Part I. *J Chem Soc* 2195 – 2203 (1931)
b) Ing H.R. Cytisine. Part II. J Chem Soc 2778 – 2780 (1932)

135. www.ibiblio.org

136. Okuda S.T.K. *Chem. Ind.* 1751 (1961)

137. Ohmiya S.; Otomasu H.; Haginiwa J.; Murakoshi I. The alkaloid constituents of Euresta japonica and the stereochemical assignment of two isomeric sophoridine N-oxides. *Chem Pharm Bull* 28, 546 – 551 (1980)

138. Ohmiya S.; Kubo H.; Nakaaze Y.; Saito K.; Murakoshi I.; Otomasu H. (-)-Camolusidine N-oxide: a new alkaloid from Maackia tashiroi. *Chem Pharm Bull* 39, 1123 – 1125 (1991)

139. Takamatsu S.; Saito K.; Ohmiya S.; Ruangrungsi N.; Mukaroshi I. Lupin alkaloids from Sophora exigua. *Phytochemistry* 30, 3793 – 3795 (1991)

140. Kinghorn A.D.; Hussain R.A.; Robbins E.F.; Balandrin M.F.; Stirton C.H.; Evans S.V. Alkaloid distribution in seeds of ormosia, pericopsis and haphormosia. *Phytochemistry* 27, 439 – 444 (1988)

141. Murakoshi I.; Kidoguchi E.; Kubota M.; Haginiwa J.; Ohmiya S.; Otomasu H. Lupin alkaloids from Echinosophora koreensis. *Phytochemistry* 21, 2385 – 2388 (1982)

142. El-Shazly A.; Sarg T.; Ateya A.; Abdel Aziz E.; Witte L.; Wink M. Quinolizidine alkaloids from Argyrolobium uniflorum. *Pharmazie* 10, 768 – 772 (1996)

143. www.botanical.com
www.ibiblio.org/herbmed
http://en.wikipedia.org

144. Moll F.; Koggel A.; Moll M. Vergiftung mit Goldregen. *Deutscher Apoth Ztg* 141, 22, 74 – 76 (2001)

145. **a)** Gündisch D.; London E.D.; Terry P.; Hill G.R.; Mukhin A. High affinity binding of [^{3}H]epibatidine to rat brain membranes. *Neuroreport* 10, 1631 – 1636 (1999)
b) Gündisch D.; Koren A.O.; Horti A.G.; Pavlova O.A.; Kimes A.S.; Mukhin A.G.; London E.D. In vitro characterization of 6-[^{18}F]fluoro-A-85380, a high-affinity ligand for α4β2* nicotinic acetylcholine receptors. *Synapse* 55, 89 – 97 (2005)

146. Parker M.J.; Beck A.; Luetje C.W. Neuronal nicotinic receptor β2 and β4 subunits confer large differences in agonist binding affinity. *Mol Pharmacol* 54, 1132 – 1139 (1998)

147. Slater Y.E.; Houlihan L.M.; Maskell P.D.; Exley R.; Bermúdez I.; Lukas R.J.; Valdivia A.C.; Cassels B.K. Halogenated cytisine derivatives as agonists at human neuronal nicotinic acetylcholine receptor subtypes. *Neuropharmacology* 44, 503 – 515 (2003)

148. Houlihan L.M.; Slater Y.; Guerra D.L.; Peng J.-H.; Kuo Y.-P.; Lukas R.J.; cassels B.K.; Bermudez I. Activity of cytisine and its brominated isosteres on recombinant human α7, α4β2 and α4β4 nicotinic acetylcholine receptors. *J Neurochem* 78, 1029 – 1043 (2001)

149. Luetje C.W.; Patrick J. Both α- and β-subunits contribute to the agonist sensitivity of neuronal nicotinic acetylcholine receptors. *J Neurosci* 11, 837 – 845 (1991)

150. Fitch R.W.; Kaneko Y.; Klaperski P.; Daly J.W.; Seitz G.; Gündisch D. Halogenated and isosteric cytisine derivatives with increased affinity and functional activity at nicotinic acetylcholine receptors. *Bioorg Med Chem Lett* 15, 1221 – 1224 (2005)

151. Dale H.H.; Landlaw P.P. The physiological action of cytisien, the active alkaloid of laburnum (Cytisus laburnum). *J Pharmacol Exp Ther* 3, 205 – 221 (1912)

152. Stolerman I.P.; Garcha H.S.; Pratt J.A.; Kumar R. Role of training dose in discrimination of nicotine and related compounds by rats. *Psychopharmacology* 84, 413 – 418 (1984)

153. Reavill C.; Walther B.; Stolerman I.P.; Testa B. Behavioural and kinetic studies on nicotine, cytisine and lobeline. *Neuropharmacol* 29, 619 – 624 (1990)

154. Pabreza L.A.; Dhawan S.; Kellar K.J. [^{3}H]Cytisine binding to nicotinic cholinergic receptors in brain. *Mol Pharmacol* 39, 9 – 12 (1991)

155. Anderson D.J.; Arneric S.P. Nicotinic receptor binding of [^{3}H]cytisine, [^{3}H]nicotine and [^{3}H]methylcarbamylcholine in rat brain. *Eur J Pharmacol* 253, 261 – 267 (1994)

156. Khan I.M.; Yaksh T.L.; Taylor P. Ligand specificity of nicotinic acetylcholine receptors in rat spinal cord: studies with nicotine and cytisine. *J Pharmacol Exp Ther* 270, 159 – 166 (1994)

157. Hall M.; Zerbe L.; Leonard S.; Freedman R. Characterization of [^{3}H]cytisine binding to human brain membrane preparations. *Brain Research* 600, 127 – 133 (1993)

158. Flesher J.E.; Scheffel U.; London E.D.; Frost J.J. I vivo labelling of nicotinic cholinergic receptors in brain with [^{3}H]cytisine. *Life Sci* 54, 1883 – 1890 (1994)

159. Valette H.; Bottlaender M.; Dollé F.; Dolci L.; Syrota A.; Crouzel C. An attempt to visualize baboon brain nicotinic receptors with N-[^{11}C]ABT-418 and N-[^{11}C]methyl-cytisine. *Nuclear Med Comm* 18, 164 – 168 (1997)

160. Kozikowski A.P.; Musachio J.; Kelar K.; Xiao Y.; Wei Z.-L. Ligands for nicotinic acetylcholine receptors, and methods of making and using them. WO2005000806

161. Scharfenberg G.; Benndorf S.; Kempe G. *Dtsche Gesundheitswesen* 26, 463 (1971)

162. Rose J.E.; Behm F.M.; Westman E.C. Nicotine-mecamylamine treatment for smoking cessation: the role of pre-cessation therapy. *Exp Clin Psychopharmacol* 6, 331 – 343 (1998)

163. Cohen C.; Bergis O.E.; Galli F.; Lochead A.W.; Jegham S.; Biton B.; Leonardon J.; Avenet P.; Sgard F.; Besnard F.; Graham A.; Coste A.; Oblin A.; Curet O.; Voltz C.; Gardes A.; Caille D.; Perrault G.; George P.; Soubrie P.; Scatton B. SSR591813, a novel selective and partial α4β2 nicotinic receptor agonist with potential as an aid to smoking cessation. *J Pharmacol Exp Ther* 306, 407 – 420 (2003)

164. a) Pfizer Products, Inc.: WO02092089 (2002)
b) Pfizer Products, Inc.: WO02092597 (2002)

165. **a)** van Tamelen E.E.; Baran T.S. The synthesis of *dl*-cytisine *J Am Chem Soc* 77, 4944 – 4945 (1955)
b) van Tamelen E.E.; Baran T.S. Total synthesis of oxygenated tetracyclic lupin alkaloids. *J Am Chem Soc* 78, 2913 – 2914 (1956)
c) van Tamelen E.E.; Baran T.S. Total synthesis of oxygenated lupin alkaloids. *J Am Chem Soc* 80, 4659 – 4670 (1958)

166. Bohlmann F.; English A.; Ottawa N.; Sander H.; Weise W. Zur Synthese des Cytisins. III.Mitteil.[1)] Totalsynthese des Cytisines. *Chem Ber* 89, 792 – 799 (1956)

167. Govindachari T.R.; Rajadurai S.; Subramanian M.; Thyagarajan B. *J Chem Soc* 3839, (1957)

168. O'Neill B.T.; Yohannes D.; Bundesmann M.W.; Arnold E.P. Total synthesis of (±)-cytisine. *Org Lett* 2, 4201 – 4204 (2000)

169. Coe J.W. Total synthesis of (±)-cytisine via the intramolecular Heck cyclization of activated N-alkyl glutarimides. *Org Lett* 2, 4205 – 4208 (2000)

170. Nshimyumukiza P.; Cahard D.; Rouden J.; Lasne M.-C.; Plaquevent J.-C. Construction of functionalized/substituted bipyridines by means of Negishi cross-coupling reactions. Formal synthesis of (±)-cytisine. *Tetrahedron Lett* 42, 7787 – 7790 (2001)

171. Botuha C.; Galley C.M.S.; Gallagher T. A short synthesis of (±)-cytisine. *Org Biomol Chem* 2, 1825 – 1826 (2004)

172. Danieli B.; Lesma G.; Passarella D.; Sacchetti A.; Silvani A.; Virdis A. Total enantioselective synthesis of (-)-cytisine. *Org Lett* 6, 493 – 496 (2004)

173. Honda T.; Takahashi R.; Namiki H. Syntheses of (+)-cytisine, (-)-kuraramine, (-)-isokuraramine and (-)-jussiaeiine A. *J Org Chem* 70, 499 – 504 (2005)

174. Luputiu G.; Moll F. Die Bromderivate des cytisins. *Archiv der Pharmazie*, 1970

175. Luputiu G.; Gilau L. N-aryl-thiocarbamyl-cytisin-Derivate. *Archiv der Pharmazie* 302, 943 – 945 (1969)

176. Moll F.; Luputiu G. Harnstoff-Derivate des Cytisins. *Archiv der Pharmazie* 305, 771 – 776 (1971)

177. Sadykov A.S.; Aslanov K.A.; Kushmuradov Y.K. Cytisine Alkaloids [in Russian], Nauka, Moscow, pp. 48 – 50 (1975)

178. Khakimova T.V.; Pukhlyakova O.A.; Shavaleeva G.A.; Fatykhov A.A.; Vasileva E.V.; Spirikhin L.V. Synthesis and stereochemistry of new N-substituted cytisine derivatives. *Chemistry of Natural Compounds* 37, 356 – 360 (2001)

179. Grebenyuk A.D.; Vinogradva V.I.; Tashmukhamedova A.K. Reaction of cytisine with 4'-substituted dibenzo-18-crown-6 sulfonylchlorides. *Chemistry of Natural Products* 38, 182 – 185 (2002)

180. Krasnov K.A.; Kartsev V.G.; Gorovoi A.S.; Khrustalev V.N. Chemical modification of plant alkaloids. III. X-ray diffraction and NMR studies of the structure of 1,3-dimethyl-5-arylmethyl-5-cytisylmethylbarbituric acids. *Chemistry of Natural Products* 38, 450 – 457 (2002)

181. Rakhimov A.A.; Vinogradova V.I.; Tashmukhamedova A.K. Synthesis of new cytisine derivatives with benzocrown-ether fragments. *Chemistry of Natural Products* 38, 344 – 346 (2002)

182. Klaperski P. Strukturvariationen des Naturstoffs (-)-cytisine. Synthese neuer nAChRs-Liganden. Marburg, *Univ., Diss.*, 2002. Shaker Verlag, Aachen 2002

183. Tilotta M.C. Novel nicotinic acetylcholine receptor ligands based on cytisine, ferruginine, anatoxin-a and choline: In vitro evaluation and structure-activity relationships, *Bonn, Univ., Diss.* (2004)

184. Marriére E.; Rouden J.; Tadino V.; Lasne M.-C. Synthesis of analogues of (-)-cytisine for in vivo studies of nicotinic receptors using positron emission tomography. *Org Lett* 2, 1121 – 1124 (2000)

185. Coe J.W.; Vetelino M.G.; Bashore C.G.; Wirtz M.C.; Brooks P.R.; Arnold E.P.; Lebel L.A.; Fox C.B.; Sands S.B.; Davis T.I.; Schulz D.W.; Rollema H.; Tingley F.D.; O'Neill B.T. In pursuit of α4β2 nicotinic receptor partial agonists for smoking cessation: Carbon analogs of (-)-cytisine. *Bioorg Med Chem Lett* 15, 2974 – 2979 (2005)

186. **a)** Miyaura N.; Yamada K.; Suzuki A. A new stereospecific cross-coupling by the palladium-catalyzed reaction of 1-alkenylboranes with 1-alkenyl or 1-alkynyl halides. *Tetrahedron Lett* 3437 – 3440 (1979)

b) Miyaura N.; Suzuki A. Stereoselective synthesis of arylated (*E*)-alkenes by the reaction of alk-1-enylboranes with aryl halides in the presence of palladium catalyst. *J Chem Soc Chem Com 19, 866 - 867 (1979)*
c) Miyaura N.; Yanagi T.; Suzuki A. The palladium-catalyzed cross-coupling reaction of phenylboronic acid with haloarenes in the presence of bases. *Synth Comm* 11, 513 – 519 (1981)
d) Suzuki A. Organoboron compounds in new synthetic reactions. *Pure & Appl Chem* 57, 1749 – 1758 (1985)

187. Knochel P.; Sapountzis I.; Gommermann N. Carbon-carbon bond-forming reactions mediated by organomagnesium reagents. In . In *Metal-catalyzed cross-coupling reactions*, de Meijere A.; Diederich F. (Eds.), Wiley-VCH, Weinheim, 2004, Chapter 12, pp 671 - 698

188. Farina V.; Krishnamurthy W.; Scott J. The Stille Reaction, Wiley, New York, 1998

189. Hatanaka Y.; Hiyama T. Cross-coupling of organosilanes with organic halides by palladium catalyst and tris(diethylamino)sulfonium difluorotrimethylsilicate. J Org Chem 53, 918 – 920 (1988)

190. **a)** Sonogashira K.; Tohda Y.; Hagihara N. A convenient synthesis of acetylenes:catalytic substitutions of acetylenic hydrogen with bromoalkenes, iodoarenes and bromopyridines. Tetrahedron Lett 16, 4467 – 4470 (1975)
b) Sonogashira K. Development of Pd-Cu catalyzed cross-coupling of terminal acetylenes with sp^2-carbon halides. J Organomet Chem 653, 46 – 49 (2002)

191. **a)** Miyaura N.; Suzuki A. Palladium-catalyzed cross-coupling reactions of organoboron compounds. Chem Rev 95, 2457 – 2483 (1995)
b) Suzuki A. Recent advances in the cross-coupling reactions of organoboron derivatives with organic electrophiles, 1995 – 1998. J Organomet Chem 576, 147 – 168 (1999)
c) Miyaura N. Metal-catalyzed cross-coupling reactions of organoboron compounds with organic halides. In *Metal-catalyzed cross-coupling reactions*, de Meijere A.; Diederich F. (Eds.), Wiley-VCH, Weinheim, 2004, Chapter 2, pp 41 - 124

192. Heck R.F.; Nolley J.P. Palladium-catalyzed vinylic hydrogen substitution reactions with aryl, benzyl and styryl halides. J Org Chem 37, 2320 – 2322 (1972)

193. March J. Advanced Organic Chemistry. Reactions, mechanisms, and structure. Fourth Edition. John Wiley&Sons (1992)

194. **a)** Gillie A.; Stille J.K. Mechanisms of 1,1-reductive elimination from palladium. *J Am Chem Soc* 102, 4933 - 4941 (1980)
b) Ozawa F.; Ito T.; Yamamoto A. Mechanism of thermal decomposition of trans-diethylbis(tertira phosphine)palladium(II). Steric effects of tertiary phosphine ligands on the stability of diethylpalladium complexes. *J Am Chem Soc* 102, 6457 (1980)

195. Coulson D.R. *Inorg Synth* 13, 121 – 124 (1972)

196. **a)** Amatore C.; Jutand A. Mechanistic and kinetic studies of palladium catalytic systems. *J Organomet Chem* 576, 254 – 278 (1999)
b) Amatore C.; Jutand A.; Suarez A. Intimate mechanism of oxidative addition to zerovalent palladium complexes in the presence of halide ions and its relevance to the mechanism of palladium-catalyzed nucleophilic substitutions. *J Am Chem Soc* 115, 9531 – 9541 (1993)

197. Watanabe T.; Miyaura N. Suzuki A. Synthesis of Sterically Hindered Biaryls via the Palladium-Catalyzed Cross-Coupling Reaction of Arylboronic Acids or their Esters with Haloarenes. *Synlett* 207 - 210 (1992)

198. Uenishi J.I.; Beau J.-M.; Armstrong R.W.; Kishi Y. Dramatic rate enhancement of Suzuki diene synthesis: its application to palytoxin synthesis. *J Am Chem Soc* 109, 4756-58 (1987)

199. Johnson C.R.; Braun M.P. A two-step, three-component synthesis of PGE1: utilization of .alpha.-iodo enones in Pd(0)-catalyzed cross-couplings of organoboranes. *J Am Chem Soc* 115, 11014 - 11015 (1993)

200. Miyaura N.; Ishiyama T.; Ishikawa M.; Suzuki A. Paladium-catalyzed cross-coupling reactions of B-alkyl-9-BBN or trialkylboranes with aryl and 1-alkenyl halides. *Tetrahedron Lett* 27, 6369 – 6372 (1986)

201. Miyaura N. Effect of bases. In *Metal-catalyzed cross-coupling reactions*, de Meijere A.; Diederich F. (Eds.), Wiley-VCH, Weinheim, 2004, Chapter 2, pp 71 - 74

202. Smith R.M.; Martell A.E. Critical stability constants, Vol. 4, Inorganic complexes, Plenum Press, New York, 1976

203. Smith G.B.; Dezeny G.C.; Hughes D.L.; King A.O.; Verhoeven T.R. Mechanistic studies of the Suzuki cross-coupling reaction. *J Org Chem* 59, 8151 – 8156 (1994)

204. Köster R. Houben-Wey Methoden der Organischen Chemie; Georg Thieme; Verlag Stuttgart 1984

205. **a)** Ishiyama T.; Murata M.; Miyaura N. Palladium(0)-Catalyzed cross-coupling reaction of alkoxydiboron with haloarenes: A Direct Procedure for Arylboronic Esters. *J Org Chem* 60, 7508 – 7510 (1995)
b) Tatsuo I., Kousaku I.; Norio M. Synthesis of pinacol arylboronates via cross-coupling reaction of bis(pinacolato)diboron with chloroarenes catalyzed by palladium(0)–tricyclohexylphosphine complexes. *Tetrahedron* 57, 9813 – 9816 (2001)

206. **a)** Brown H.C.; Gupta S.K. 1,3,2-Benzodioxaborole, a convenient monofunctional hydroborating agent. Simple new synthesis of alkaneboronic esters and acids from olefins via hydroboration. *J Am Chem Soc* 93, 1816 - 1818 (1971)
b) Brown H.C.; Gupta S.K. Catecholborane (1,3,2-benzodioxaorole) as a new, general monohydroboration reagent for alkynes. Convenient synthesis of alkeneboronic esters and acids from alkynes via hydroboration. *J Am Chem Soc* 94, 4370 - 4371 (1972)

207. **a)** Colberg J.C.; Rane A.; Vaquer J.; Soderquist J.A. *trans*-Vinylboranes from 9-borabicyclo[3.3.1]nonane through dehydroborylation. *J Am Chem Soc* 115, 6065 – 6071 (1993)
b) Soderquist J.A.; Matos K.; Rane A.; Ramos J. Alkynylboranes in the Suzuki-Miyaura coupling. *Tetrahedron Lett* 36, 2401-2402 (1995)

208. Fürstner A.; Seidel G. Suzuki reactions with B-allyl-9-borabicyclo[3.3.1]nonane (B-allyl-9-BBN). *Synlett* 161 – 162 (1998)

209. Miyaura N.; Ishiyama T.; Sasaki H.; Ishikawa M.; Satoh M.; Suzuki A. palladium-catalyzed inter- and intramolecular cross-coupling reactions of B-alkyl-9-borabicyclo[3.3.1]nonane derivatives with 1-halo-1-alkenes or haloarenes. Syntheses of functionalized alkenes, arenas, and cycloalkenes via hydroboronation-coupling sequence. *J Am Chem Soc* 111, 314 – 321 (1989)

210. **a)** Chemler S.R.; Trauner D.; Danishefsky S.J. The B-alkyl Suzuki-Miyaura coupling reaction: Development, Mechanistic study and Applications in natural product synthesis. *Angew Chem Int Ed* 40, 4544 - 4568 (2001)
b) Meng D.F.; Bertinato P.; Balog A.; Su D.-S.; Kamenecka T.; Sorensen E.J.; Danishefsky S.J. Total Syntheses of Epothilones A and B. *J Am Chem Soc* 119, 10073 – 10092 (1997)
c) Stachel S.J.; Chappell M.D.; Lee C.B.; Danishefsky S.J.; Chou T.-C.; He L.; Horwitz S.B. On the total synthesis and preliminary biological evaluations of 15(R) and 15(S) aza-dEpoB: A Mitsunobu inversion at C15 in pre-epothilone fragments. *Org Lett* 2, 1637 – 1639 (2000)
d) Balog A.; Meng D.F.; Kamenecka T.; Bertinato P.; Su D.-S.; Sorensen E.J.; Danishefsky S.J. Total Synthesis of (-)-Epothilone A. *Angew Chem Int Ed* 35, 2801 – 2803 (1996)
e) Harris C.R.; Kuduk S.D.; Balog A.; Savin K.; Glunz P.W.; Danishefsky S.J. New chemical synthesis of the promising cancer chemotherapeutic agent 12,13-desoxyepothilone B: Discovery of a suprising long-range effect on the diastereoselectivity of an aldol condensation. *J Am Chem Soc* 121, 7050 – 7062 (1999)

211. Zhang H.; Chan K.S. Base effect on the cross-coupling of bulky arylboronic acid with halopyridines. *Tetrahedron Lett* 37, 1043 – 1044 (1996)

212. Cempi E.M.; Jackson W.R.; Maruccio S.M.; Naeslund C.G.M. *J Chem Soc Chem Commun* 2395 (1994)

213. Badone D.; Baroni M.; Cardamone R.; Ielmini A.; Guzzi U. Highly efficient palladium-catalyzed boronic acid coupling reactions in water: scope and limitations. *J Org Chem* 62, 7170 – 7173 (1997)

214. **a)** Cammidge A.N.; Crépy K.V.L. The first asymmetric Suzuki cross-coupling reaction. *Chem Commun* 1723 – 1724 (2000)
b) Yin J.; Buchwald S.L. A catalytic asymmetric Suzuki coupling for the synthesis of axially chiral biaryl compounds. *J Am Chem Soc* 122, 12051 – 12052 (2000)

215. Miyaura N.; Yamada K.; Suginome H.; Suzuki A. Novel and convenient method for stereo- and regiospecific synthesis of conjugated alkadienes and alkenynes via palladium-catalyzed cross-coupling reaction of 1-alkenylboranes with bromoalkenes and bromoalkynes. *J Am Chem Soc* 107, 972 – 980 (1985)

216. Miyaura N.; Suzuki A. Palladium-catalyzed reaction of 1-alkenylboronates with vinylic halides: (1*Z*,3*E*)-1-phenyl-1,3-octadiene. *Org Synth* 68, 130 – 135 (2000)

217. Pazos Y.; de Lera A.R. Stereoselective synthesis of 9-cis-retinoic acid by Suzuki reaction. *Tetrahedron Lett* 40, 8287-8290 (1999)

218. **a)** Scheidt K.A.; Tasaka A.; Bannister T.D.; Wendt M.D.; Roush W.R. Total synthesis of (-)-bafilomycin A_1: Application of diastereoselective crotylboration and methyl ketone aldol reactions. *Ang Chem Int Ed* 38, 1652-1655 (1999)
b) Scheidt K.; Bannister T.D.; Tasaka A.; Wendt M.D.; Savall B.M.; Fegley G.J.; Roush W.R. Total synthesis of (-)-bafilomycin A_1. *J Am Chem Soc* 124, 6981-6990 (2002)

219. Ritter K. Synthetic transformations of vinyl and aryl triflates. *Synthesis* 735 - 762 (1993)

220. **a)** Stang P.J.; Hanack M.; Subramanian L.R. Perfluoroalkanesulfonic esters: methods of preparation and applications in organic chemistry. *Synthesis* 85 – 126 (1982)
b) Comins D.L.; Dehghani A. Pyridine-derived triflating reagents: an improved preparation of vinyl triflates from metallo enolates. *Tetrahedron Lett* 33, 6299 – 6302 (1992)

221. Milstein D.; Stille J.K. Palladium-catalyzed coupling of tetraorganotin compounds with aryl and benzyl halides. Synthetic utility and mechanism. *J Am Chem Soc* 101, 4992 – 4998 (1979)

222. Mitchell T.N. Organotin reagents in cross-coupling reactions. In *Metal-catalyzed cross-coupling reactions*, de Meijere A.; Diederich F. (Eds.), Wiley-VCH, Weinheim, 2004, Chapter 3, pp 125 - 161

223. **a)** Casado A.L.; Espinet P. Mechanism of the Stille reaction. 1. The transmetallation step. Coupling of R^1I and R^2SnBu_3 catalyzed by trans-$[PdR^1IL_2]$ ($R^1 = C_6Cl_2F_3$; R^2 = vinyl, 4-methoxyphenyl; L = $AsPh_3$). *J Am Chem Soc* 120, 8978 – 8985 (1998)
b) Casado A.L.; Espinet P.; Gallego A.M. Mechanism of the Stille reaction. 2. Couplings of aryl triflates with vinyltributyltin. Observations of intermediates. A more comprehensive scheme. *J Am Chem Soc* 122, 11771 – 11782 (2000)

224. Handy S.T.; Zhang X. Organic synthesis in ionic liquids: the Stille coupling. *Org Lett* 3, 233 – 23 (2001)

225. **a)** Shin K.; Ogasawara K. A facile construction of the woodward ketone by a zinc(II) chloride-catalyzed Stille coupling reaction. *Heterocycles* 50, 427 – 431 (1999)
b) Han X.; Stoltz M.; Corey E.J. Cuprous chloride accelerated Stille reaction. A general and effective coupling system for sterically congested substrates and for enantioselective synthesis. *J Am Chem Soc* 121, 7600 – 7605 (1999)

226. Nicolaou K.C., Sorensen E.J. Classics in Total Synthesis: Targets, Strategies, Methods. Wiley-VCH Verlag GmbH & Co. KGaA, Weinheim (1996)

227. Sirisoma N.S.; Johnson C.R. α-Iodocycloalkenones: Synthesis of (±)-epibatidine. *Tetrahedron Lett* 39, 2059 – 2062 (1998)

228. **a)** Gedye R.; Smith F.; Westaway K.; Ali H.; Baldisera L.; Laberge L.; Rousell J. The use of microwave ovens for rapid organic synthesis. *Tetrahedron Lett* 27, 279 – 282 (1986)
b) Giguere R.J.; Bray T.L.; Duncan S.M.; Majetich G. Application of commercial microwave ovens to organic synthesis. *Tetrahedron Lett* 27, 4945 – 4958 (1986)

229. **a)** Kappe C.O. Controlled microwave heating in modern organic synthesis. *Angew Chem Int Ed* 43, 6250 – 6284 (2004)
b) Larhed, M.; Moberg, C., Hallberg, A. Microwave-accelerated homogenous catalysis in organic chemistry. *Acc Chem Rev* 35, 717 – 727 (2002)
c) Mavandadi F.; Lindström P. Microwave-assisted Chemistry in drug discovery. *Curr Topics Med Chem* 2004, 4, 773 - 792

230. **a)** Hayes B.L. Microwave synthesis. Chemistry at the speed of light. CEM Publishing, Matthews NC, 2002
b) Loupy A.(Ed.) Microwaves in organic synthesis. Wiley-VCH, Weinheim, 2002
c) Lindström P.; Tierney J.P. (Eds.) Microwave-assisted organic synthesis, Blackwell, Oxford, 2004

231. Stuerga D.; Delmotte M. Wave-material interactions, Microwave technology and equipment. In *Microwaves in Organic Synthesis* (Ed. Loupy A.), Wiley-VCH, Weinheim, 2002, pp. 1-34

232. Baghurst D.R.; Mingos D.M.P. Applications of microwave dielectric heating effects to synthetic problems in chemistry. *Chem Soc Rev* 20, 1 – 47 (1991)

233. Macquer P. Dictionnaire de Chymie contenant la théorie et la pratique de cette science, Lacombe, Paris, II, 503, 1766

234. Baghurst D.R.; Mingos D.M.P. Superheating effects associated with microwave dielectric heating. *J Chem Soc Chem Commun* 674 – 677 (1992)

235. Gabriel C.; Gabriel S.; Grant E.H.; Halstead B.S.; Mingos D.P.M. Dielectric parameters relevant to microwave dielectric heating. *Chem Soc Rev* 27, 213 (1998)

236. **a)** Kuhnert N. Microwave-Assisted Reactions in Organic Synthesis - Are There Any Nonthermal Microwave Effects? *Ang Chem Int Ed* 41, 1863 – 1866 (2002)
b) Perreux L., Loupy A. A tentative rationalization of microwave effects in organic synthesis according to the reaction medium, and mechanistic considerations. *Tetrahedron* 57, 9199 – 9223 (2001)
c) Perreux L.; Loupy A. Nonthermal effects of microwaves in organic synthesis. In Loupy A.(Ed.) *Microwaves in organic synthesis*. Wiley-VCH, Weinheim, 2002, Ch 3, pp 61 - 114

237. **a)** Gedye R.N.; Wei J.B.; Rate enhancement of organic reactions by microwaves at atmospheric pressure. *Can J Chem* 76, 525 – 532 (1998)
b) Perreux L.; Loupy A. A tentative rationalization of microwave effects in oganic synthesis according to the reaction medium and mechanistic considerations. *Tetrahedron* 57, 9199 – 9223 (2001)
c) Kuhnert N. Microwave-assisted reactions in organic synthesis – are there any nonthermal microwave effects? *Angew Chem Int Ed* 41, 1863 – 1866 (2002)
d) Strauss C.R. Response to the Highlight by N. Kuhnert. *Angew Chem Int Ed* 41, 3589 – 3590 (2002)

238. Larhed M.; Halberg A. Microwave-promoted palladium catalyzed coupling reactions. *J Org Chem* 61, 9582 – 9584 (1996)

239. Larhed M.; Lindeberg G.; Hallberg A. Rapid microwave-assisted Suzuki coupling on solid phase. *Tetrahedron Lett* 37, 8219 – 8222 (1996)

240. Blettner C.G.; König W.A.; Stenzel W.; Schotten T. Microwave-assisted aqueous Suzuki cross-coupling reactions. *J Org Chem* 64, 3885 – 3890 (1999)

241. Leadbeater N.; Marco M. Ligand-free palladium catalysis of Suzuki reaction in water using microwave heating. *Org Lett* 4, 2973 – 2976 (2002)

242. Bedford R.B.; Butts C.P.; Hurst T.E.; Lidström P. The Suzuki coupling of aryl chlorides under microwave heating. *Adv Synth Catal* 346, 1627 – 1630 (2004)

243. Leadbeater N.E., Marco M. Transition-metal-free Suzuki-type coupling reactions. *Angew Chem Int Ed* 12, 1407 – 1409 (2003)

244. Li C.-J. Suzuki reaction takes a „naked hot bath": coupling in high-temperature water without transition metals. *Angew Chem Int Ed* 42, 4856 – 4858 (2003)

245. Bojadschiewa M.; Issaev IW.; Totev IL.; Dimov CHR. Eine neue Methode zur Gewinnung von Cytisin aus Samen von Cytisus laburnum. *Pharmazie* 26, 643 (1971)

246. Jarowicki K.; Kocienski P. Protecting groups**.** *J Chem Soc Perkin Trans 1*, 2495 – 2527 (2000)

247. Padwa A. Application of cascade processes toward heterocyclic synthesis. *Pure Appl. Chem* 75, 47–62 (2003)

248. Hansen J.B.; Nielsen M.C.; Ehrbar U.; Buchardt O. Partially Protected Polyamines. *Synthesis* 404 (1982)

249. Greene T.W.; Wuts P.G.M. Protection for the amino group. *In* Protective groups in organic synthesis. 3rd Edition. John Wiley & Sons, Inc., pp 494 – 653 (1999)

250. Sugasawa T.; Sasakura K.; Toyoda T. *Chem Pharm Buletin* 22, 763 (1974)

251. Misra R.; Pandey R.C.; Silverton J.V. Fredericamycin A, an antitumor antibiotic of a novel skeletal type. *J Am Chem Soc* 104, 4478 (1982)

252. Williams D.R.; Sit S.-Y. Synthesis of racemic tenellin. *J Org Chem* 47, 2846 - 2851 (1982)

253. Earl R.A.; Vollhardt K.P.C. The preparation oh 2(1*H*)-pyridinone and 2,3-dihydro-5(1*H*)-indolizinones via transition metal mediated cocyclization of alkynes and isocyanates. A novel construction of the antitumor agent captothecin. *J Org Chem* 49, 4786 – 4795 (1984)

254. Pendrak I.; Wittrock R.; Kingsbury W.D. Synthesis and anti-HSV activity of methylenedioxy mappicine ketone analogs. *J Org Chem* 60, 2912 – 2915 (1995)

255. Barr S.A.; Neville C.F.; Grundon M.F.; Boyd D.R.; Malone J.F.; Evans T.A. Quinoline cycloaddition as a potential route to dimeric quinoline alkaloids. *J Chem Soc Perkin Trans I*, 4, 445 – 452 (1995)

256. Parreira R.L.T.; Abrahão O.; Galembeck S.E. Conformational preference of non-nucleoside HIV-1 reverse transcriptase inhibitors. *Tetrahedron* 57, 3243 – 3253 (2001)

257. Steinhilber D.; Schubert-Zsilavecz M.; Roth H.J. Medizinische Chemie. Deutscher Apotheker Verlag Stuttgart, pp 206 (2005)

258. **a)** Dragovich P.S.; Prins T.J.; Zhou R.; Brown E.L.; Maldonado F.C.; Fuhrman S.A.; Zalman L.S.; Tuntland T.; Lee C.A.; Patick A.K.; Matthews D.A.; Hendrickson T.F.; Kosa M.B.; Liu B.; Batugo M.R.; Gleeson J.-P. R.; Sakata S.K.; Chen L.; Guzman M.C.; Meador J.W.; Ferre R.A.; Worland S.T. Structure-based design, synthesis and biological evaluation o irreversible human rhinovirus 3C protease inhibitors. 6. Structure – activity studies of orally bioavailable, 2-pyridone-containing peptidomimetics. *J Med Chem* 45, 1607 – 1623 (2002)
b) Dragovich P.S.; Prins T.J.; Zhou R.; Johnson T.O.; Brown E.L.; Maldonado F.C.; Fuhrman S.A.; Zalman L.S.; Patick A.K.; Matthews D.A.; Hou X.; Meador J.W.; Ferre R.A.; Worland S.T. Structure-based design, synthesis and biological evaluation o irreversible human rhinovirus 3C protease inhibitors. 7. Structure – activity studies bicyclic 2-pyridone-containing peptidomimetics. *Bioorg Med Chem Lett* 12, 733 – 738 (2002)

259. **a)** Semple G.; Andersson B.-M.; Chhajlani V.; Georgsson J.; Johansson M.; Lindschoten M.; Pontén F.; Rosenquist A.; Sörensen H.; Swanson L.; Swanson M. 3-Aryl pyridone derivatives. Potent and selective kappa opiod receptor agonists. *Bioorg Med Chem Lett* 12, 197 – 200 (2002)
b) Semple G.; Andresson B.-M.; Chhajlani V.; Georgsson J.; Johansson M.J.; Rosenquist A.; Swanson L. Synthesis and biological activity of kappa opiod receptor agonists. Part 2: Preparation of 3-aryl-2-pyridone analogues generated by solution- and solid-phase parallel synthesis methods. *Bioorg Med Chem Lett* 13, 1141 – 1145 (2003)

260. **a)** Gorobetz N.Y.; Yousefi B.H.; Belaj F.; Kappe C.O. Rapid microwave-assisted solution phase synthesis of substituted 2-pyridone libraries. *Tetrahedron* 60, 8633 – 8644 (2004)
b) Sutherland A.; Gallagher T. Versatile synthesis of 3,5-disubstituted 2-fluoropyridines and 2-pyridones. *J Org Chem* 68, 3352 – 3355 (2003)
c) Sheehan S.M.; Padwa A. New synthetic route to 2-pyridones and its application toward the synthesis of (±)-ipalbidine. *J Org Chem* 62, 438 – 439 (1997)
d) Mont N.; Fernandez-Megido L.; Teixidó J.; Kappe C.O.; Borrell J.I. A diversity-orientated, microwave-assisted synthesis of 4-oxo and 4-chloropyrido[2,3-d]pyrimidin-7(8*H*)-ones. *QSAR & Comb Sci* 23, 836 – 849 (2004)

261. Organikum. Organisch-chemisches Grundpraktikum, 21. Auflage. Wiley-VCH. Weinheim-New York-Chichester-Brisbane-Singapore-Toronto (2001)

262. Timári G.; Soós T.; Hajós G. A Convenient synthesis of two new indoloquinoline alkaloids. *Synlett* 1067 – 1068 (1997)

263. Collins I.; Castro J.L. A Convenient synthesis of highly substituted 2-pyridones. *Tetrahedron Lett* 40, 4069 – 4072 (1999)

264. Potoski J. Timely synthetic support for medicinal chemist. *Drug Discovery Today* 10, 115 – 120 (2005)

265. **a)** Schaal W.; Karlsson A.; Ahlsen G.; Lindberg J.; Andersson H.O.; Danielson U.H.; Classon B.; Unge T.; Samuelsson B.; Hultén J.; Hallberg A.; Karlén A. Synthesis and comparative molecular field analysis (CoMFA) of symmetric and nonsymmetric cyclic sulfamide HIV-1 protease pnhibitors *J Med Chem* 44, 155 – 169 (2001)
b) Luo G.; Chen L.; Pointdexter G.S. Microwave-assisted synthesis of aminopyrimidines. *Tetrahedron Lett* 43, 5739 – 5742 (2002)
c) Gong Y.; He W. A Direct approach to the synthesis of 5-aryl-4-chloropyridazinone: From microwave assisted catalyst screen to room temperature regio- and chemoselective Suzuki arylation. *Heterocycles* 62, 851 – 856 (2004)
d) Melucci M.; Barbarella G.; Zambianchi M.; Di Pietro P.; Bongini A. Solution-phase microwave-assisted synthesis of unsubstituted and modified α-quinque- and sexithiophenes. *J Org Chem* 69, 4821 – 4828 (2004)
e) Wang Y.; Sauer D.R. Use of polymer-supported Pd reagents for rapid and efficient Suzuki reactions using microwave heating. *Org Lett* 6, 2793 – 2796 (2004)

266. Nadin A.; Harrison T. Synthesis of tricyclic pyridones by radical cyclization. *Tetrahedron Lett* 40, 4073 – 4076 (1999)

267. Fu J.; Chen Y.; Castelhano A.L. Synthesis of functionalized pyridones via palladium catalyzed cross coupling reactions. *Synlett* 1408 – 1410 (1998)

268. Unger K.K.; Weber E. Handbuch der HPLC. Teil 2 - Präparative Säulenflüssig-Chromatographie, 2. Auflage, GIT Verlag, 1994,

269. Morita D.K.; Stille J.K.; Norton J.R. Methyl/Phenyl Exchange between Palladium and a Phosphine Ligand. Consequences for Catalytic Coupling Reactions. *J Am Chem Soc* 117, 8576 – 8581 (1995)

270. Miyaura N. Oxygen-induced homocoupling. In *Metal-catalyzed cross-coupling reactions*, de Meijere A.; Diederich F. (Eds.), Wiley-VCH, Weinheim, 2004, Chapter 2, pp 79

271. Brown H.C.; Molander G.A. Vinylic organoboranes. 2. Improved procedures for the protonolysis of alkenyldialkylboranes providing a simplified stereospecific synthesis of (Z)-alkenes. *J Org Chem* 51, 4512 – 4514 (1986)

272. Scheidel M.S.; Briehn C.A.; Bäuerle P. C---C Cross-coupling reactions for the combinatorial synthesis of novel organic materials. *J Organomet Chem* 653, 200 – 208 (2002)

273. Stahl G.L.; Walter R.; Smith C.W. General procedure for the synthesis of mono-N-acylated 1,6-diaminohexanes. *J Org Chem* 43, 2285 - 2286 (1978)

274. Houghten R.A.; Beckman A.; Ostresh J.M. *Int J Pept Protein Res* 27, 653 (1986)

275. Rawal V.H.; Jone R.J.; Cava M.P. Photocyclization strategy for the synthesis of antitumor agent CC-1065: synthesis of dideoxy PDE-I and PDE-II. Synthesis of

thiophene and furan analogues of dideoxy PDE-I and PDE-II. *J Org Chem* 52, 19 – 28 (1987)

276. Kolb H.C.; Finn M.G.; Sharpless K.B. Click chemistry: Diverse chemical function from a few good reactions. *Ang Chem Int Ed* 40, 2004-2021 (2001)

277. Wasserman H.H.; Berger G.D.; Cho K.R. Transamidation reactions using β-lactams. The synthesis of homaline *Tetrahedron Lett* 23, 465 - 468 (1982)

278. **a)** Varma R.S.; Chatterjee A.K.; Varma M. Alumina-mediated deacetylation of benzaldehyde diacetates. A simple deprotection method. *Tetrahedron Lett* 34, 3207 - 3210 (1993)
b) Varma R.S.; Chatterjee A.K.; Varma M. Alumina-mediated microwave thermolysis: A new approach to deprotection of benzyl esters. *Tetrahedron Lett* 34, 4603 - 4606 (1993)
c) Heravi M.M.; Ajami D.; Mojtahedi M.M.; Ghassamzadeh M. A convenient oxidative deprotection of tetrahydropropanyl ethers with iron (III) nitrate and clay under microwave irradiation in solvent free conditions. *Tetrahedron Lett* 40, 561 – 562 (1999)

279. Bose D.S.; Lakshminarayana V. An efficient and highly selective cleavage of *N-tert*-butoxycarbonyl group under microwave irradiation. *Tetrahedron Lett* 39, 5631 - 5634 (1998)

280. Siro J.G.; Martin J.; García-Navío J.L.; Remuiñan, Vaquero J.J. Easy microwave assisted deprotection of N-Boc derivatives. *Synlett* 147 – 148 (1998)

281. Babu V.; Patil B.; Vasanthakumar G.-R. MW-Enhanced high-speed deprotection of Boc group using p-TsOH and concommitant formation of N-Me-amino acid benzyl ester p-TsOH salts. *Synth Commun* 35, 1795 – 1802 (2005)

282. Mathieson D.W. Nuclear magnetic resonance for organic chemists. Academic press Inc. (London) 1967

283. Pihlaja K.; Kleinpeter E. Carbon-13 NMR chemical shifts in structural and stereochemical analysis. VCH Publishers, Inc. (1994)

284. Croasmun W.R.; Carlson R.M.K. Two-dimensional NMR spectroscopy. VCH, New York 1994

285. Buddrus J.; Lambert J. Connectivities in molecules by INADEQUATE: recent developments. *Magn Reson Chem* 40, 3 – 23 (2002)

286. Hesse M.; Meier H.; Zeeh B. Spektroskopische Methoden in der organischen Chemie. 7., überarbeitete Auflage. Thieme Stuttgart, New York (2005)

287. Braun S.; Kalinowski H.-O.; Berger S. 100 and more basic NMR Experiments. VCH Weinheim (1996)

288. Liu Z.; Yang L.; Jia Z.; Chen J. Stereochemical study of anagyrine-type quinolizidine alkaloids by ^{15}N and 2D NMR spectroscopy. *Magn Reson Chem* 30, 511 – 514 (1992)

289. calculated with *ChemDraw Ultra 7.0* Program

290. Buccafusco J.J.; Beach J.W.; Terry A.; `Doad G.S.; Sood A.; Arias E.; Misawa H.; Masai M.; Fujii T.; Kawashima K. Novel analogs of choline as potential neuroprotective agents. *J Alzheim Disease* 6, S85 – S92 (2004)

291. Simsek R.; Chang-Fong J.; Lee M.; Dukat M.; Damaj M.I.; Martin B.R.; Glennon R.A. Quaternary ammonium 3-(aminoethoxy)pyridines as antinociceptive agents. *Bioorg Med Chem Lett* 13, 2917 – 2920 (2003)

292. **a)** Andrä M. Synthese und In-vitro-Pharmakologie neuer Phenylcarbamate als Liganden für nicotinische Acetylcholin-Rezeptoren (nAChR). *Bonn, Univ, Diss* (2005)
b) Gündisch D.; Ändra M.; Munoz L.; Tilotta M.C. Synthesis and evaluation of phenylcarbamate derivatives as ligands for nicotinic acetylcholine receptors. *Bioorg Med Chem* 12, 4953 – 4962 (2004)

293. a) Brown B.G.; Hey P. Brit Choline phenyl ethers as inhibitors of amine oxidase. *Brit J Pharmacol* 11, 56 – 58 (1956)
b) Hey P. On relationships between structure and nicotine-like stimulant activity in choline esters and ethers. *Br J Pharmacol* 7, 117 – 129 (1952)

294. University of Kansas Research Foundation, *U.S. Patent* 863, 197 (1959)

295. Zielinsky J.; Kenilworth N.J. U.S.Patent 3,535,328 (1970), Chem Abstr. 73, P 130899t

296. **a)** Gómez-Parra V.; Sánchez F.; Torres T. Carbamates from Secondary Amines and Alkyl Chlorides under Phase-Transfer Conditions. *Synthesis* 282 – 385 (1985)
b) Gómez-ParraV.; Sánchez F.; Torres T. A study of the phase-transfer alkoxycarbonylation of secondary alkyl amines. Application of a factorial design. *J Chem Soc Perkin Trans 2*, 6, 695 – 699 (1987)

297. Fukuoka S.; Chono M.; Kohno M. A novel catalytic synthesis of carbamates by the oxidative alkoxycarbonylation of amines in the presence of platinum group metal and alkali metal halide or onium halide. *J Org Chem* 49, 1458 – 1460 (1984)

298. Alper H.; Vasapollo G. Carbonylation of nitrosobenzenes to carbamate esters catalyzed by palladium and cupric acetates under ambient conditions. *Tetrahedron Lett* 28, 6411 – 6412 (1987)

299. Bodrikov J.A., Danova T.P. *J Org Chem USSR* 4, 1611 (1968)

300. **a)** Leppänen J.; Huuskonen J.; Nevalainen T.; Gynther J.; Taipale H.; Järvinen T. Design and synthesis of a novel L-dopa-Entacapone codrug. *J Med Chem* 45, 1379 – 1382 (2002)
b) Sasse A., Kiec-Kononowicz K., Stark H., Motyl M., Reidemeister S., Ganellin S.R., Ligneau X., Schwartz J.-C., SchunackW. Development of Chiral *N*-Alkylcarbamates as New Leads for Potent and Selective H_3-Receptor Antagonists: Synthesis, Capillary Electrophoresis, and in Vitro and Oral in Vivo Activity. *J Med Chem* 42, 593 – 600 (1999)
c) Soulier J.-L., Yang D., Brémont B., Croci T., Guzzi U., Langlois M. Arylcarbamate Derivatives of 1-Piperidineethanol as Potent Ligands for 5-HT_4 Receptors. *J Med Chem* 40, 1755 - 1761 (1997)

301. **a)** Duggan M.E.; Imagire J.S. Copper(I) Chloride Catalyzed Addition of Alcohols to Alkyl Isocyanates. A Mild and Expedient Method for Alkyl Carbamate Formation. *Synthesis* 131 (1989)
b) Hazzard G., Lamminan S.A., Poon N.L., Satchell D.P.N., Satchell R.S. The kinetics of the addition of ethanol to *p*-chlorophenyl isocyanate in diethyl ether solution in the presence of covalent metal halides. *J Chem Soc Perkin Trans 2*, 7, 1029 – 1035 (1985)

302. McManus S.P., Bruner H.S.; Coble H.D.; Ortiz M. Studies of the catalyzed reaction between alcohols and alkyl isocyanates. Evidence for a light-assisted reaction. *J Org Chem* 42, 1428 – 1433 (1977)

303. Beyer H.; Walter W. Lehrbuch der organischen Chemie, 23. Auflage, S.Hirzel Verlag Stuttgart Leipzig (1998)

304. Macor J.; Wu E. PCT Int Appl 2001; 35 (WO 97/30998); Chem Abstr 127, 1804p (1997)

305. Naito R.; Takeuchi M.; Morihira K.; Hayakawa M.; Ikeda K.; Shibanuma T.; Isomura Y. Selective muscarinic antagonists II. Synthesis and antimuscarinic properties of biphenylcarbamate derivatives. *Chem Phar Bulletin* 46, 1286 – 1294 (1998)

306. a) Mazurov A.; Klucik J.; Miao L.; Phillips T.Y.; Seamans A.; Schmitt J.D.; Hauser T.A.; Johnson R.T.; Miller C. 2-(Arylmethyl)-3-substituted quinuclidines as selective α7 nicotinic receptor ligands. *Bioorg Med Chem Lett* 15, 2073 – 2077 (2005)
b) Bodnar A.L.; Cortes-Burgos L.A.;Cook K.K.; Dinh D.M.; Groppi V.E.; Hajos M.; Higdon N.R.; Hoffmann W.E.; Hurst R.S.; Myers J.; Rogers B.N.; Wall T.M.; Wolfe M.L.; Wong E. Discovery and structure-activity relationship of quinuclidine benzamides as agonists of α7 nicotinic acetylcholine receptors. *J Med Chem* 48, 905 – 908 (2005)
c) Hurst R.; Hajos M.; Raggenbass M.; Wall T.M.; Higdon N.R.; Lawson J.A.; Rutherford-Root K.L.; Berkenpas M.B.; Hoffmann W.E.; Piotrowski D.W.; Groppi V.E.; Allaman G.; Ogier R.; Bertrand S.; Bertrand D., Arneric S.P. A novel positive allosteric modulator of the α7 neuronal nicotinic acetylcholine receptor: In vitro and in vivo characterization. *J Neurosci* 25, 4396 – 4405 (2005)

LIST OF PUBLICATIONS

2005 **Munoz L**., Abdelrahman A., Fleischer R., Gündisch D.: *Design, Synthesis and Biological Evaluation of Novel Cytisine Derivatives as Ligands for Nicotinic Acetylcholine Receptors*
Manuscript in preparation

2004 Gündisch D, Andrä M, **Munoz L**., Tilotta C.M.: *Synthesis and Evaluation of Phenylcarbamate Derivatives as Ligands for Nicotinic Acetylcholine Receptors*
Bioorganic & Medicinal Chemistry 12 (2004) 4953 – 4962

2002 **Gyűrösiová L**., Sedlárová E., Čizmárik J.: *Study of local anaesthetics, part 156: Some physicochemical and lipophilic properties of o-, m-, p-alkoxysubstituted pyrrolidinoethylesters of phenylcarbamic acid*
Chemical Papers 56 (2002) 340-344

2002 **Gyűrösiová L**., Laitinen L., Raiman J., Čizmárik J., Sedlárová E., Hirvonen J.: *Permeability profiles of m-alkoxysubstituted pyrrolidinoethylesters of phenylcarbamic acid across Caco-2 monolayers and human skin*
Pharmaceutical Research 19 (2002) 162-169

LIST OF POSTER PRESENTATIONS

2005 D. Gündisch, A. Abdelrahman, R. Fleischer, **L. Munoz**. *Novel cytisine analogs as potent nicotinic acetylcholine receptor (nAChR) ligands.*
Society for Neuroscience, Annual Meeting, Nov 12 –16, 2005, Washington, DC, USA

2005 **Munoz L**., Abdelrahman A., Fleischer R., Gündisch D.: *Novel Cytisine Analogues: Synthesis and Biological Activity*
2nd UK Nicotinic Receptor Club Meeting, May 20, 2005, GlaxoSmithKline, Harlow, UK

2004 Gündisch D.; Andrä M.; **Munoz L**.: *Novel ligands for nicotinic acetylcholine receptors (nAChRs) based on choline and cytisine: Synthesis and in vitro evaluation for different subtypes and tissues.*
Society for Neuroscience, Annual Meeting, Oct 23 –27, 2004, San Diego, USA

2004 **Munoz, L**.; Hennen S.; Gündisch D. *Novel Cytisine Analogues: Synthesis and Biological Activity*
29th National Medicinal Chemistry Symposium, June 27 – July 1, 2004, University of Wisconsin – Madison, USA

2004 Özbolat, A.; **Munoz, L**.; Guhlke, U.; Wüllner, D.; Schmaljohann, J. *Synthesis of the receptorligand [^{131}I]-3-Iodo-cytisine for in vivo imaging of the nAChReceptor*
6th International Conference on Nuclear and Radiochemistry, Aug 29 – Sept 3, 2004, Aachen, Germany

2004 Özbolat, A.; **Munoz, L**.; Guhlke, U.; Wüllner, D.; Schmaljohann, J. *Synthesis of the receptorligand [^{131}I]-3-Iodo-cytisine for in vivo imaging of the nAChReceptor*
Eur J Nucl Med 2004, 31 (suppl 2): P220, European Association of Nuclear Medicine Congress, Sept 4 – 8, 2004, Helsinki, Finland

2004 Özbolat, A.; **Munoz, L**.; Guhlke, U.; Wüllner, D.; Schmaljohann, J. *Synthesis of the receptorligand [^{131}I]-3-Iodo-cytisine for in vivo imaging of the nAChReceptor*
World Journal of Nuclear Medicine 2004, 3, 237, International Congress of radiopharmacy and Radiopharmaceutical Chemistry, Sept 25 – 27, 2004, Istanbul, Turkey

2003 **Munoz L**., Andrä M., Tilotta C.M., Gündisch D.: *Synthesis and In Vitro Evaluation of Phenylcarbamates and Choline Phenyl Ether Derivatives for Nicotinic Acetylcholine Receptors (nAChRs)*
Society for Neuroscience, Annual Meeting, Nov 8 – 12, 2004,
New Orleans, USA
Travel Award of "The Parkinson's Institute, Sunnyvale, CA, USA"

2003 Gündisch, D.; Seitz, G.; Tilotta, M.C.; Schwarz, S.; Wegge, T.; Klaperski, P.; Seifert, S.; Stehl, A.; Eichler, G.; **Munoz, L**.; Andrä, M.; Limbeck, M. *Synthesis and in vitro evaluation of structural variants of choline, cytisine, ferruginine, anatoxin-a, diazabicyclononane- and quinuclidin-2-ene based ligands for nicotinic acetylcholine receptors*
14th Camerino-Noordwijkerhout Symposium, Sept 7 – 11, 2003,
Camerino, Italy

2003 Gündisch, D.; Seitz, G.; Tilotta, M.C.; Schwarz, S.; Wegge, T.; Klaperski, P.; Seifert, S.; Stehl, A.; Eichler, G.; **Munoz, L**.; Andrä, M.; Limbeck, M. *Synthesis and In Vitro Evaluation of Novel Ligands for Nicotinic Acetylcholine receptors (nAChRs): Structural Variants of Choline and Alkaloidal Toxins and 3,9-Diazabicyclo[4.2.1]nonane and Quinuclidin-2-ene based Derivatives*
1st UK Nicotinic Receptor Club Meeting, July 1st, 2003, Lilly Research Centre, Earl Wood Manor, Windlesham, UK

ACKNOWLEDGEMENTS

The following is my heartfelt appreciation to those people, both past and present, who gave me the spirit and encouragement to start, conduct and complete this thesis, as well as to those people who made me feel home in Germany…...

First of all I would like to thank **Daniela**, my supervisor, for introducing me to the nAChR world. Daniela, you have been a wonderful supervisor and a scientist I admire. I am particularly grateful that you have never stopped believing in my ability and that you did not let me to leave. Thank you for the independence and freedom you gave me. I've learnt so much in the last 4 years and I know that all this development is a result of your hidden, but constant supervising. But what impress me even more are your personality and the love you have for your children and family. You are a super-woman – you have a great career and you have a beautiful family. Daniela, your friendship means very much to me (you can't stop me to use the adjectives here!), as people like you are difficult to meet.

Thank you very much goes to **Frau Müller**, our "*Chefin*" for giving me the opportunity to conduct the research at this institute. I greatly respect your career and success, which has inspired me to always be willing to learn more and work hard. I will always remember your very nice speeches at the farewell parties and your great performance at the last X-mas party!

I could not have reached this stage of my life if it wasn't for the great teachers throughout my studies. I am particularly thankful to my chemistry teacher from high school, **Mrs. Barthova** (*Trudi, ďakujem za všetko*), my diploma and rigorous thesis supervisor, **Prof. Sedlarova** (*vďaka za podporu*) and my first real teacher of the "serious" science, Prof. Hirvonen, my supervisor during the research visit to the Uni of Hki, who taught me the most important statement of the science "*there is always a light at the end of the tunnel*". **Jouni**, I can't count how many times this went through my mind over the past 4 years. Kiitos for that and thanks for coming to Bonn.

Ein grosses Danke schön goes to Ralf Mayer, a supervisor? a colleague? a friend? No **Ralph,** you have been a bit of everything. Thank you for teaching me how to "squeeze" the Goldregen-Samen in order to get some white, oh so precious cytisine. Danke for all the NMR help. Danke for being a proof-reader, Danke for taking care of my *Sicherheit*, Danke für "*die Einweisung für den Umgang mit Lenca*" and especially thanks for calling me "*meine Lieblingsdoktorandin*". Wishing you and your increasing family all the best for the future.

Mi Amor, Mi Amor **Jörgi** how can I thank you? You are not just a great chemist, but a beautiful person. You have been the colleague who had time and patience for everyone, every day! I don't think I can ever repay you for all you've done for me but I won't forget it. Thanks for helping me with the chemistry, for being such an uncomplicated *Semesterleiter*, for all the lunch/dinner outings once in a while and for getting me drunk for the very first (and last) time in my life!

Joe, Big **Joe**, you are absolutely the best teacher. Whatever I asked you, you explained it in an excellent way on the little blackboard in your lab until it was all clear in my head. Sometimes the information just didn't stay in my brain, and I came back with the same question. And once again I got a lecture on the blackboard. Vielen Dank dafür. Und auch für die Witze. Und die Freundschaft. Wishing you all the best, always.

Carlito, moving up to your Denkraum was the best thing that happened to me in Poppelsdorf. I am so grateful that I could overtake your greatly organised and tidy working place, and keep the greatest Suzuki chemistry alive in Poppelsdorf. Danke für showing me the tricks with the argon bomb. Danke für das hömeopathisch verdünte Kaffee. Für die leckersten Nussecken. Und für die netten Briefe die Du mir geschrieben hast. Aber noch mehr bin ich Dir dankbar für die wunderbare and langhaltige Freundschaft die sich zwischen uns entwickelt hat. I wish we were colleagues for the whole period. But I am appreciative that I had the chance to meet you and get to know you.

Thanks goes to my colleagues and friends in the research group – the old (in the meaning of being the first PhD student in our group) and wise **Marcus** L., **Matthias** (immer gut gelaunt und hilfsbereit, Danke für das Goldregen!), **Cristina** Pelota (oops, Tilotta) – the Sicilian treasure we were honoured to hold for a while and the diploma student – **Jeannette**. Although we spent only 6 months together, we became good friends. Jeannette, danke für Deine wunderbare Hilfe am Anfang, für die Freundschaft und tolle Begleitung bei der Tagung in New Orleans. Du hast mir immer gefehlt.

Thanks to the "old school" that was in Poppelsdorf when I arrived and are now nearly gone, but some people are not forgotten, especially **Steffi** – thanks for your generous help with HPLC and the smile you always had for me; **Till** – thanks for the nice chats about the science behind the scenes; **Mark** Thorand (oh, how did we managed without you? ☺); **Phu** for creating a very peaceful working atmosphere; **Gunawan** (the most relaxed and patient person I have ever met) and the smiling **Heiko K**. **Fritzi** sei Dank für die Freundschaft und für die Motivation die Du durch Deinen Kraft und Ausdauer verbreitest.

Thanks to the "staff" in Poppelsdorf - **Marcus A.** - thanks for the odd looks you gave me when I asked something about the EDV and the help that came afterwards. And Marcus, for the very last time – Lance is clean! **Herr Neugebauer** (please remember, after my graduation you will be Michael) for the great company at the parties and the crisp-a-la-Neugebauer humour; thanks to **Wolfgang** for always being so happy to see me (and for maintaining all the instruments *im Haus*); thanks to Herr Kriechel for being **Herr Kriechel** ("*Die Chemikalien sind da*"); thanks to **Herr Belasin**, my Hungarian grandfather for the nice words he had every evening for me and for calling me "*szepség*"; **Frau Spychala** for her wonderful smile and immediate help; **Stefan** for being such a great organiser of our chemical treasure, for constant help when needed and the company during our lunches at the Turkish corner. Vielen Vielen Dank goes to our secretaries – **Beate** und **Martina**, I have to say that I was always happy when I had to go to the *Sekretariat,* as you always had a nice word and a solution for every bureaucratic problem. Last, but not least, *Danke schön* für **Marion** und **Sabine** for all the excellent (really excellent) work with the NMR spectroscopy! Your efforts are truly appreciated.

Another big Thanks goes to the **Prof. Gütschow** for putting up with me as one of the loudest element in his surroundings and to his very nice research group; Danke **Manuela** und viel Glück in Mainz; Danke **Agnieszka** – the peaceful nice Agnieszka, the stability of the group; **Reiki**, thanks for scaring the living days out of me!, **Marcus** – the leader, you are simply "*süss*" in the way you are; **Paul** – Danke nochmals für die Hilfe mit 2Ds. **Sonja**, Danke für das nette Lächeln und die Freundschaft, und **Camino** – Niñita, que suerte, que nos hemos conocido! Eres una maravilla!

"No-group-member", but excellent colleague - **Svenja** – thanks for being always nice and helpful.

And now it's time to mentioned "*die Jungs*", meine Jungs – Fabian, Andreas, Heiko und Frank – **Fabianito**, you have been a wonderful and very easy-going lab-mate and honestly, I will miss you, thanks for everything. Viva HSV! I am sure one day they will be champions! **Andreas** – I know, I know, the Russian jazz and trekking in Siberia, maybe one day we all meet there, don't stop living your dreams!! **Frank** – Danke für alle Komplimente, ich überlege noch… – und **Heiko**, you were the last one joining Poppelsdorf, but it feels I have known you for years! Great colleagues, all of you….I have enjoyed every lunch and coffee break with you, honestly.

Und meine **Mery**, thanks for everything. No words can describe how much I appreciate our friendship and how grateful I am for your listening. Sometimes I would talk and complain for hours and hours and you would just try to cheer me up. Whenever I felt like talking to a soul mate, there was Mery and this helped me through the toughest time. Mery, ich wünsche mir so sehr dass Dein Leben ein bisschen unkomplizierter wird. All you deserve is happiness and however I can contribute to this, I'll do my best to do so.

And a BIG, BIG THANKS to my friends in the "real world"…..the Barulhos – we might not be welcome in the Cologne night scene anymore, but we definitely are the funniest bunch of people in Cologne – **Antonio A**. – our founder and his missus **Nicole**, **Célia** – the loudest member and always a great company, **Sergio C**. – the most peaceful member who somehow managed to get into a trouble with *Ordnungsamt* , **Rosa** (pronounced Rousa) – einfach eine tolle Freundin, und **Antonio C.** and of course, **Pedro Pinto** – always together – whenever I saw you or heard you, I felt happy – **Andrea** (tio Baresi, ueu ueu bum bum bum casino casino) thanks for driving us around and being always helpful, **Sergio G.** – you were the highlight of every party! – **Jean-Marc** ("*put the pizza in the oven*….") – great person in his special way, and **Ana** – disappearing for months but luckily always coming back – **Andreas** – you were the only German who managed with us more than one night and **Sofia**, "big-stuff-Samba-queen"! You guys are great and my only regret is that we didn't meet each other sooner, but both the fun & friendship made up for the lost time. I miss you already.

A special Thanks for our oldest "German" friend **Sebastian**, not only for looking after my flowers when we were on holidays, but for being such a nice person and bringing the warm Argentinean soul to Köln. Sebastian, gracias por la amistad y todo…..nos vemos, seguramente

Danke, Danke schön goes to my Brazilian dancing group, to which I became addictive over the years. I could not miss out on anything, the great dancing classes, the organised chaos we produced every time when planning things, the absolutely amazing trip to Hamburg and Lindenthal, but most of all the friendship that kept us together, is one of the most beautiful things that ever happened to me. Ihr meine Lieben – **Beatriz**, **Julie**, **Ingrid**, **Elena**, **Christina**, **Marivaldo** und **Delsinho** (the best dancer ever!) – ihr seid meine Familie in Köln und seitdem ich euch habe, fühle ich mich in Kölle zu Hause und glücklich. Ich liebe euch…

And finally, Ďakujem to my wonderful **parents**, for their endless love, care, support, freedom and coping so great with the distance that is between us. Maminka, tatík – ďakujem vám za všetku lásku a pochopenie počas celého štúdia. Gracias to my wonderful **parents-in-law** for being such a wonderful parents-in-law, for their love and nice time together. I am happy that I married into such a nice family…

Four years ago the life got beautiful, my deepest thanks to the one responsible.